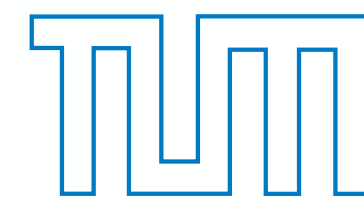
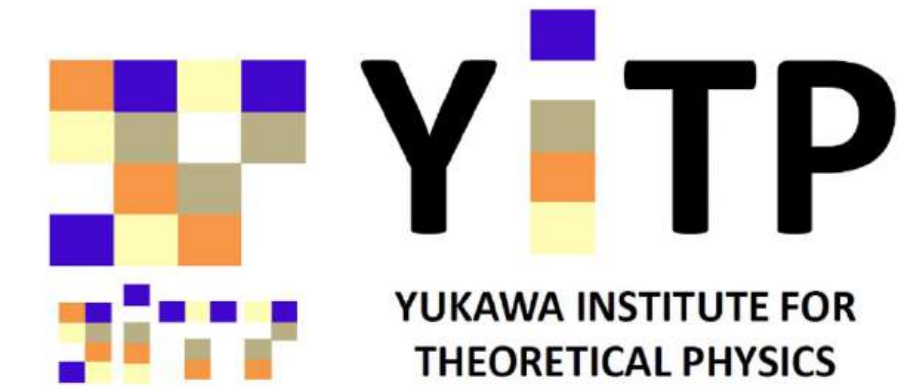




Dense Baryonic Matter :

From Quarks to Nuclei and Neutron Stars



Wolfram Weise
Technische Universität München



★ Phases of QCD Matter

- **High temperatures : Constraints from High-energy heavy-ion collisions and Lattice QCD thermodynamics**
- **High baryon densities : Constraints from neutron star matter**
- **Moderate temperatures and densities : nuclear thermodynamics**
- **Low-energy structure of the nucleon**

★ Dense and Cold Baryonic Matter

- **Inference of the Equation of State from neutron star observations**
- **Theoretical methods and strategies : Effective Field Theory Functional Renormalisation Group**
- **Neutron star matter as a Relativistic Fermi liquid**
- **Strangeness ? Quark Matter ? Hadron - Quark Continuity**

1.

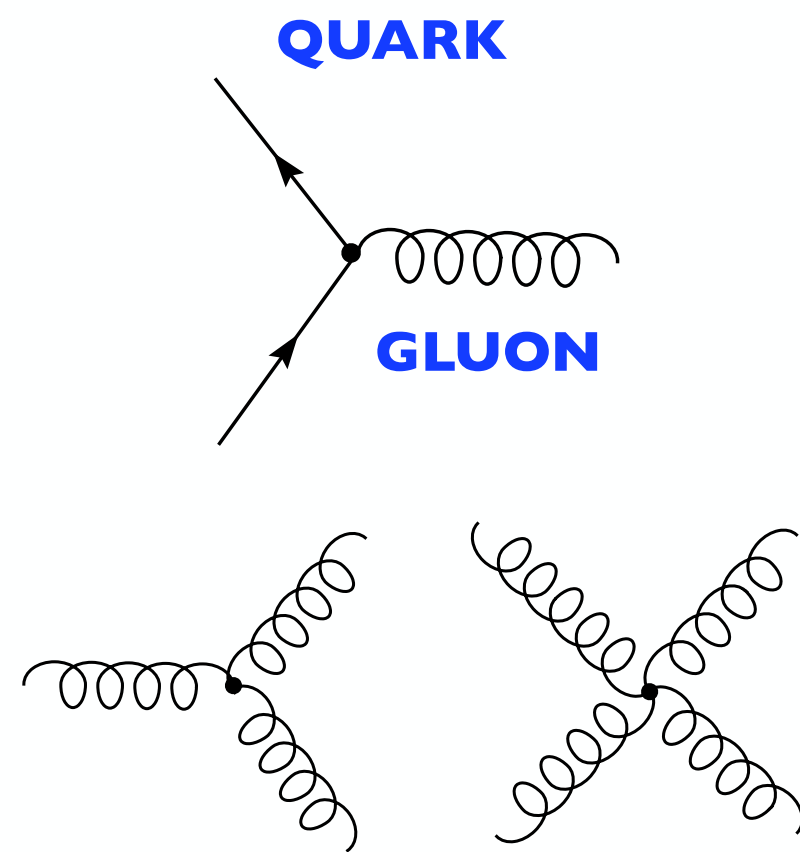
*Preliminaries :
QCD and Cold Quark Matter*

QUANTUM CHROMO

DYNAMICS

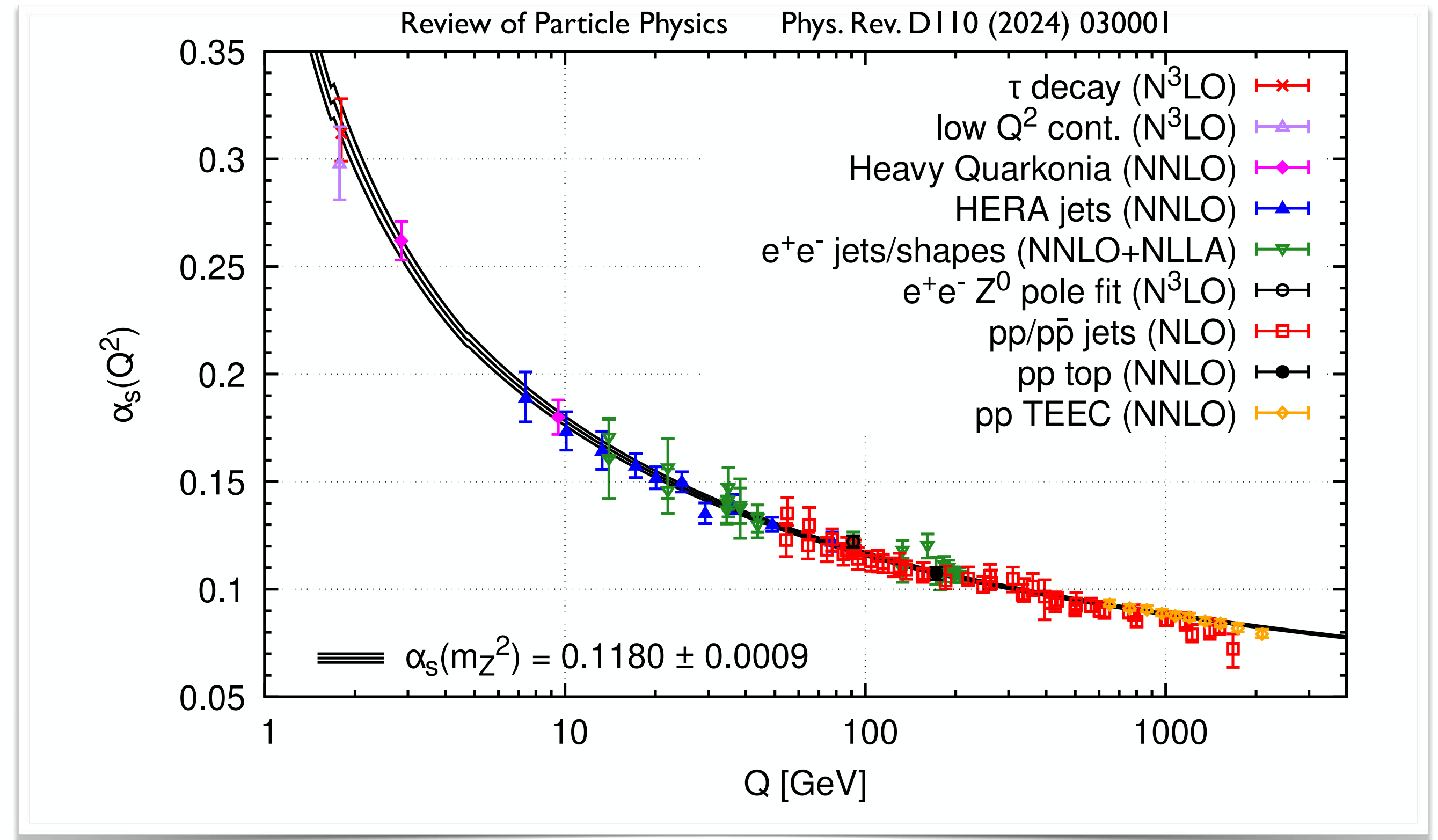
$$\mathcal{L}_{\text{QCD}} = \bar{\psi} (i\gamma_{\mu} D^{\mu} - m) \psi - \frac{1}{4} \mathbf{G}_{\mu\nu} \mathbf{G}^{\mu\nu}$$

Quarks spin = 1/2		
Flavor	Approx. Mass GeV/c ²	Electric charge
u up	0.002	2/3
d down	0.005	-1/3
C charm	1.3	2/3
S strange	0.1	-1/3
t top	173	2/3
b bottom	4.2	-1/3



QCD running coupling

$$\lambda_R \frac{d\alpha_s}{d\lambda_R} = \beta(\alpha_s) = - \left(\frac{33 - 2N_f}{12\pi^2} \alpha_s^2 + \frac{153 - 19N_f}{24\pi^2} \alpha_s^3 + \dots \right)$$



► Scale-setting example : **cold gas of massless quarks** (quark chemical potential $\mu \simeq p_F$)

Quark density : $n_q = N_f p_F^3 / \pi^2 = 3\mu^3 / \pi^2$
 ($N_f = 3$)

Baryon number density : $n_B = \mu^3 / \pi^2$

Range of applicability for **perturbative QCD** :

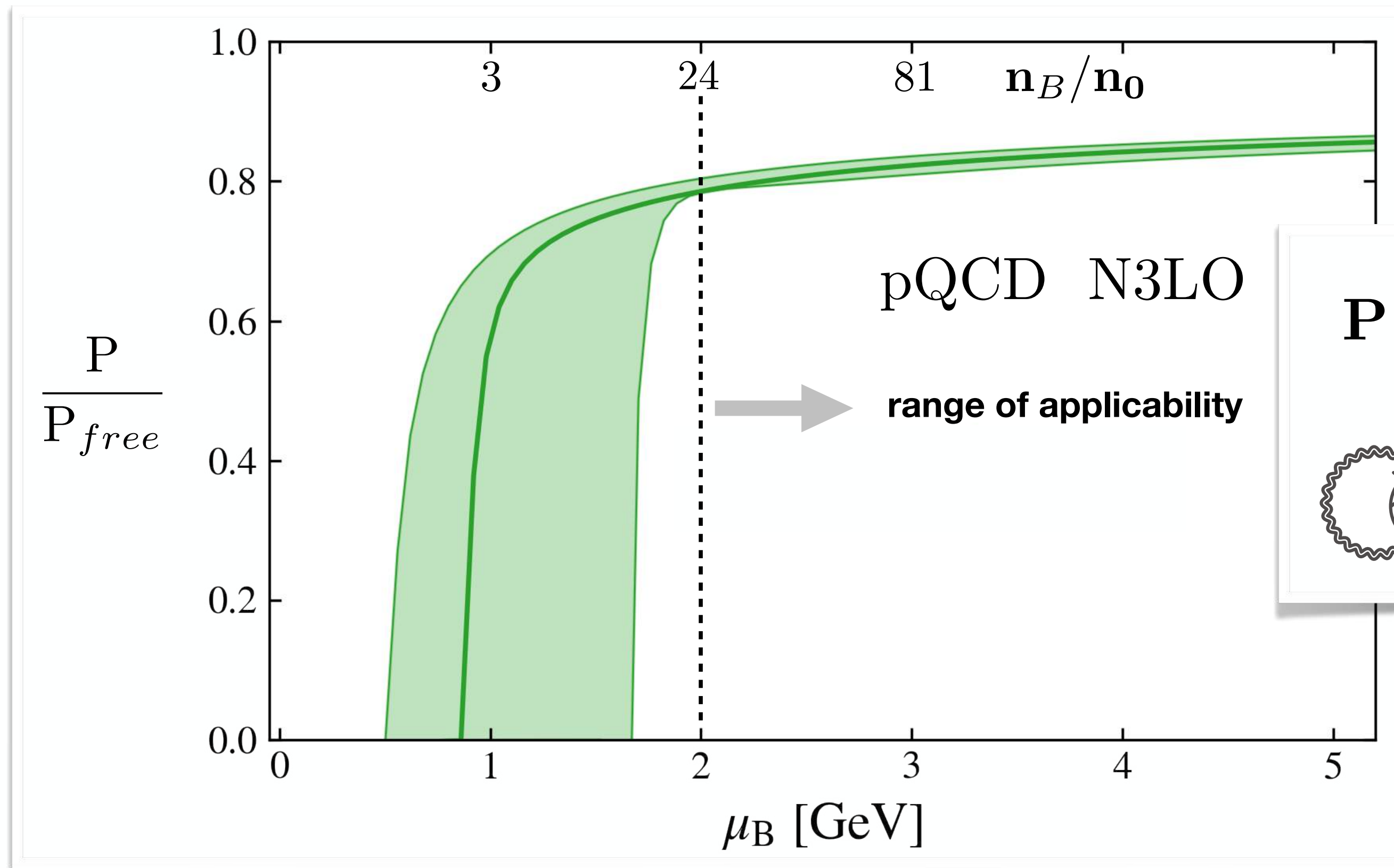
$\mu > 1 \text{ GeV} \rightarrow n_B > 80 n_0$!
 ($n_0 = 0.16 \text{ fm}^{-3}$)



COLD QUARK MATTER in pQCD

- State-of-the-art : next-to-next-to-next-to leading order in α_s ($N_f = 3$ massless quarks)

- Pressure
$$\frac{P}{P_{free}} = 1 - \frac{\alpha_s}{\pi} - 3 \left(\frac{\alpha_s}{\pi} \right)^2 f \left[\ln \left(\frac{\alpha_s}{\pi} \right), \mu \right] + 9 \left(\frac{\alpha_s}{\pi} \right)^3 g \left[\ln \left(\frac{\alpha_s}{\pi} \right), \mu \right]$$



$$P_{free} = \frac{3\mu^4}{4\pi^2} \quad \mu = \frac{\mu_B}{3}$$

$$P = \dots \left[\text{diagrams} \right] + \dots$$

The diagram shows a series of Feynman diagrams representing the perturbative expansion of the pressure. The first row contains four diagrams: a gluon loop, a ghost loop, a quark loop, and a four-gluon vertex diagram. The second row contains five diagrams: a gluon self-energy diagram, a ghost self-energy diagram, a quark self-energy diagram, a gluon-gluon vertex diagram, and a ghost-gluon vertex diagram. Each diagram is enclosed in a circular boundary representing the pressure calculation.

T. Gorda, R. Paatelainen, S. Säppi, K. Seppänen
 Phys. Rev. Lett. 131 (2023) 181902

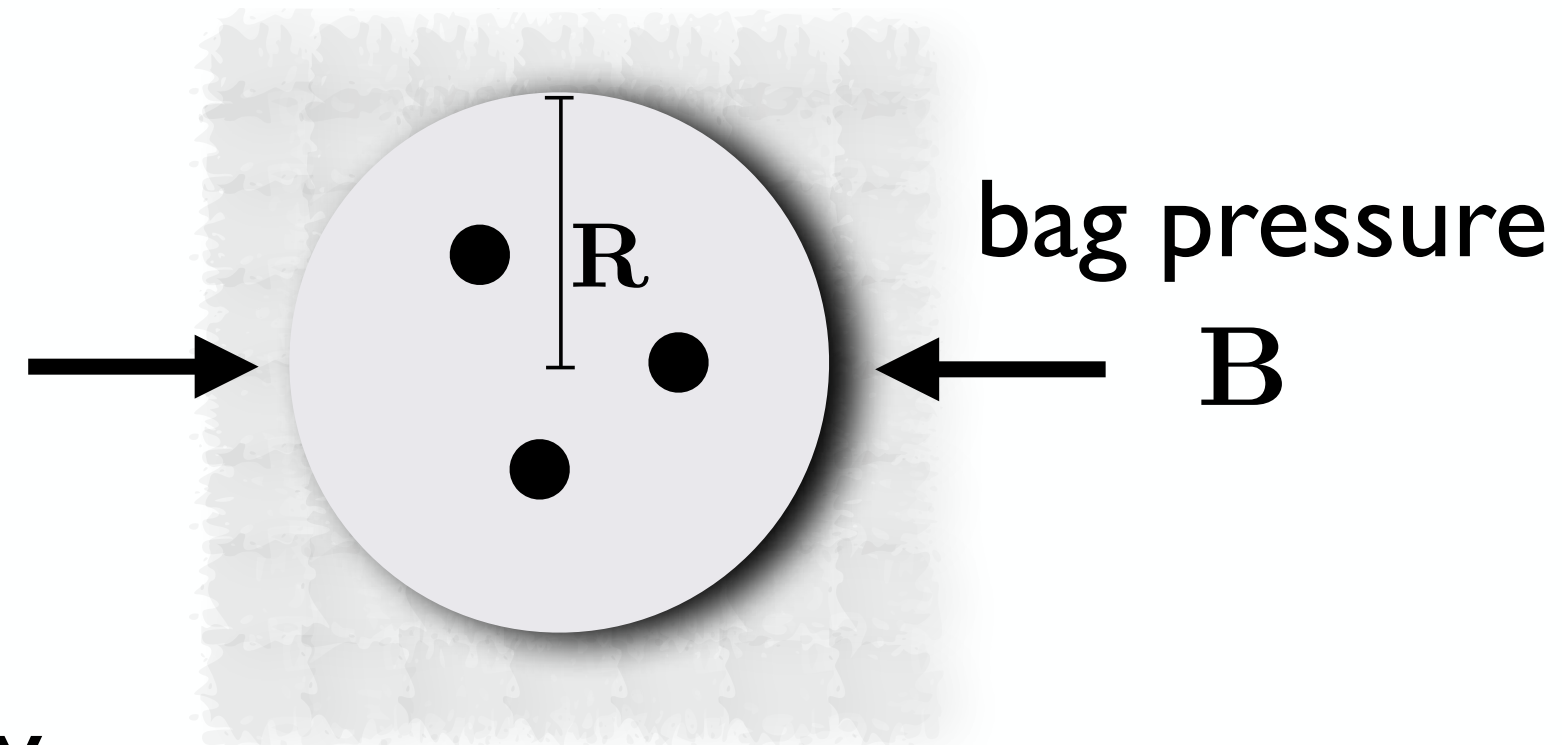


Basic schematic exercises:

Massless Quarks under Pressure

- Baryons vs. Quark Fermi Gas -

- Valence quarks in a confining bag



- Energy

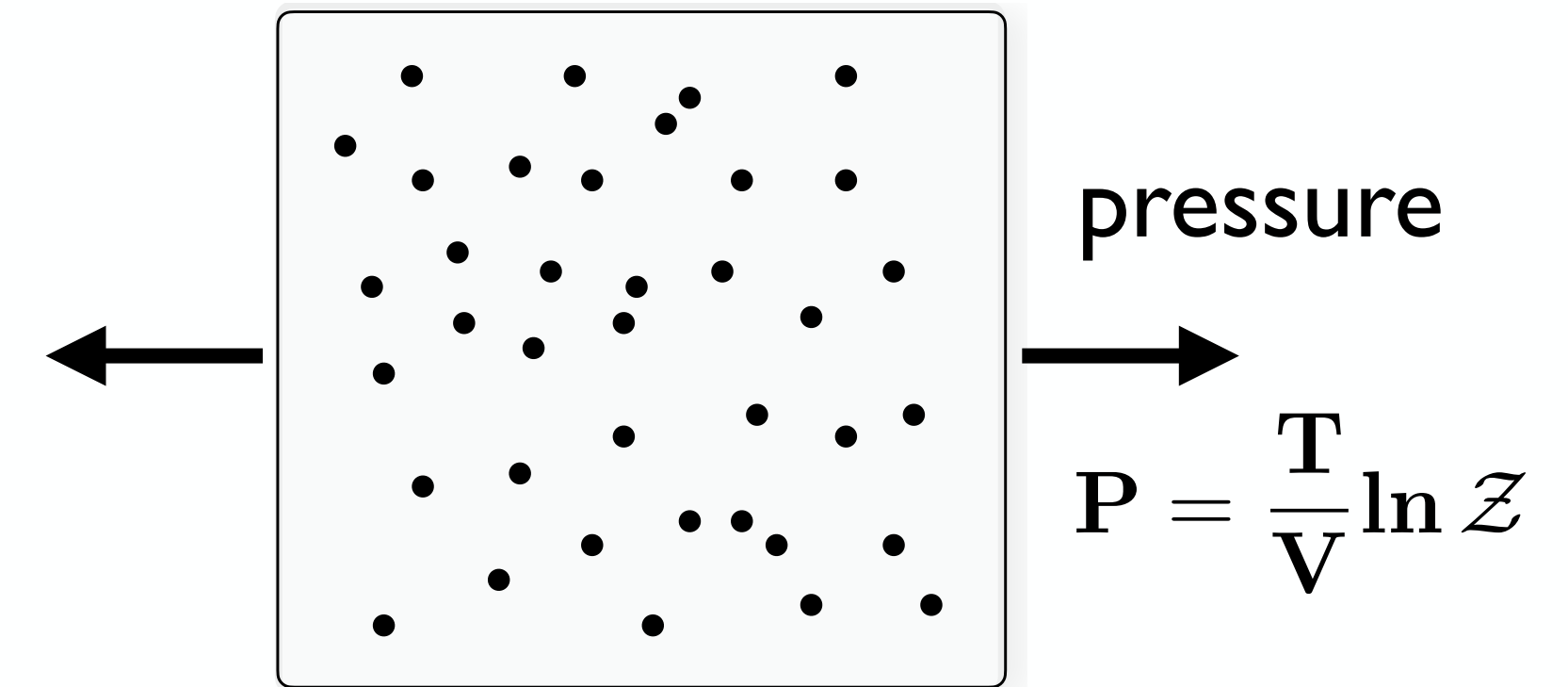
$$E = \frac{C}{R} + \frac{4\pi}{3} B R^3 = M \quad \frac{\partial E}{\partial R} = 0$$

$$B = \frac{3}{16\pi} \frac{M}{R^3} \quad C = \frac{3}{4} M R$$

- Example: $M \sim 1 \text{ GeV}$ $R \sim 0.6 \text{ fm}$

bag constant: $B^{1/4} \simeq 0.22 \text{ GeV} \sim \Lambda_{\text{QCD}}$

- Gas of ultrarelativistic quarks and gluons



$$P = P_Q + P_G$$

- Fermi gas of massless quarks ($g_Q = 2 N_f N_c$)

$$P_Q = \frac{g_Q}{12} T^4 \left[\frac{7\pi^2}{30} + \left(\frac{\mu}{T}\right)^2 + \frac{1}{2\pi^2} \left(\frac{\mu}{T}\right)^4 \right]$$

μ : chemical potential of quarks ($\mu = p_F$)

- Gluon gas ($g_G = 2(N_c^2 - 1) = 16$)

$$P_G = g_G \frac{\pi^2}{90} T^4$$

Basic schematic exercise (contd.)

Massless Quarks under Pressure

- Baryons vs. Quark Fermi Gas -

• total pressure ($N_f = 3$) $P(T, \mu) = \frac{19}{36} \pi^2 T^4 + \frac{3}{2} \mu^2 T^2 + \frac{3}{4\pi^2} \mu^4$
 • baryon density $n_B = \frac{1}{3} \frac{\partial P}{\partial \mu} = \mu T^2 + \frac{\mu^3}{\pi^2}$

- Critical temperature at deconfinement crossover

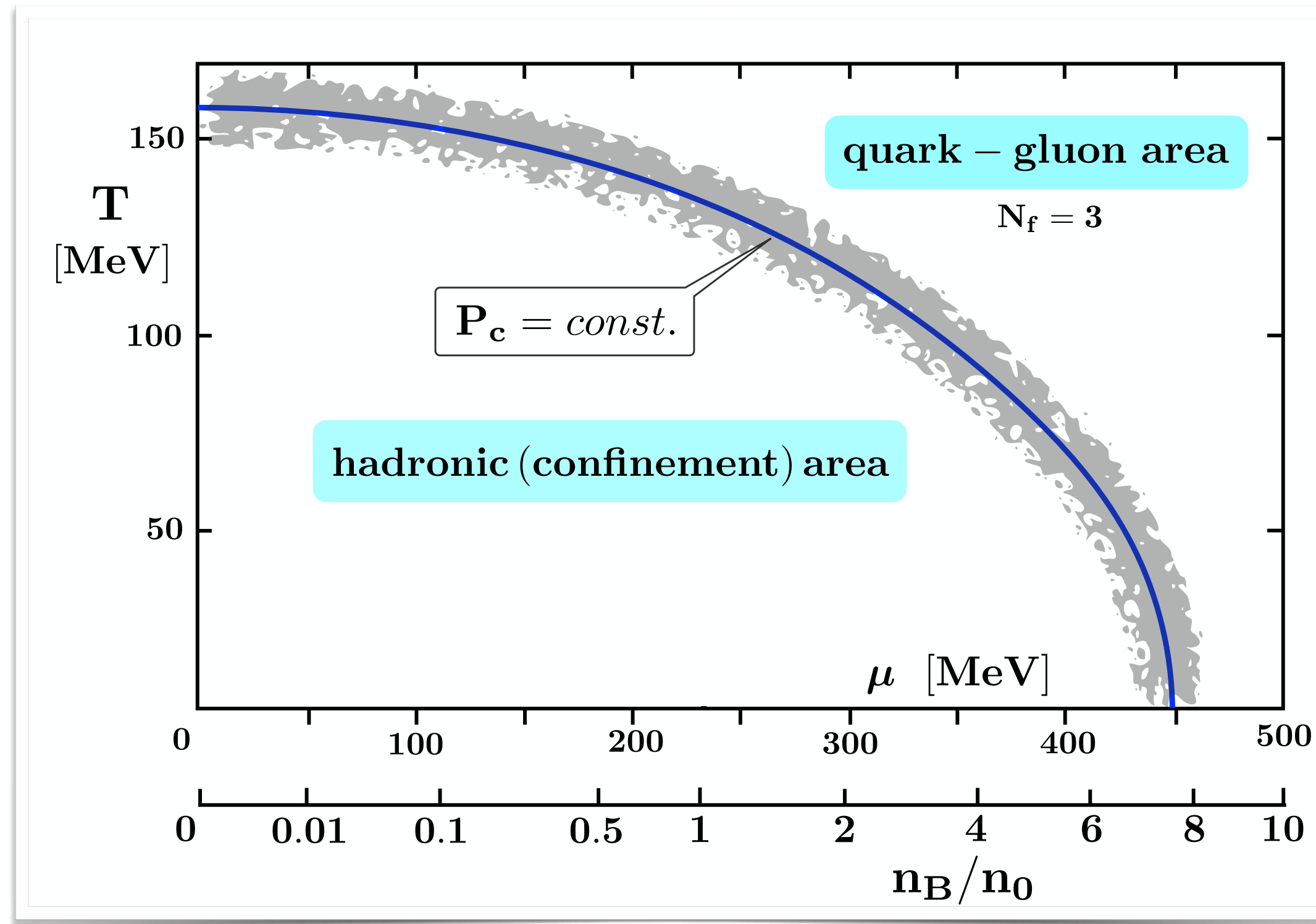
$$T = T_c = 156 \text{ MeV}, \mu = 0$$

- Critical pressure

$$P_c = P(T_c, \mu = 0) \simeq 0.4 \text{ GeV}/\text{fm}^3 \quad (N_f = 3)$$

- Note: assuming $P_c = B$

$$\rightarrow B^{1/4} \simeq 0.23 \text{ GeV}$$



Prototype of a phase diagram

quark chemical potential

baryon density

$$(n_0 = 0.16 \text{ fm}^{-3})$$

Critical isobaric curve (line of constant P_c) in the $T - \mu$ diagram

2.

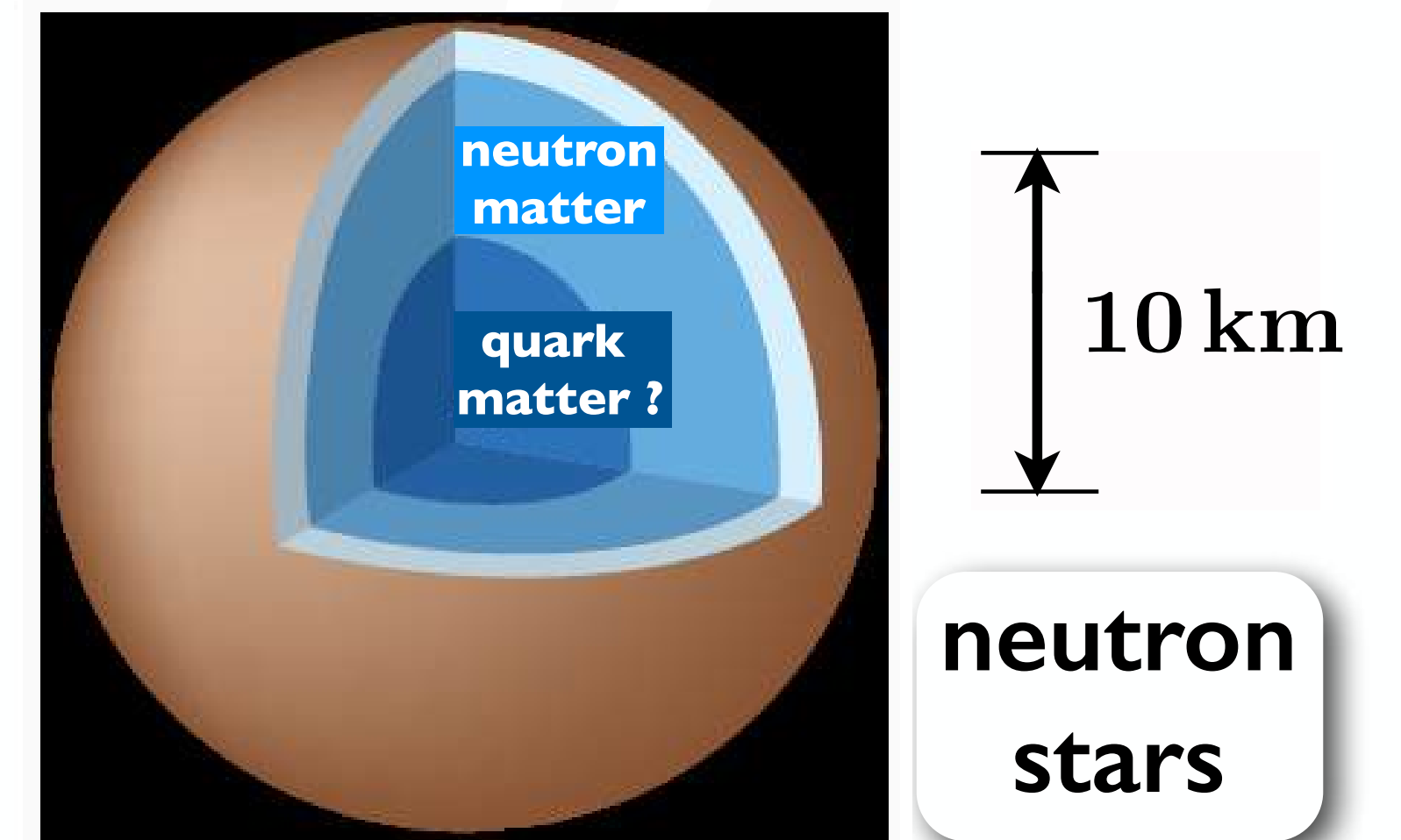
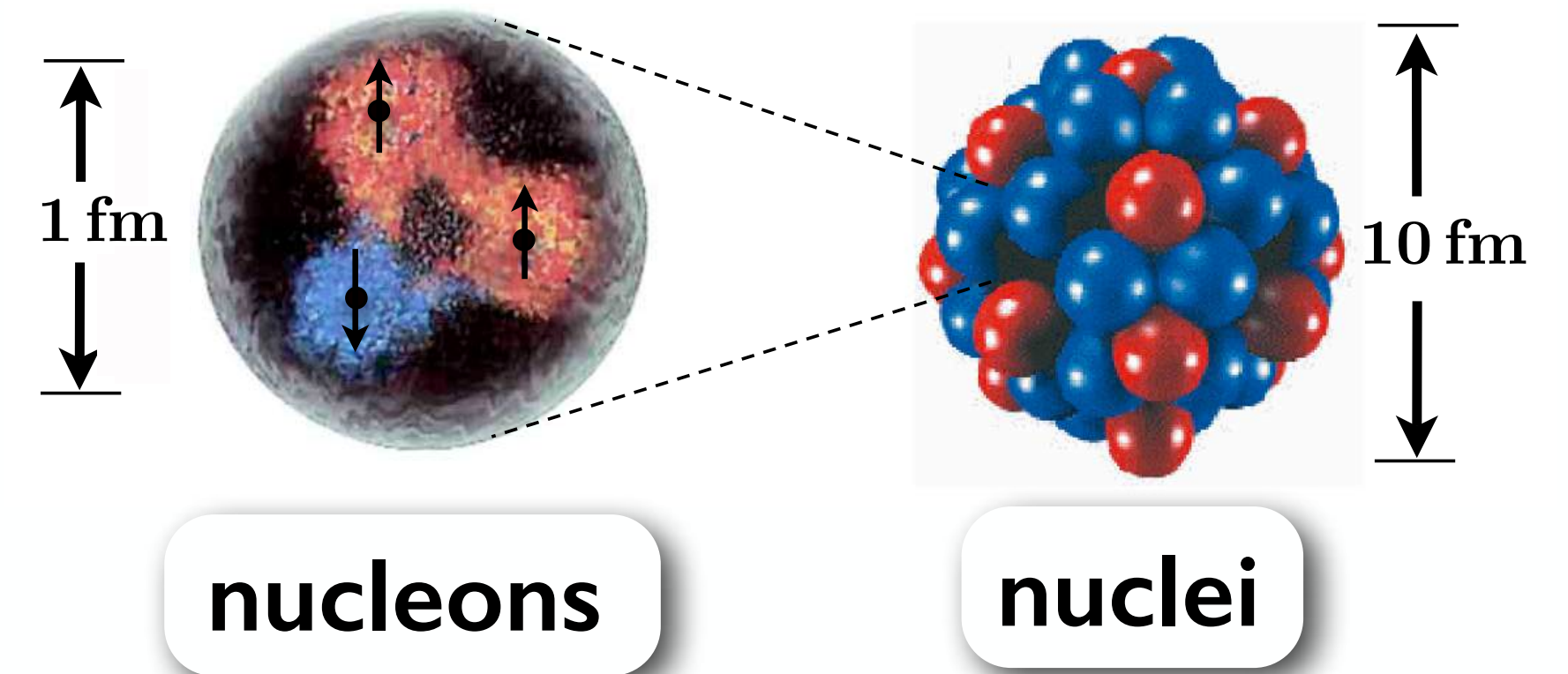
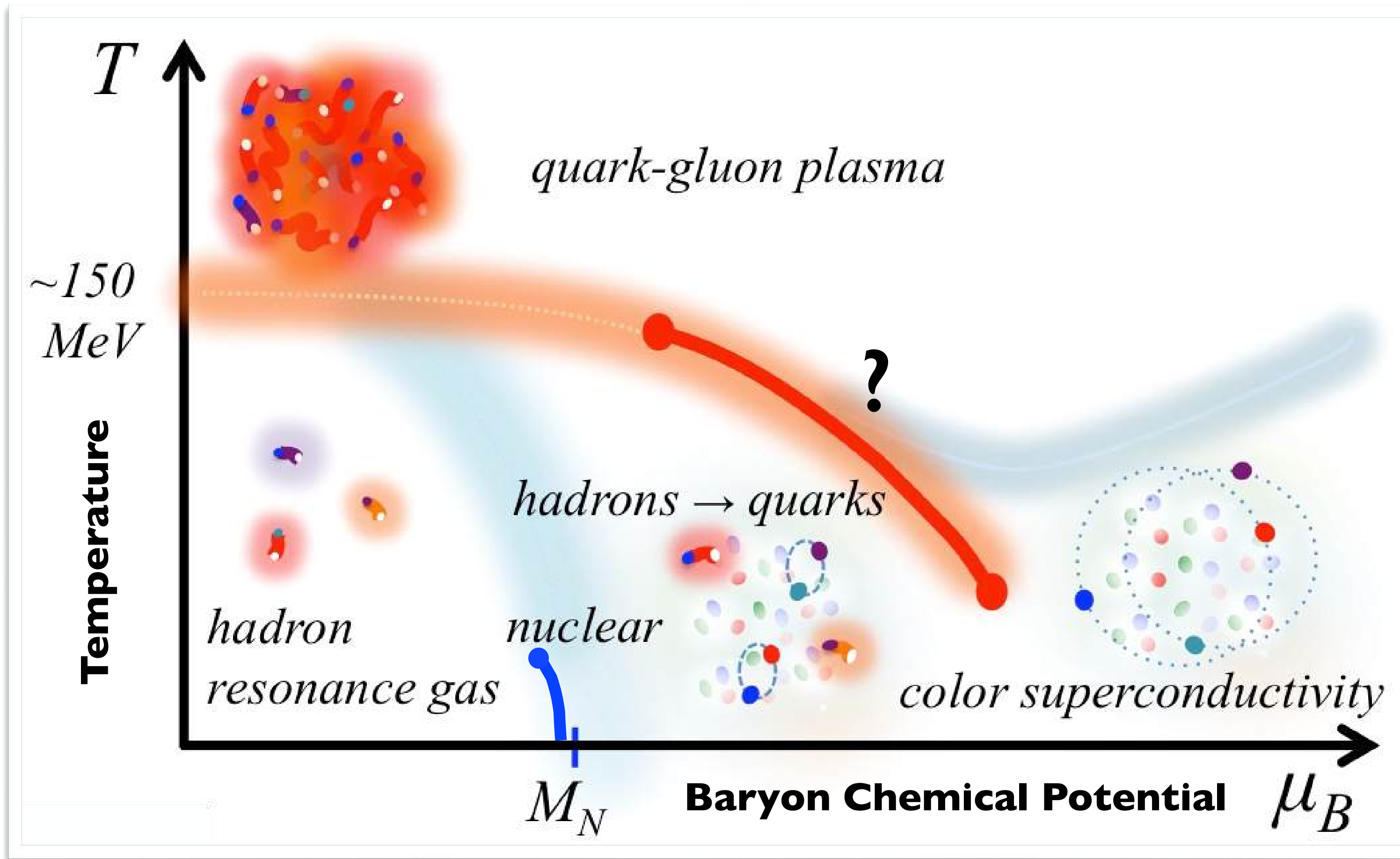
Status :

*What do we know about the
PHASES of QCD ?*



PHASES and STRUCTURES of QCD

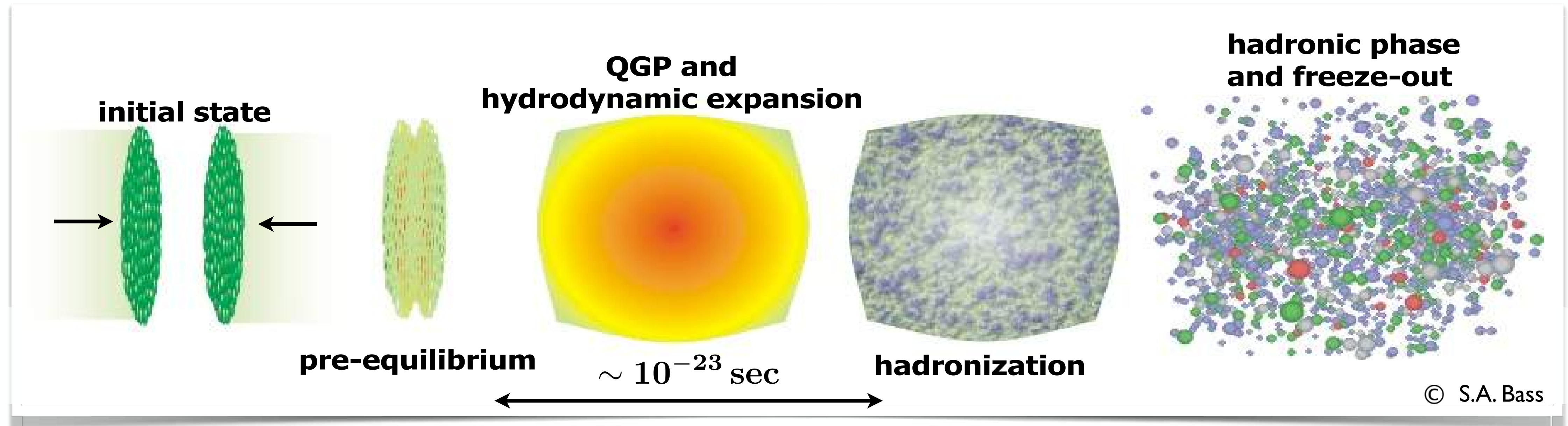
QCD PHASE DIAGRAM : Theorist's Vision



G. Baym, T. Hatsuda, T. Kojo, P.D. Powell, Y. Song, T. Takatsuka : Rept. Prog. Phys. 81 (2018) 056902

Strategies PART I: **Heavy-Ion Collisions**

- **High Energy Nuclear Collisions @ CERN/SPS, RHIC, LHC**

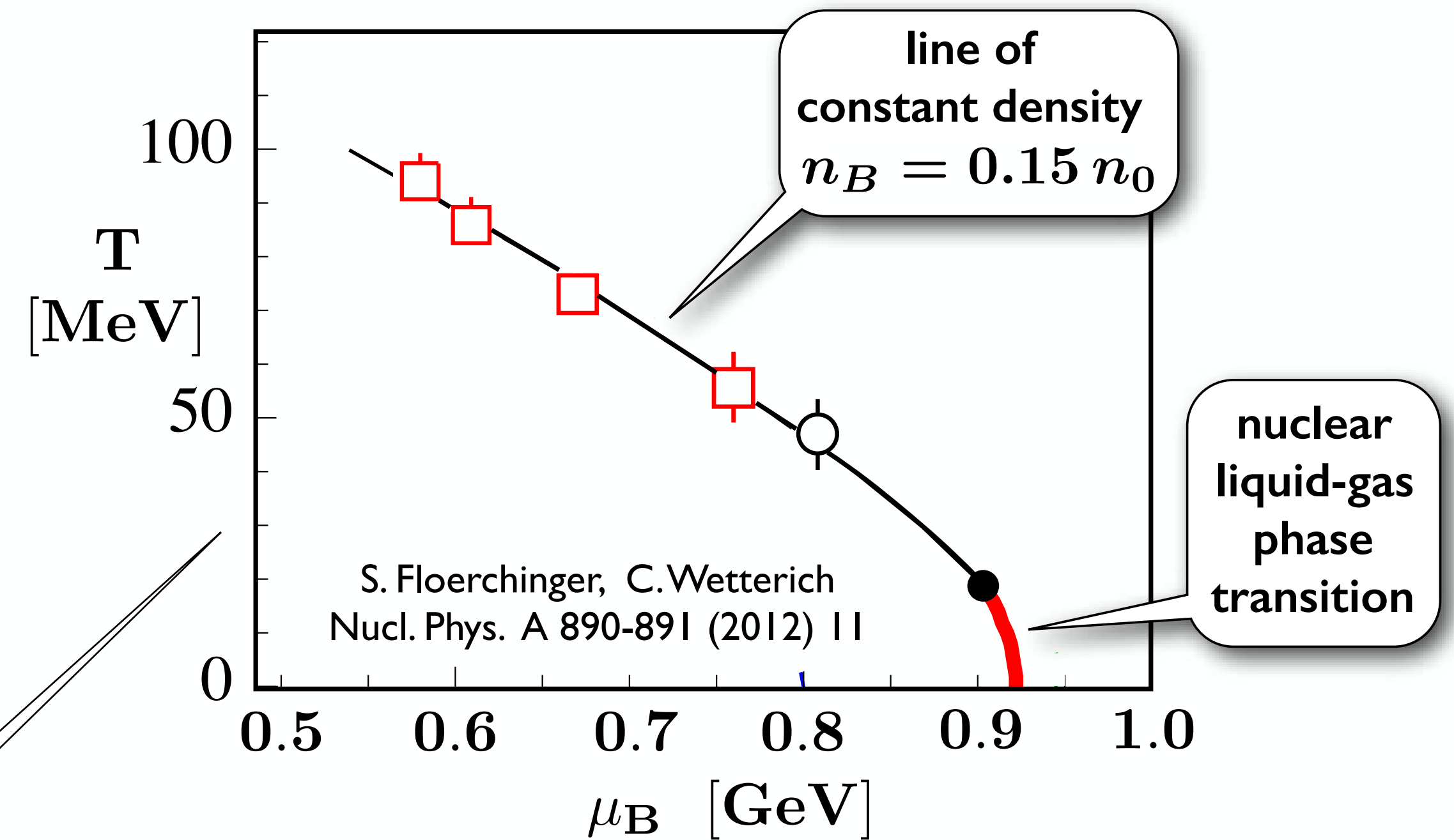
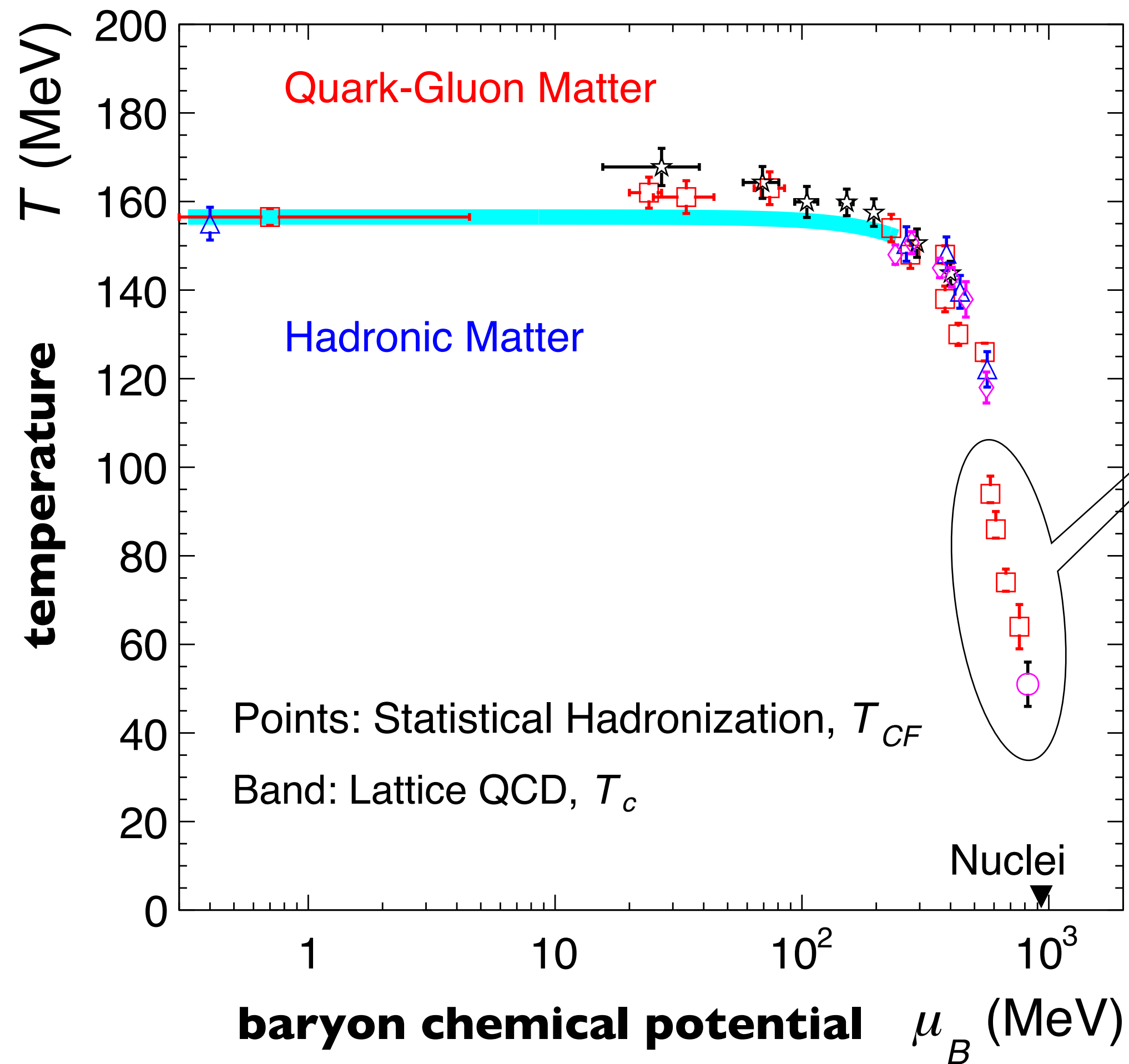


- Analysis of **RHIC** and **LHC** data:

- ▶ **Initial temperatures 300 - 500 MeV**
- ▶ **Fast equilibration**
- ▶ **Strongly correlated quark-gluon matter**

CHEMICAL FREEZE-OUT

A. Andronic, P. Braun-Munzinger, K. Redlich, J. Stachel
 Nature 561 (2018) 321 arXiv:2101.05747



- **Freeze-out temperature**
 $T_{CF} = 156 \pm 2 \text{ MeV}$ at $\mu_B \simeq 0$
- **Nuclear matter in equilibrium**
baryon density $n_0 = 0.16 \text{ fm}^{-3}$
 at $T = 0$ and $\mu_B = M_N - \frac{|E_b|}{A} = 923 \text{ MeV}$
- **Low-temperature freeze-out trajectory :**
NOT a first-order phase transition line

Strategies PART II: **Lattice QCD**

$$\mathcal{L}_{\text{QCD}} = \bar{\psi} (i\gamma_{\mu} \mathcal{D}^{\mu} - \mathbf{m}) \psi - \frac{1}{4} \mathbf{G}_{\mu\nu} \mathbf{G}^{\mu\nu}$$

- Large-scale computer simulations on **EUCLIDEAN SPACE-TIME** Lattices
- Euclidean time $\hat{=}$ inverse **temperature** $\tau = 1/T$

quarks on lattice sites

$$\psi(n)$$

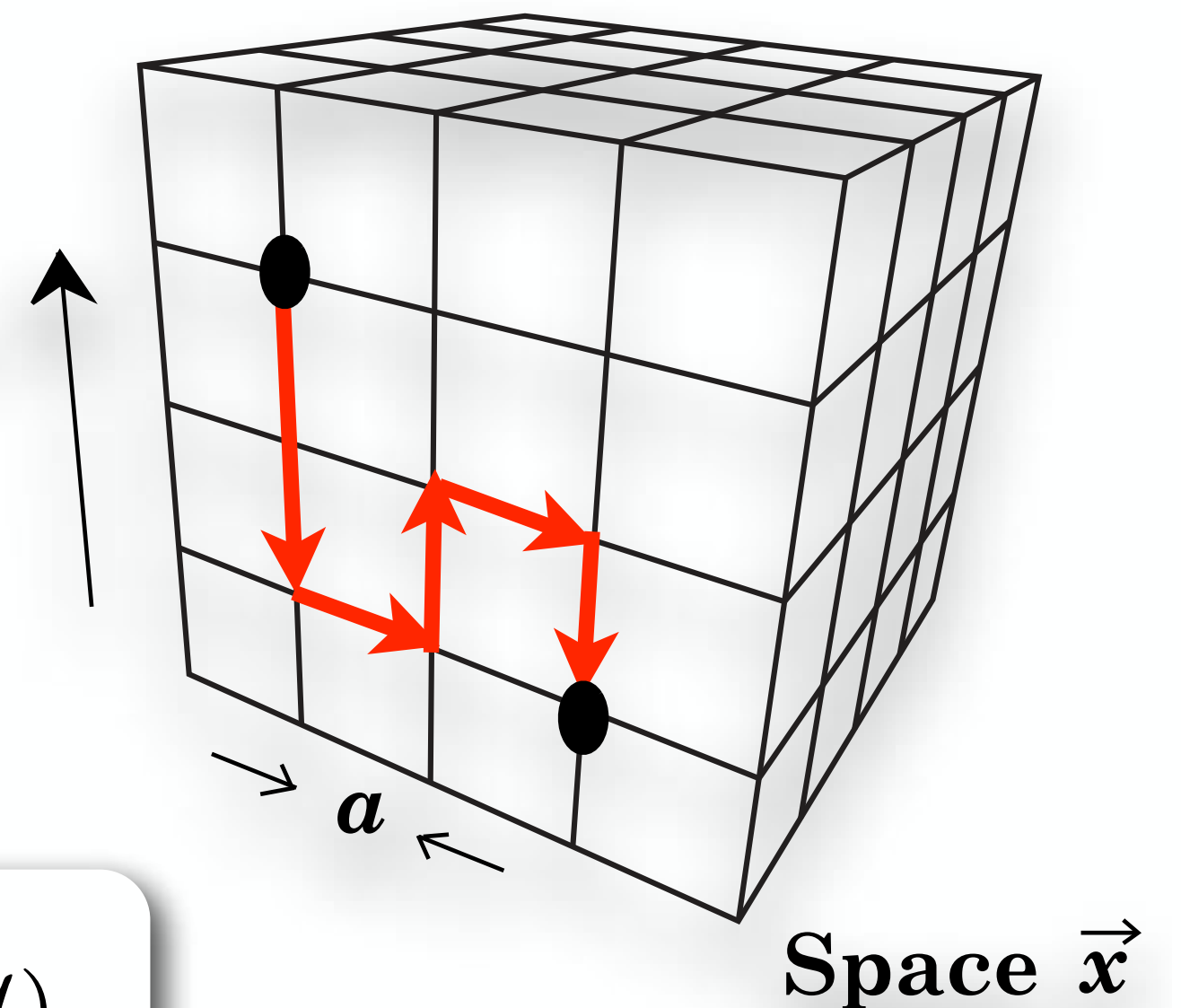
gluon fields on links $\mathcal{U}_{\mu}(n) = 1 + iaA_{\mu}(n) + \mathcal{O}(a^2)$

Euclidean time τ

- **QCD THERMODYNAMICS**

Partition function

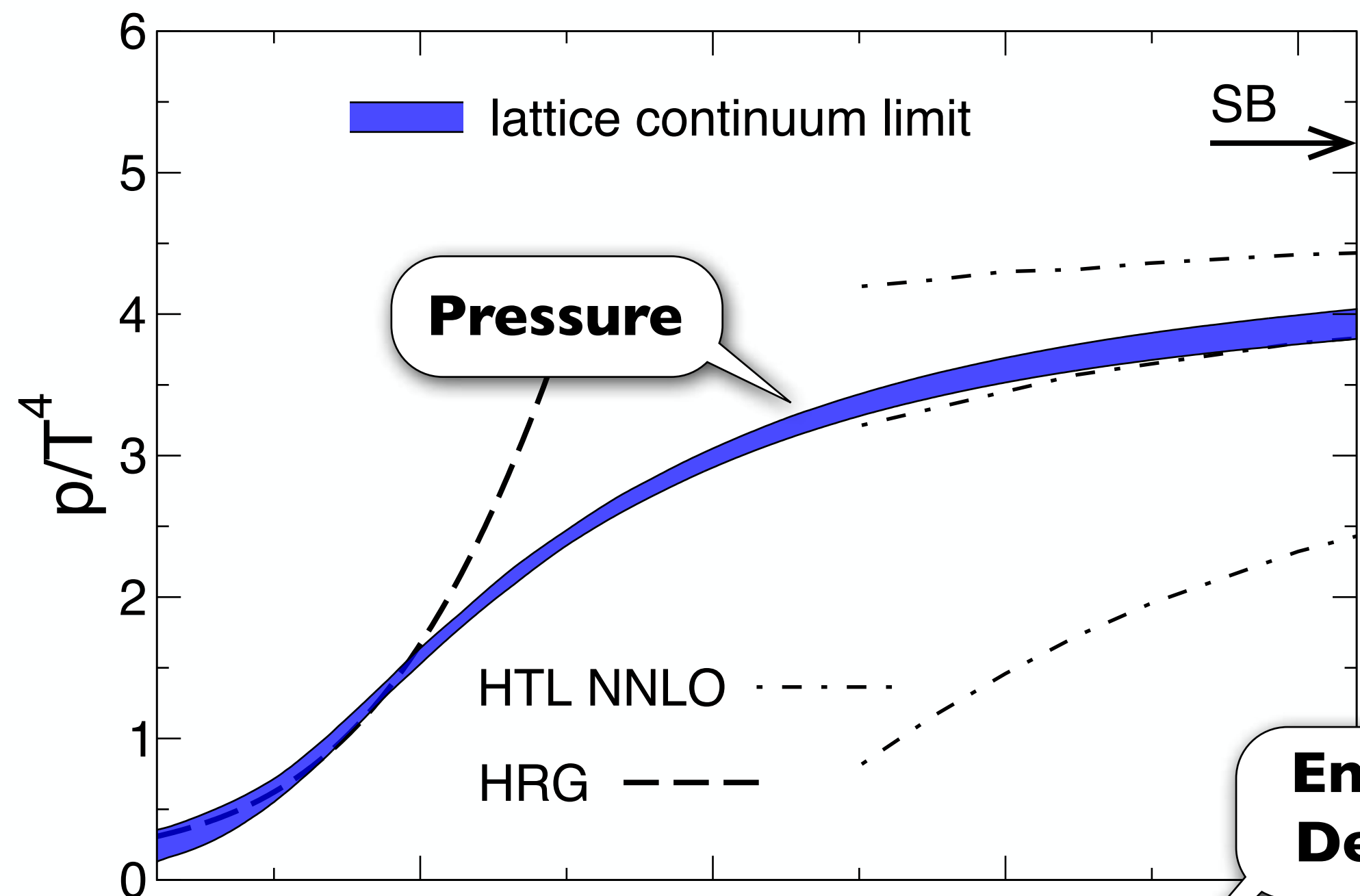
$$\mathcal{Z} = \int [d\mathcal{U} d\psi d\bar{\psi}] e^{-S_{\text{G}}(\mathcal{U}) - S_{\text{q}}(\psi, \bar{\psi}, \mathcal{U})}$$



► **Non-perturbative “condensed matter physics” of QCD**



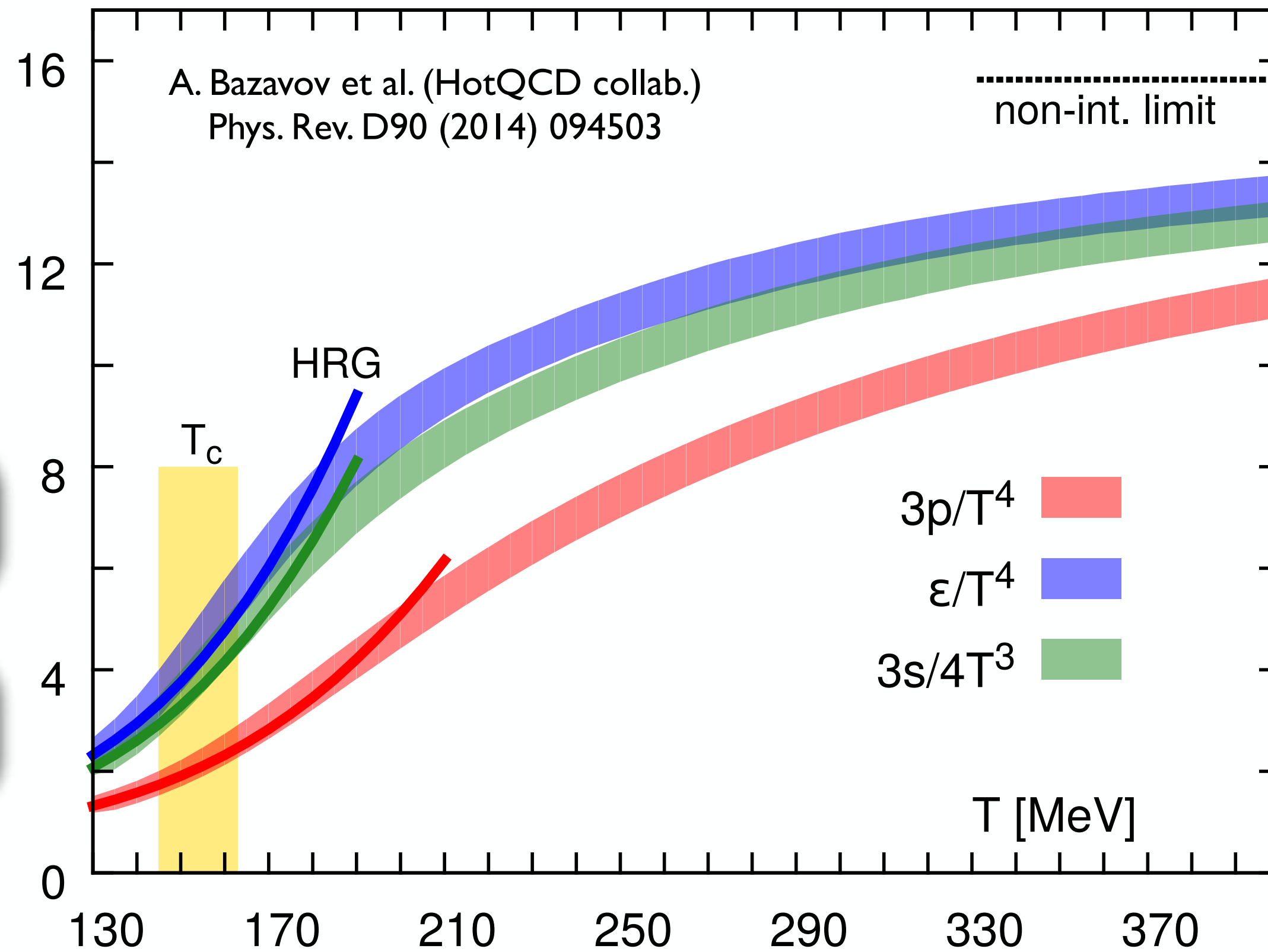
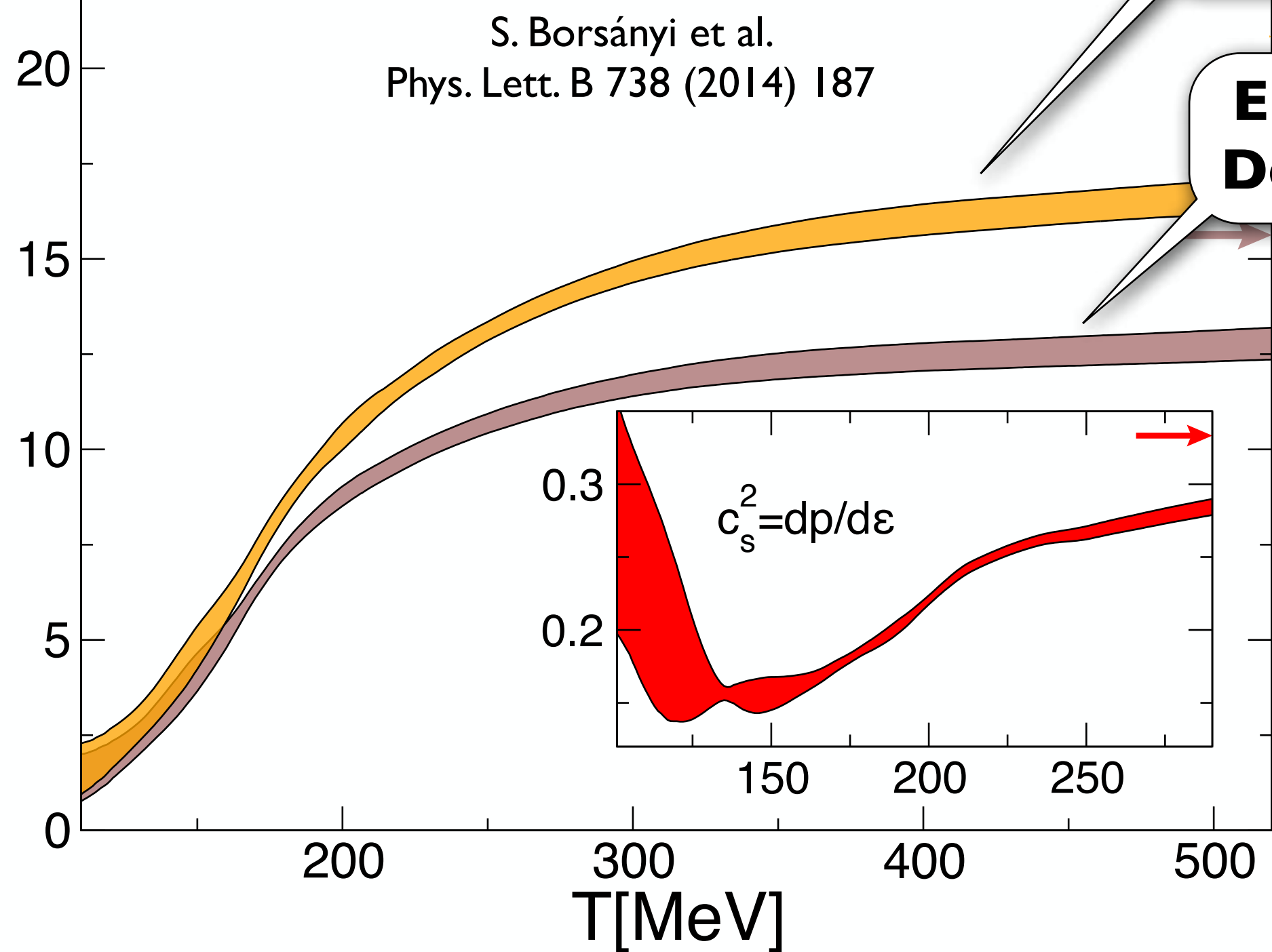
QCD THERMODYNAMICS on the LATTICE



Baryon chemical potential
 $\mu_B = 0$

Entropy Density s/T^3

Energy Density ϵ/T^4



- **Continuous crossover** (not a phase transition)
- **Transition temperature** $T_c = 156.5 \pm 1.5$ MeV

A. Bazavov et al. (HotQCD collab.) Phys. Lett. B795 (2019) 15

QCD THERMODYNAMICS on the LATTICE

- **Extrapolations to non-zero baryon chemical potential μ_B**

S. Borsányi et al. : Phys. Rev. Lett. 126 (2021) 232001

- **Pressure**

$$P(T, \mu_B) = T^4 \sum_{n=0} \frac{\chi_{2n}(T, 0)}{(2n)!} \left(\frac{\mu_B}{T}\right)^{2n}$$

$$\chi_j(T, \mu_B) = \left(\frac{\partial}{\partial \mu_B/T}\right)^j \frac{P(T, \mu_B)}{T^4}$$

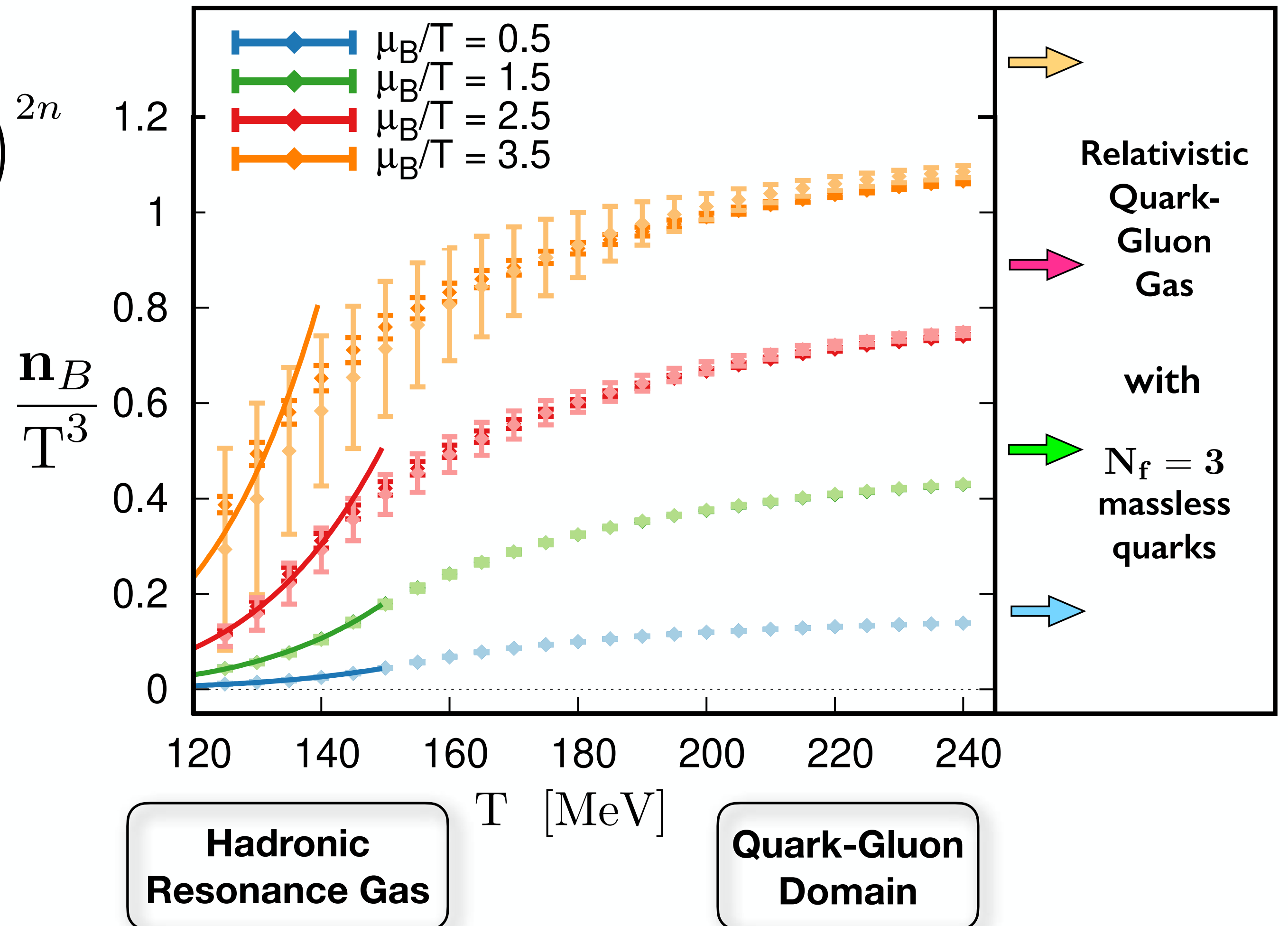
- **Baryon density**

$$\mathbf{n}_B = \frac{\partial P(T, \mu_B)}{\partial \mu_B}$$

Example:

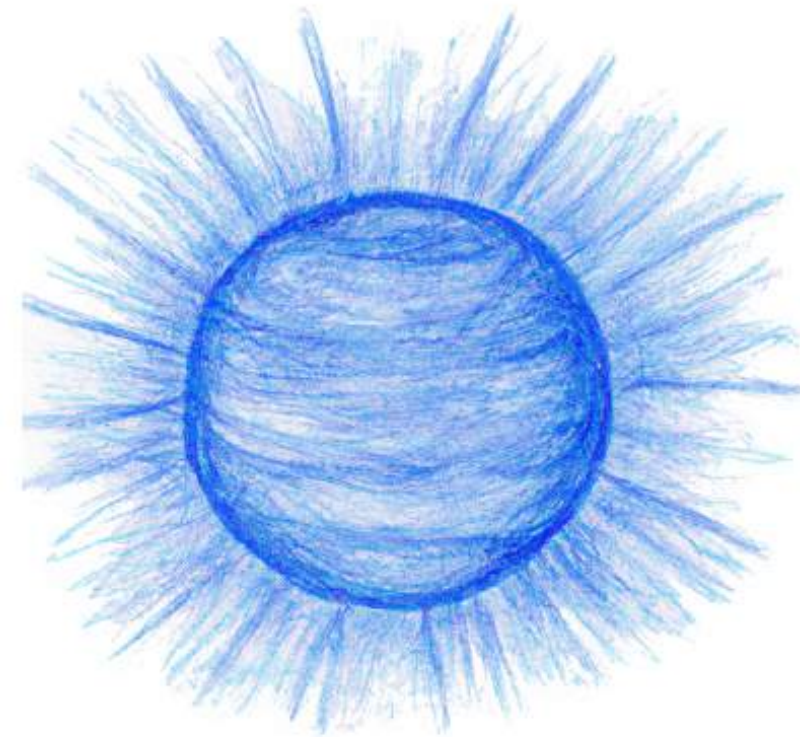
$$\mathbf{n}_B(T, \mu_B) \lesssim 0.2 \text{ fm}^{-3}$$

for $T \lesssim 150 \text{ MeV}$ and $\mu_B/T = 2.5$



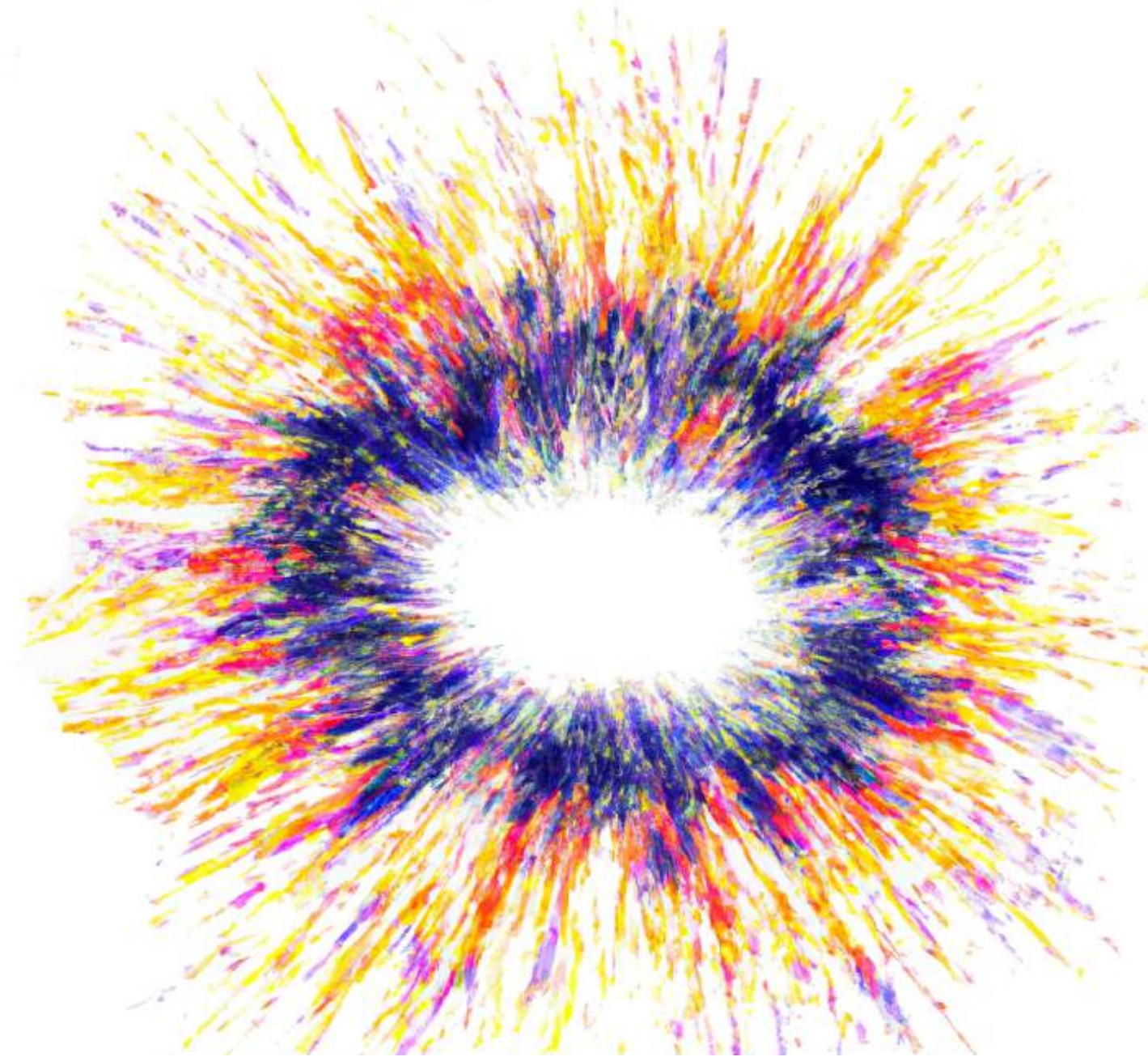
Strategies PART III: **Astrophysical Observations**

blue supergiant

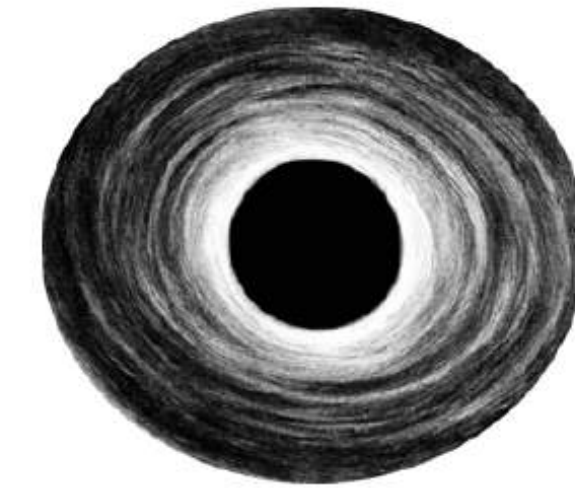


© Len Brandes

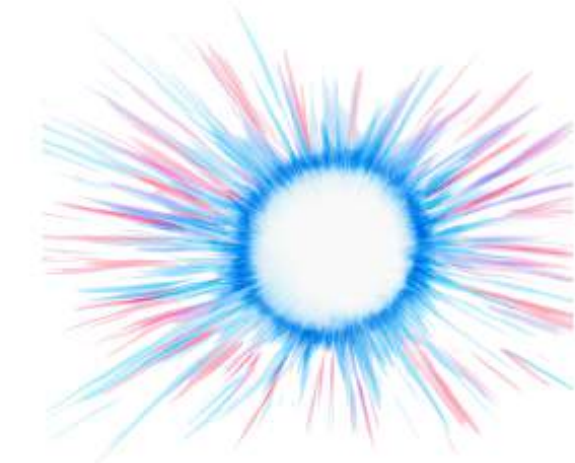
supernova



black hole



neutron star



nature

NEWS FEATURE | 04 March 2020

The golden age of neutron-star physics has arrived

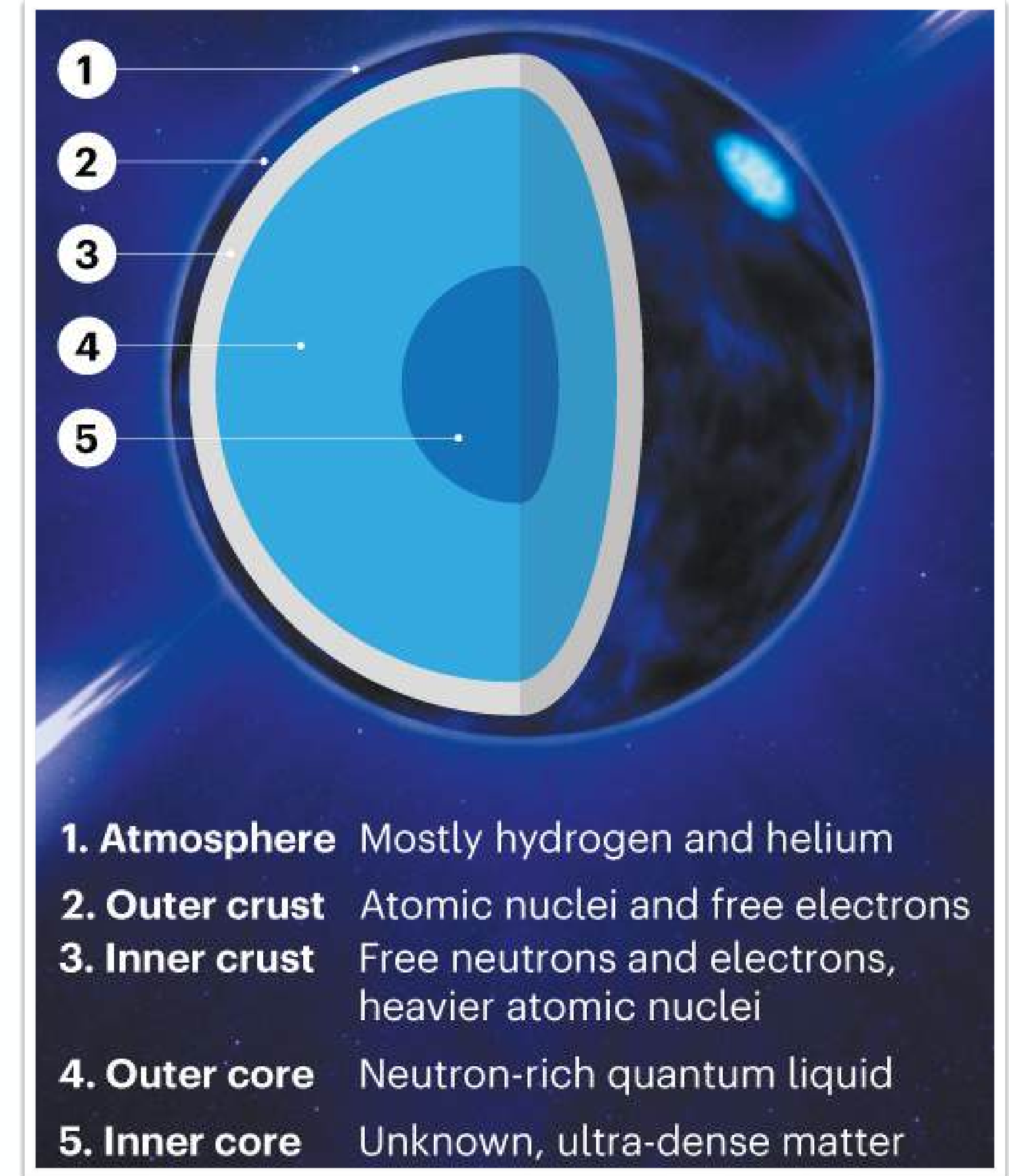
These stellar remnants are some of the Universe's most enigmatic objects – and they are finally starting to give up their secrets.



Neutron Star Matter

★ Constraints on the **Equation-of-State** of **COLD** and **DENSE BARYONIC MATTER**

- **Neutron star mass** measurements
(Shapiro delay, Radioastronomy)
- **Neutron star radius** measurements
(Neutron star Interior Composition ExploreR :
NICER telescope @ ISS)
- **Gravitational wave** signals of
neutron star mergers
(LIGO and Virgo collaborations)

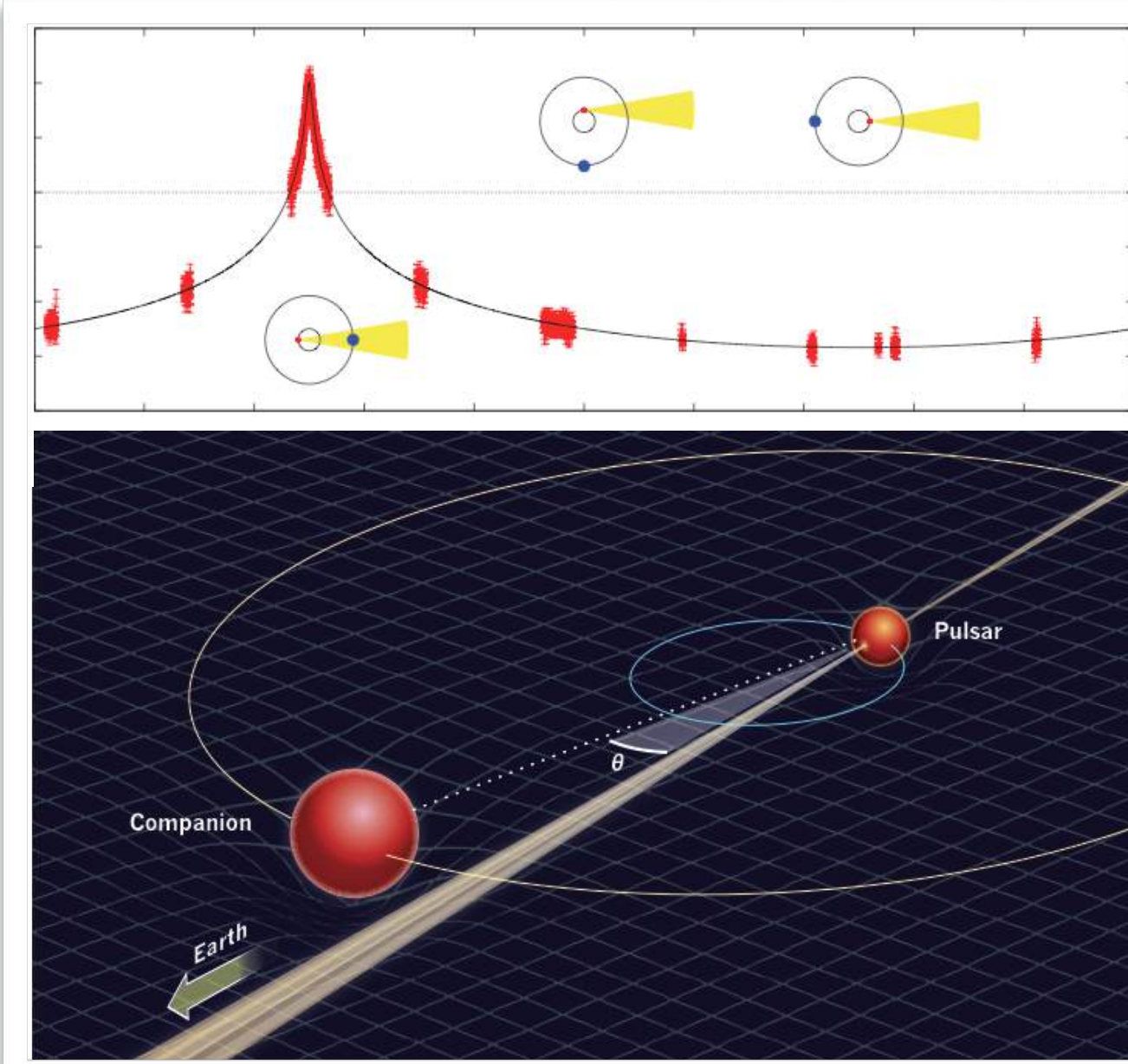


Layers of a Neutron Star

MASSIVE NEUTRON STARS

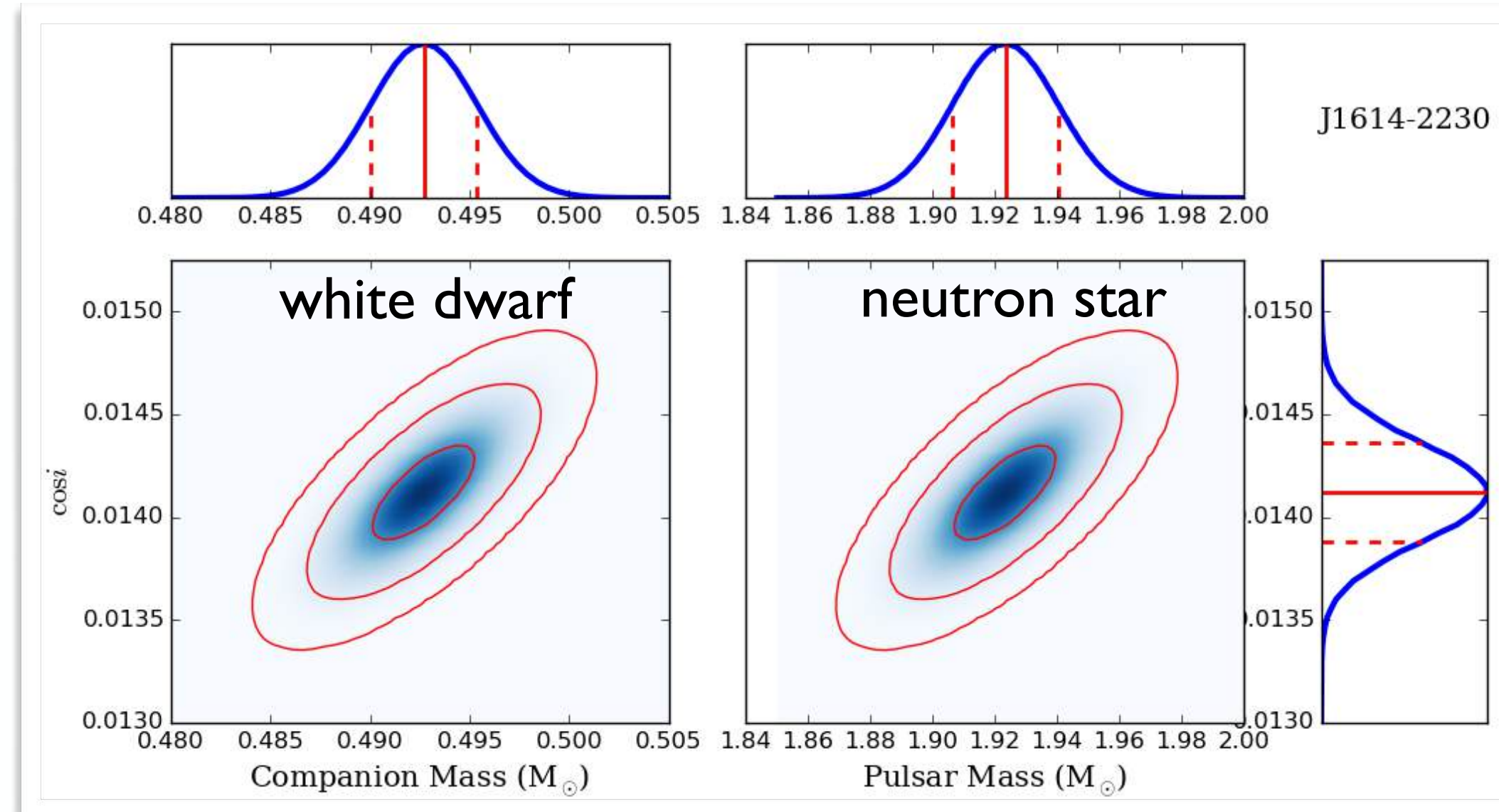
- Neutron Star - White Dwarf binaries

Shapiro delay measurements



P.B. Demorest et al.
Nature 467 (2010) 1081

PSR J1614+2230

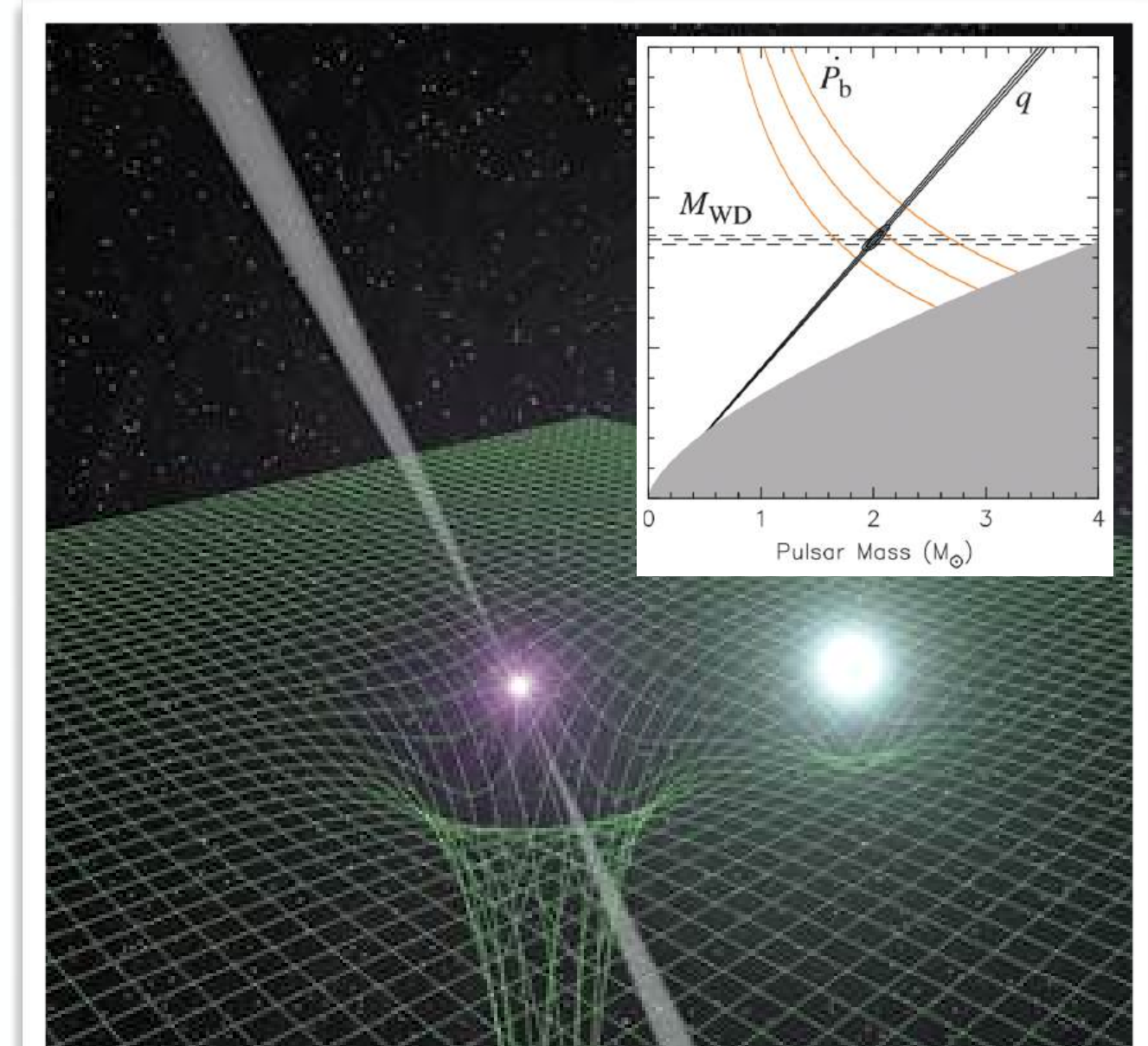


E. Fonseca et al., Astrophys. J. 832 (2016) 167

PSR J1614+2230

$$M = 1.928 \pm 0.017 M_{\odot}$$

PSR J0348+0432



J. Antoniadis et al.
Science 340 (2013) 6131

PSR J0348+0432

$$M = 2.01 \pm 0.04 M_{\odot}$$

- Strong constraints for the stiffness of the Equation-of State of cold & dense baryonic matter



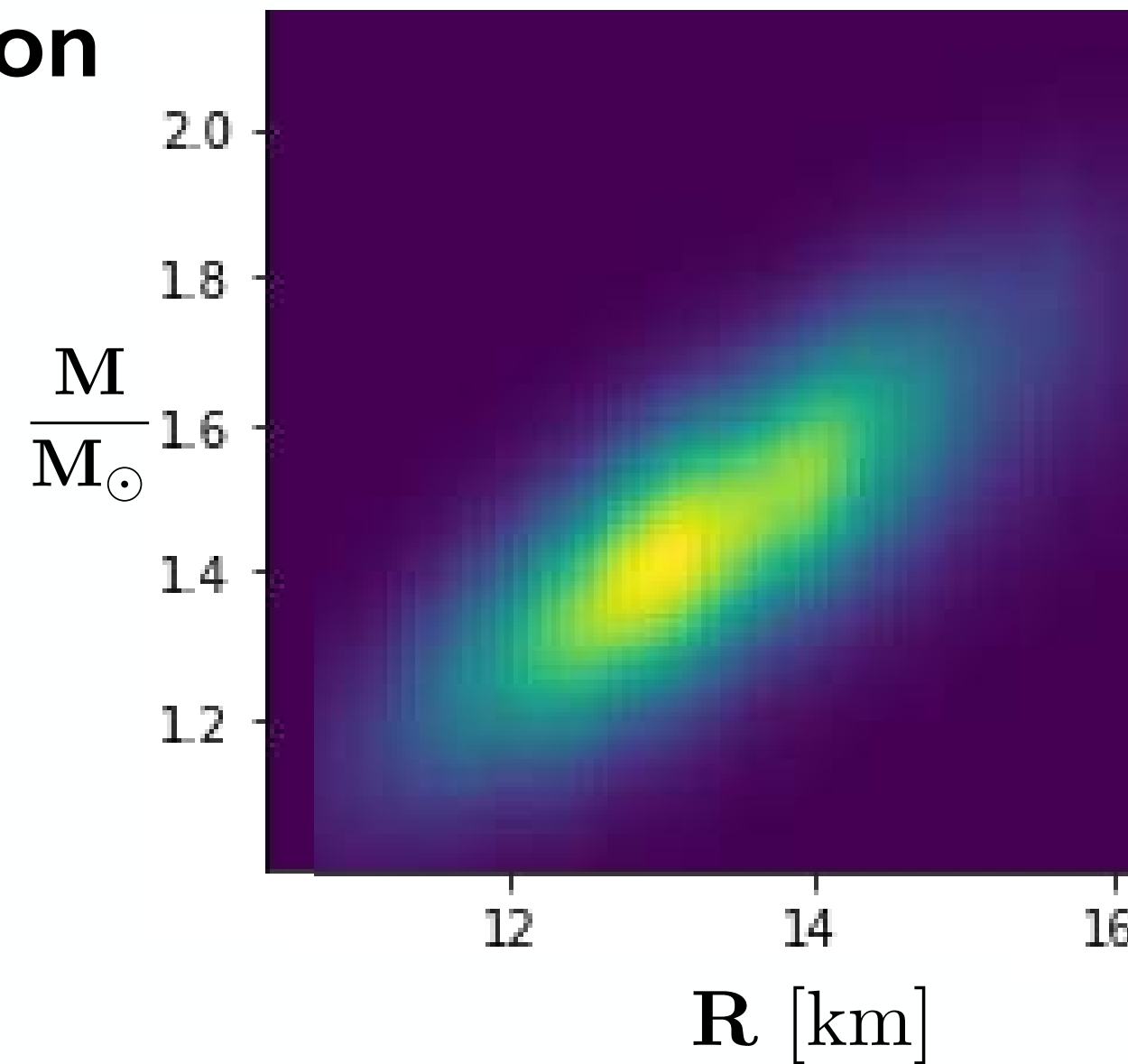
MASSES & RADII of NEUTRON STARS

- **NICER @ International Space Station**

Neutron Star Interior Composition Explorer



- X rays from hot spots at the surface of rotating neutron stars

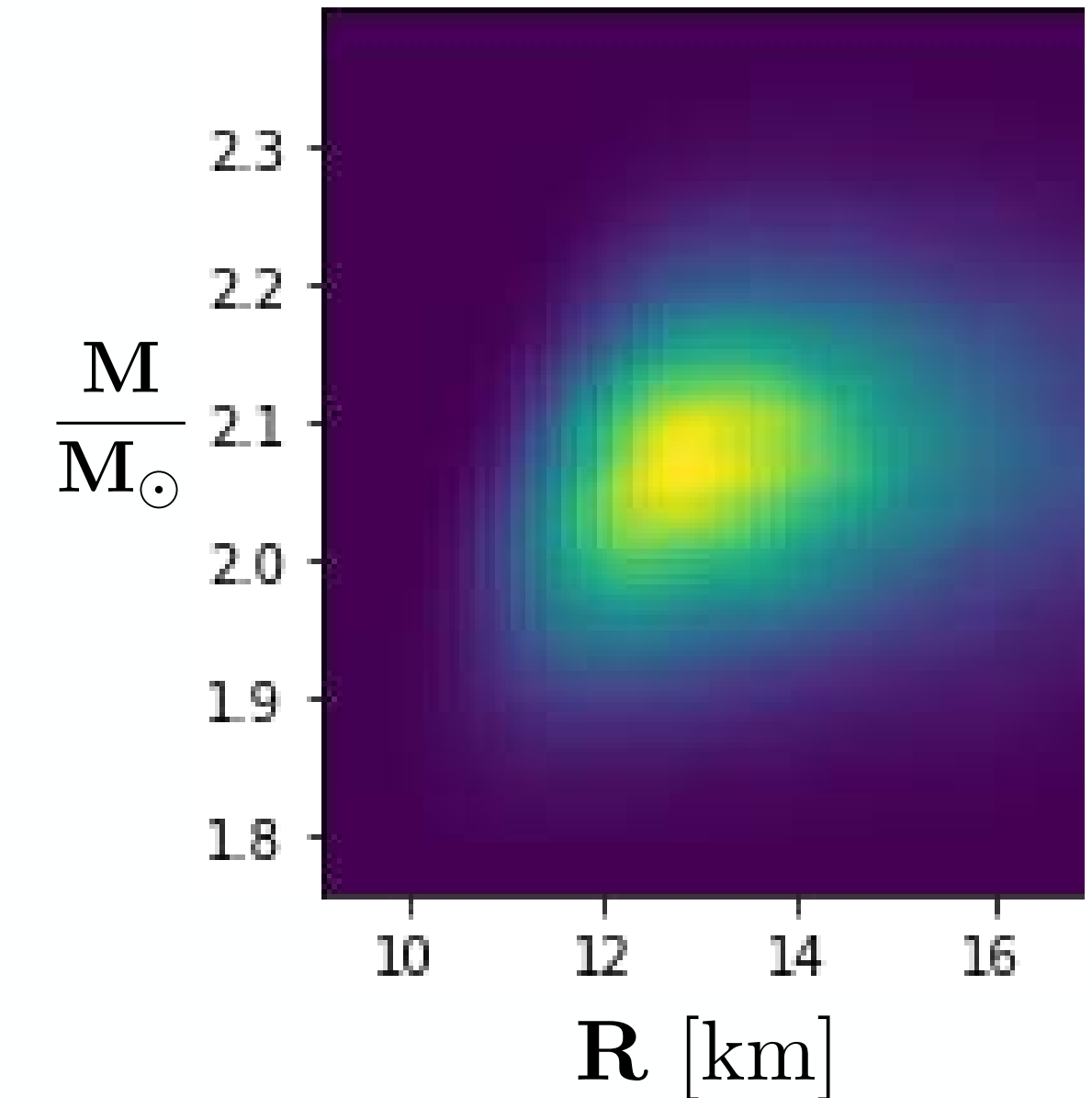


- *PSR J0030 + 0451*

$$M = 1.44 \pm 0.15 M_{\odot}$$

$$R = 13.02^{+1.24}_{-1.06} \text{ km}$$

M.C. Miller et al. (NICER)
Astroph. J. Lett. 887 (2019) L24



- *PSR J0740 + 6620*

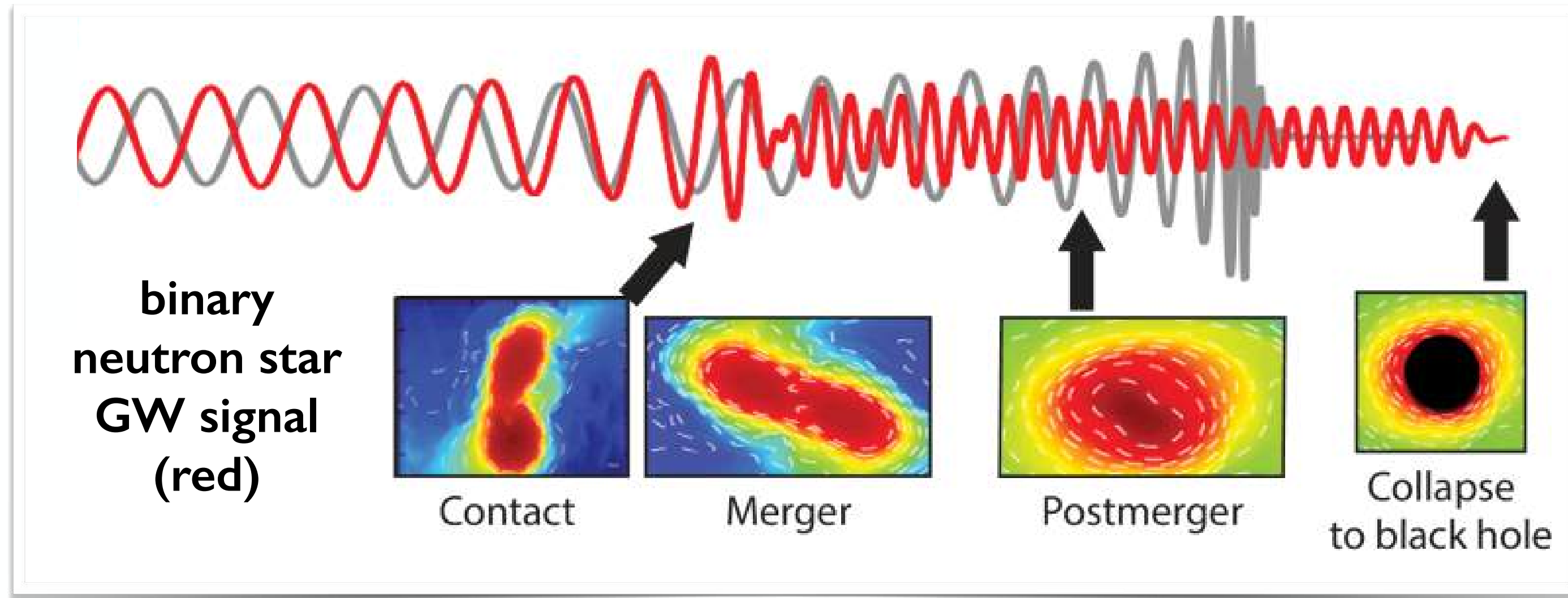
$$M = 2.08 \pm 0.07 M_{\odot}$$

$$R = 13.7^{+2.6}_{-1.5} \text{ km}$$

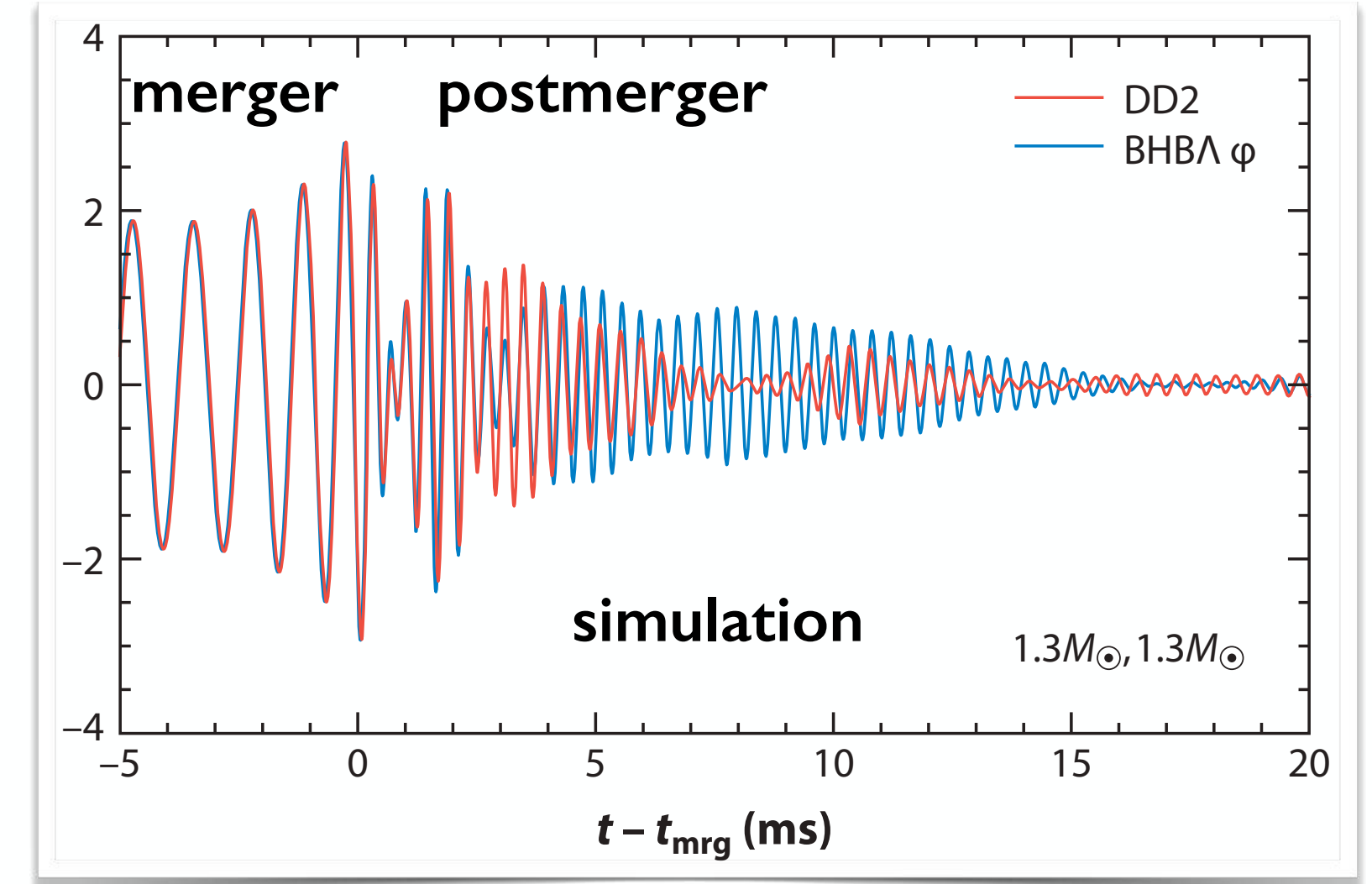
M.C. Miller et al.
(NICER + XMM Newton)
Astroph. J. Lett. 918 (2021) L28

GRAVITATIONAL WAVES from BINARY NEUTRON STAR MERGERS

LIGO and Virgo Collaborations 2017 - 2020



J.S. Lattimer : Ann. Rev. Nucl. Part. Sci. 71 (2021) 433



D. Radice, S. Bernuzzi, A. Perego : Ann. Rev. Nucl. Part. Sci. 70 (2020) 95

- Additional constraints on Equation-of-State:

Binary tidal deformability

$$\tilde{\Lambda} = \frac{16 (M_1 + 12 M_2) M_1^4 \Lambda_1}{13 (M_1 + M_2)^5} + (1 \leftrightarrow 2) \quad \Lambda_i \sim \left(\frac{R_i}{M_i} \right)^n$$

- **GW 170817** : $M = M_1 + M_2 = 2.74_{-0.01}^{+0.04} M_{\odot}$

B.P. Abbot et al. : Phys. Rev. Lett. 119 (2017) 161101 Phys. Rev. X9 (2019) 011001

- **GW 190425** : $M = M_1 + M_2 = 3.3 \pm 0.1 M_{\odot}$

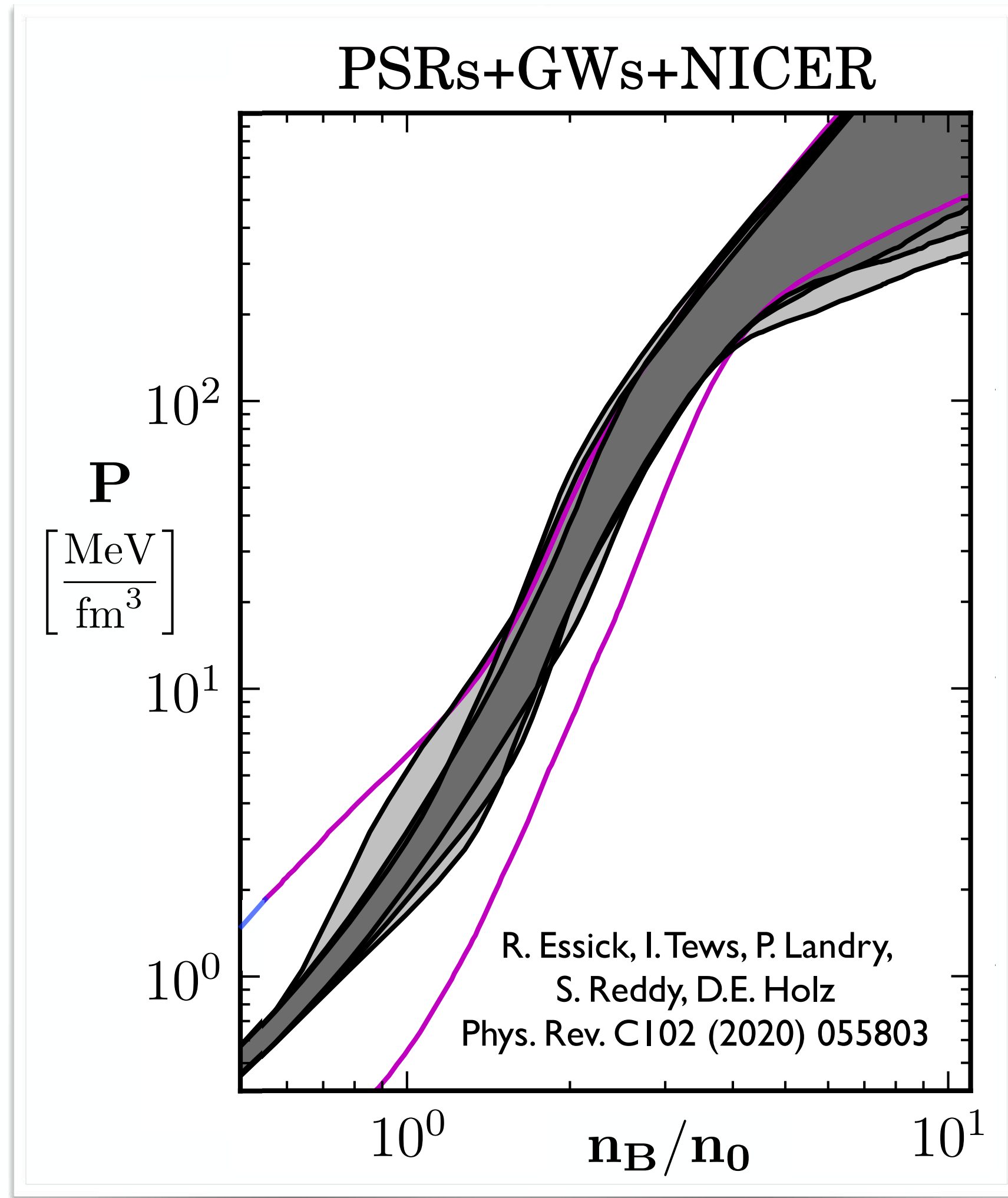
B.P. Abbot et al. : Astroph. J. Lett. 892 (2020) L3

$$\Lambda_{1.4} = 190_{-120}^{+390}$$

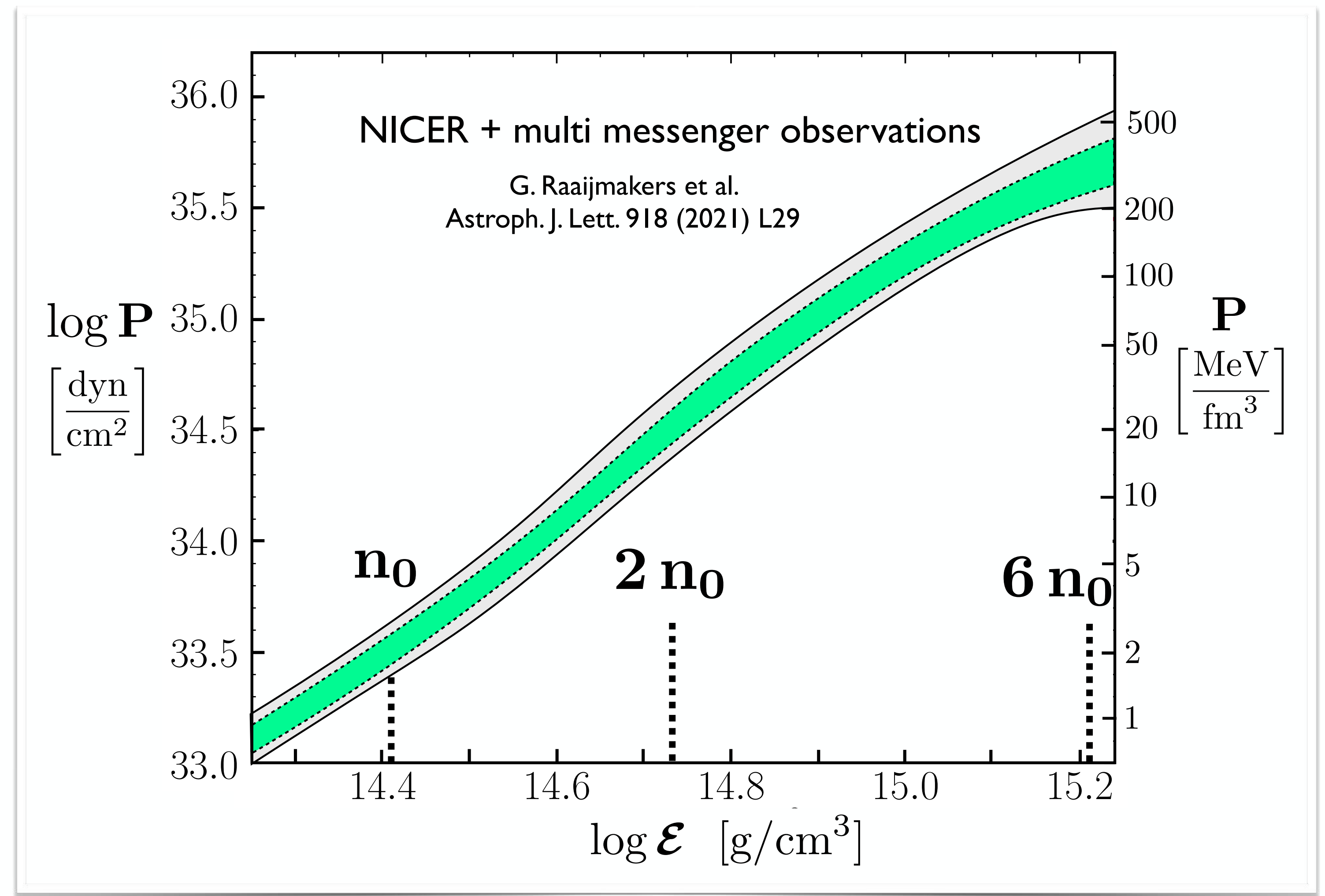
B.P. Abbot et al. : Phys. Rev. Lett. 121 (2018) 161101

NEUTRON STAR MATTER EQUATION-of-STATE

- Examples of **EoS analyses** based on multimessenger data



$(n_0 = 0.16 \text{ fm}^{-3})$



3.

Equation-of-State of Dense Baryonic Matter :

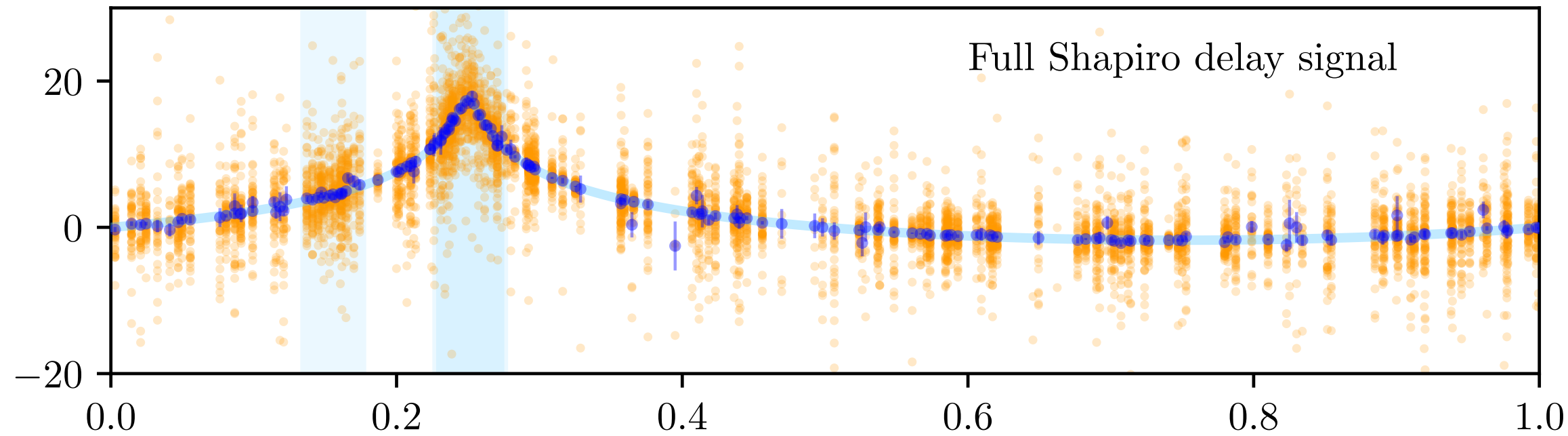
Empirical Constraints from Neutron Stars

Bayesian Inference Results



NEUTRON STARS : DATA

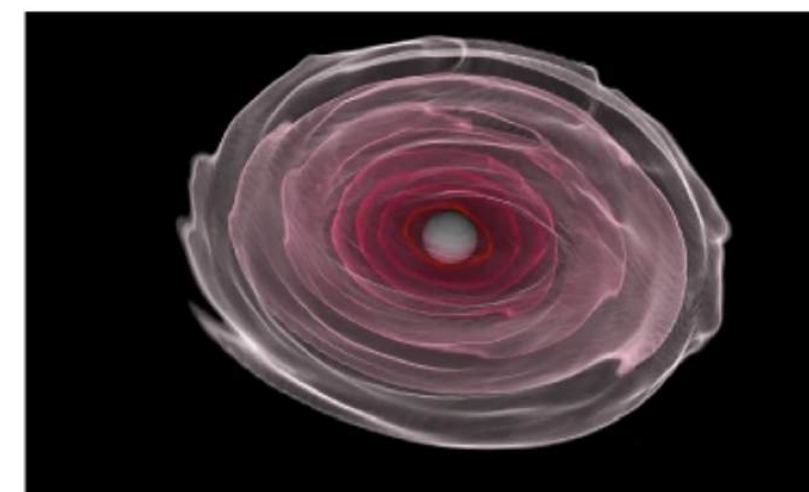
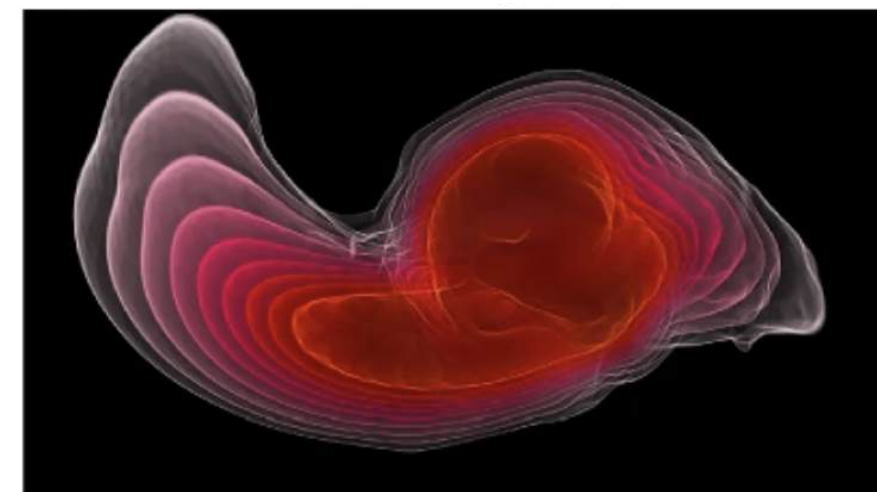
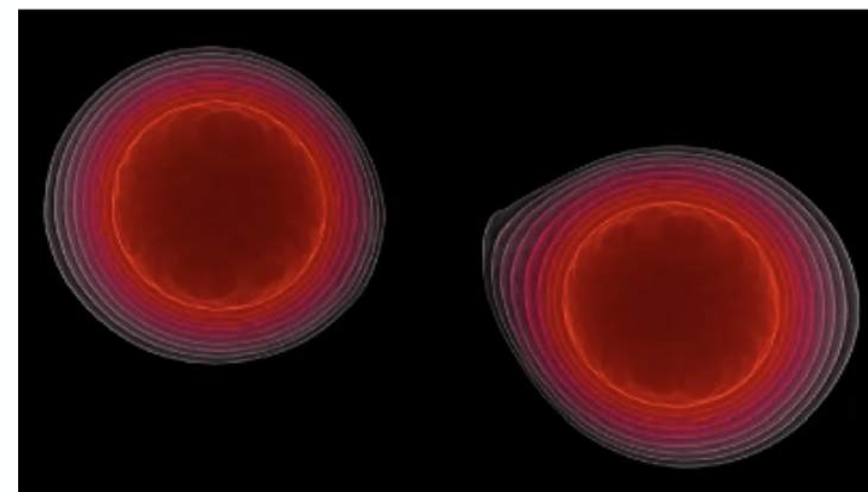
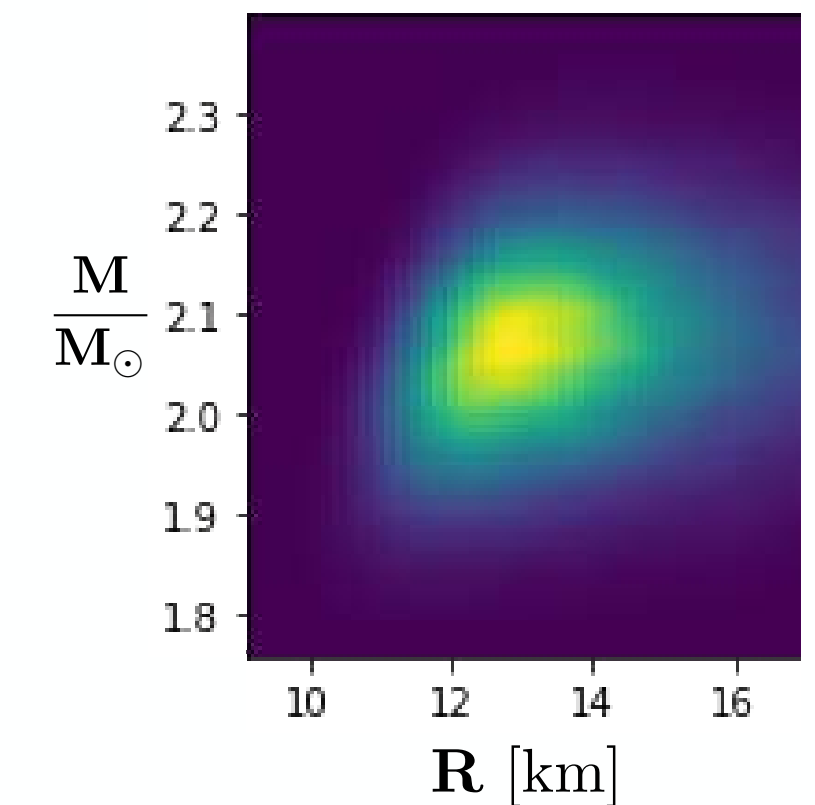
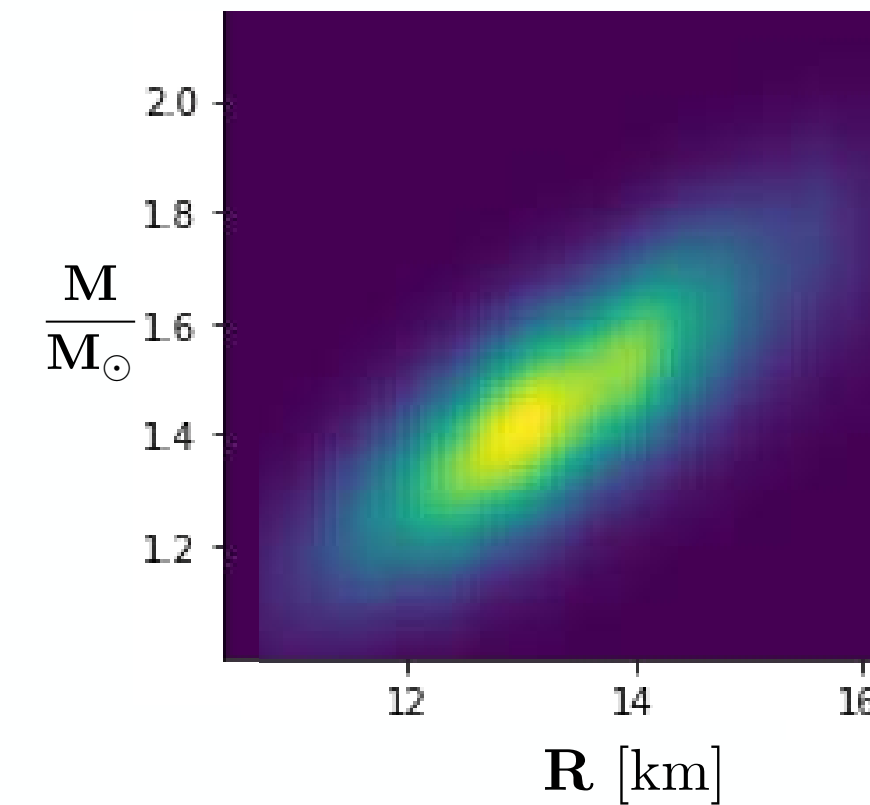
- Database for **inference of Equation-of-State** and other properties of neutron stars



- **Neutron star masses** from Radio Telescopes (Green Bank, Effelsberg)



- **Masses and radii**
X rays from hot spots on the surface of rotating neutron stars (NICER Telescope @ ISS)



- **Tidal deformabilities**
Gravitational wave signals of neutron star mergers (LIGO and Virgo Collaborations)



NEUTRON STARS : DATA

- **Masses of $2 M_{\odot}$ n-stars**
(Shapiro delay & radio observations)

PSR J0348+0432

$$M = 2.01 \pm 0.04 M_{\odot}$$

J. Antoniadis et al.: Science 340 (2013) 1233232

PSR J1614-2230

$$M = 1.908 \pm 0.016 M_{\odot}$$

Z. Arzoumanian et al., Astrophys.J. Suppl. 235 (2018) 37

PSR J0740+6620

$$M = 2.08 \pm 0.07 M_{\odot}$$

E. Fonseca et al., Astrophys.J. Lett. 915 (2021) L12

- **Masses and Radii (NICER)**

PSR J0030+0451

$$M = 1.34 \pm 0.16 M_{\odot} \quad R = 12.71^{+1.14}_{-1.19} \text{ km}$$

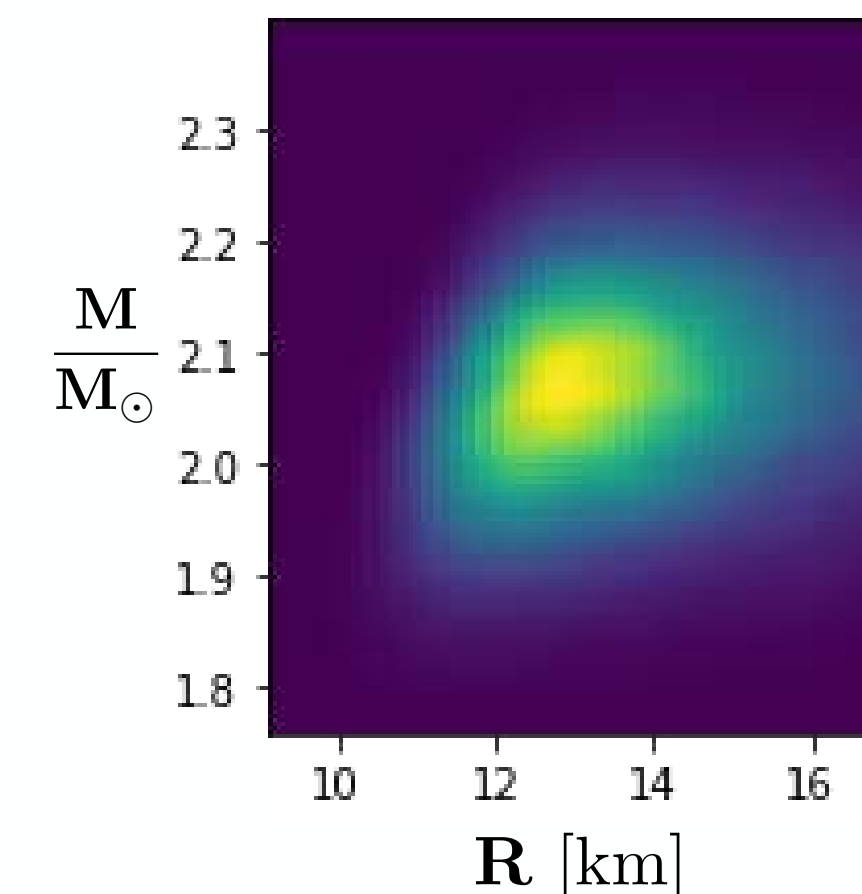
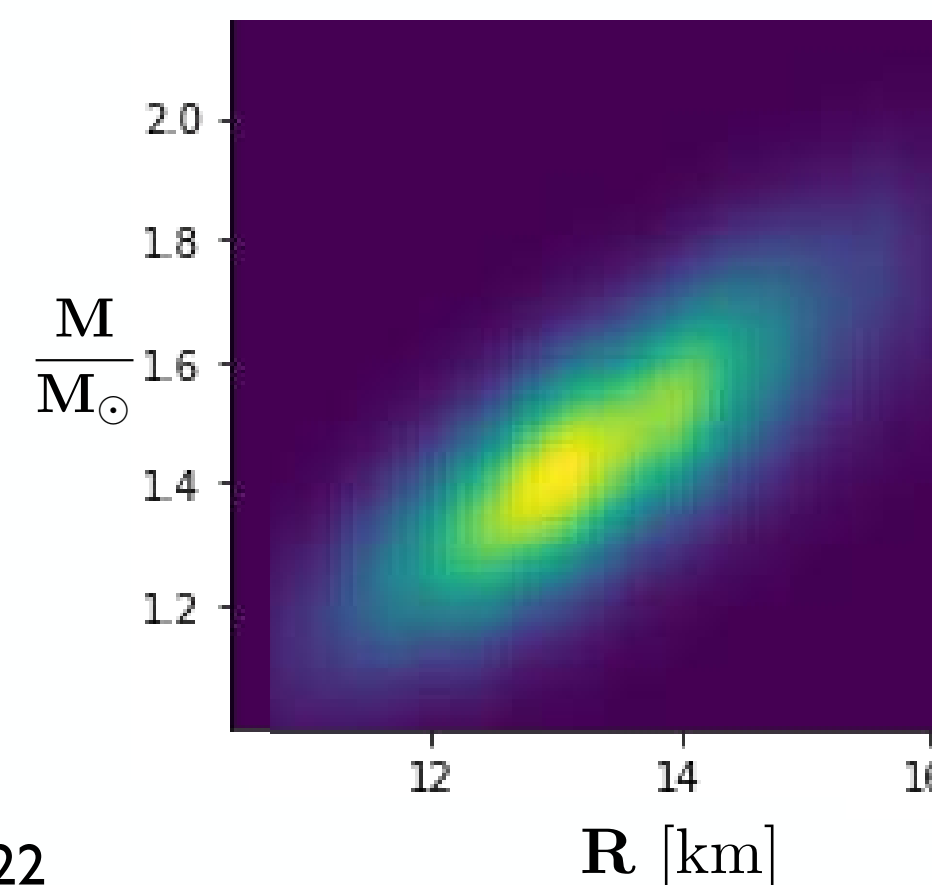
T.E. Riley et al. (NICER), Astroph.J. Lett. 887 (2019) L21

PSR J0740+6620

$$M = 2.073 \pm 0.069 M_{\odot} \quad R = 12.49^{+1.28}_{-0.88} \text{ km}$$

T.E. Riley et al. (NICER + XMM Newton), Astroph.J. Lett. 918 (2021) L27

T. Salmi et al. (NICER), arXiv:2406.14466



NEUTRON STARS : DATA (contd.)

- **Very massive and fast rotating galactic neutron star**

PSR J0952-0607

$$M = 2.35 \pm 0.17 M_{\odot}$$

R.W. Romani et al. : *Astroph. J. Lett.* 934 (2022) L17



(Keck Observatory)

→ equivalent non-rotating mass
after rotational correction : $M = 2.3 \pm 0.2 M_{\odot}$

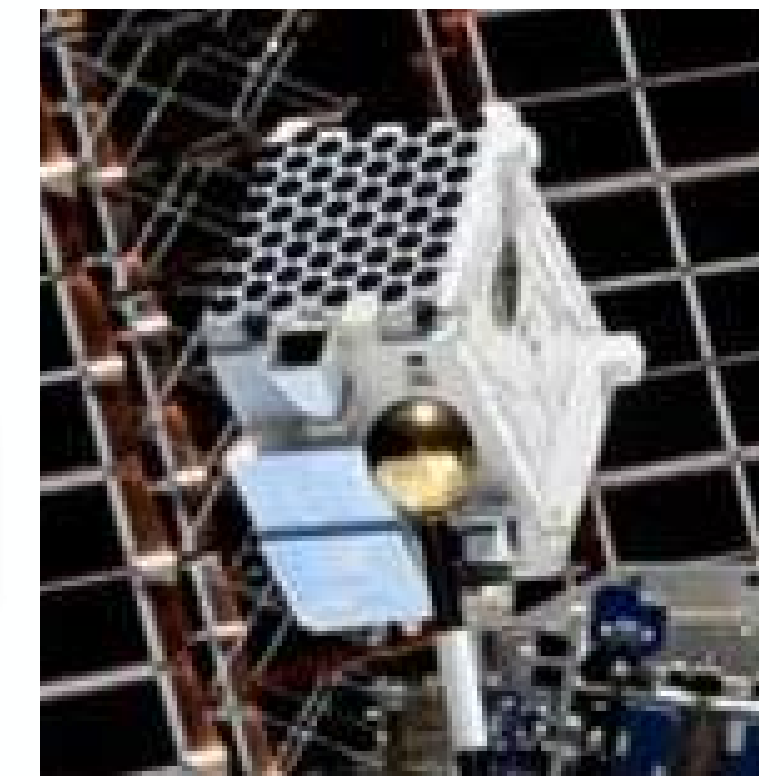
- **New accurate data from NICER**

PSR J0437-4715

$$M = 1.418 \pm 0.037 M_{\odot}$$

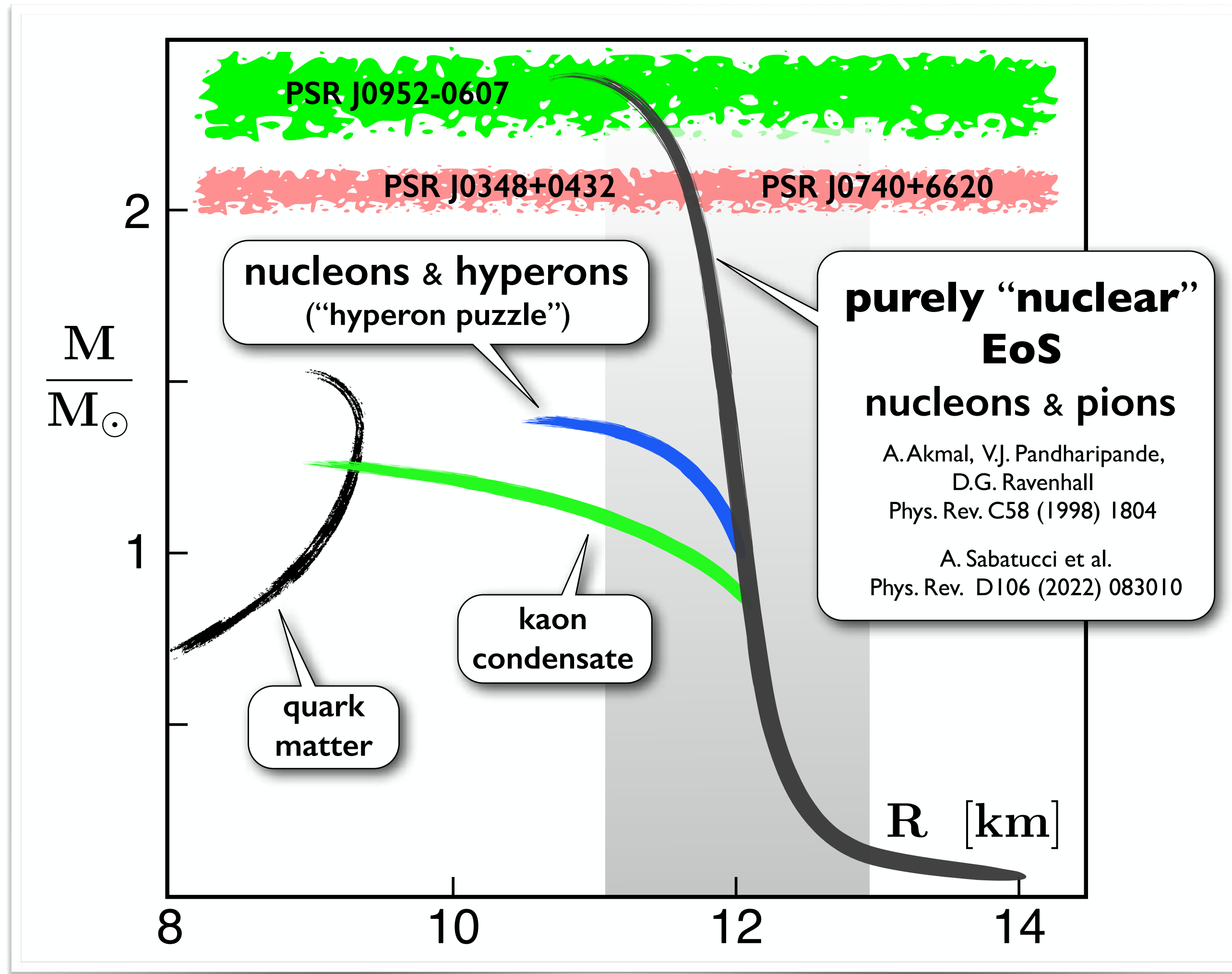
$$R = 11.36^{+0.95}_{-0.63} \text{ km}$$

D. Choudhury et al. : *Astroph. J. Lett.* 971 (2024) L20



CONSTRAINTS on EQUATION of STATE $P(\epsilon)$

- from observations of massive neutron stars



Tolman - Oppenheimer - Volkov Equations

$$\frac{dP(r)}{dr} = \frac{G [\epsilon(r) + P(r)] [m(r) + 4\pi r^3 P(r)]}{r [r - 2Gm(r)]}$$

$$\frac{dm(r)}{dr} = 4\pi r^2 \epsilon(r)$$

$$M = m(R) = 4\pi \int_0^R dr r^2 \epsilon(r)$$

- Stiff equation-of-state $P(\epsilon)$ required
- Simplest forms of exotic matter (kaon condensate, quark matter, ...) **ruled out**

SOUND VELOCITY and EQUATION of STATE

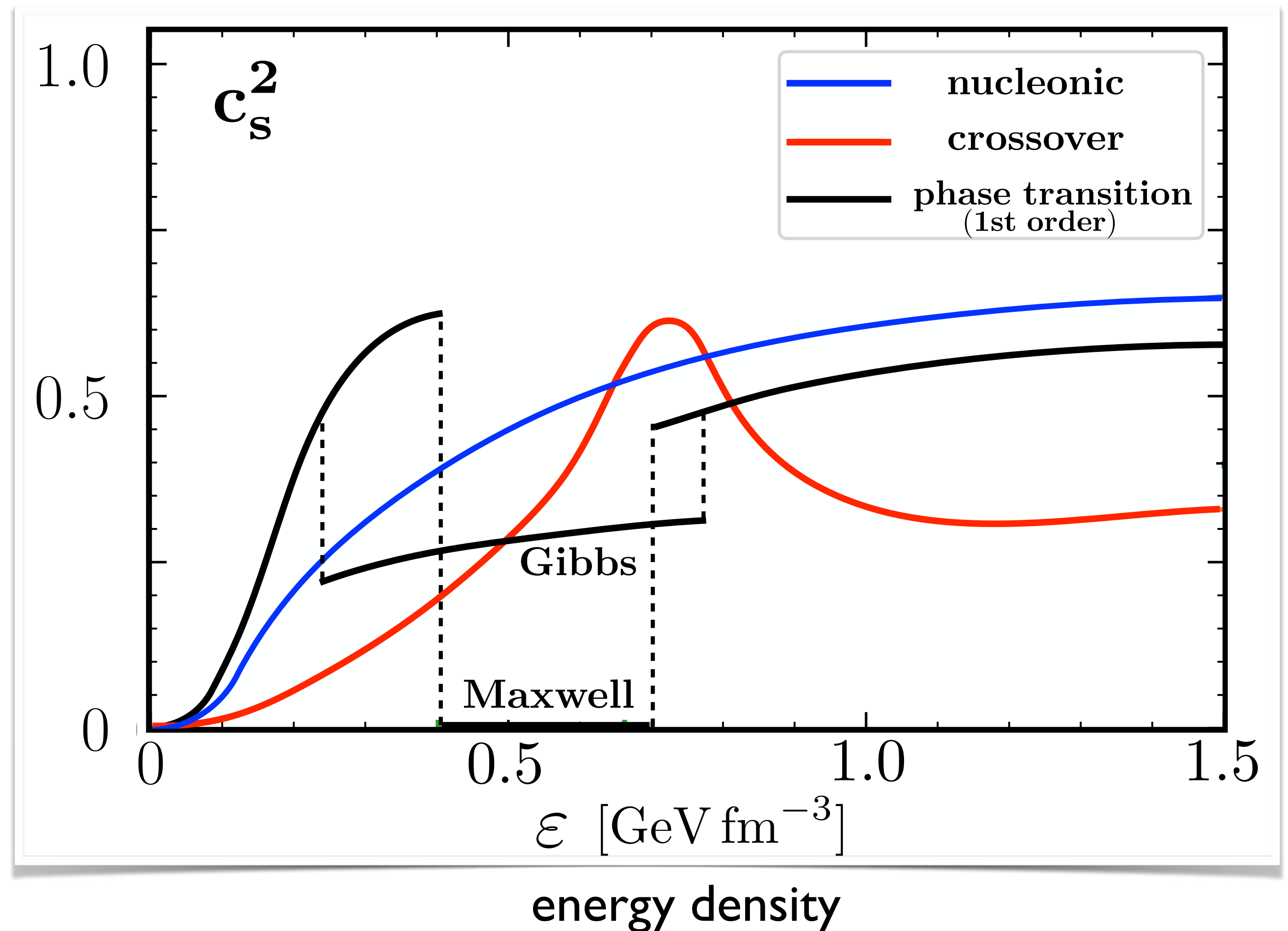
- Key quantity : **Speed of Sound**

$$c_s^2(\epsilon) = \frac{\partial P(\epsilon)}{\partial \epsilon}$$

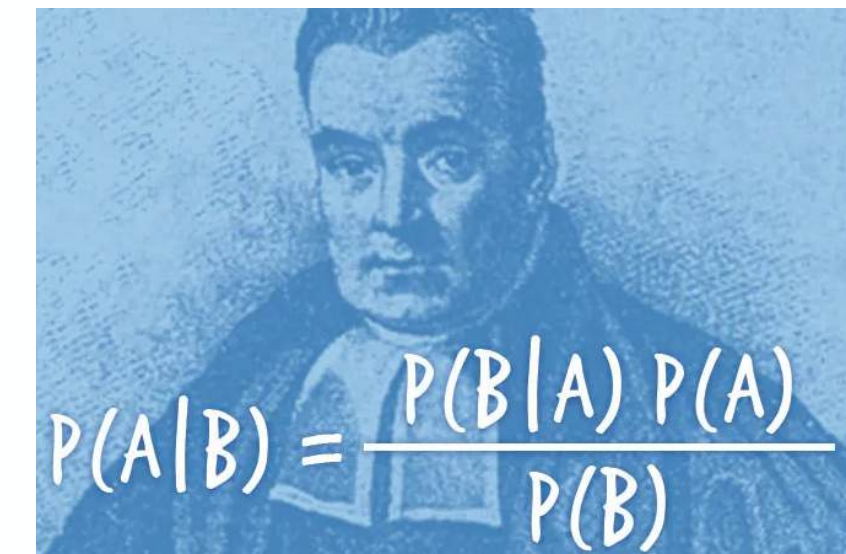
displays
characteristic signature
of
phase transition
or
crossover

- Equation of State :**

$$P(\epsilon) = \int_0^\epsilon d\epsilon' c_s^2(\epsilon')$$



INFERENCE of SOUND SPEED and RELATED PROPERTIES of NEUTRON STARS



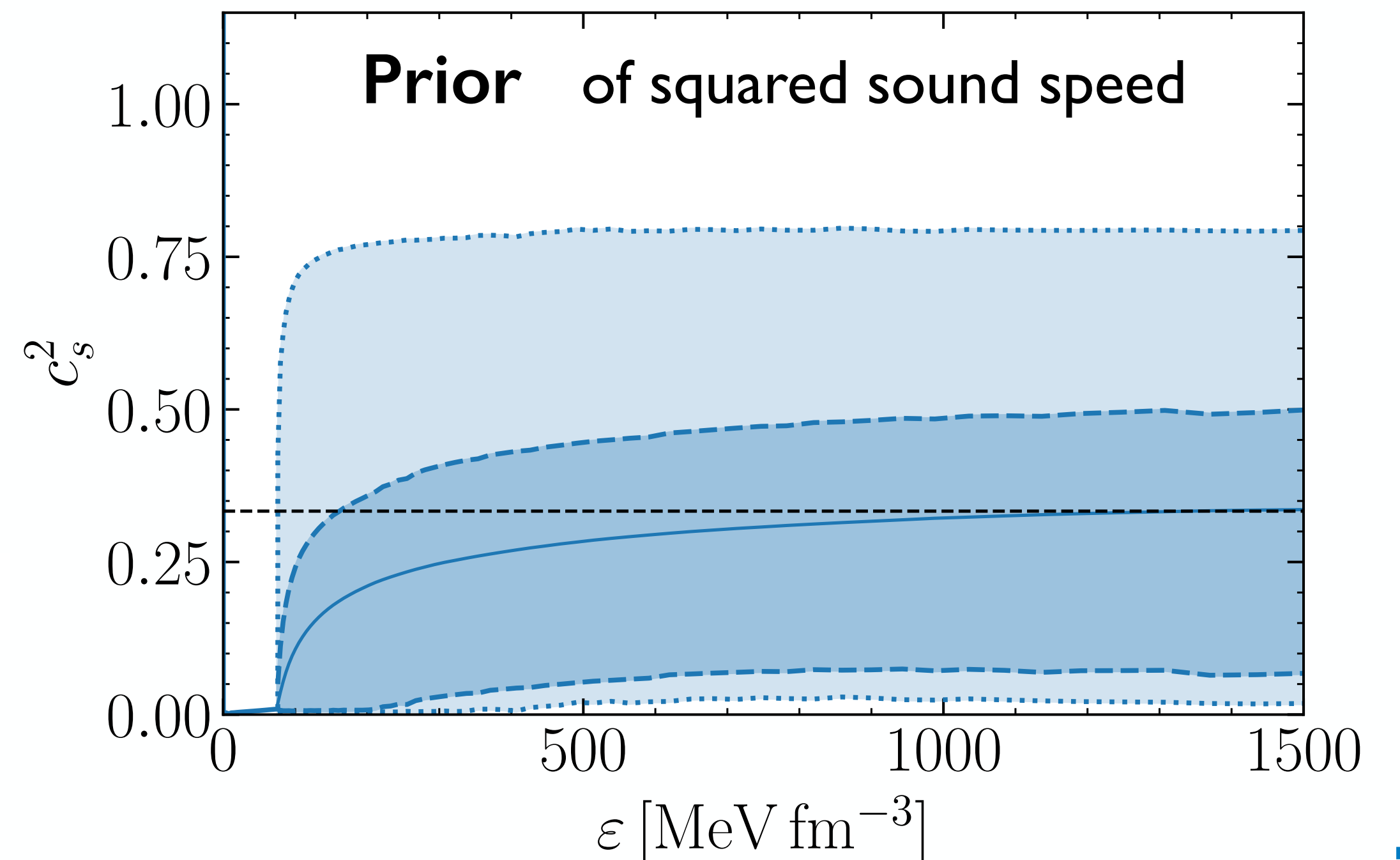
- Introduce general parametrization of sound velocity by segment-wise representation :

$$c_s^2(\varepsilon, \theta) = \frac{(\varepsilon_{i+1} - \varepsilon) c_{s,i}^2 + (\varepsilon - \varepsilon_i) c_{s,i+1}^2}{\varepsilon_{i+1} - \varepsilon_i}, \quad \text{parameter set } \theta = (c_{s,i}^2, \varepsilon_i) \quad (i = 1, \dots, N)$$

- Constrain parameters θ by Bayesian inference using nuclear and astrophysical data \mathcal{D} :

$$\Pr(\theta|\mathcal{D}) \propto \Pr(\mathcal{D}|\theta) \Pr(\theta)$$

- Choose Prior $\Pr(\theta)$
- Compute Posterior $\Pr(\theta|\mathcal{D})$ from Likelihood $\Pr(\mathcal{D}|\theta)$
- Quantify Evidences for hypotheses H_1 vs. H_0 in terms of Bayes factors $\mathcal{B}_{H_0}^{H_1} = \frac{\Pr(\mathcal{D}|H_1)}{\Pr(\mathcal{D}|H_0)}$



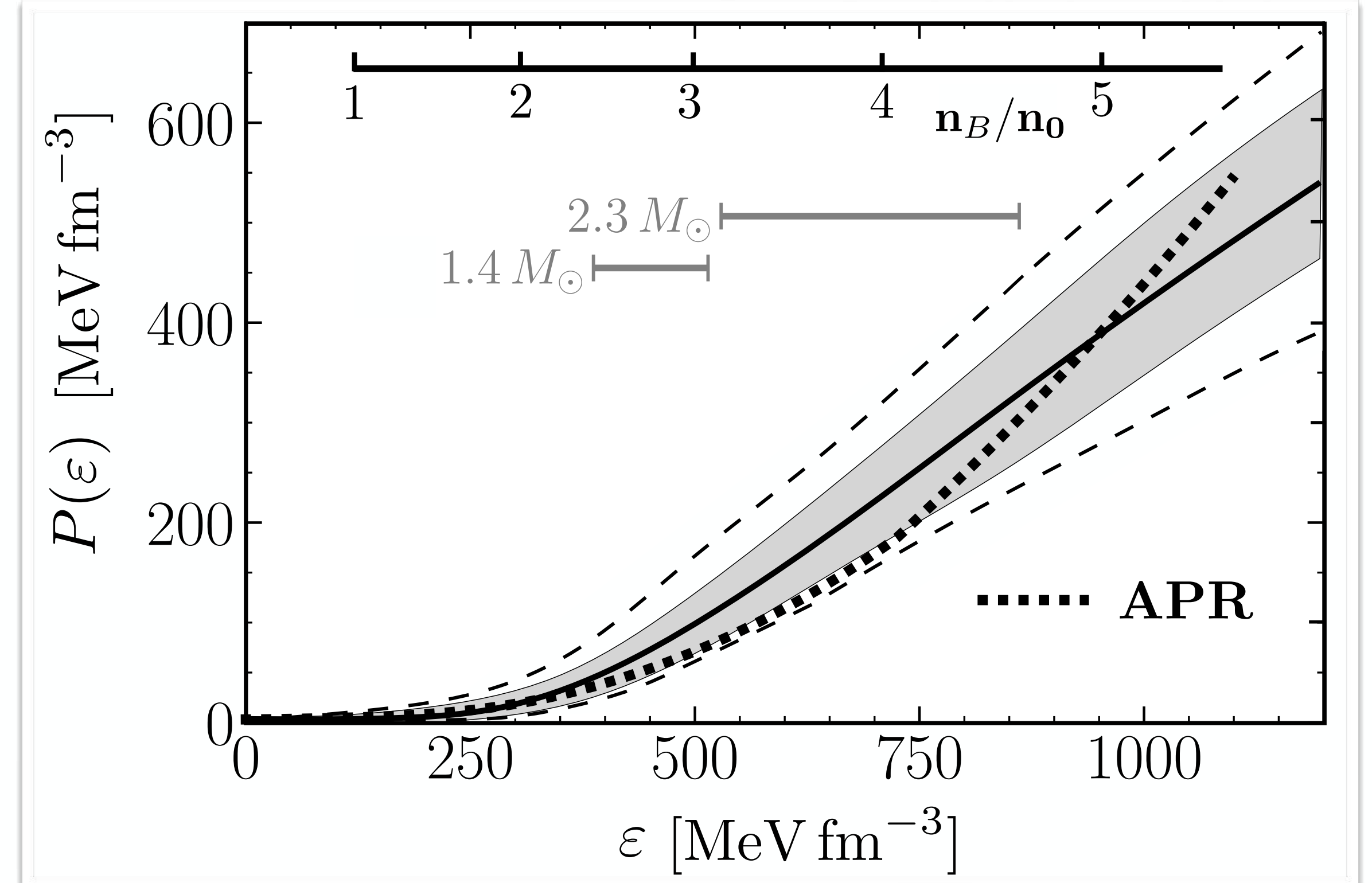
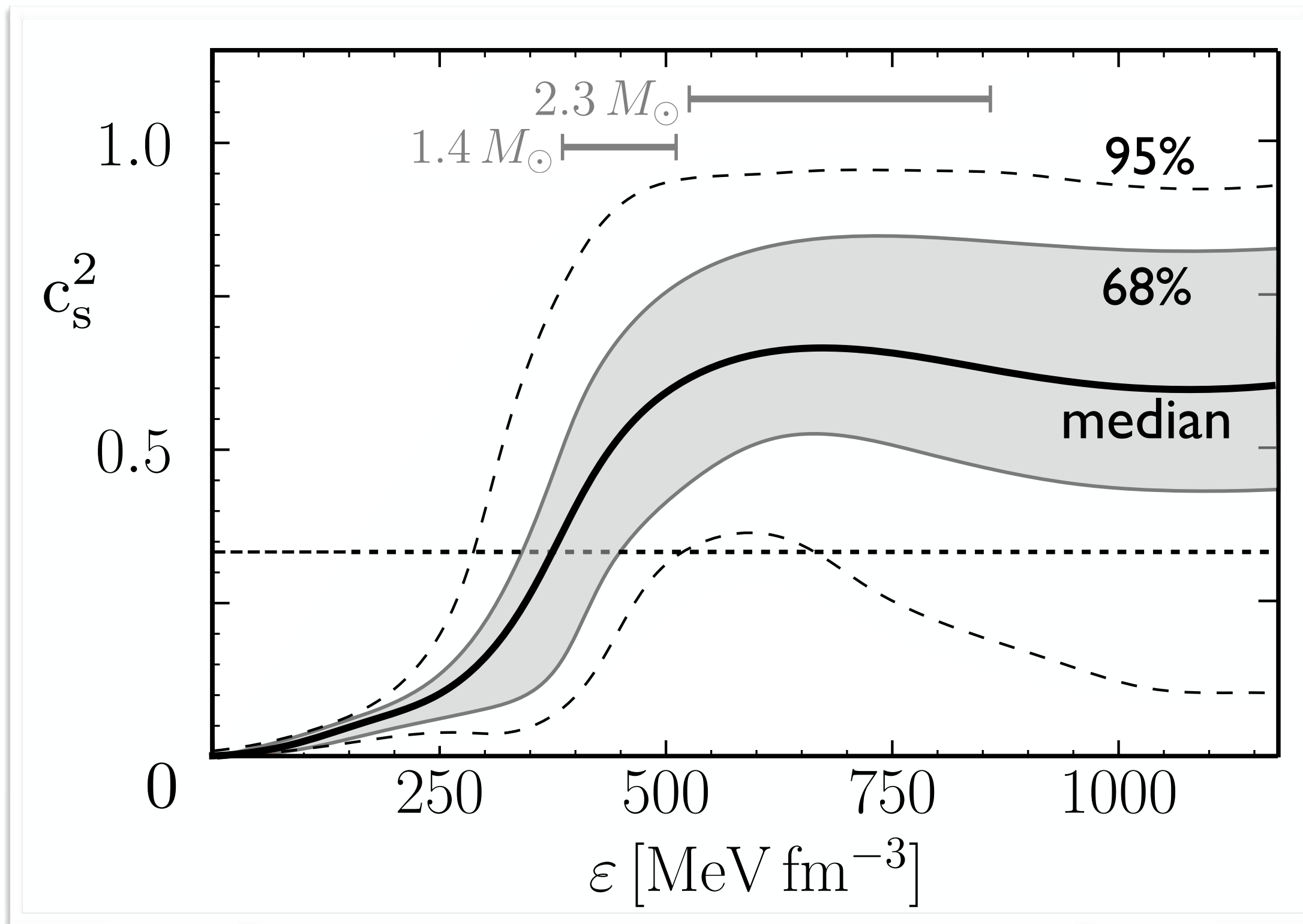
NEUTRON STAR MATTER : EQUATION of STATE

$P(\varepsilon)$

- Bayesian inference of sound speed and EoS

PSR masses, NICER & GW data, low-density constraints (ChEFT), asymptotic constraints (pQCD)

L. Brandes, W.W., N. Kaiser : Phys. Rev. D 107 (2023) 014011 ; Phys. Rev. D 108 (2023) 094014 - L. Brandes, W.W.: Symmetry 16 (2024) 111

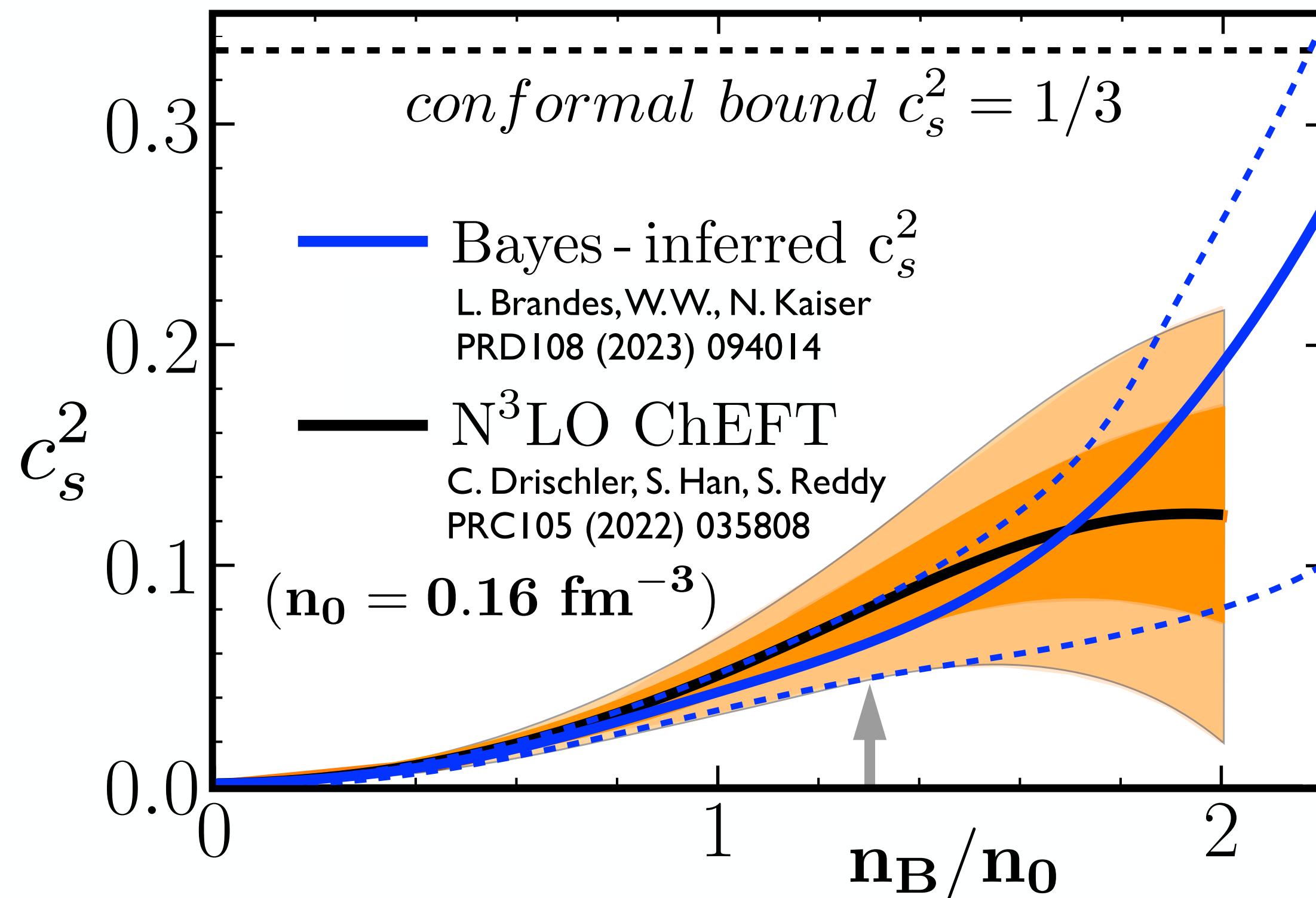


- **Speed of sound** exceeds conformal bound $c_s = 1/\sqrt{3}$ at baryon densities $n_B > 2 - 3 n_0$
- **Strongly repulsive correlations** in dense baryonic matter

EQUATION of STATE and SOUND VELOCITY

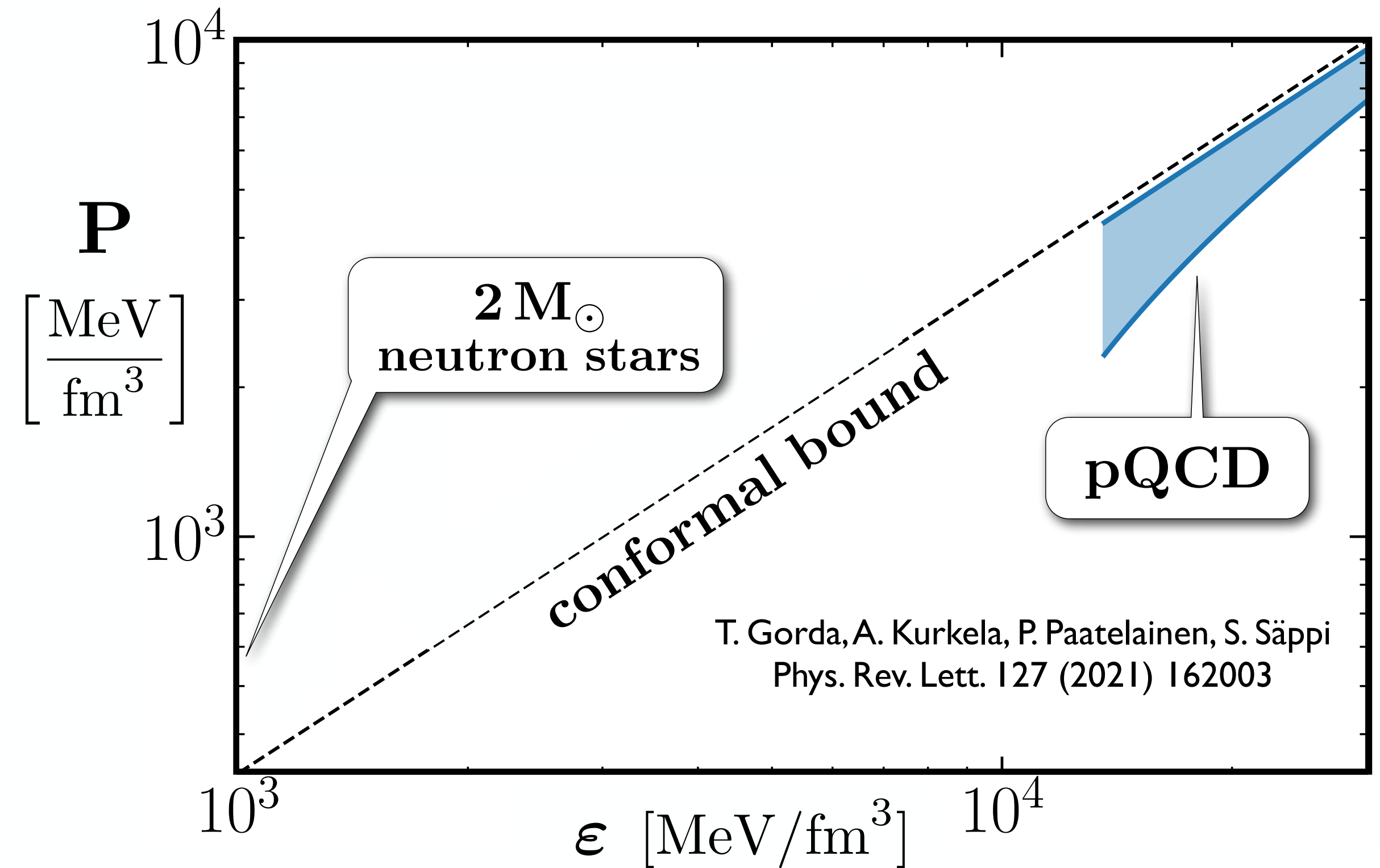
- boundary conditions -

- Low densities : Chiral EFT @ $n_B \lesssim 2 n_0$



- Employ ChEFT constraint at $n_B = 1.3 n_0$ in Bayes inference as **Likelihood, NOT Prior**

- Extremely high densities : $n_B \gg n_c(2M_\odot)$



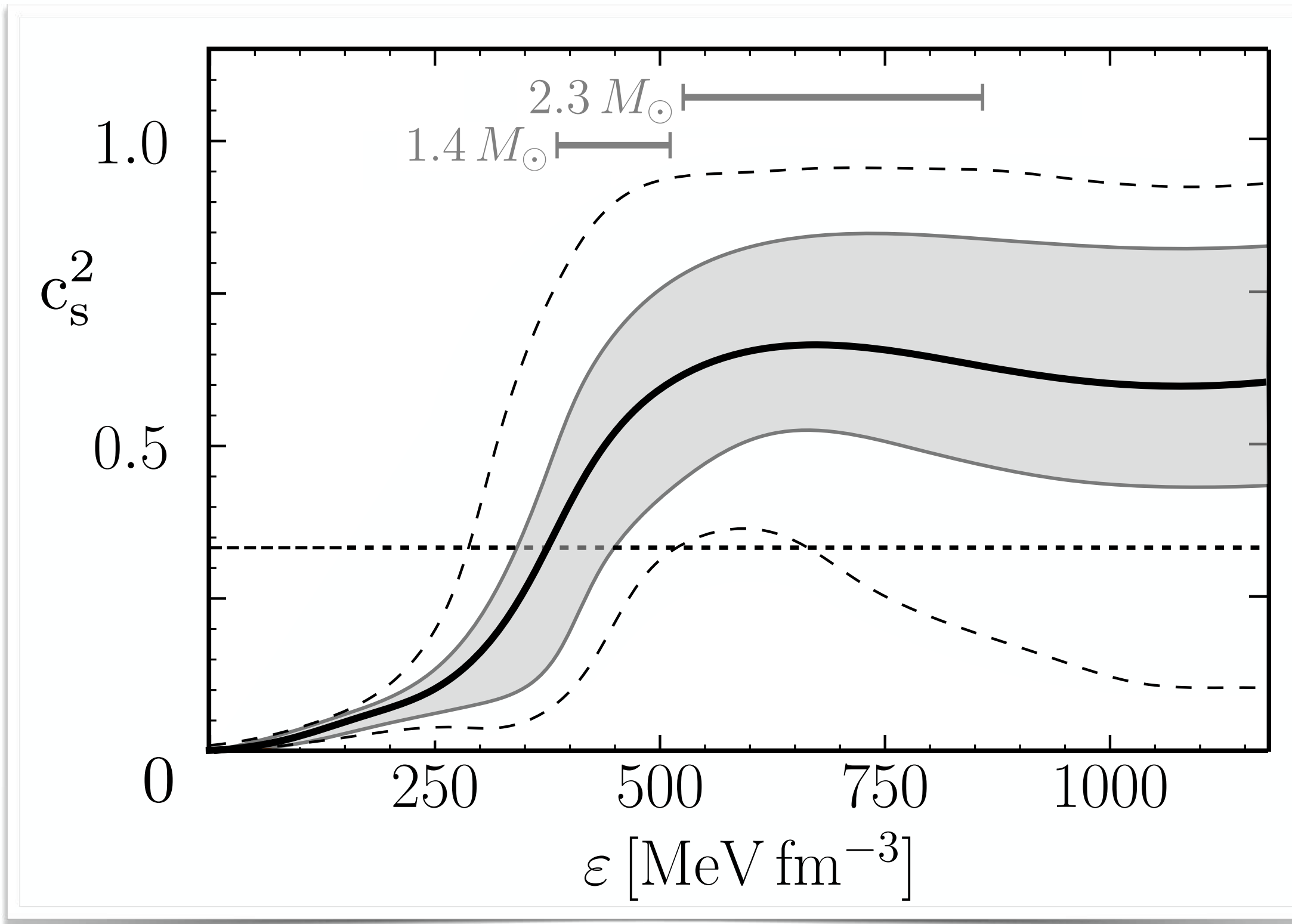
- **Conformal bound** $c_s^2 = \frac{1}{3}$ reached asymptotically



Comment : **SPEED of SOUND** exceeding **CONFORMAL BOUND**

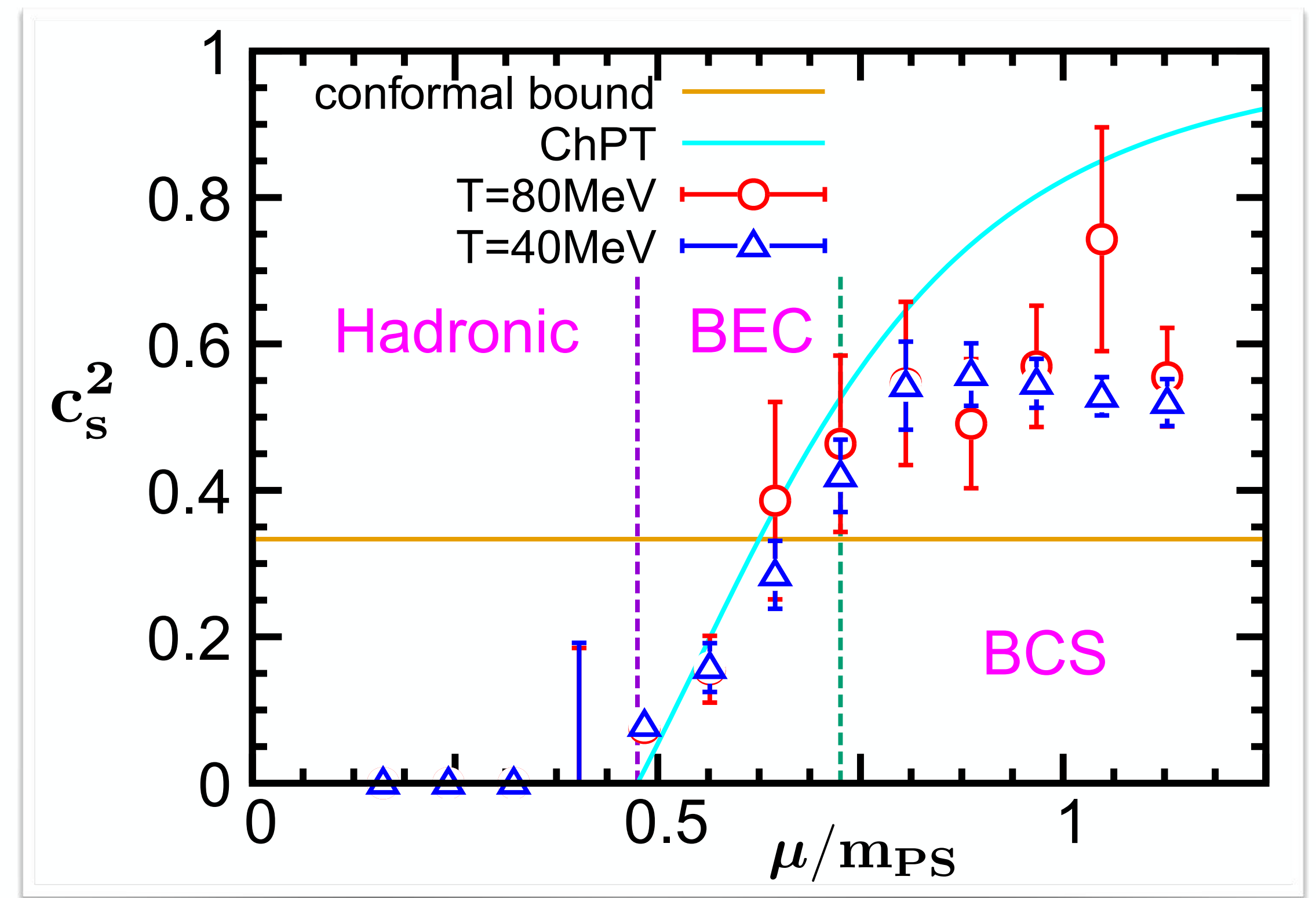
- **Bayesian inference of sound speed in neutron star matter**

L. Brandes, W.W., N. Kaiser : Phys. Rev. D 108 (2023) 094014



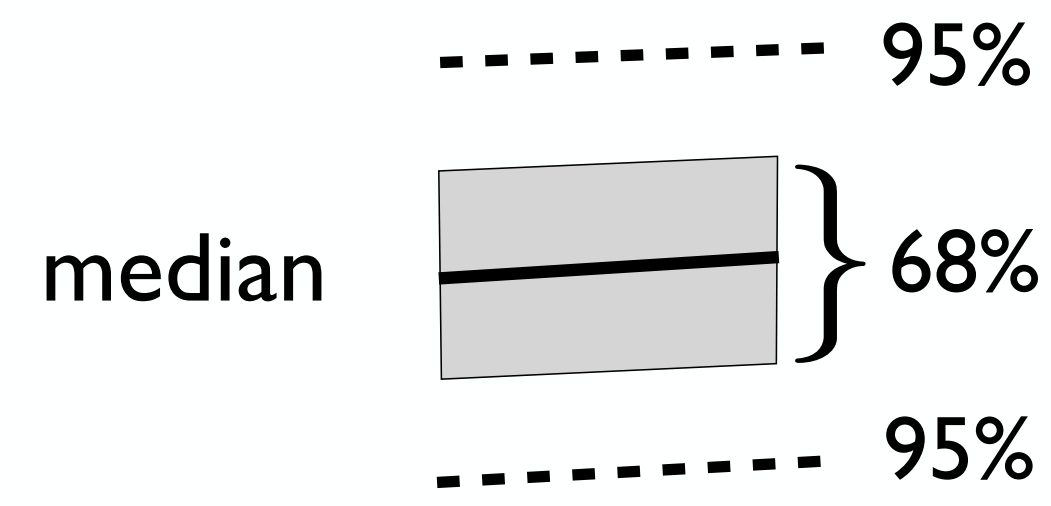
- **Sound speed as function of baryon chemical potential in $N_c = 2$ LQCD**

K. Iida, E. Itou, K. Murakami, D. Suenaga : arXiv:2405.20566



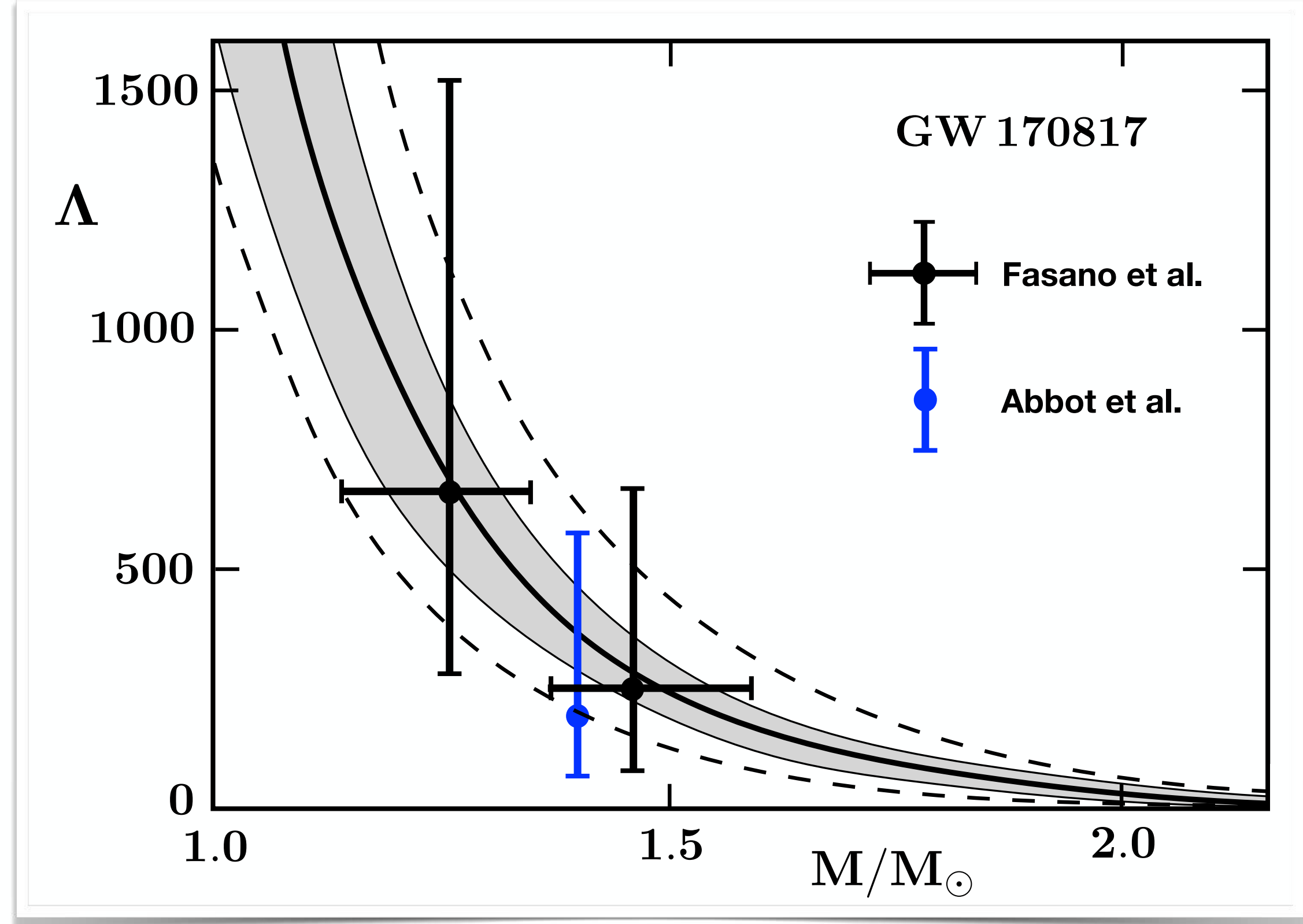
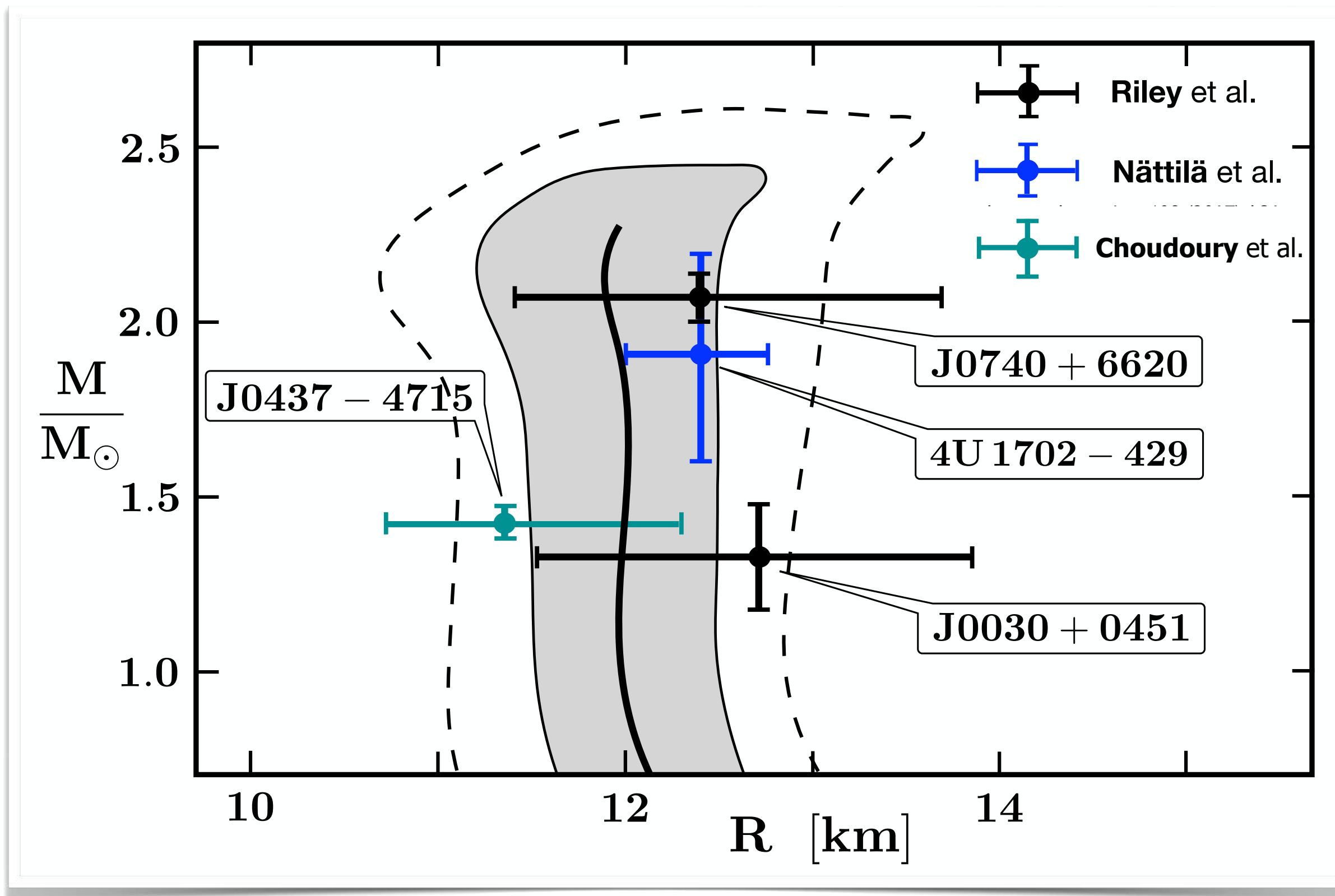
- **Speed of sound** exceeds conformal bound $c_s = 1/\sqrt{3}$ at baryon densities $n_B > 2 - 3 n_0$

NEUTRON STAR PROPERTIES

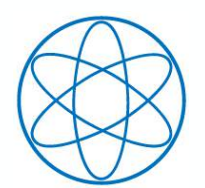


- Bayesian inference posterior bands (68% and 95% c.l.)
- Mass - Radius relation (TOV)

- Tidal deformability



L. Brandes, W. W., N. Kaiser : Phys. Rev. D 107 (2023) 014011 ; Phys. Rev. D 108 (2023) 094014 L. Brandes, W. W. (2024)



NEUTRON STAR PROPERTIES (contd.)

- Baryon chemical potential

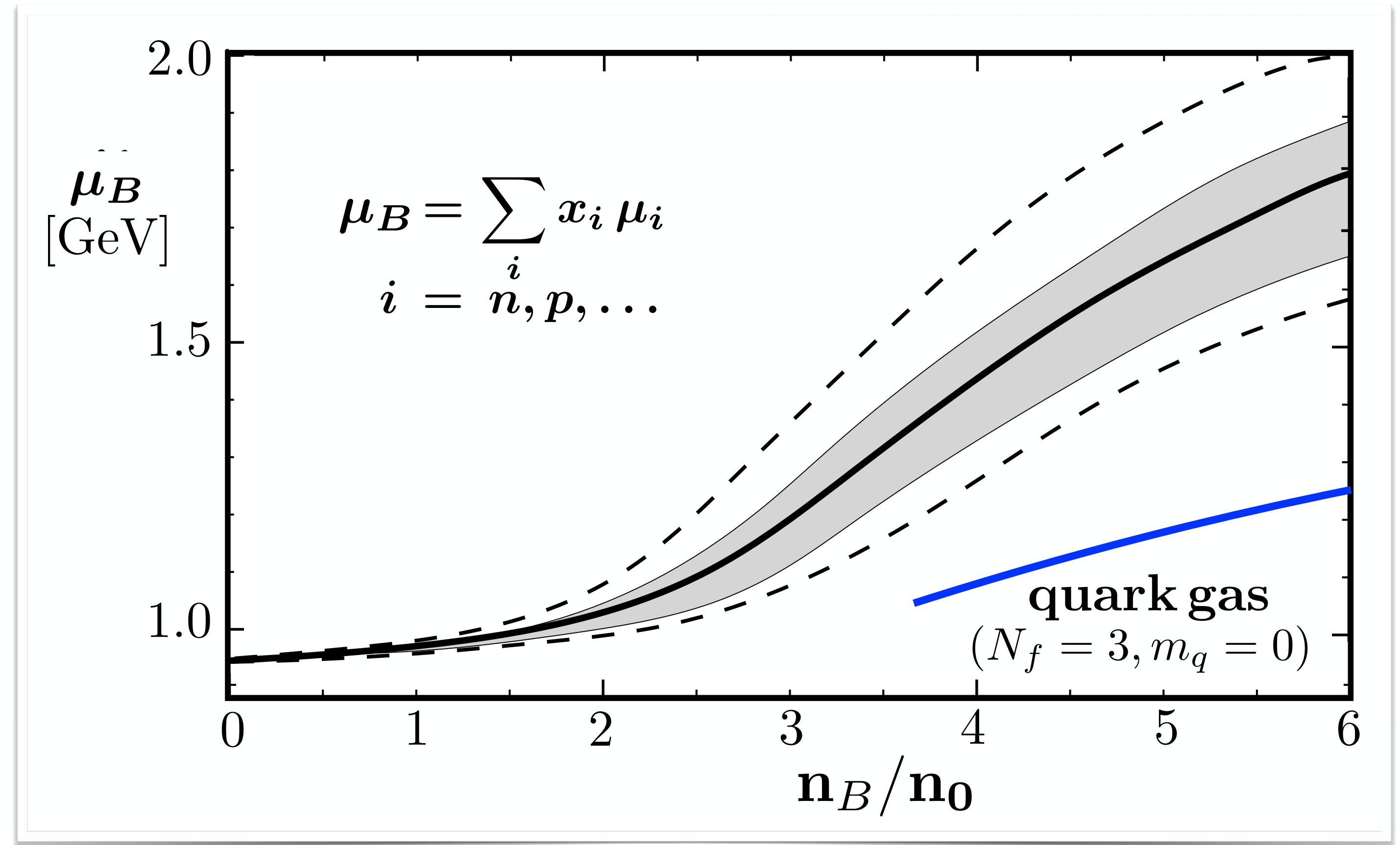
$$\mu_B = \frac{\partial \varepsilon}{\partial n_B}$$

- Stiff equation of state



strongly repulsive
correlations at work
between baryons / quarks

- Quark gas ruled out
at densities $n_B \sim 4 - 6 n_0$



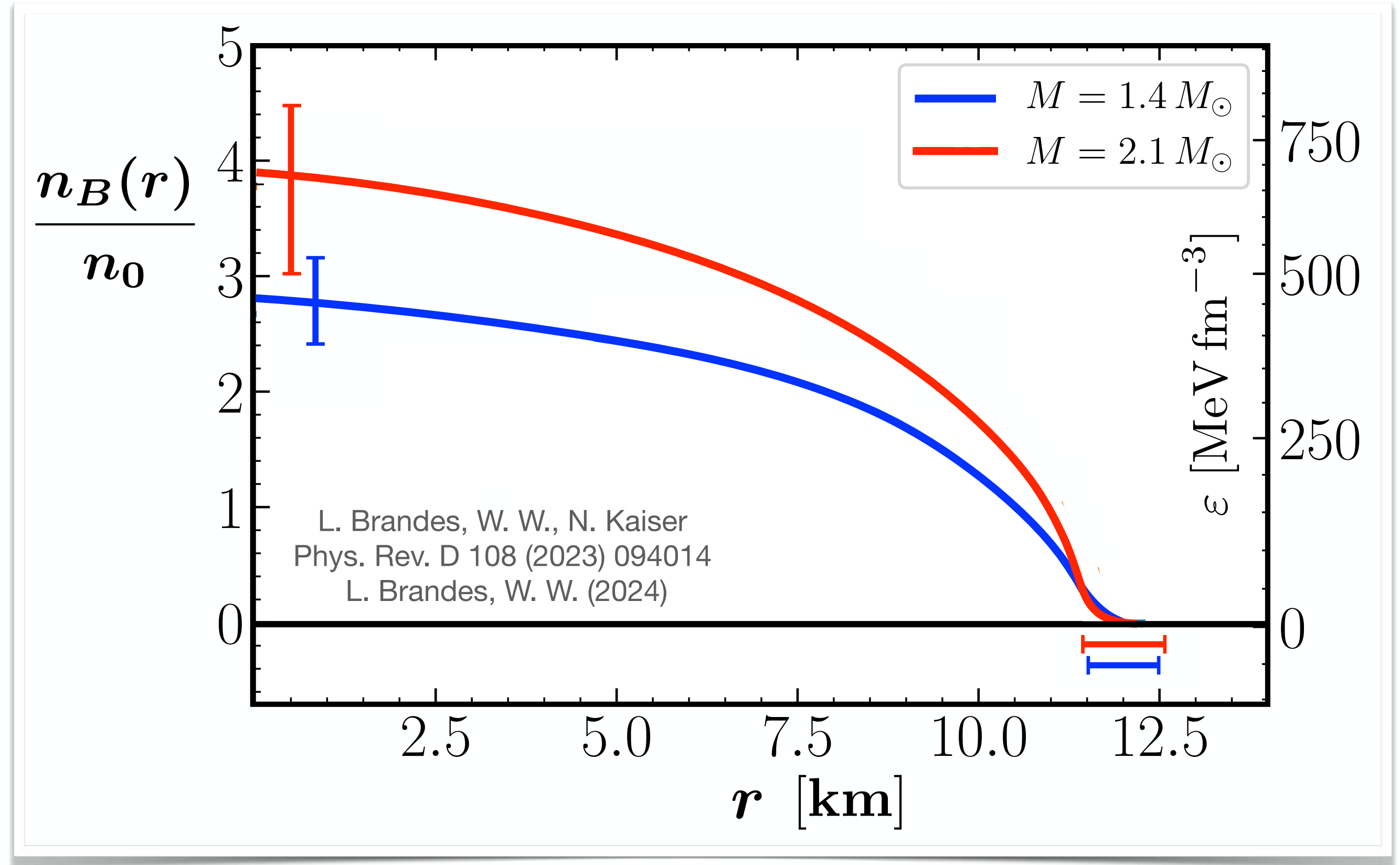
L. Brandes, W. W., N. Kaiser : Phys. Rev. D 108 (2023) 094014



NEUTRON STAR PROPERTIES (contd.)

- Density profiles of neutron stars using inferred median of $P(\varepsilon)$

- Central core densities in neutron stars are **NOT** extreme
- Average distance between baryons : $d \gtrsim 1 \text{ fm}$ even for the heaviest neutron stars



$$n_c(1.4 M_\odot) = 2.8 \pm 0.4 n_0 \quad n_c(2.1 M_\odot) = 3.9_{-0.9}^{+0.6} n_0 \quad n_c(2.3 M_\odot) = 4.0_{-0.8}^{+0.7} n_0$$

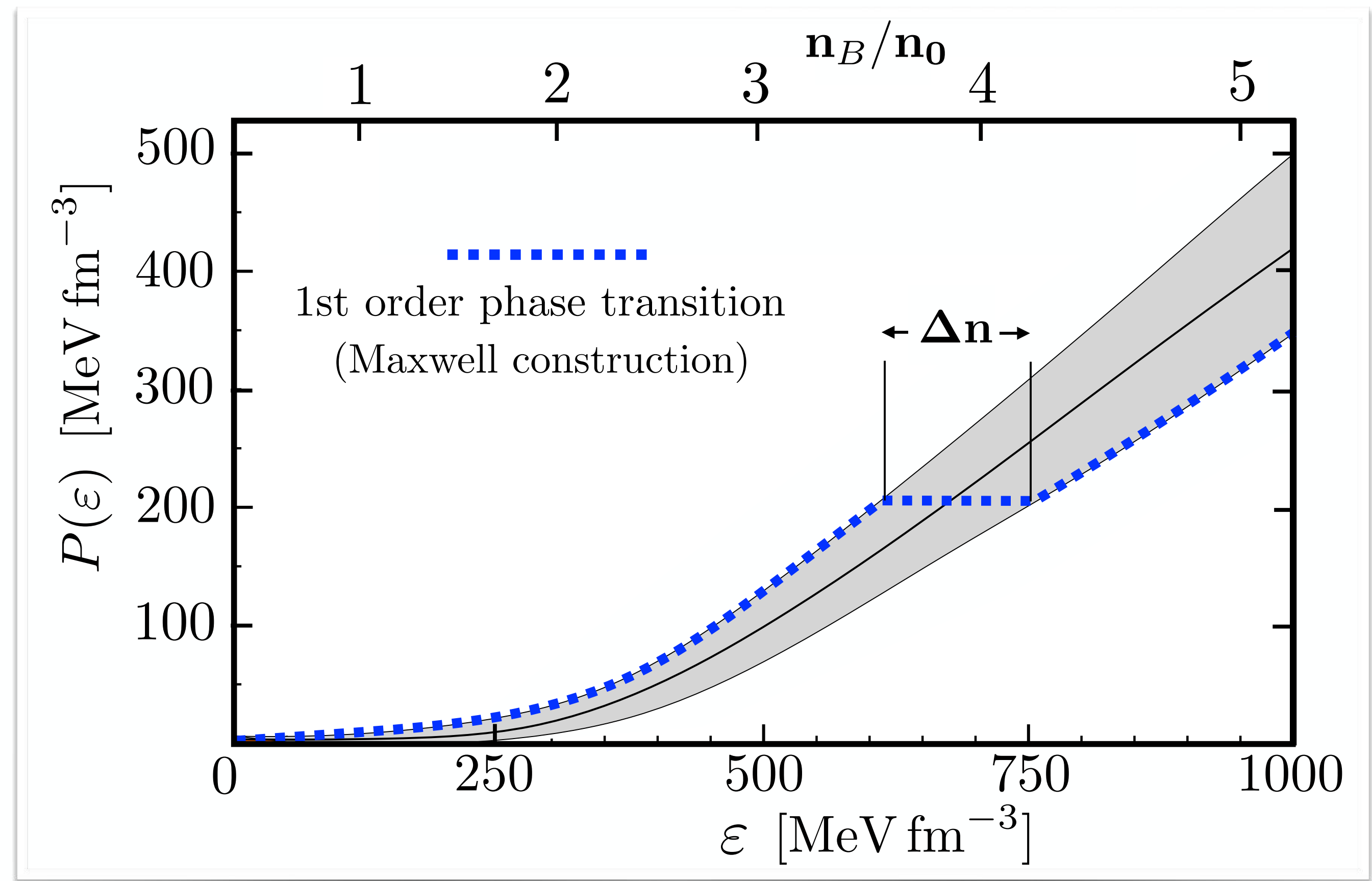
(68% c.l. — including new NICER data and “black widow” PSR J0952-0607)



Constraints on FIRST-ORDER PHASE TRANSITION in NEUTRON STAR MATTER

- Bayes factor analysis :
 - ➔ Extreme evidence for sound velocities $c_s > 0.5$ in cores of all neutron stars with $1.4 \leq M/M_\odot \leq 2.3$

- Evidence against **strong** 1st order phase transition :
 - ➔ Maximum possible extension of phase coexistence domain $\Delta n/n_B \lesssim 0.2$ (68% c.l.)



L. Brandes, W.W., N. Kaiser : Phys. Rev. D 108 (2023) 094014 - L. Brandes, W.W.: Symmetry 16 (2024) 111

- ➔ For comparison :
Maxwell construction for nuclear 1st order liquid-gas phase transition ($\Delta n/n_B > 1$)



QCD TRACE ANOMALY and CONFORMALITY in NEUTRON STARS

Y. Fujimoto, K. Fukushima, L.D. McLerran, M. Praszalowicz : Phys. Rev. Lett. 129 (2022) 252702

- Trace of energy-momentum tensor : $T^\mu_\mu = \Theta = \frac{\beta}{2g} G^a_{\mu\nu} G^{a\mu\nu} + (1 + \gamma_m) \sum_f m_f \bar{q}_f q_f$
- Finite T and μ_B :

$$\langle \Theta \rangle_{T, \mu_B} = \varepsilon - 3P$$

- Trace anomaly measure

$$\Delta \equiv \frac{\langle \Theta \rangle_{T, \mu_B}}{3\varepsilon} = \frac{1}{3} - \frac{P}{\varepsilon}$$

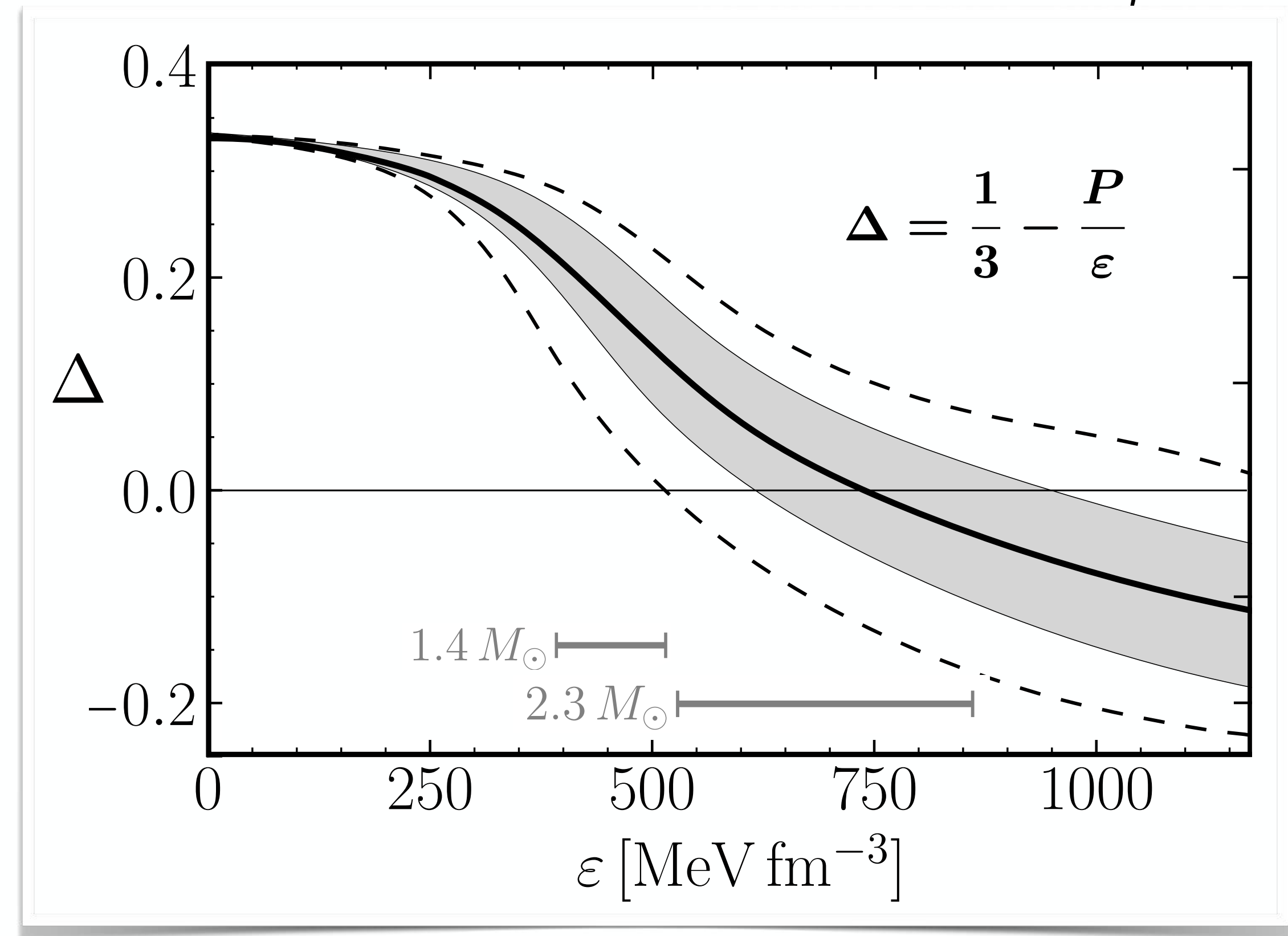
- Conformal limit : $\Delta \rightarrow 0$

- Bayes factor analysis:

Strong evidence for

$$\Delta < 0 \quad (P > \varepsilon/3)$$

at densities $n_B \gtrsim 4 n_0$



L. Brandes, W.W., N. Kaiser Phys. Rev. D 108 (2023) 094014
L. Brandes, W.W. (2024)



INTERMEDIATE SUMMARY

★ Bayesian inference analysis

including heavy ($M = 2.35 \pm 0.17 M_{\odot}$) galactic neutron star and NICER news

→ even **stiffer equation of state** required than previously expected

→ almost **constant neutron star radii** ($R \simeq 12 \pm 1$ km) for all masses

★ Extreme evidence for sound velocities $c_s > 1/\sqrt{3}$ in neutron star cores

→ **strongly repulsive correlations** at work

★ Evidence against **strong 1st order phase transition** in neutron star cores

→ **not excluded: baryonic matter or hadron-quark continuous crossover**

★ **No extreme central core densities** even in the heaviest neutron stars:

$$n_B < 5 n_0 \quad \text{for } M \leq 2.3 M_{\odot} \quad (68\% \text{ c.l.})$$

→ average baryon-baryon distance in the core: $d \gtrsim 1$ fm



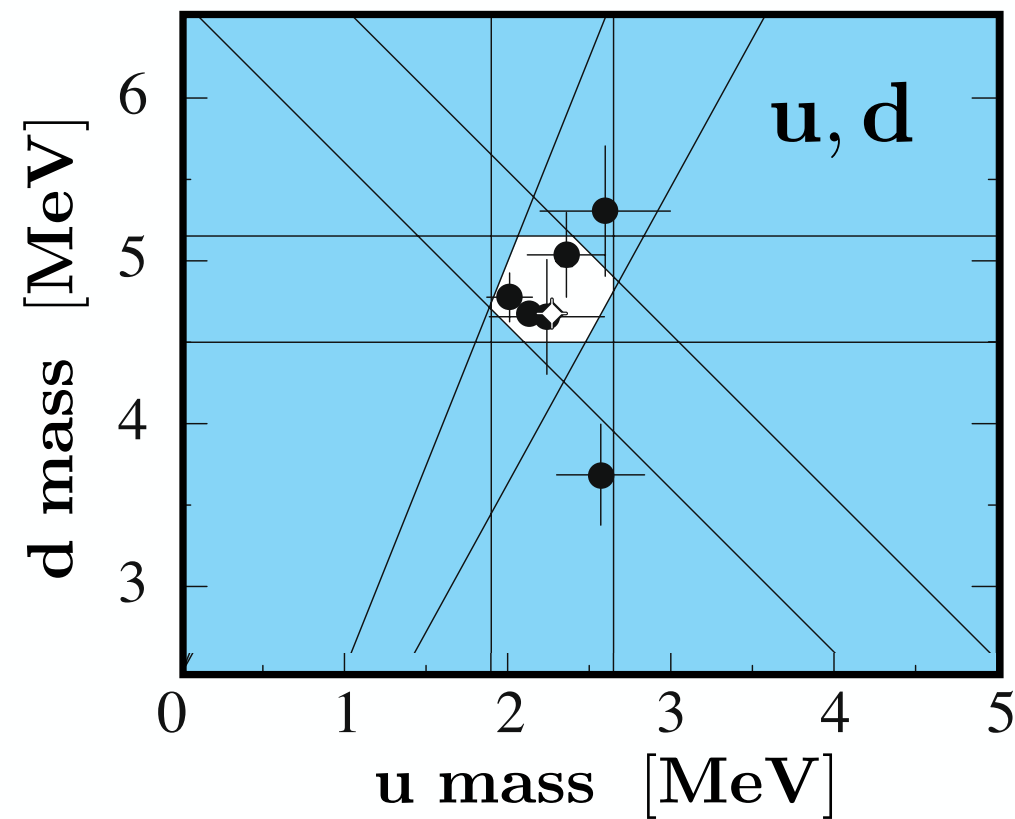
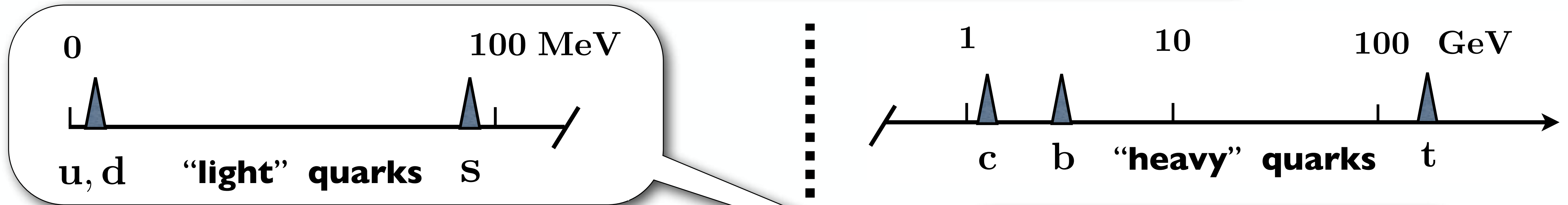
4.

*Further preparations :
QCD Symmetries,
Symmetry Breaking Patterns
and Scales*



Hierarchy of **QUARK MASSES** in **QCD**

- Separation of Scales -



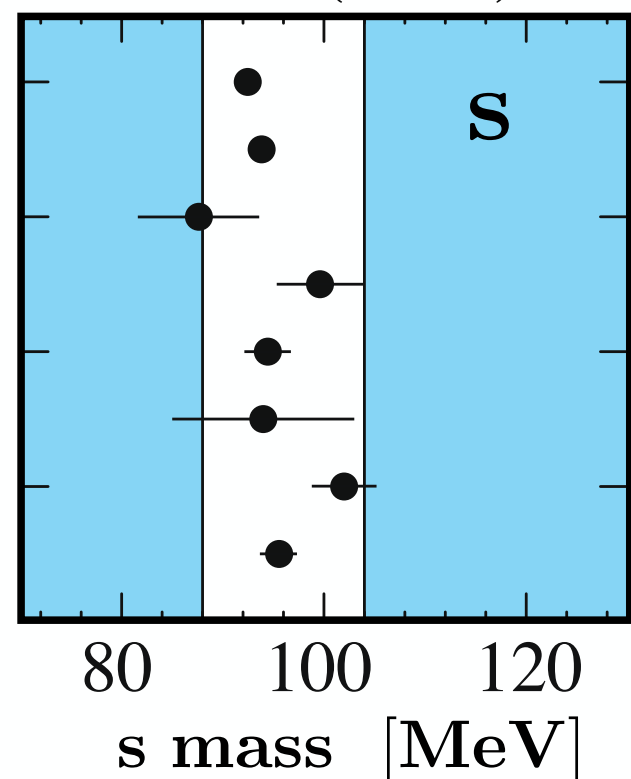
$$m_u = 2.16 \pm 0.07 \text{ MeV}$$

$$m_d = 4.70 \pm 0.07 \text{ MeV}$$

$$m_s = 93.5 \pm 0.8 \text{ MeV}$$

($\lambda = 2 \text{ GeV}$) PDG 2024

PDG 2020



CHIRAL EFFECTIVE FIELD THEORY
of
Pseudoscalar Nambu-Goldstone Bosons
coupled to **Baryons**

★ **Idealised QCD**
 $m_{u,d} \rightarrow 0$ ($m_s \rightarrow 0$)

★ **Scale Invariance**
and **Trace Anomaly**
from **massless quarks**
to **massive nucleons**

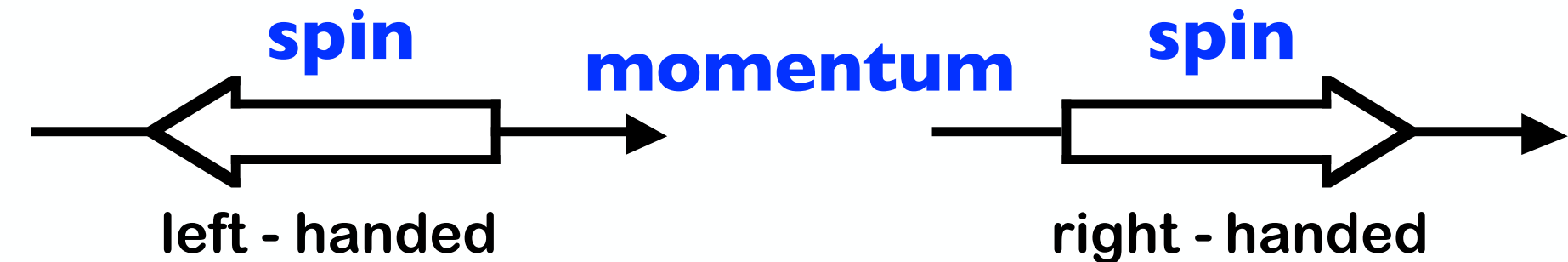
★ **Chiral Symmetry**
 $SU(N_f)_L \times SU(N_f)_R$
spontaneously broken
at low energy

Low-Energy QCD : CHIRAL SYMMETRY

- QCD with (almost) **MASSLESS** u- and d-QUARKS

$$SU(2)_L \times SU(2)_R$$

$$\psi = (u, d)$$



pseudoscalar

isovector

$$\pi \leftrightarrow \bar{\psi} i\gamma_5 \tau \psi$$

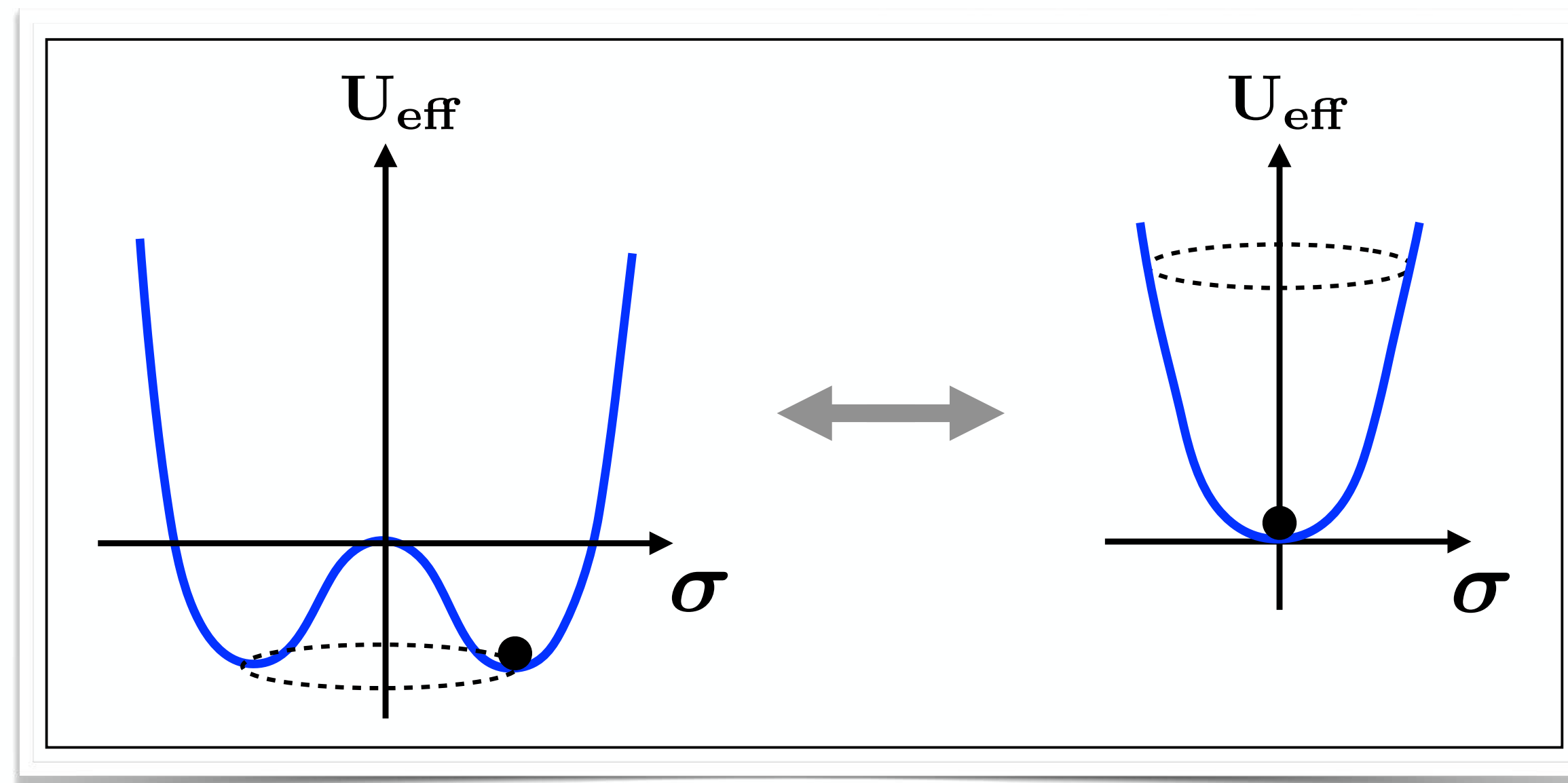
scalar isoscalar

$$\sigma \leftrightarrow \bar{\psi} \psi$$

invariant :

$$\sigma^2 + \pi^2 = f_\pi^2$$

- Realisations of **CHIRAL SYMMETRY**:



Nambu - Goldstone

$$\langle \bar{\psi} \psi \rangle \neq 0$$

low energy

low temperature

Wigner - Weyl

$$\langle \bar{\psi} \psi \rangle = 0$$

high energy

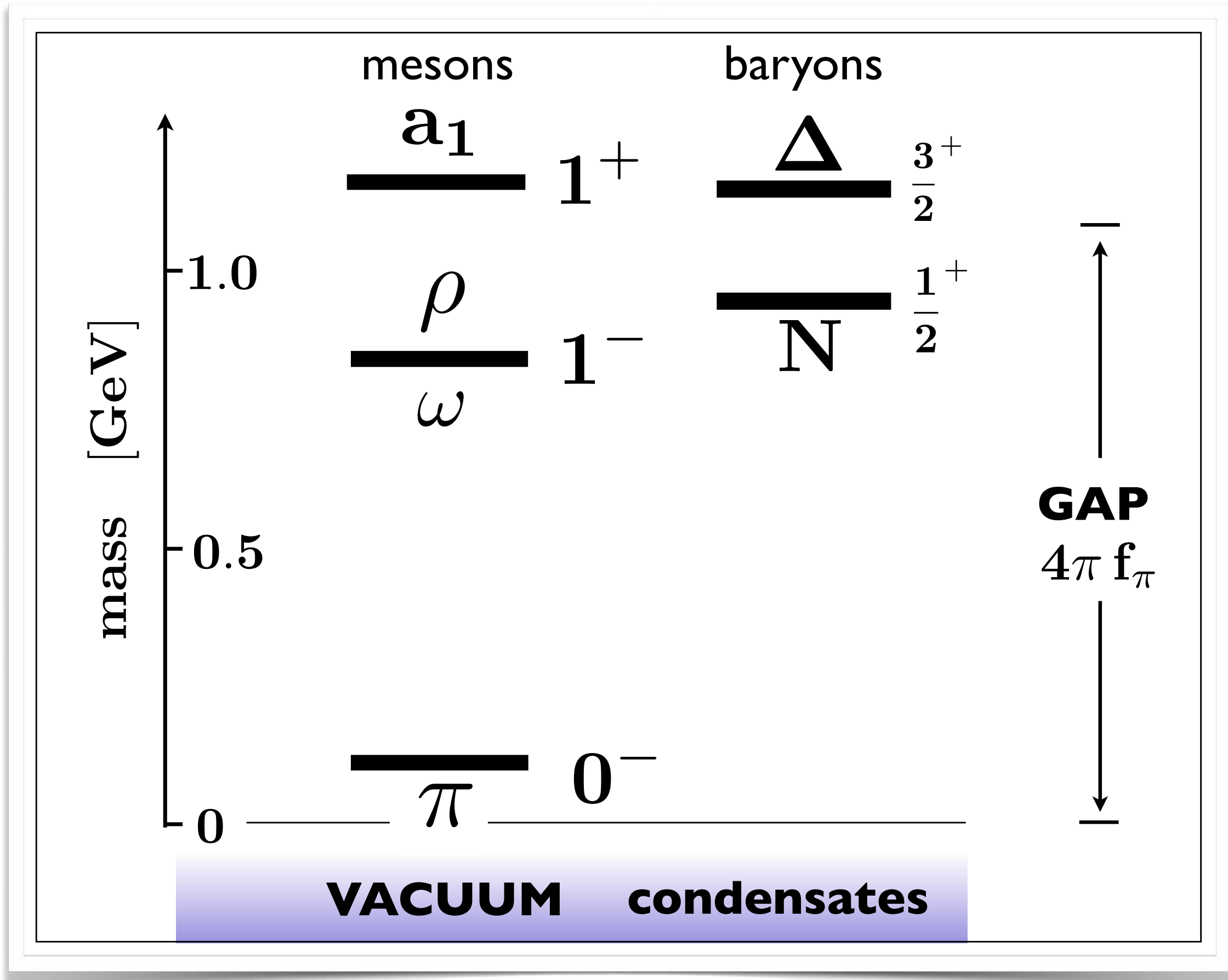
high temperature

**2nd order
phase
transition**

(for $m_{u,d} = 0$)

CHIRAL SYMMETRY

- Low energy : **spontaneous chiral symmetry breaking**
- **PIONS** as (almost) **massless Nambu-Goldstone bosons**

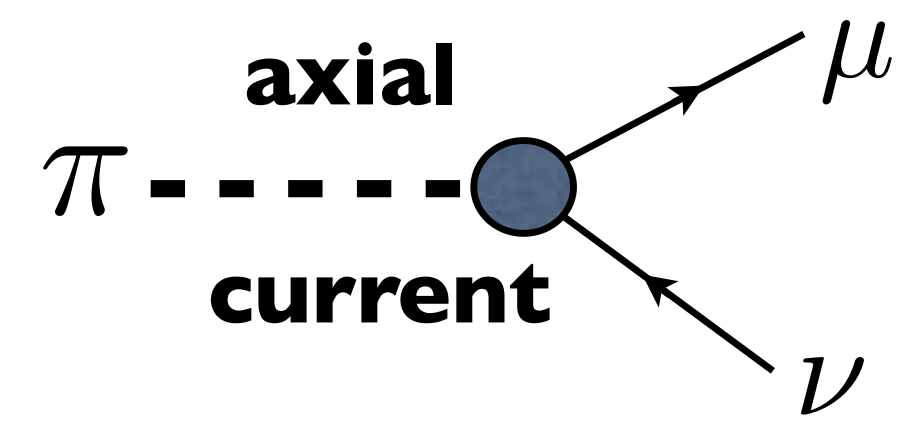


★ **Symmetry breaking scale :**

$$\Lambda_\chi = 4\pi f_\pi \sim 1 \text{ GeV}$$

• **Pion decay constant :**

$f_\pi^{(0)} \simeq 86 \text{ MeV}$ (chiral limit)
 $f_\pi \simeq 92 \text{ MeV}$ (empirical)

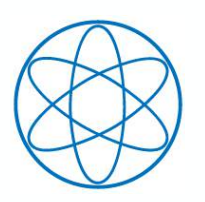


★ **Order parameter :** Pion decay constant

• **Chiral condensate and sigma field**

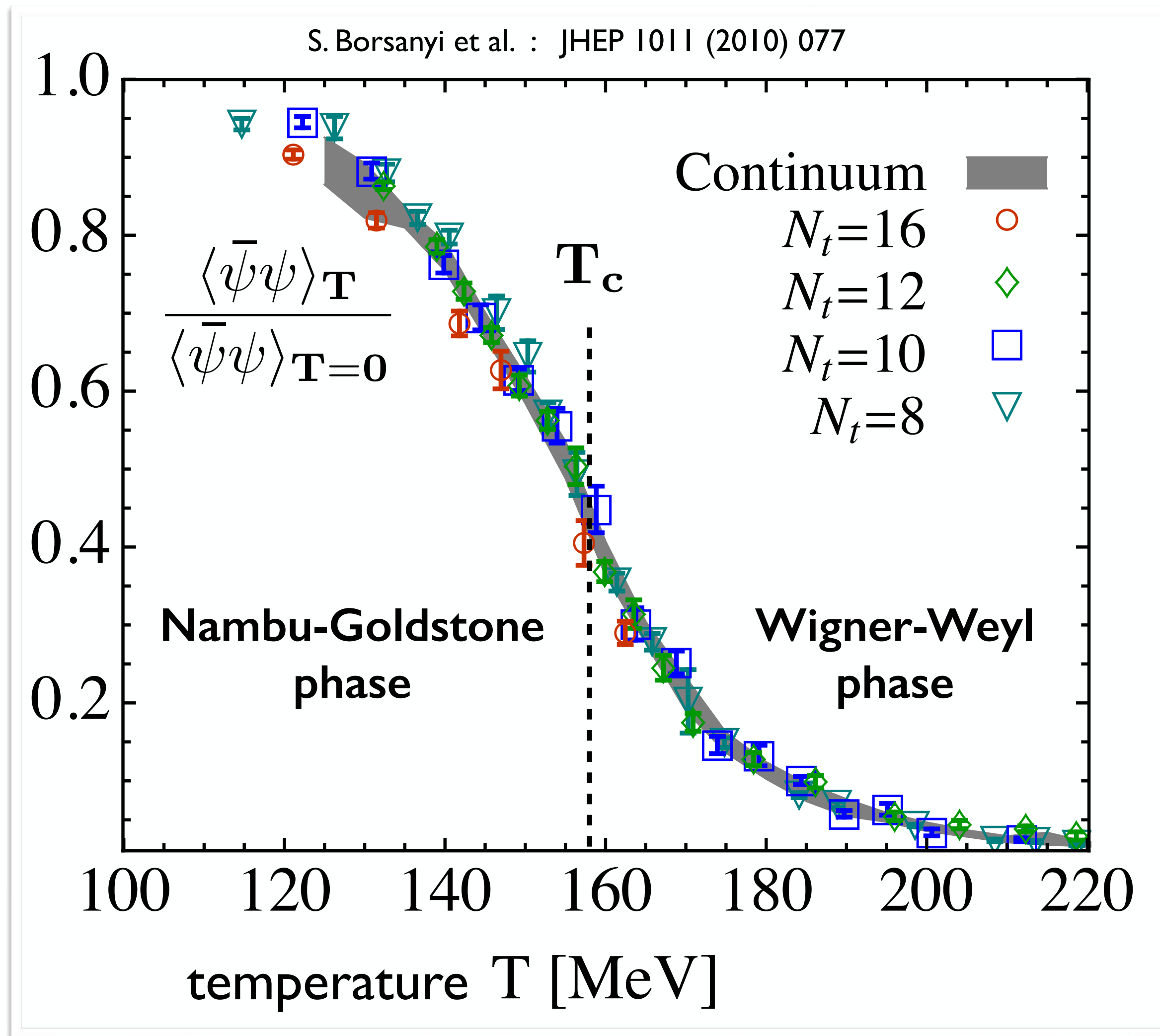
$$f_\pi^2 = -\frac{m_u + m_d}{2 m_\pi^2} \langle \bar{u}u + \bar{d}d \rangle = \langle \sigma \rangle^2$$

Gell-Mann - Oakes - Renner relation



LATTICE QCD THERMODYNAMICS: CHIRAL CROSSOVER TRANSITION

$$\mu_{\text{baryon}} = 0$$



Chiral (Quark) Condensate

**Crossover
transition temperature**

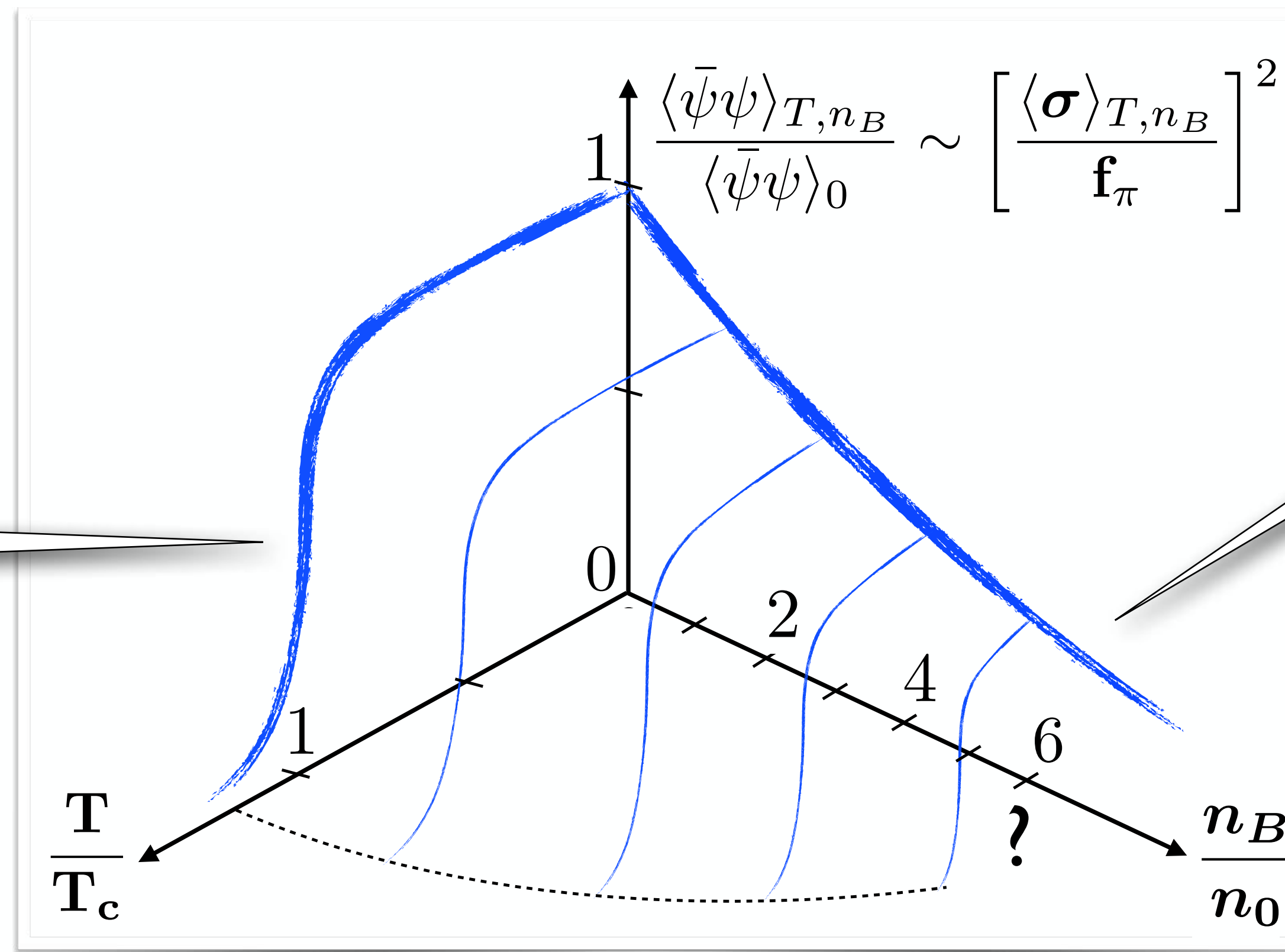
$$T_c = 158.0 \pm 0.6 \text{ MeV}$$

C. Ratti et al. : J. Phys. Conf. Ser. 1602 (2020) 012011

CHIRAL and **DECONFINEMENT**
crossover transitions
appear to be closely **connected**

CHIRAL SYMMETRY RESTORATION

- From **Nambu-Goldstone** to **Wigner-Weyl** realisations of chiral symmetry
- Key issue : **Thermodynamics** of **chiral order parameter**
its dependence on **temperature** and **baryon chemical potential / baryon density**



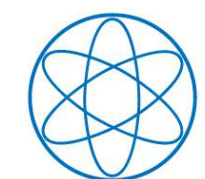
$\mu_B = 0$
 $T_c \simeq 158 \text{ MeV}$
crossover
 Lattice QCD
 HIC Freeze-out

$\mu_B > M_N$
 low - T
crossover ?
phase transition ?

(P)NJL type quark models,
 chiral quark-meson models,
 ...
 suggest first-order
 chiral phase transition,
BUT ...

5.

Low-Energy Structure of the Nucleon: Mass and Size(s)



SCALE INVARIANCE, TRACE ANOMALY and **MASS** of the **NUCLEON**

★ QCD with massless quarks : no dimensional parameter

- Invariance under scale transformations $x \rightarrow \lambda x$
- Trace of energy-momentum tensor $T^{\mu\nu}$ vanishes classically ...

★ ... but - QCD as a quantum field theory introduces renormalisation scale, and so :

$$T_{\mu}^{\mu} \propto \text{Tr} [G_{\mu\nu} G^{\mu\nu}] \text{ non-vanishing (TRACE ANOMALY)}$$

★ From **MASSLESS QUARKS** to **MASSIVE NUCLEONS** :

$$M_N^{(0)} = \langle N | T_{\mu}^{\mu} | N \rangle = \frac{9}{4} \langle N | \frac{\alpha}{\pi} (\mathbf{B}^2 - \mathbf{E}^2) | N \rangle \simeq 0.8 \text{ GeV}$$

- **Physical nucleon mass** : $M_N = M_N^{(0)} + \sigma_N + \sigma_s = 0.94 \text{ GeV}$
- **Sigma terms** : $\sigma_N = \frac{1}{2} (m_u + m_d) \langle N | \bar{u}u + \bar{d}d | N \rangle$ $\sigma_s = m_s \langle N | \bar{s}s | N \rangle$

NUCLEON MASS

- Aspects of Broken Symmetry -

$$M_N = M_N^{(0)} + \sigma_N + \sigma_s = 0.94 \text{ GeV}$$

~ 90 %
of the nucleon mass from
gluonic trace anomaly

~ 10 %
of the nucleon mass from
quark mass terms
(sigma terms)

M_N

$$M_N^{(0)} \propto \langle N | \text{Tr}[G_{\mu\nu} G^{\mu\nu}] | N \rangle$$

TRACE ANOMALY sum rule
broken scale invariance

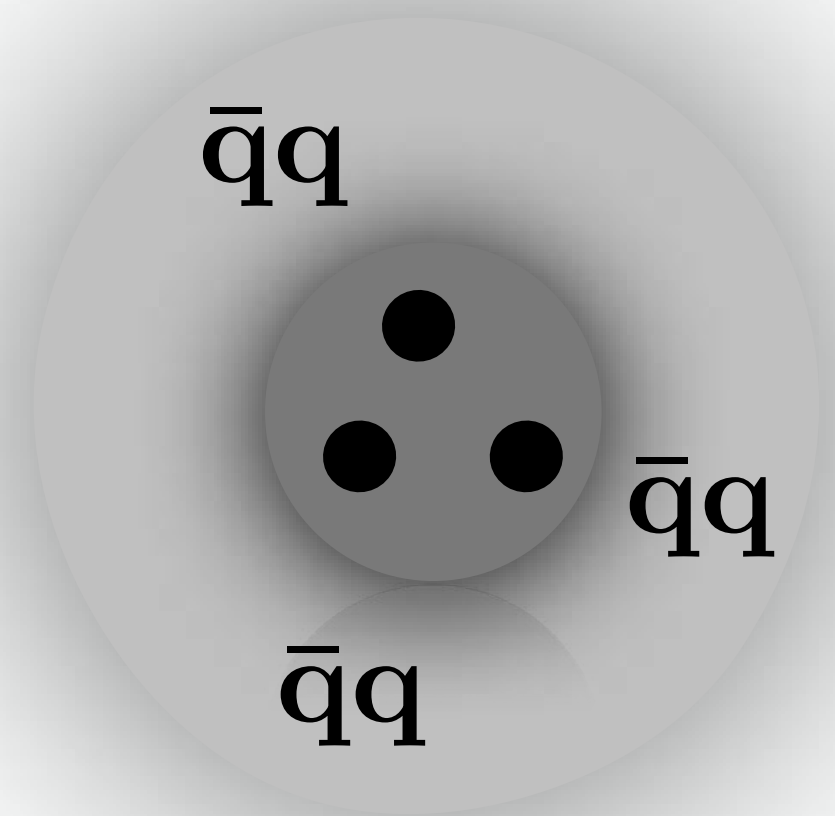
$$M_N = g f_\pi \equiv g \langle \sigma \rangle \quad \left(g = \frac{g_{\pi N}}{g_A} \right)$$

spontaneously broken
CHIRAL SYMMETRY
Goldberger - Treiman relation

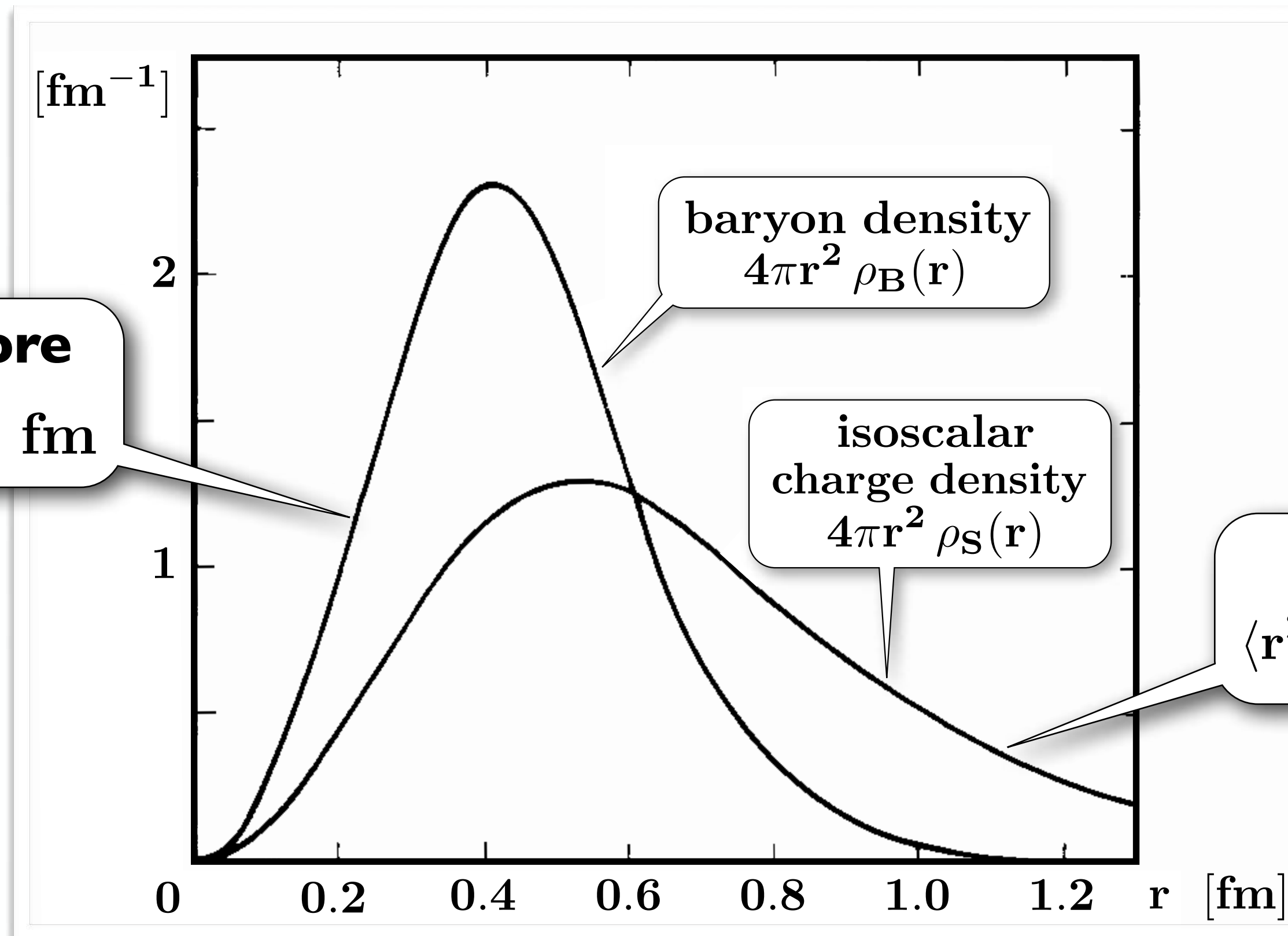
SIZES of the NUCLEON

Low-energy QCD: spontaneously broken chiral symmetry + localisation (confinement)

- **NUCLEON** : compact valence quark core + mesonic (multi $\bar{q}q$) cloud
 - Historic example: Chiral Soliton Model of the Nucleon



baryonic core
 $\langle r^2 \rangle_B^{1/2} \simeq 0.5 \text{ fm}$



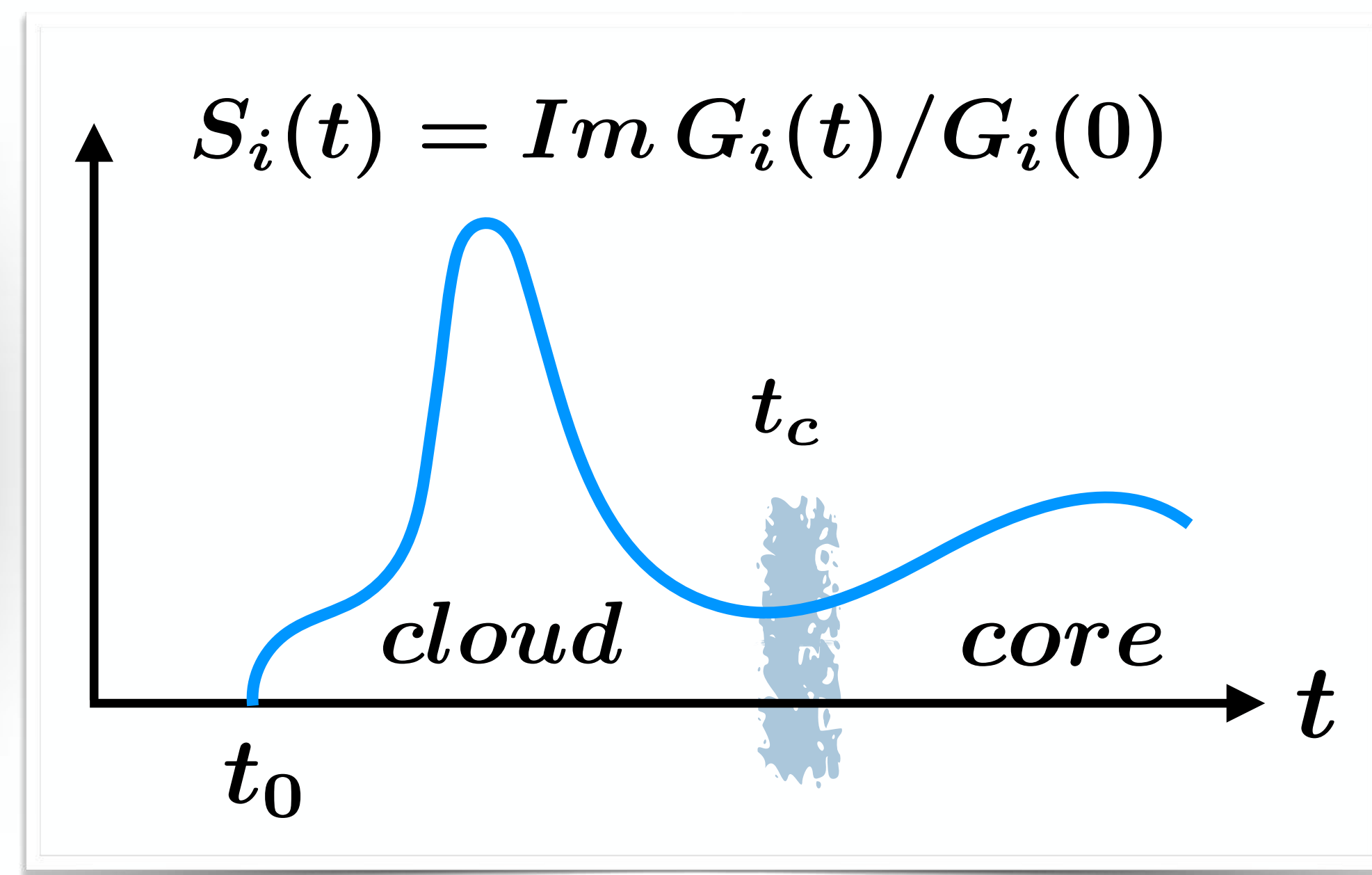
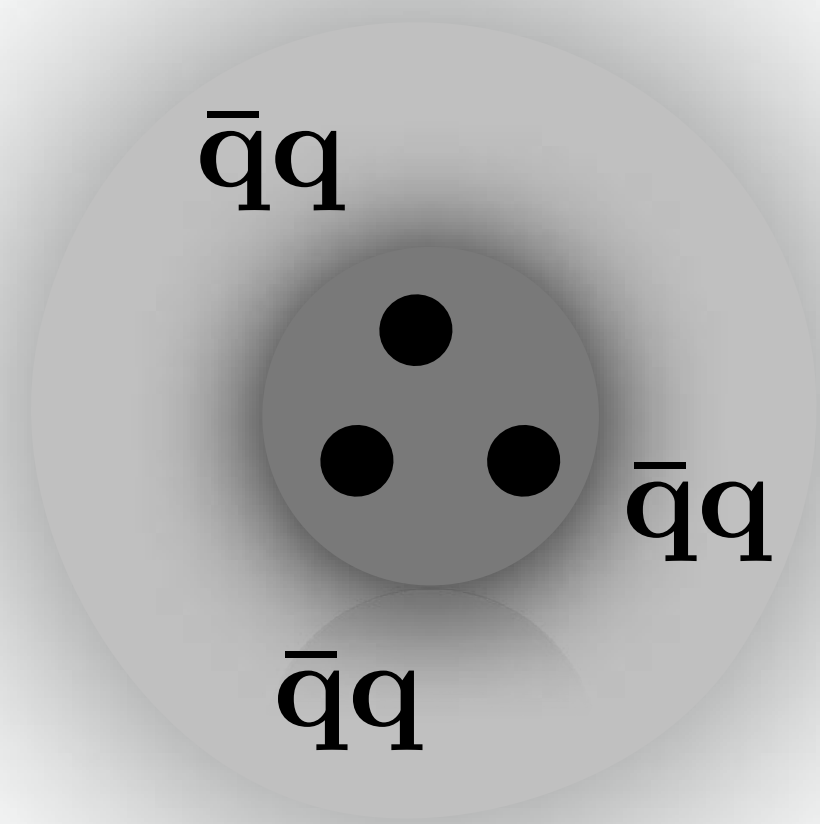
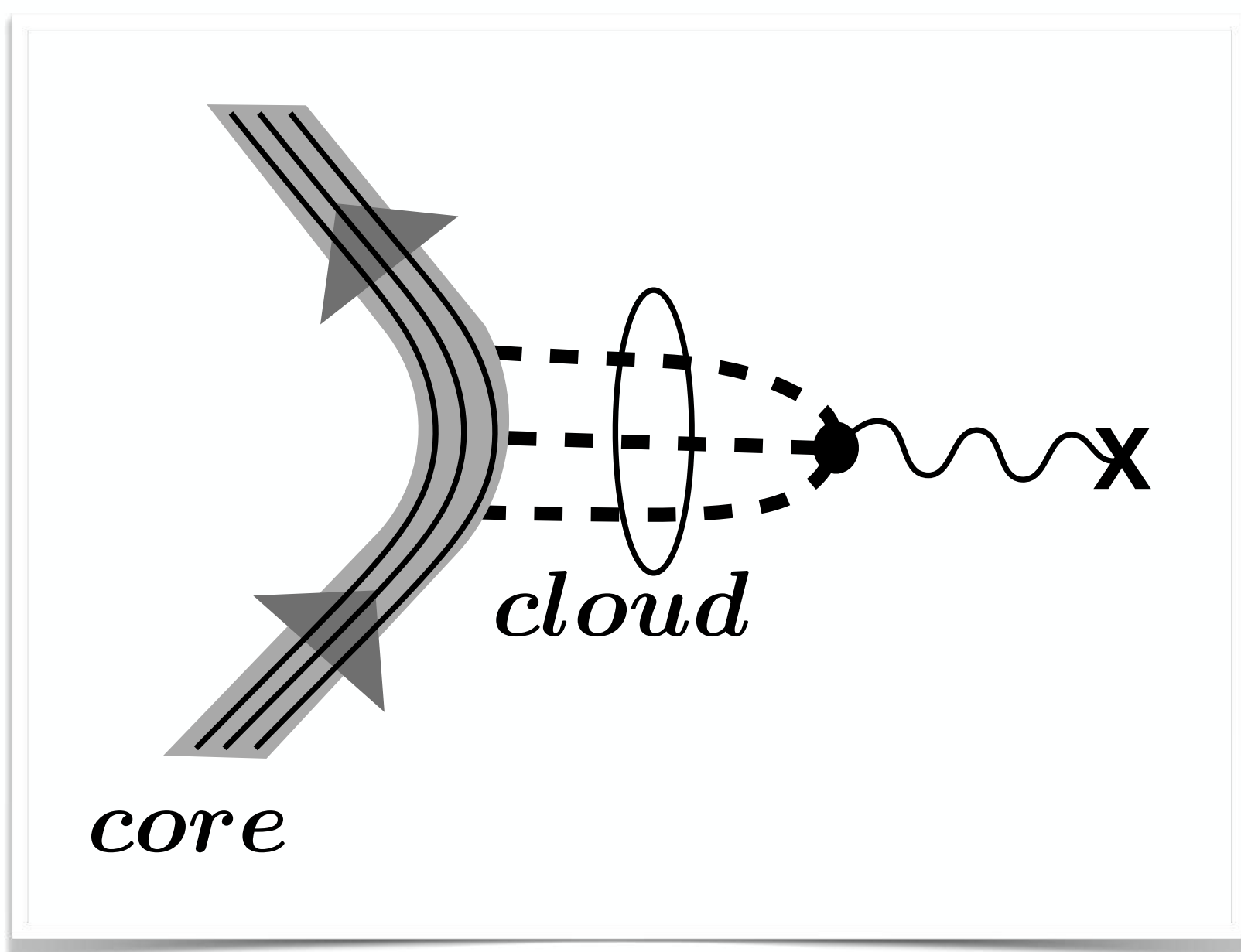
mesonic cloud
 $\langle r^2 \rangle_{E, \text{isoscalar}}^{1/2} \simeq 0.8 \text{ fm}$

N. Kaiser,
 U.-G. Meißner,
 W.W.
 Nucl. Phys. A466 (1987) 685

• **Separation of scales**
 $\left(\frac{R_{cloud}}{R_{core}} \right)^3 \gg 1$

FORM FACTORS of the NUCLEON

$$G_i(q^2) = G_i(0) + \frac{q^2}{\pi} \int_{t_0}^{\infty} dt \frac{\text{Im } G_i(t)}{t(t - q^2 - i\epsilon)} \quad \langle r_i^2 \rangle = \frac{6}{G_i(0)} \left. \frac{dG_i(q^2)}{dq^2} \right|_{q^2=0} = \frac{6}{\pi} \int_{t_0}^{\infty} \frac{dt}{t^2} S_i(t)$$



$$\langle r_i^2 \rangle = \langle r_i^2 \rangle_{\text{cloud}} + \langle r_i^2 \rangle_{\text{core}} = \frac{6}{\pi} \left[\int_{t_0}^{t_c} \frac{dt}{t^2} S_i(t) + \int_{t_c}^{\infty} \frac{dt}{t^2} S_i(t) \right]$$

Example I: ISOSCALAR ELECTRIC FORM FACTOR of the NUCLEON

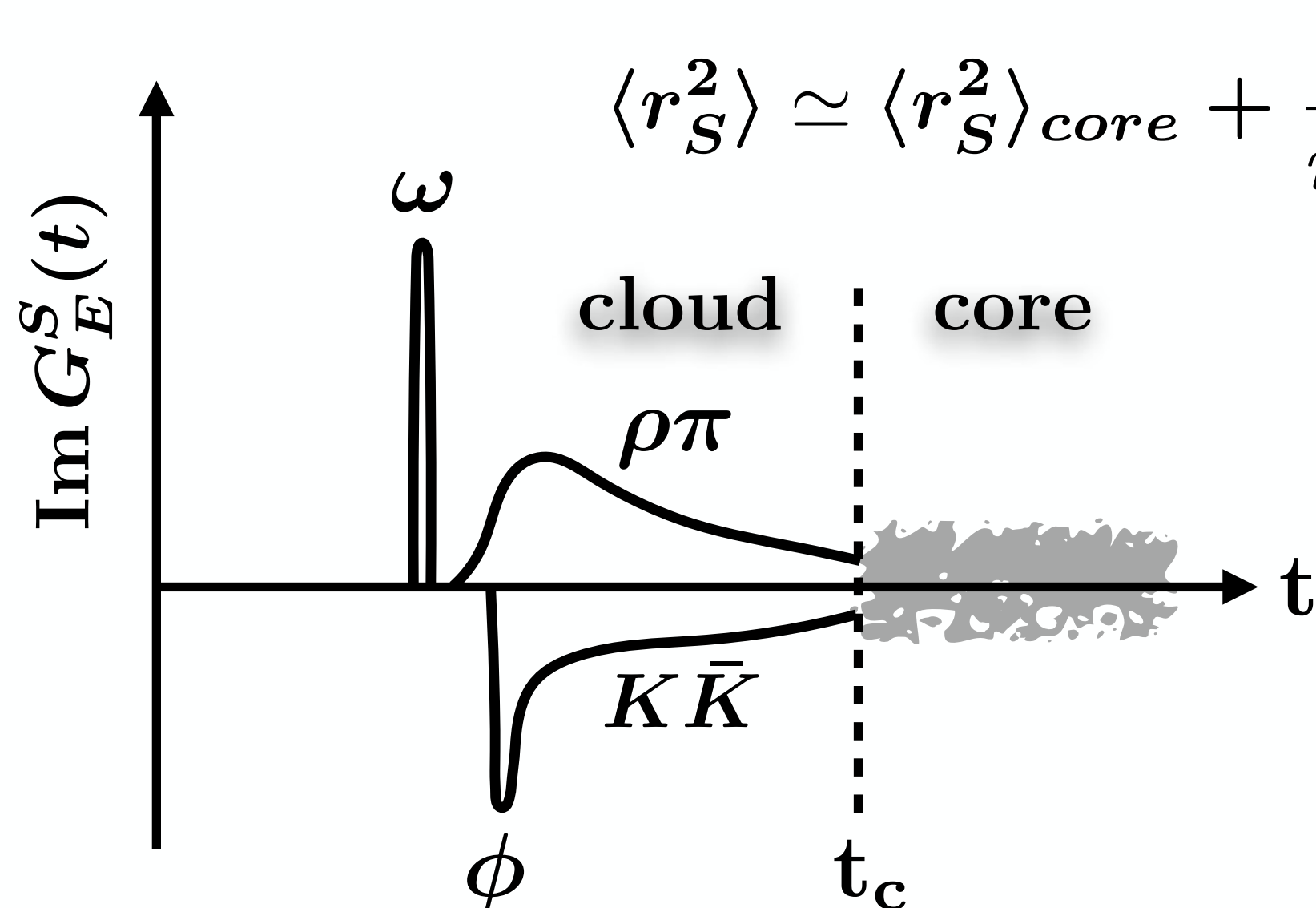
- Isoscalar electric form factor $G_E^S(q^2) = \frac{1}{2} [G_E^p(q^2) + G_E^n(q^2)]$ $\langle r_S^2 \rangle = \langle r_p^2 \rangle + \langle r_n^2 \rangle$

Empirical : $\langle r_p^2 \rangle^{1/2} = 0.840 \pm 0.004 \text{ fm}$ $\langle r_S^2 \rangle^{1/2} = 0.775 \pm 0.011 \text{ fm}$
 $\langle r_n^2 \rangle = -0.105 \pm 0.006 \text{ fm}^2$

Y.H. Lin,
H.-W. Hammer,
U.-G. Meißner
PRL 128 (2022) 052002

... based on precision fits to form factors at both spacelike and timelike q^2

- Simplest Vector Dominance Model: “cloud” dominated by ω meson



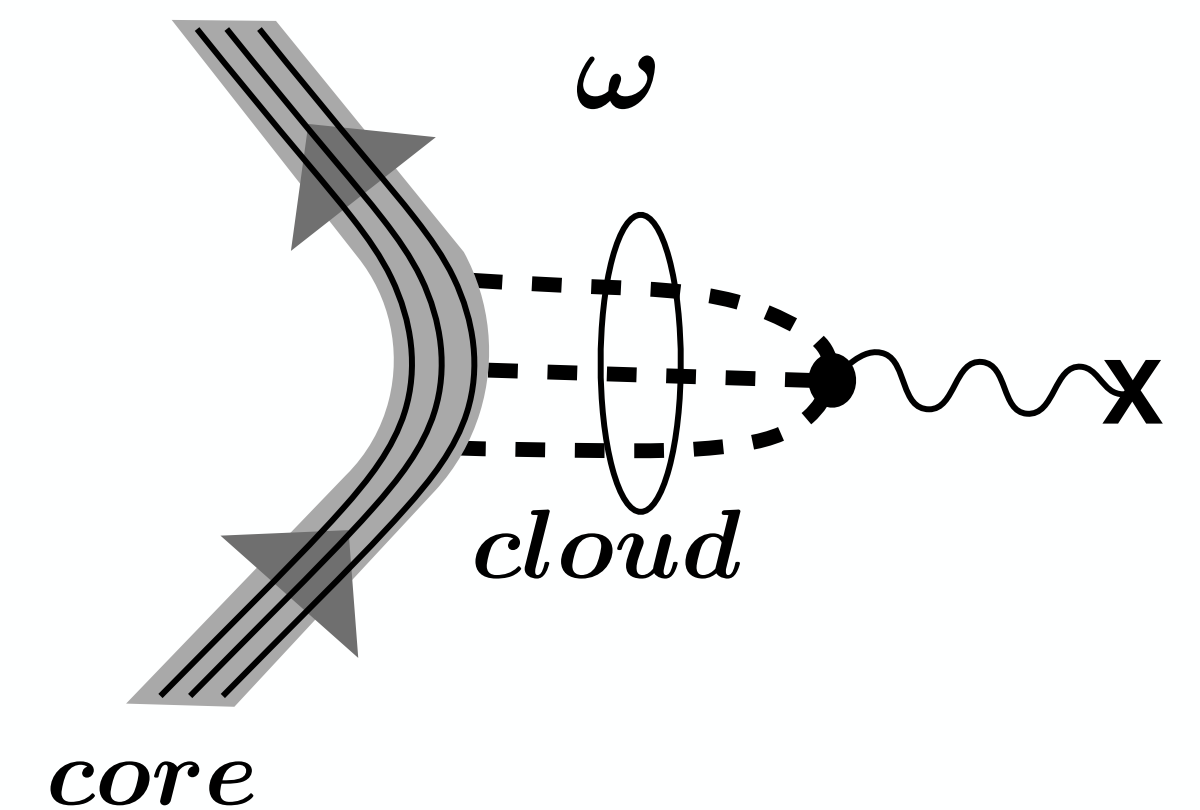
$$\langle r_S^2 \rangle \simeq \langle r_S^2 \rangle_{core} + \frac{6}{m_\omega^2}$$



$$\langle r_S^2 \rangle_{core}^{1/2} \simeq 0.47 \text{ fm}$$

- Detailed analysis using best-fit spectral functions :

$$\langle r_S^2 \rangle_{core}^{1/2} \equiv \langle r_B^2 \rangle^{1/2} = 0.50 \pm 0.01 \text{ fm}$$



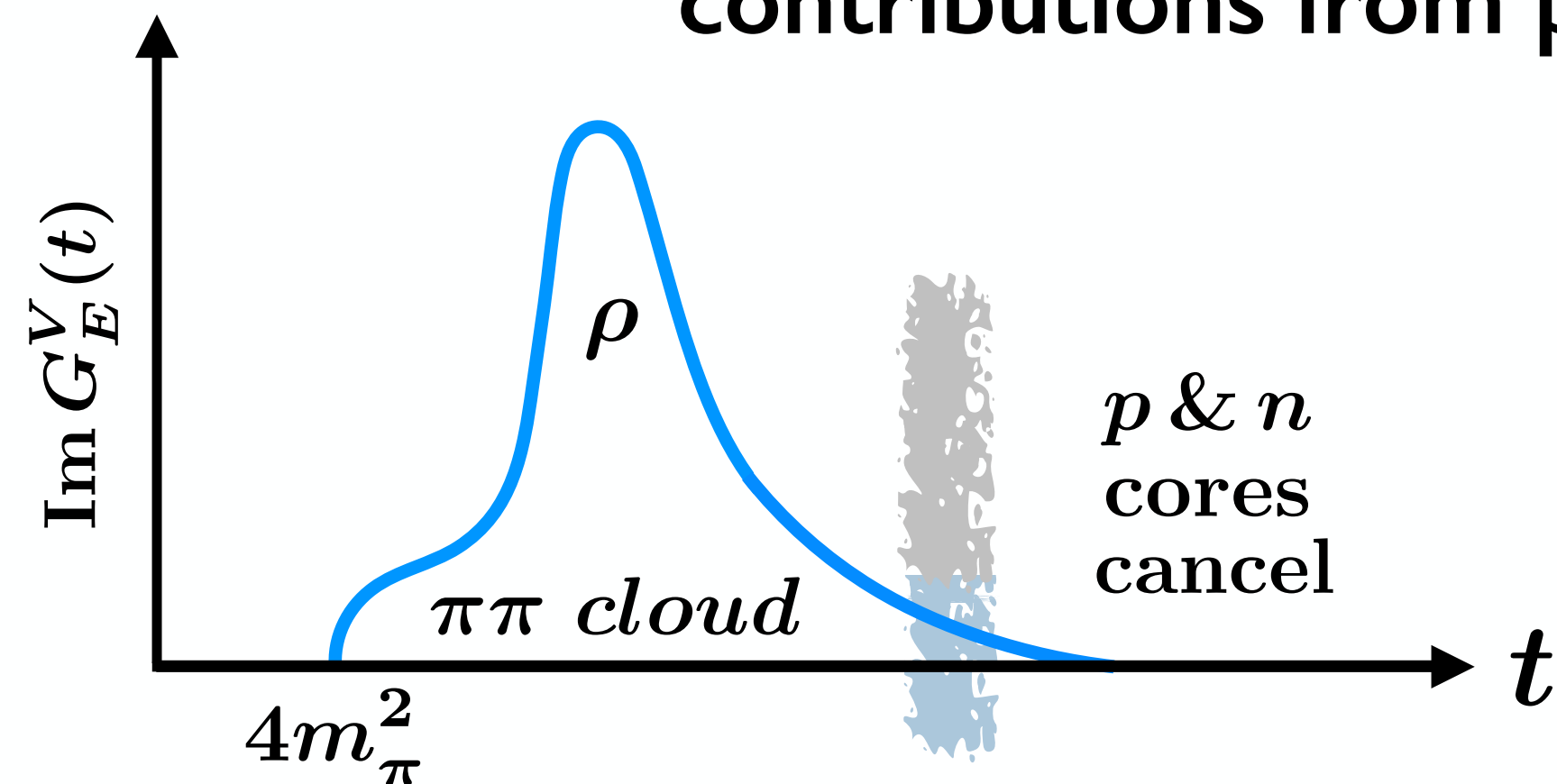
N. Kaiser, W.W.
Phys. Rev.
C110 (2024) 015202

Example II: ISOVECTOR ELECTRIC FORM FACTOR of the NUCLEON

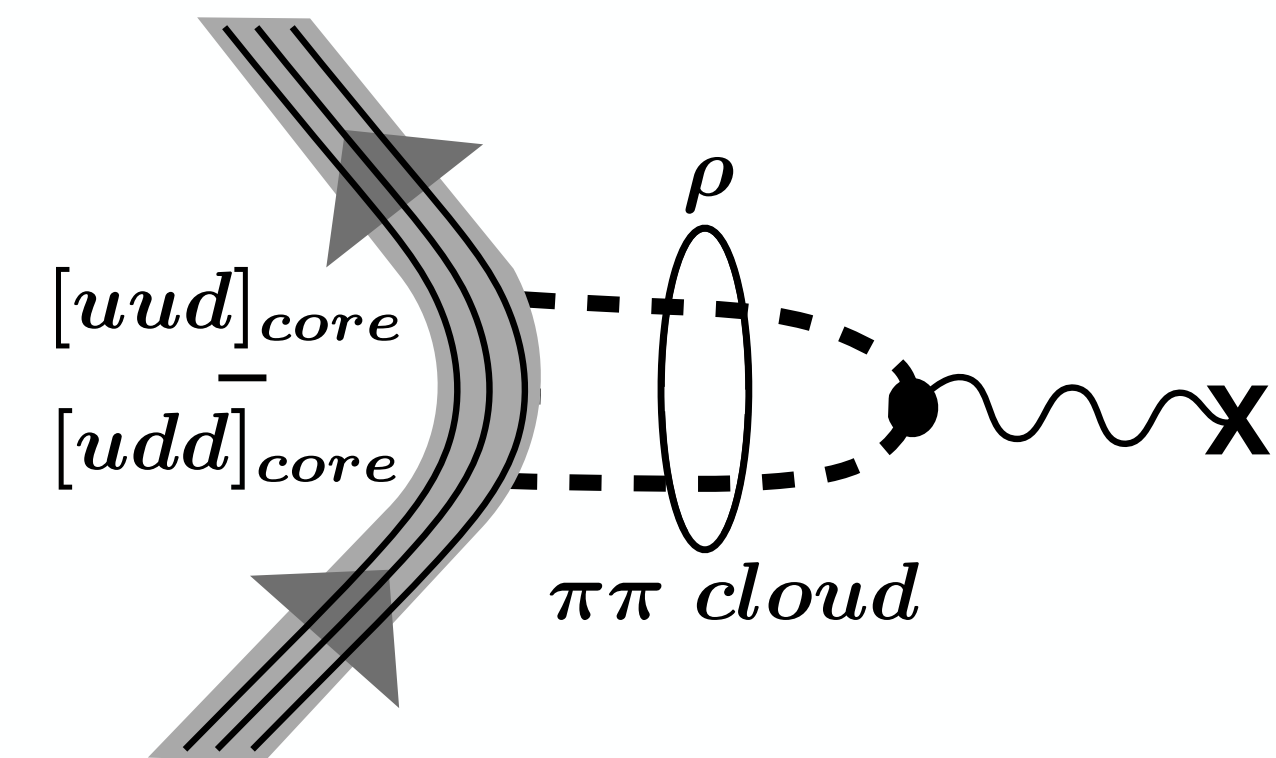
- Isovector electric form factor $G_E^V(q^2) = \frac{1}{2} [G_E^p(q^2) - G_E^n(q^2)]$ $\langle r_V^2 \rangle = \langle r_p^2 \rangle - \langle r_n^2 \rangle$

Empirical : $\langle r_V^2 \rangle^{1/2} = 0.901 \pm 0.009$ fm Y.H. Lin, H.-W. Hammer, U.-G. Meißner PRL 128 (2022) 052002

... clue and test case : in the limit of exact isospin symmetry, contributions from proton and neutron valence quark cores **CANCEL**



- Detailed analysis using best-fit spectral functions :

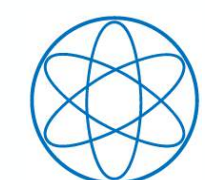


$$\langle r_V^2 \rangle_{core} = \langle r_p^2 \rangle_{core} - \langle r_n^2 \rangle_{core} = -0.025 \text{ fm}^2$$

... almost vanishing

- Isovector charge radius almost entirely determined by two-pion cloud

N. Kaiser, W.W. Phys. Rev. C110 (2024) 015202



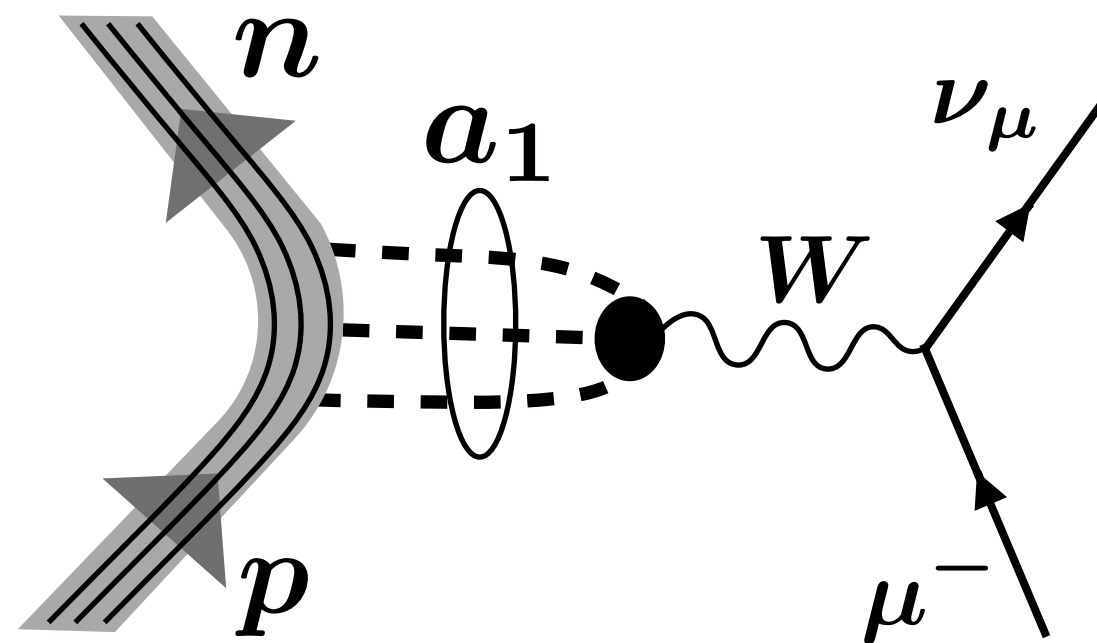
Example III: ISOVECTOR AXIAL FORM FACTOR of the NUCLEON

- Axial form factor** $G_A(q^2) = g_A \left[1 + \frac{1}{6} \langle r_A^2 \rangle q^2 + \dots \right]$

R.J. Hill, P. Kammel, W.C. Marciano, A. Sirlin
Rep. Prog. Phys. 81 (2018) 096301

Empirical :

a) $\langle r_A^2 \rangle = 0.454 \pm 0.013 \text{ fm}^2$
(from νd scattering and
 $ep \rightarrow en\pi^+$ dipole fits)



b) $\langle r_A^2 \rangle = 0.46 \pm 0.16 \text{ fm}^2$
(from μp capture and
 νd scattering analysis)

Axial radius significantly smaller than proton charge radius ($\langle r_p^2 \rangle = 0.71 \pm 0.01 \text{ fm}^2$)

- Detailed analysis using three-pion spectrum dominated by broad a_1 meson :**

$$\langle r_A^2 \rangle = \langle r_A^2 \rangle_{core} + \frac{6}{m_a^2} (1 + \delta_a) \quad \delta_a = -\frac{m_a^3}{\pi} \int_{9m_\pi^2}^{t_{max}} dt \frac{\Gamma_a(t)}{t^2(t - m_a^2)}$$

→ $\langle r_A^2 \rangle_{core}^{1/2} = 0.53 \pm 0.02 \text{ fm}$

N. Kaiser, W.W.
Phys. Rev. C 110 (2024) 015202

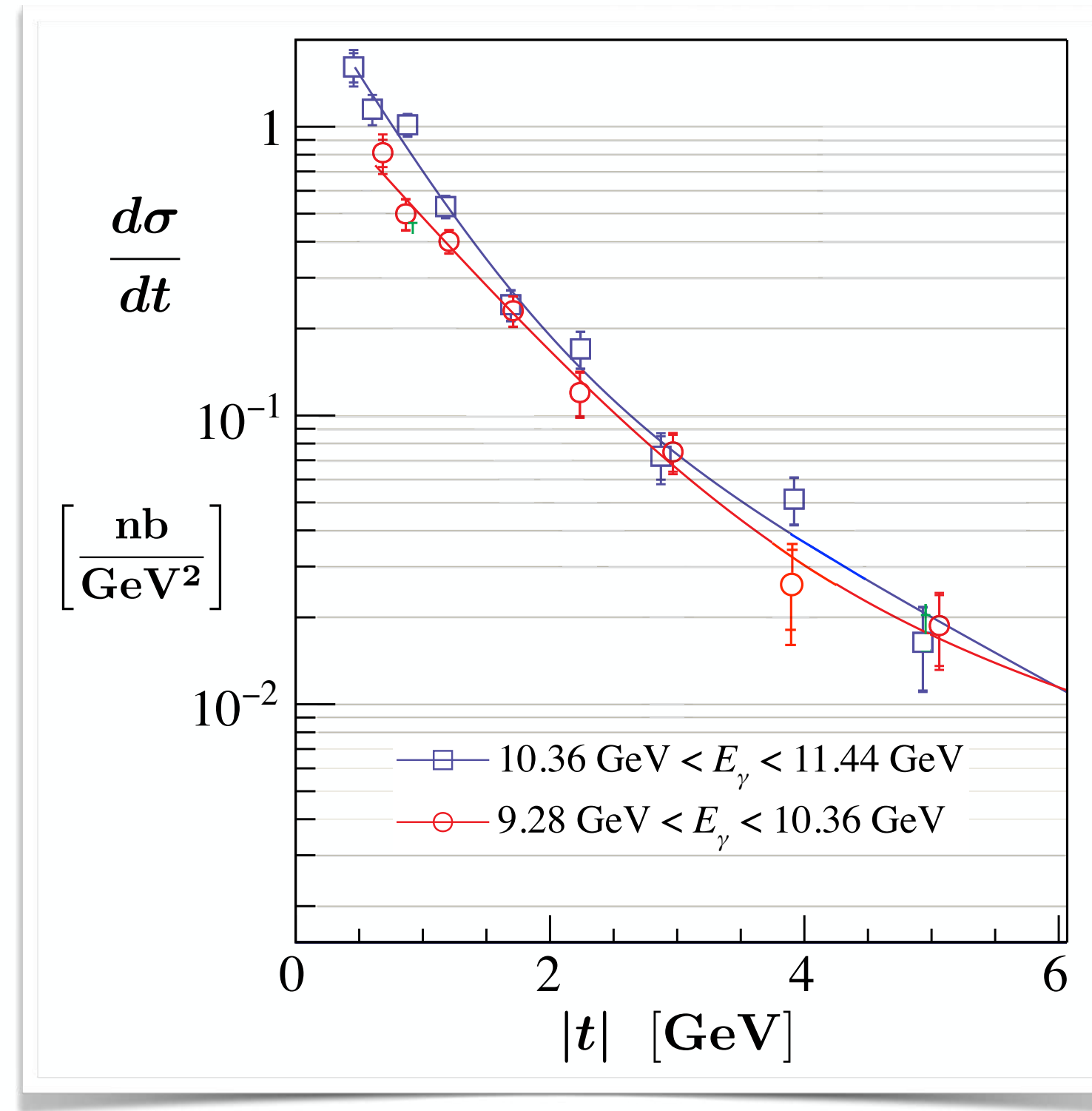
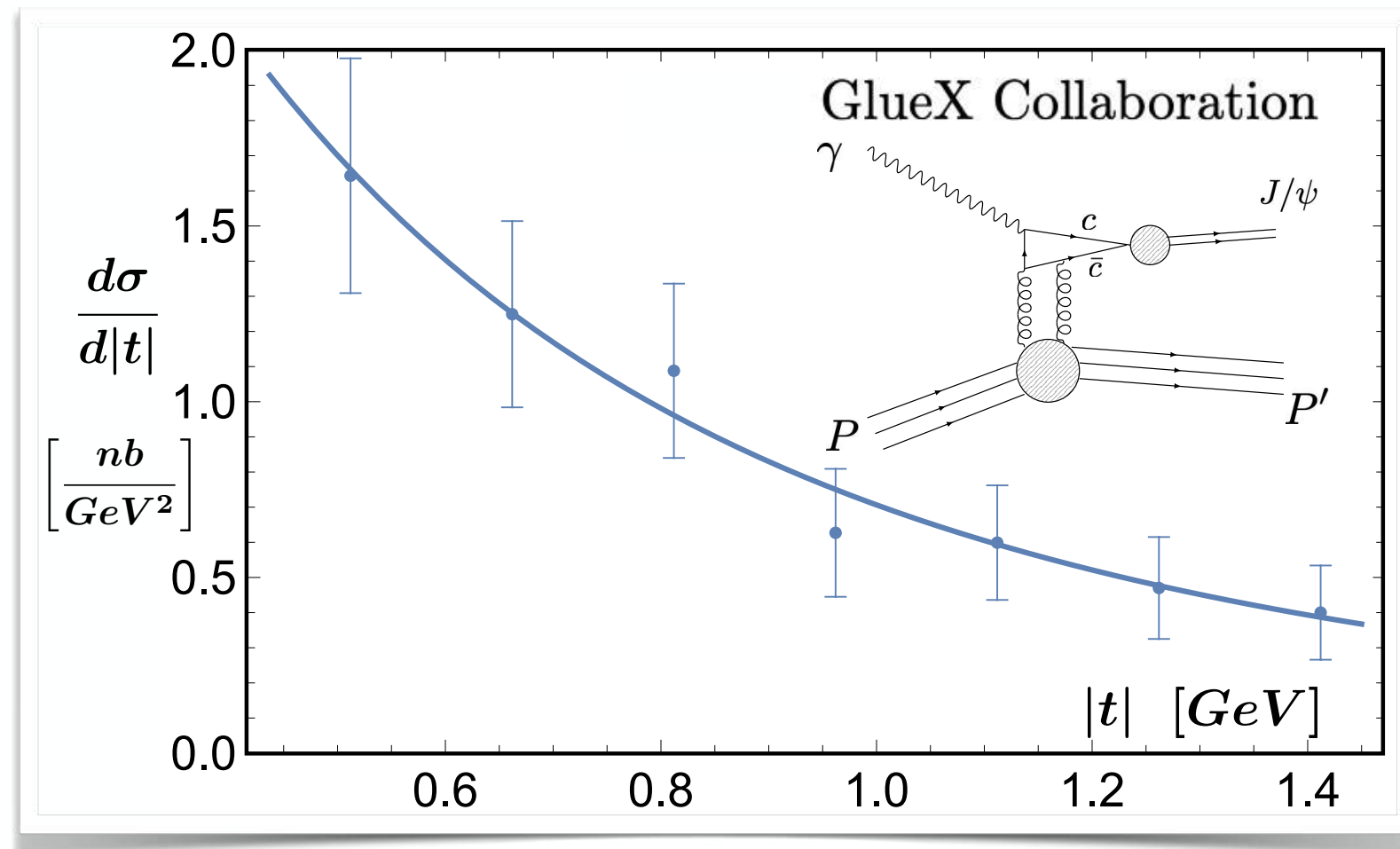
(based on a) — correspondingly larger uncertainty when using b))

Example IV: MASS RADIUS of the NUCLEON

- Mass (“gravitational”) form factor

- Trace of QCD energy-momentum tensor

$$G_m(q^2) = \langle P' | T_\mu^\mu | P \rangle = \langle P' | \frac{\beta(g)}{2g} G_a^{\mu\nu} G_{\mu\nu}^a + m_q(\bar{u}u + \bar{d}d) + m_s\bar{s}s | P \rangle$$



$$G_m(0) = M_N \simeq 0.94 \text{ GeV}$$

$$M_N = M_0 + \sigma_N + \sigma_s$$

$$(M_0 \gtrsim 0.9 M_N)$$

$$\langle r_m^2 \rangle = \frac{6}{M_N} \left. \frac{dG_m(q^2)}{dq^2} \right|_{q^2=0}$$

$$\langle r_m^2 \rangle^{1/2} = (0.53 \pm 0.04) \text{ fm}$$

- Empirical mass radius

$$\langle r_m^2 \rangle^{1/2} = (0.55 \pm 0.03) \text{ fm}$$

D. Kharzeev : Phys. Rev. D104 (2021) 054015

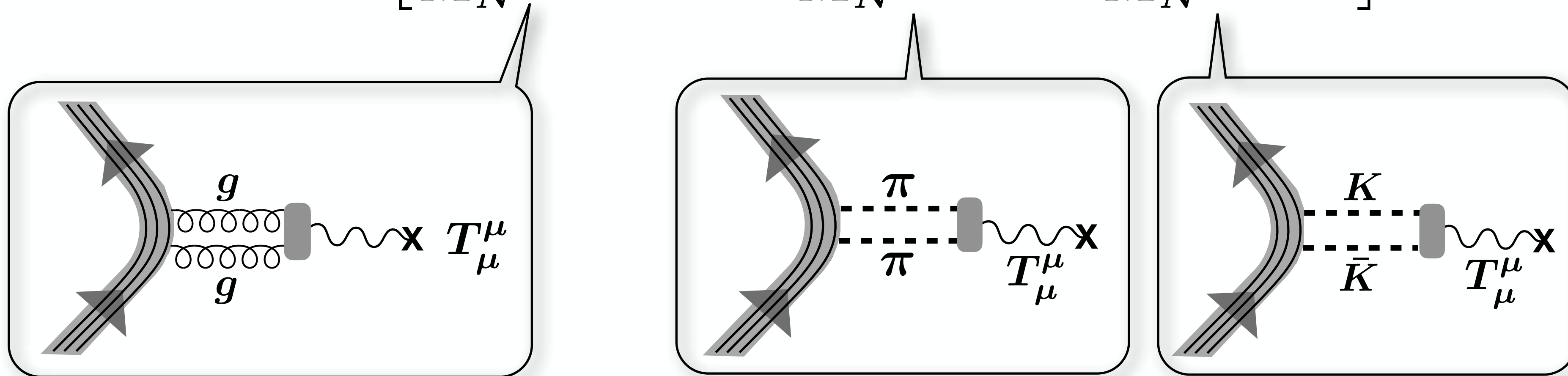
Recent GlueX update:

S. Adhikari et al. ; arXiv:2304.03845

Example IV: MASS RADIUS of the NUCLEON (contd.)

- Core (**gluon**) dominance plus small corrections from sigma terms

$$\langle r_m^2 \rangle = \left[\frac{M_0}{M_N} \langle r_m^2 \rangle_{core} + \frac{\sigma_N}{M_N} \langle r_{\pi\pi}^2 \rangle + \frac{\sigma_s}{M_N} \langle r_{K\bar{K}}^2 \rangle \right]$$



- Estimates of sigma terms and associated radii from Lattice QCD and ChPT

$$\sigma_N \simeq 40 - 60 \text{ MeV} , \quad \sigma_s \simeq 30 \text{ MeV} \quad \langle r_{\pi\pi}^2 \rangle^{1/2} \simeq 1.3 \text{ fm} , \quad \langle r_{K\bar{K}}^2 \rangle \sim (m_\pi/m_K)^2 \langle r_{\pi\pi}^2 \rangle$$

→ $\langle r_m^2 \rangle_{core}^{1/2} = 0.48 \pm 0.05 \text{ fm}$

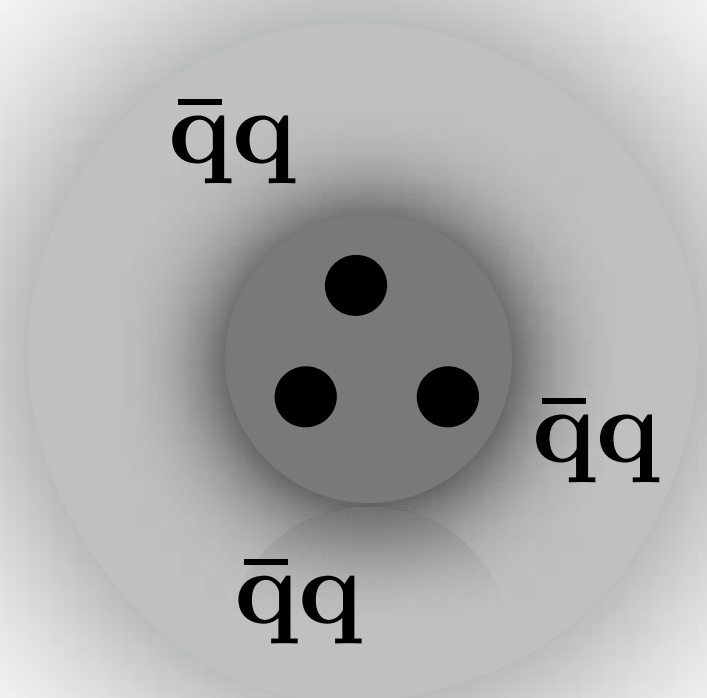
N. Kaiser, W.W.
Phys. Rev. C110 (2024) 015202

TWO-SCALES Picture of the NUCLEON : Implications for DENSE BARYONIC MATTER

$$\langle r_S^2 \rangle_{core}^{1/2} \simeq \langle r_A^2 \rangle_{core}^{1/2} \simeq \langle r_m^2 \rangle_{core}^{1/2} \equiv R_{core} \simeq \frac{1}{2} \text{ fm}$$

$$R_{core} \sim \frac{1}{2} \text{ fm}$$

$$R_{cloud} \sim 1 \text{ fm}$$



- **Separation of scales**

$$\left(\frac{R_{cloud}}{R_{core}} \right)^3 \gg 1$$

- **Soft mesonic (multi-pion) cloud**

expected to **expand** with increasing baryon density along with

decreasing in-medium pion decay constant $f_\pi^*(n_B)$

- **Hard baryonic core governed by gluon dynamics**

expected to remain **stable** with increasing baryon density up until

hard compact cores begin to touch and overlap

TWO-SCALES Scenario for DENSE BARYONIC MATTER

- Baryon densities

$$n_B \sim n_0 = 0.16 \text{ fm}^{-3}$$

tails of mesonic clouds overlap :
two-body exchange forces
between nucleons

- $n_B \gtrsim 2 - 3 n_0$

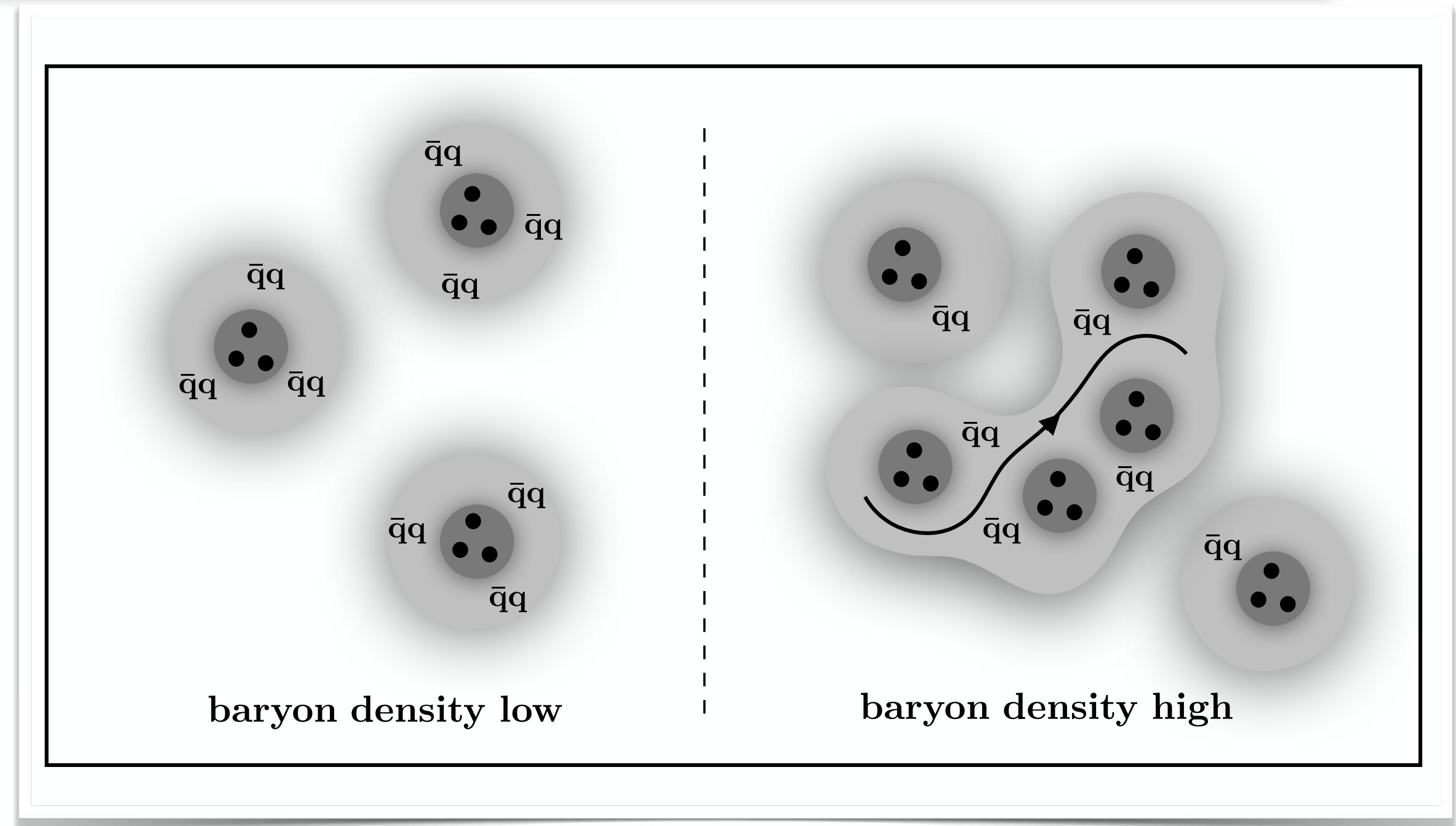
Soft $\bar{q}q$ clouds delocalize:

percolation → many-body forces

baryonic cores still separated, but subject to increasingly strong repulsive Pauli effects

- $n_B > 5 n_0$ (beyond central densities of neutron stars)

compact nucleon cores begin to touch and overlap at distances $d \lesssim 1 \text{ fm}$
(but still have to overcome repulsive NN hard core)



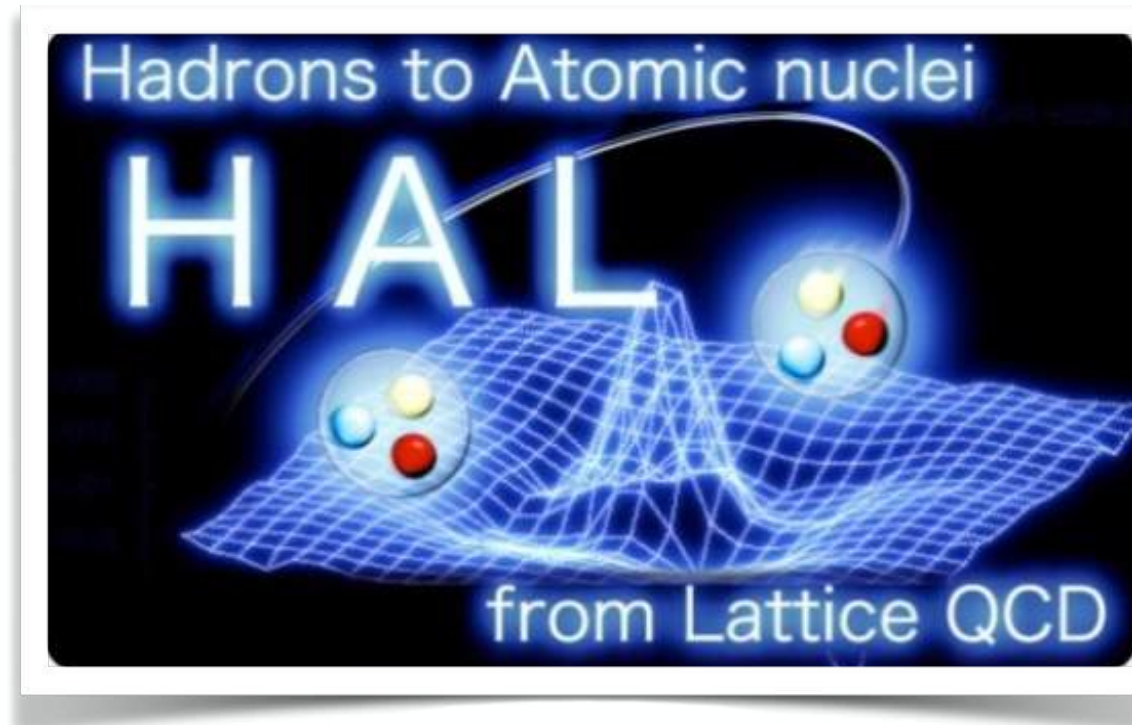
K. Fukushima, T. Kojo, W.W.
Phys. Rev. D 102 (2020) 096017

Key words: **hadron-quark continuity** and **crossover**

NUCLEAR FORCES from LATTICE QCD

NN Central Potential ($S = 0, l = 1$)

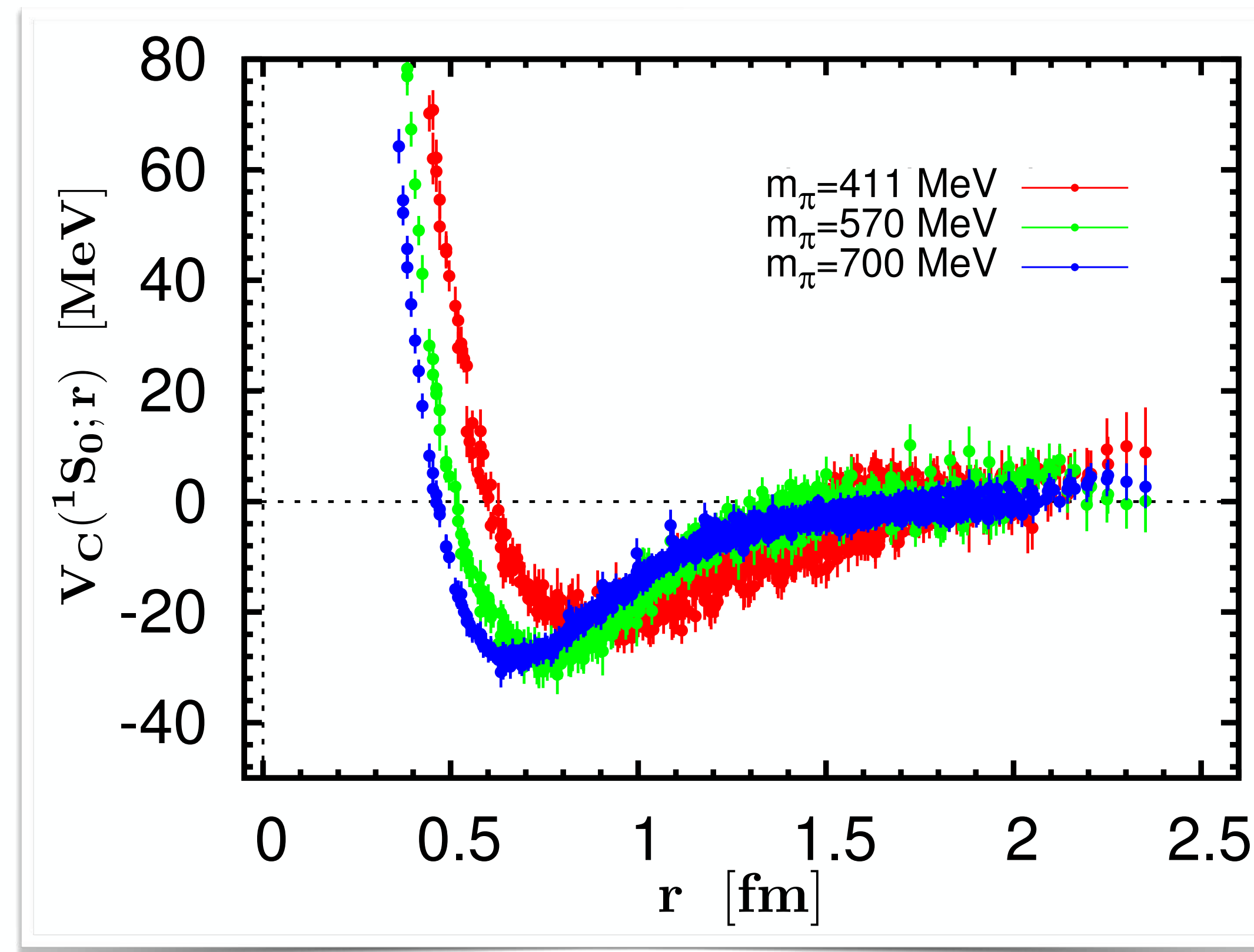
deduced from LQCD two-nucleon (6-quark) correlation function



S.Aoki, T. Hatsuda, N. Ishii
Prog. Theor. Phys. 123 (2010) 89

S.Aoki
Eur. Phys. J. A49 (2013) 81

S.Aoki, T. Doi
arXiv:2402.11759

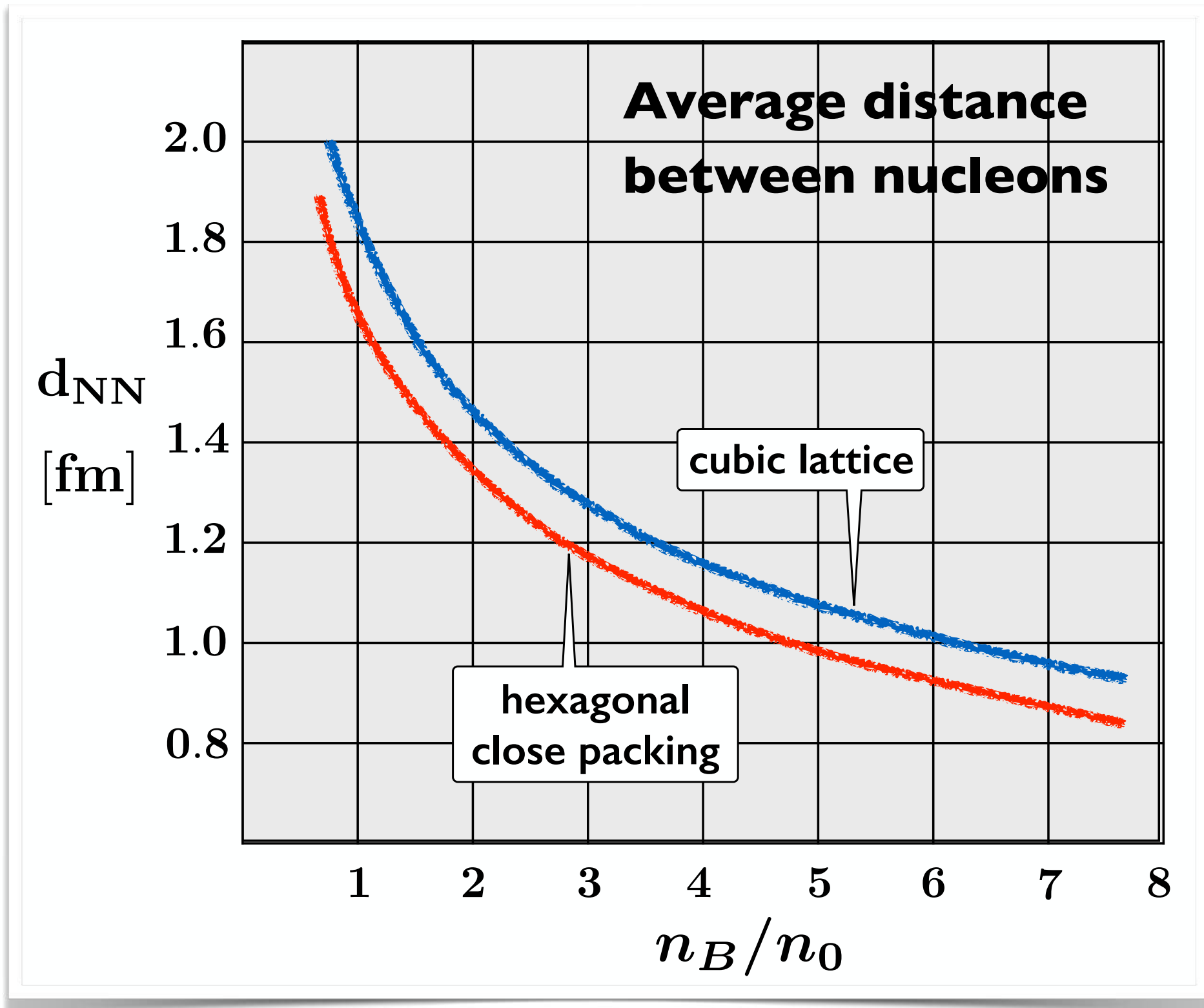


Nuclear Physics
Phenomenology:

Short-Range
Repulsive Core

- **Compression of baryonic matter is energetically expensive**

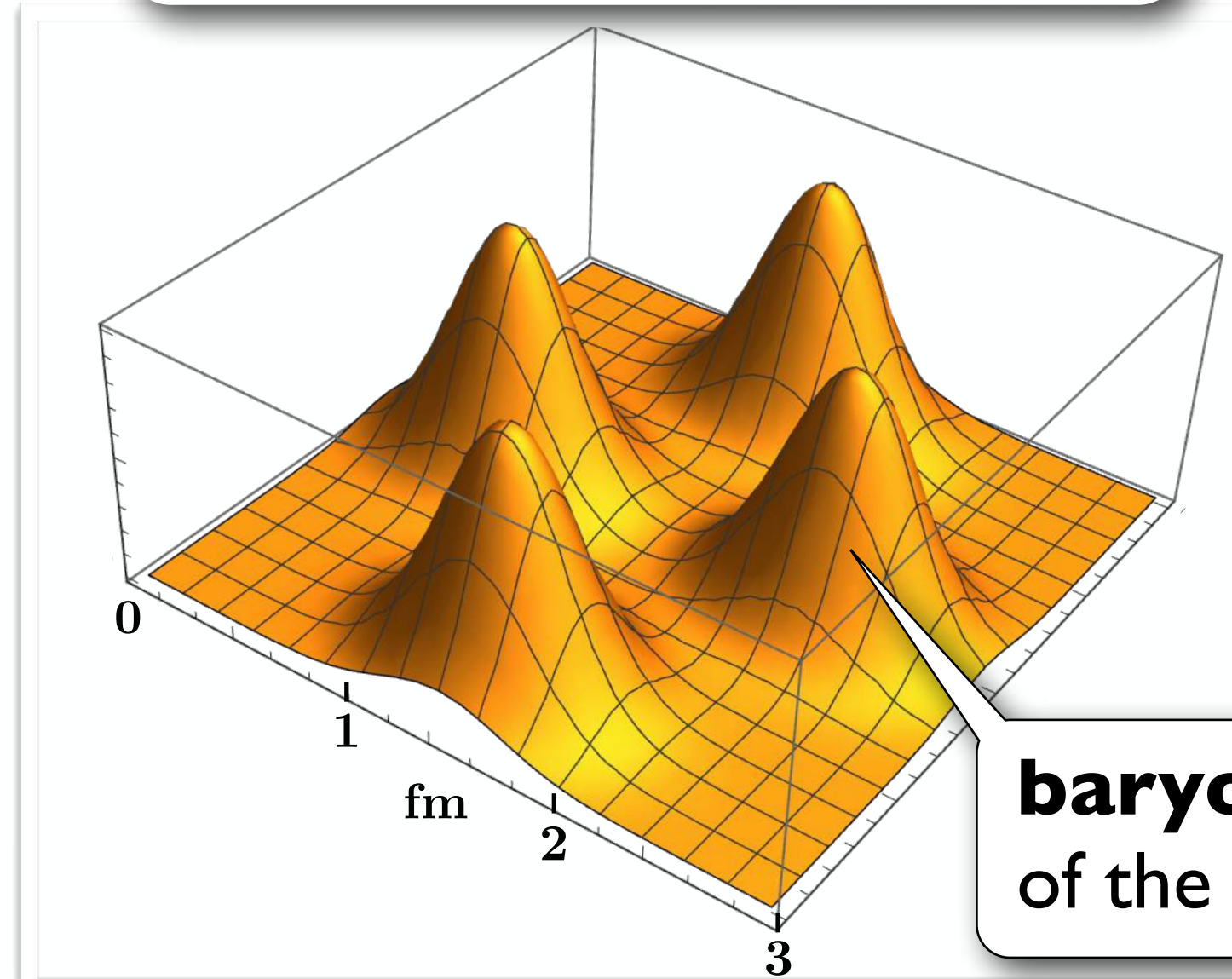
Densities and Distance Scales in Baryonic Matter



normal nuclear matter

$$n_B \simeq n_0 = 0.16 \text{ fm}^{-3}$$

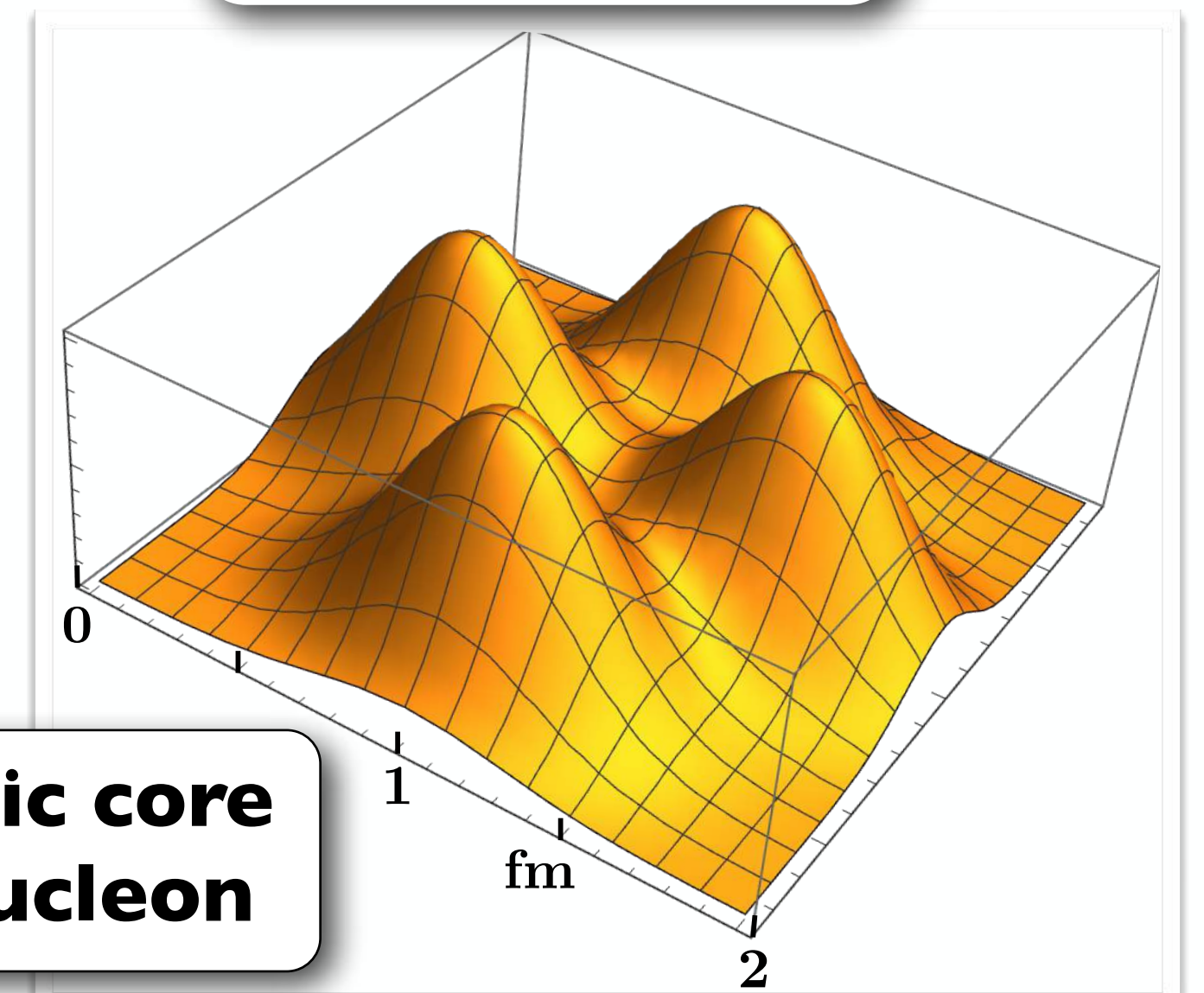
$$d_{NN} \simeq 1.7 \text{ fm}$$



neutron star core matter

$$n_B \sim 4 n_0$$

$$d_{NN} \gtrsim 1 \text{ fm}$$



- (Multi-) pion fields populate space between baryonic sources
- **Quark cores of nucleons start overlapping at baryon densities $n_B > 5 n_0$**
- **Reminder: Density at random close packing of spheres (radius R) : $n_{cp} \simeq 0.16/R^3$**

6.

*Chiral Effective Field Theory,
Nuclear Many-Body Problem
and
Dense Baryonic Matter*



Minimal Conditions to be satisfied by theories of Dense Baryonic Matter

★ Vacuum :

- Low-energy theorems of spontaneously broken **CHIRAL SYMMETRY** (Gell-Mann, Oakes, Renner ; Goldberger-Treiman ; ...)
- Low-energy pion-pion and pion-nucleon scattering
- Realistic nucleon-nucleon interaction

★ Low density ($n_B \lesssim 1.5 n_0$) :

- Realistic EoS of symmetric nuclear matter and neutron matter
- Asymmetric nuclear matter and symmetry energy
- Nuclear thermodynamics : liquid-gas phase transition

★ High density :

- Neutron star maximum mass $M_{max} \gtrsim 2 M_\odot$
- Neutron star radii (NICER) $11 \text{ km} \lesssim R \lesssim 13 \text{ km}$
- Tidal deformability constraints from neutron star mergers (GW signals)



Physics at low densities and temperatures :
PIONS and **NUCLEI** in the context of **LOW-ENERGY QCD**

- **CONFINEMENT** of quarks and gluons in hadrons
 - Spontaneously broken **CHIRAL SYMMETRY**



LOW-ENERGY QCD

at (energy and momentum) scales $Q < 4\pi f_\pi \sim 1 \text{ GeV}$ is realised as an

Effective **F**ield **T**heory

of Nambu-Goldstone Bosons (**PIONS**) coupled to
NUCLEONS as (heavy) Fermion sources



CHIRAL EFFECTIVE FIELD THEORIES and MODELS

- Underlying symmetries and symmetry breaking pattern

$$\mathrm{SU}(2)_L \times \mathrm{SU}(2)_R \rightarrow \mathrm{SU}(2)_{\text{Isospin}}$$

- **Pions and Nucleons** as active degrees of freedom in a **Nuclear Fermi Sea**

- Perturbative methods:
Chiral Effective Field Theory
and
Nuclear Many-Body Problem
(baryon densities $n_B \lesssim 1.5 n_0$)

- Non-perturbative methods:
Chiral Nucleon-Meson Field Theory
and
Functional Renormalisation Group
(towards higher densities : $n_B \lesssim 5 n_0$)

NUCLEON-NUCLEON INTERACTION

from CHIRAL EFFECTIVE FIELD THEORY

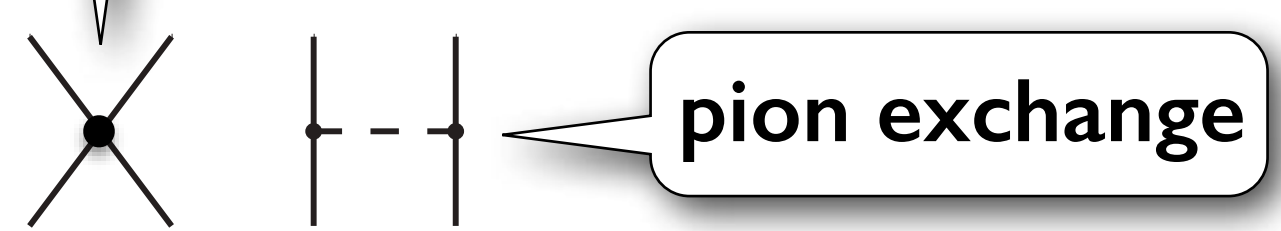
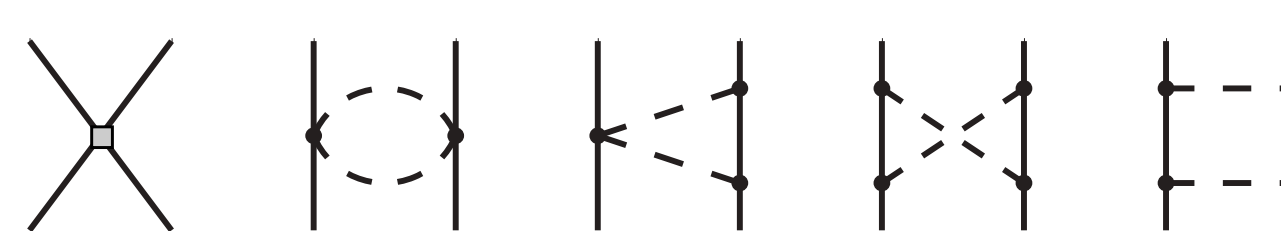

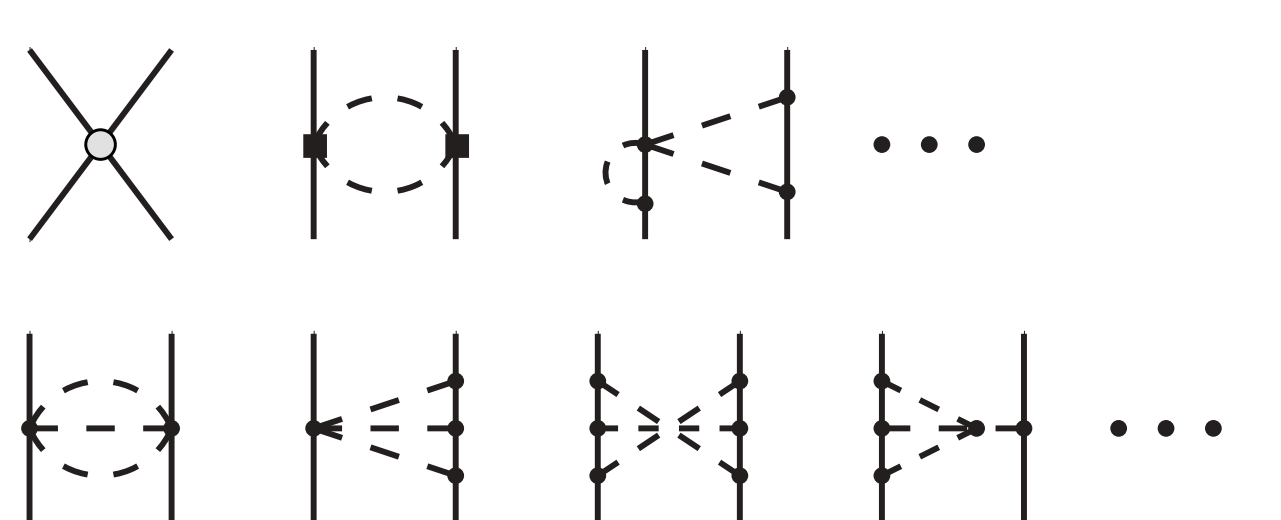
Weinberg

Bedaque & van Kolck

Bernard, Epelbaum, Kaiser, Meißner

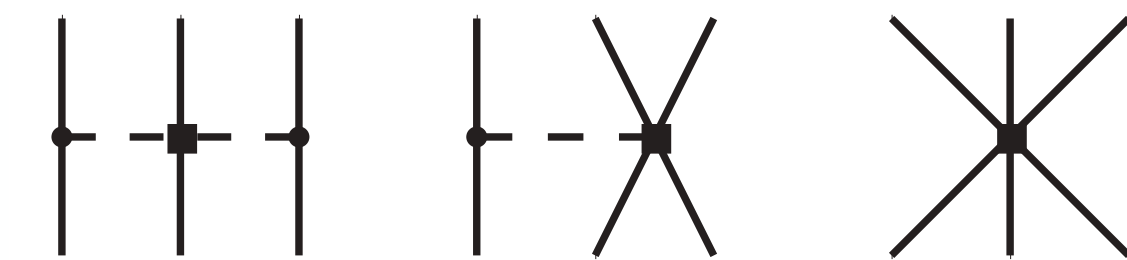
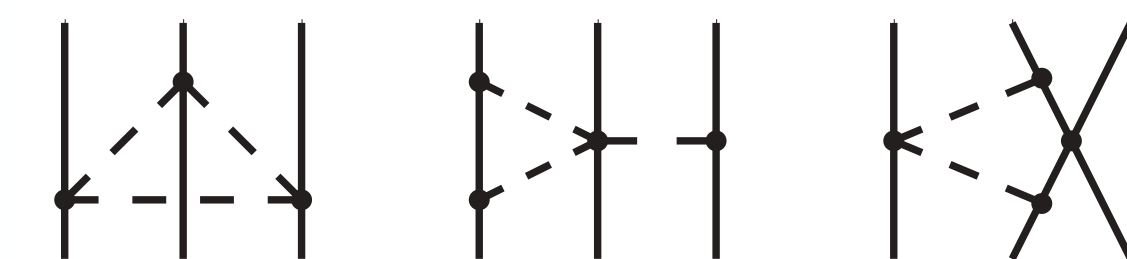
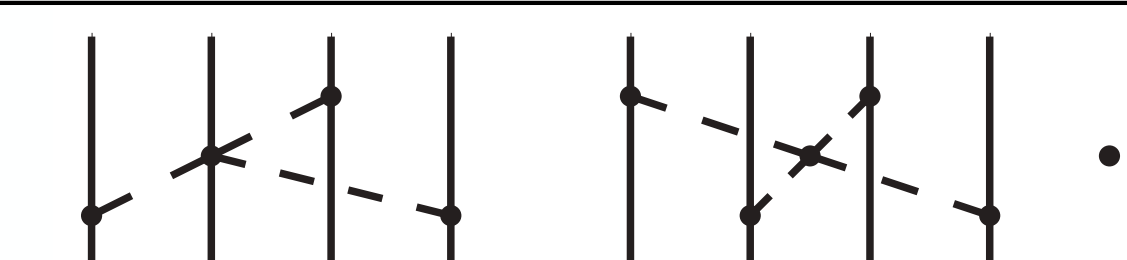
short distance contact terms

NN interaction

LO	
NLO	
N ² LO	
N ³ LO	

pion exchange

- Systematically organized hierarchy in powers of $\frac{Q}{\Lambda}$
 (Q: momentum, energy, pion mass ; $\Lambda < \Lambda_\chi = 4\pi f_\pi$)

3 – body forces	
N ² LO	
N ³ LO	
4 – body forces	
N ³ LO	

- NN interaction state-of-the-art: N⁴LO
 plus convergence tests at N⁵LO



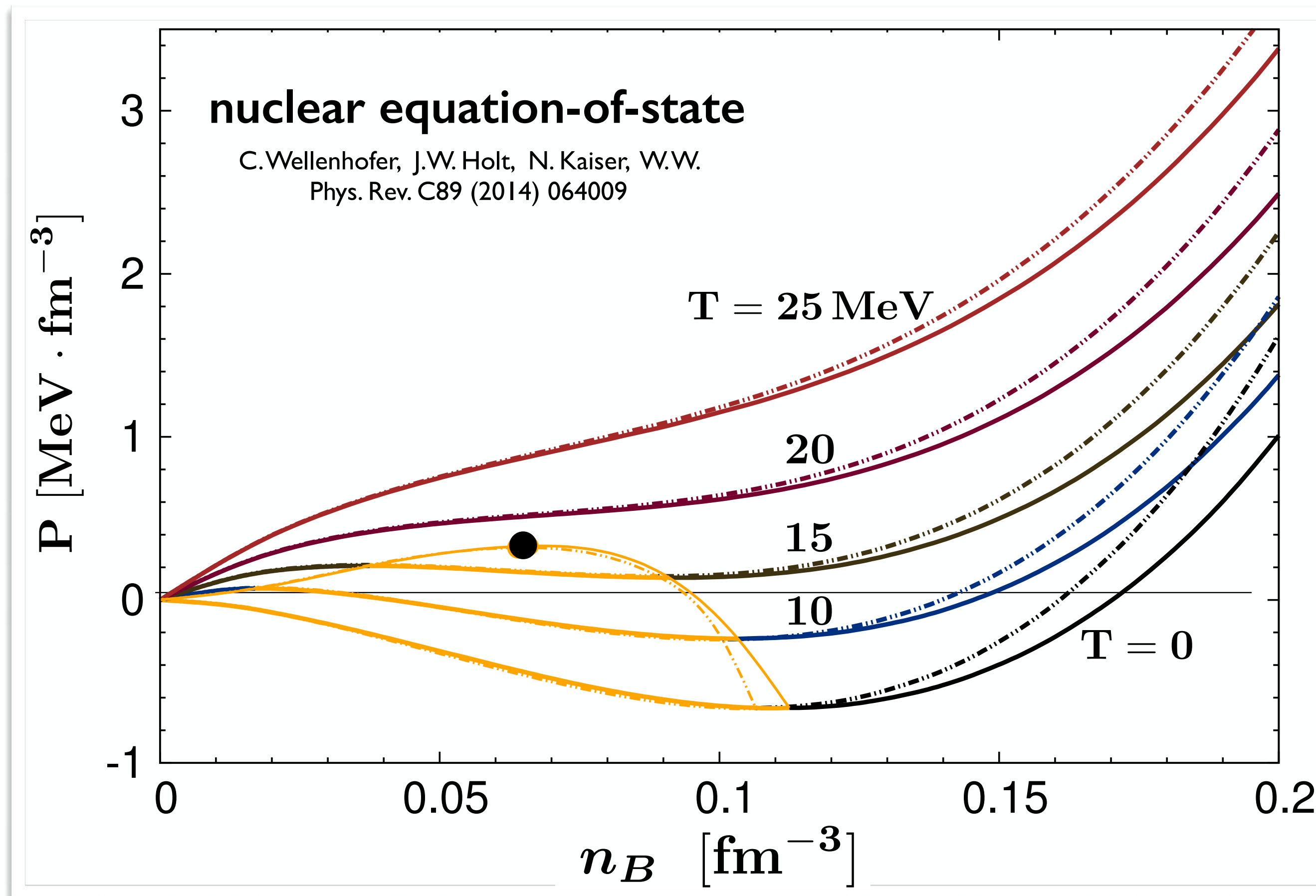
NUCLEAR THERMODYNAMICS from CHIRAL EFT

- Symmetric nuclear matter : first-order liquid-gas phase transition
- **N3LO chiral NN interactions + N2LO 3-body forces**
Finite - T many-body perturbation theory calculations

Critical temperature of liquid-gas first-order transition :

$$T_c = 17.4 \text{ MeV}$$

C. Wellenhofer, J.W. Holt, N. Kaiser,
Phys. Rev. C92 (2015) 015801



Empirical position of liquid-gas critical point :

$$T_c = 17.9 \pm 0.4 \text{ MeV}$$

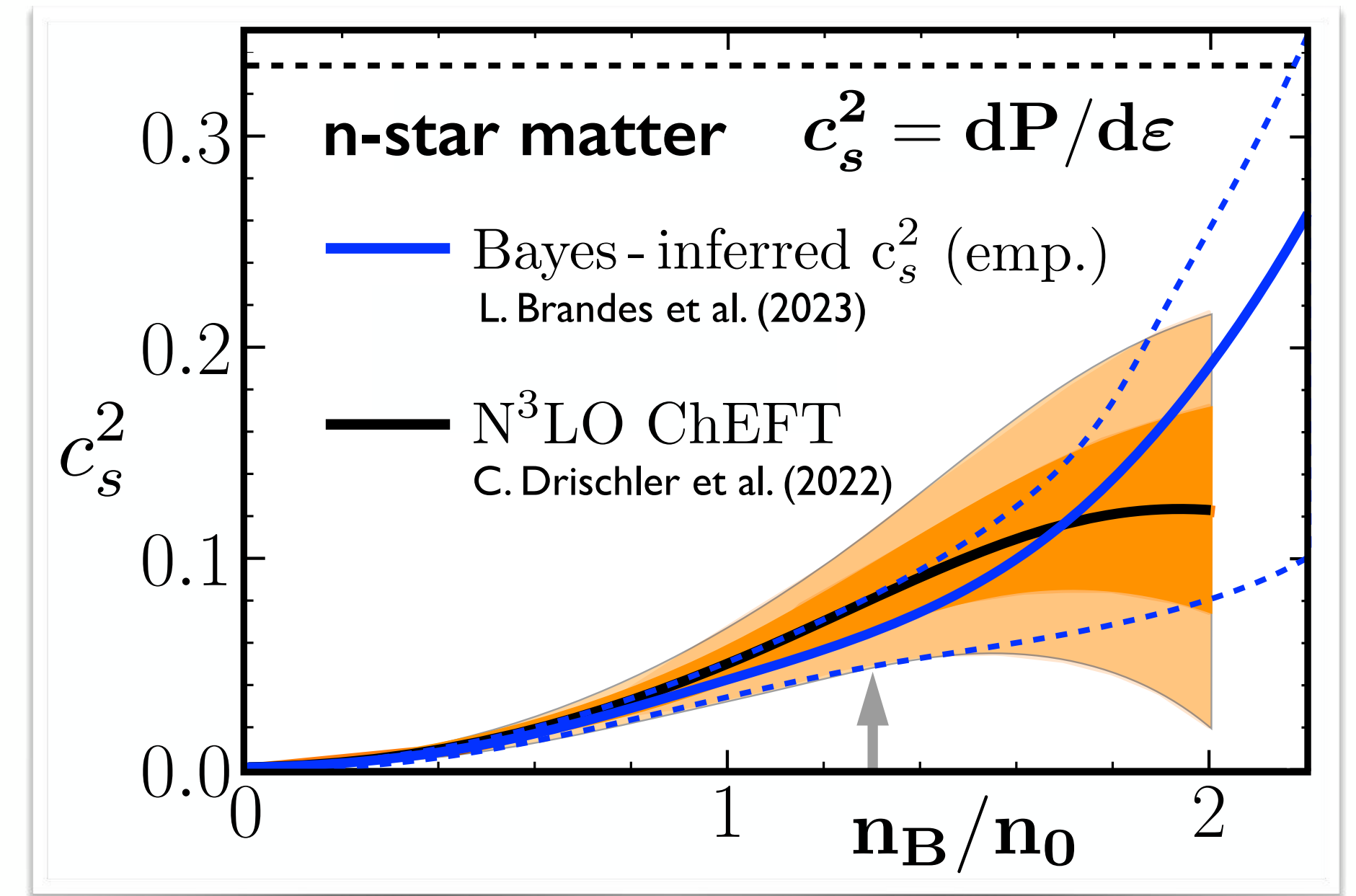
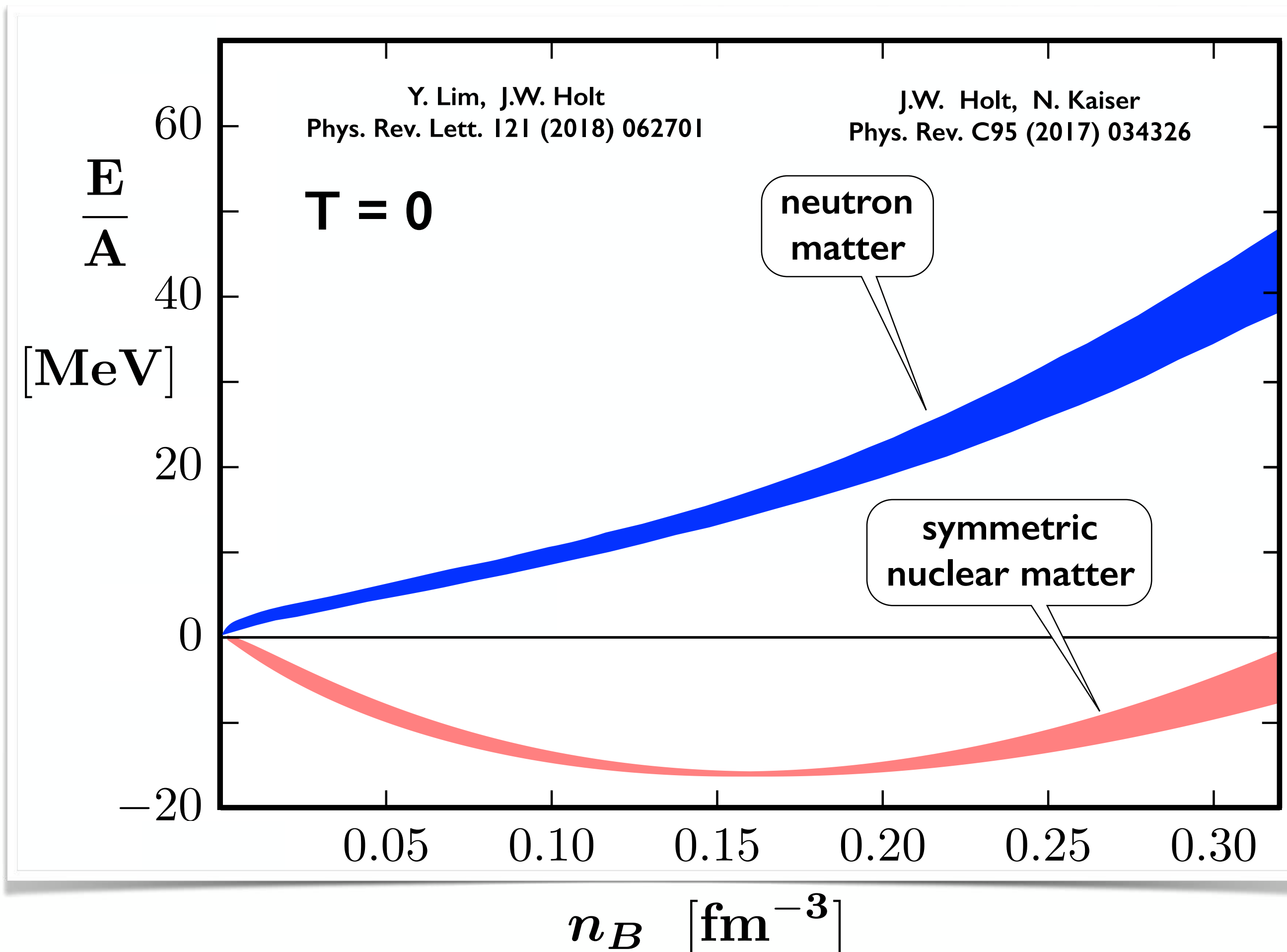
$$n_c = 0.06 \pm 0.01 \text{ fm}^{-3}$$

$$P_c = 0.31 \pm 0.07 \frac{\text{MeV}}{\text{fm}^3}$$

J. B. Elliot et al.
Phys. Rev. C87 (2013) 054622

NEUTRON and NUCLEAR MATTER from CHIRAL EFT

- **N3LO chiral NN interactions + N2LO 3-body forces**
- **Many-body perturbation theory (3rd order)**



- **Perturbative Chiral EFT :**
applicable up to baryon densities
 $n_B \lesssim 1.5 n_0$

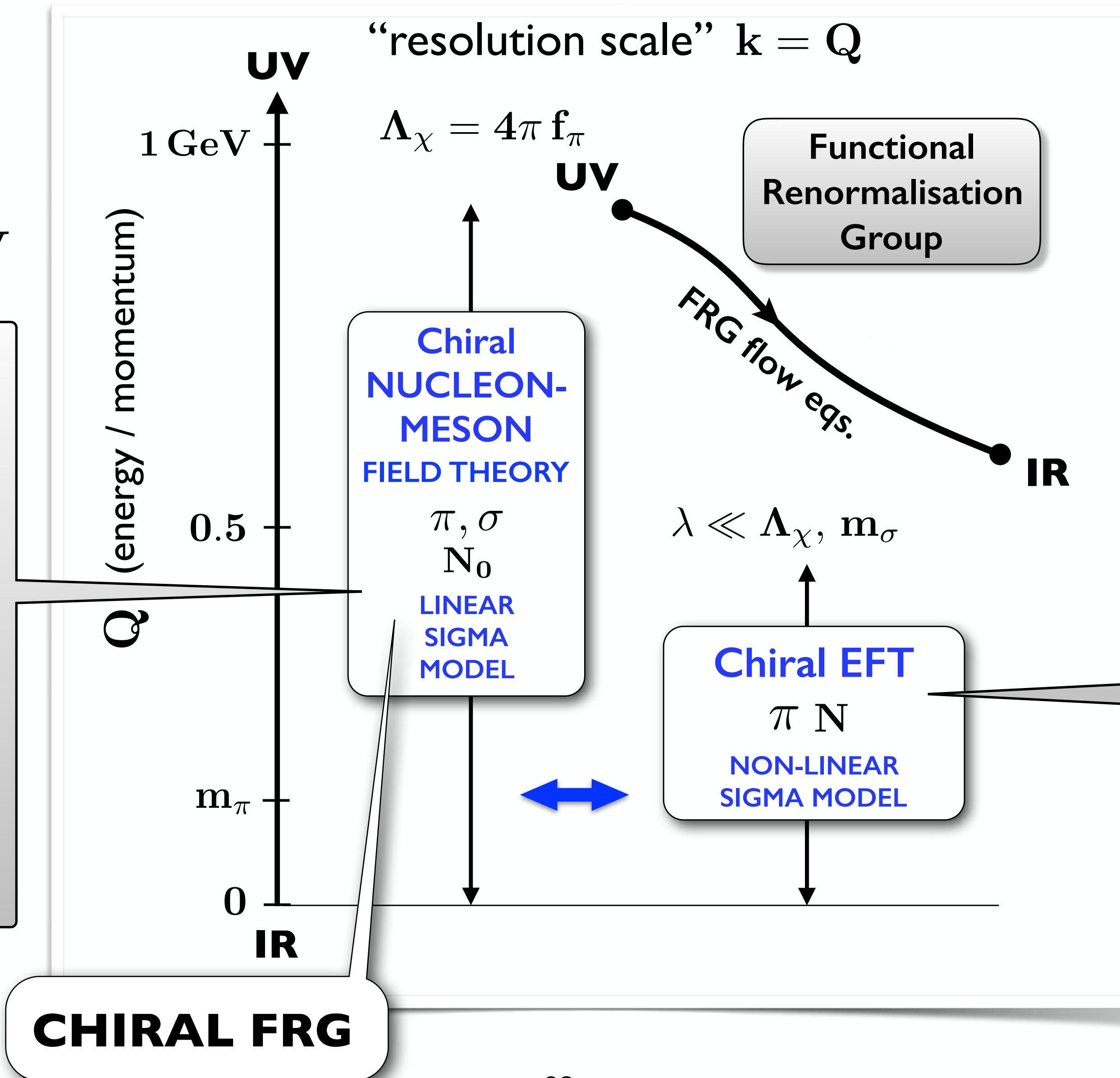
Theoretical FRAMEWORKS and METHODS

- **UV** initialization at :

$$\Lambda_{UV} \gtrsim$$

$$\Lambda_\chi = 4\pi f_\pi \sim 1 \text{ GeV}$$

Non-perturbative methods:
Chiral Nucleon-Meson Field Theory
 and
Functional Renormalisation Group
 towards high densities
 $n_B \lesssim 5 n_0$



Perturbative methods:
Chiral Effective Field Theory
 and
 Nuclear Many-Body Problem
 baryon densities
 $n_B \lesssim 1.5 n_0$

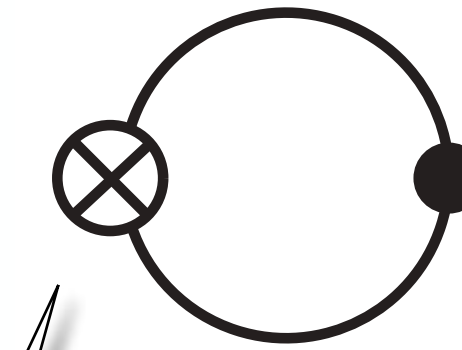
- **IR** limit : $Q \rightarrow 0$
 full effective action

Renormalisation Group strategies

k-dependent action

Wetterich's FRG flow equations

$$k \frac{\partial \Gamma_k[\Phi]}{\partial k} = \frac{1}{2} \text{Tr} \left[k \frac{\partial R_k}{\partial k} \cdot \left(\Gamma_k^{(2)}[\Phi] + R_k \right)^{-1} \right]$$



full propagator

$$\Gamma_{k=\Lambda}[\Phi] = S$$

UV

$\Gamma_k[\Phi]$

IR

$$\Gamma_{k=0}[\Phi] = \Gamma[\Phi]$$

scale regulator R_k

C. Wetterich
Phys. Lett. B 301 (1993) 90

Thermodynamics :

$$k \partial_k \bar{\Gamma}_k(T, \mu) = \left(\text{diagram with nucleon and pion loops} \right) \Big|_{T, \mu}$$

$$- \left(\text{diagram with nucleon and pion loops} \right) \Big|_{T=0, \mu=\mu_c}$$

nucleons

pions

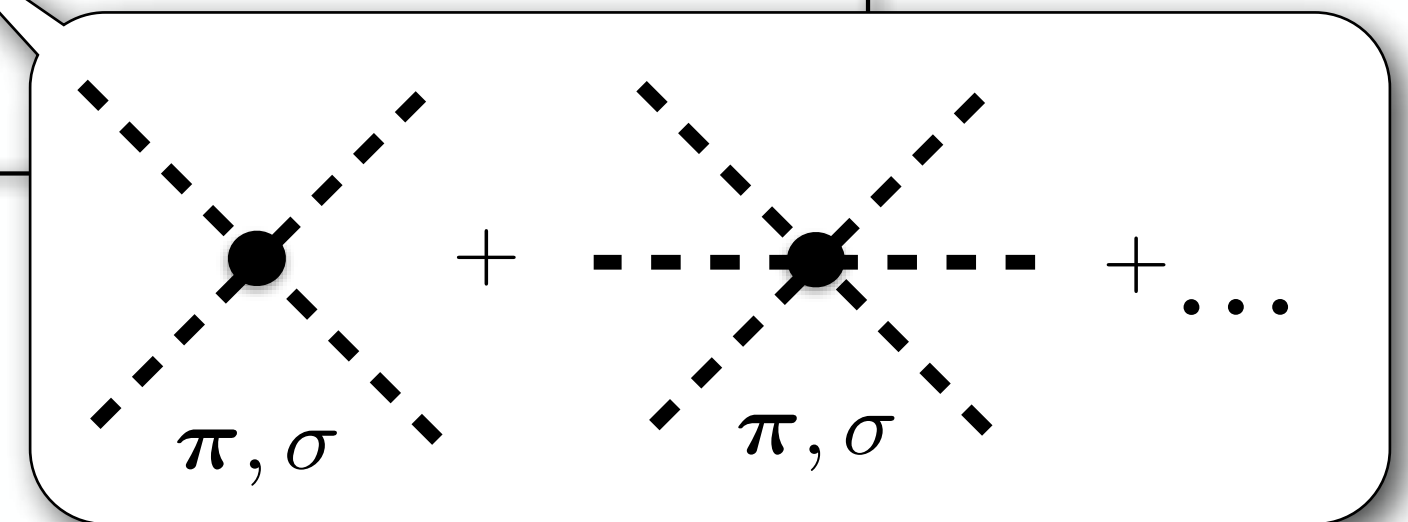
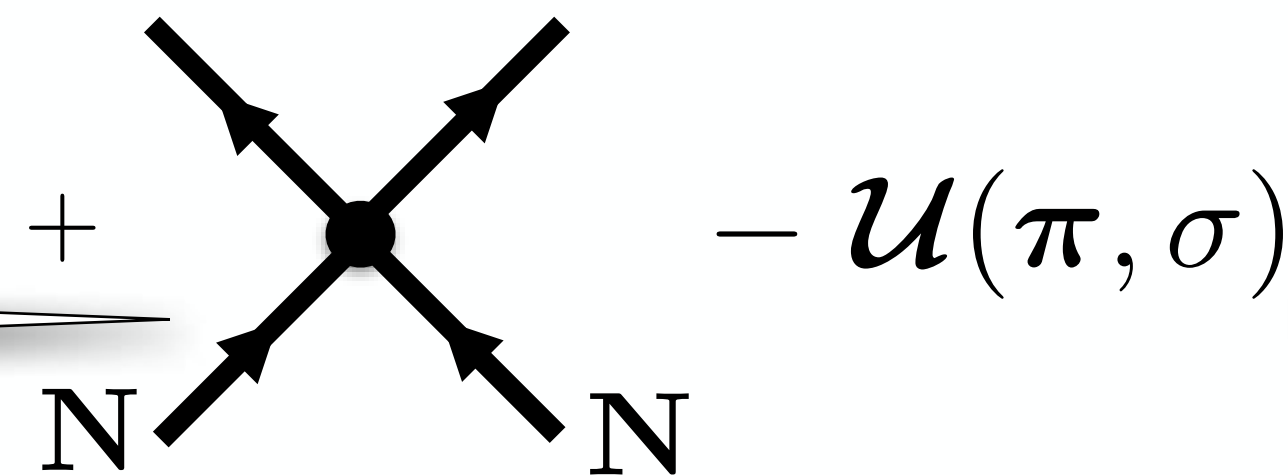
- **multi-pion exchange** processes
- **nucleonic** excitations of Fermi sea
- **multi-nucleon** correlations

Mesons, Nucleons, Nuclear Matter and Functional Renormalization Group

- **Chiral Nucleon - Meson Lagrangian**

$$\mathcal{L} = \bar{\mathbf{N}} i \gamma_\mu \partial^\mu \mathbf{N} + \frac{1}{2} (\partial_\mu \sigma \partial^\mu \sigma + \partial_\mu \boldsymbol{\pi} \cdot \partial^\mu \boldsymbol{\pi}) + \text{---} \pi, \sigma \text{---} \bullet \begin{cases} \nearrow \mathbf{N} \\ \searrow \mathbf{N} \end{cases}$$

isoscalar & isovector current-current interactions



- **Nambu-Goldstone bosons π and “heavy” σ**
- **Potential $\mathcal{U}(\sigma, \pi)$: Polynomial** in $\chi = \pi^2 + \sigma^2$
constructed to reproduce **vacuum physics** and **equilibrium nuclear matter**

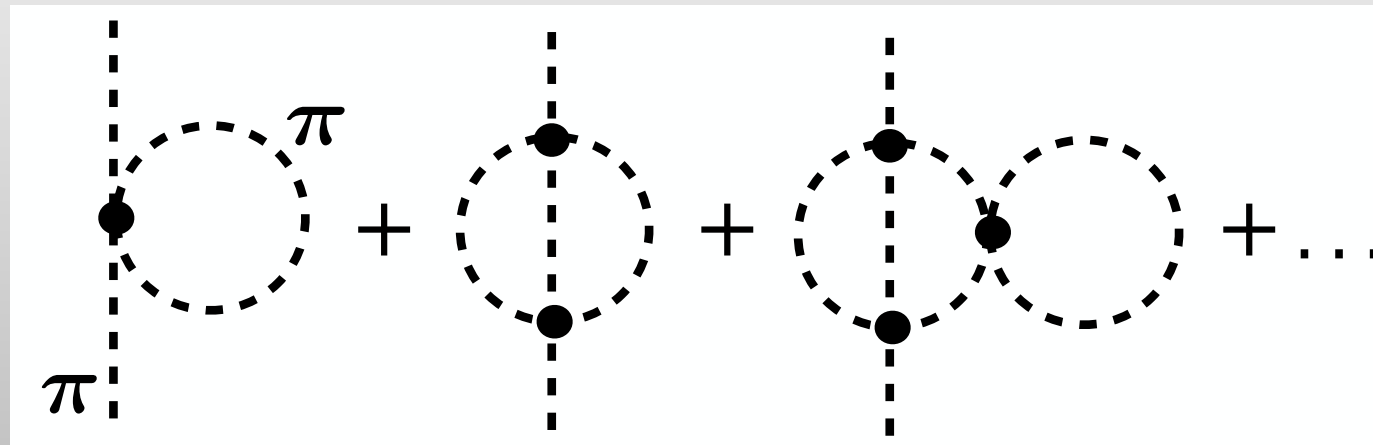
- **Pionic fluctuations**, **nucleonic particle-hole excitations** and **many-body correlations** treated **non-perturbatively** using **FRG**



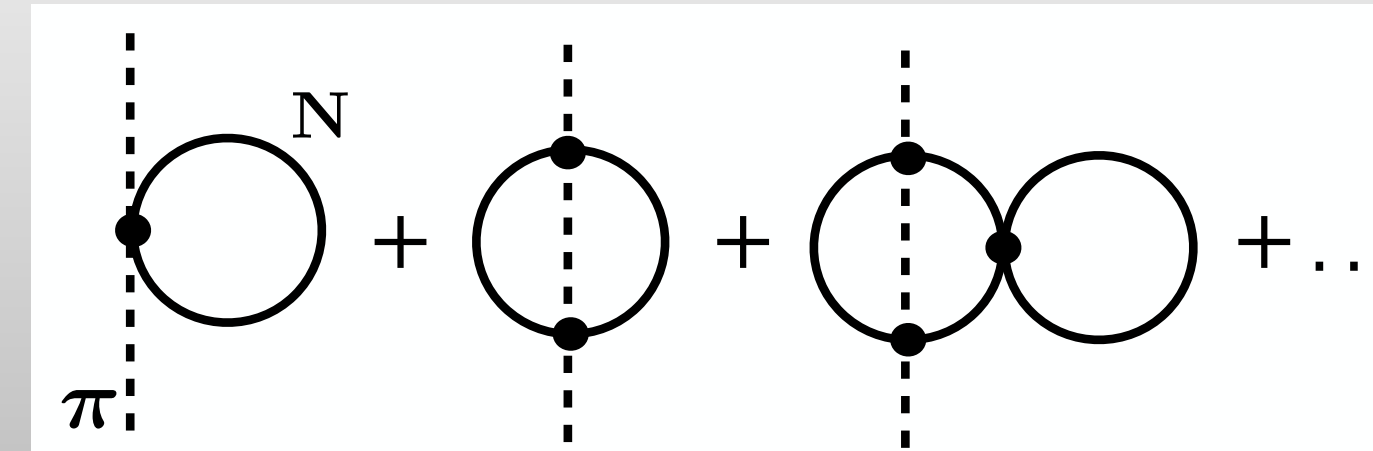
Categories of mesonic and baryonic fluctuations treated non-perturbatively in the FRG approach

● Pion propagator

$$D_\pi(\mathbf{x}_1, \mathbf{x}_2) = \left[\frac{\delta^2 \Gamma}{\delta \pi(\mathbf{x}_1) \delta \pi(\mathbf{x}_2)} \right]^{-1}$$



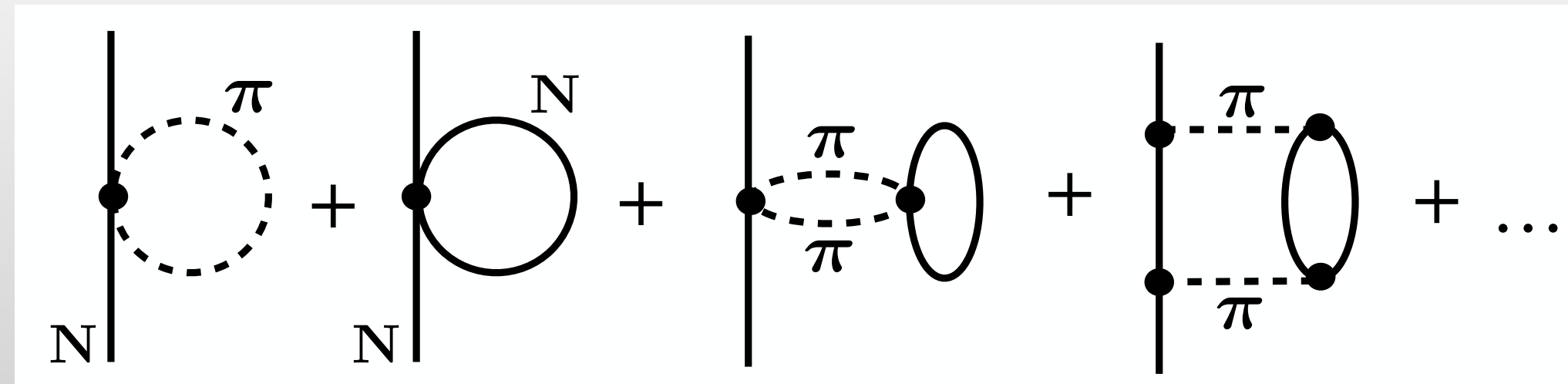
Pion propagation in pionic heat bath



Pion propagation in **nuclear Fermi sea**

● Nucleon propagator

$$D_N(\mathbf{x}_1, \mathbf{x}_2) = \left[\frac{\delta^2 \Gamma}{\delta N(\mathbf{x}_1) \delta N^\dagger(\mathbf{x}_2)} \right]^{-1}$$

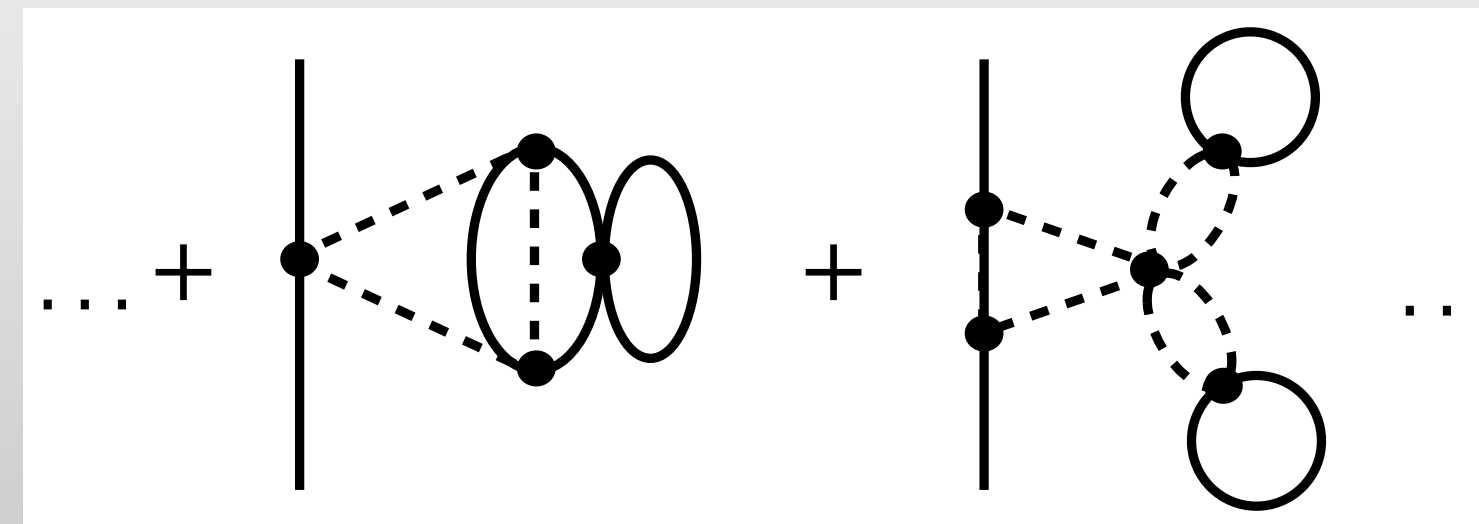


thermal pion cloud

Hartree (MF)

Two-pion exchange

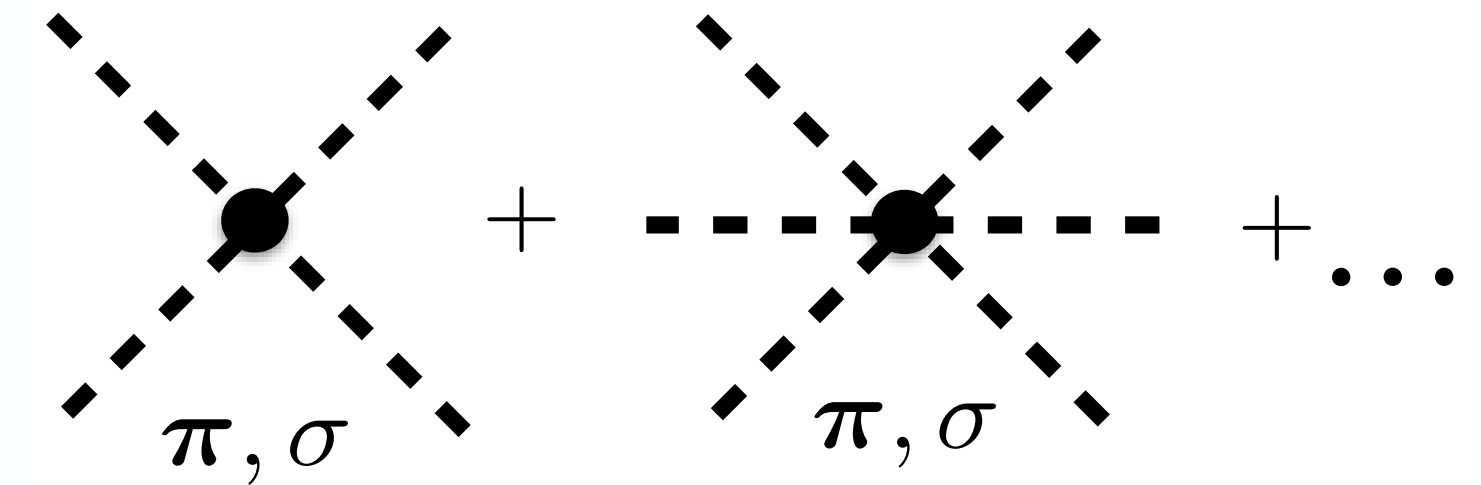
2nd order tensor force



multi-nucleon correlations

Loops & ladders involving **excitations** of the **nucleonic Fermi sea**

Fixing the input



- **Potential** $\mathcal{U}(\sigma, \pi) = \mathcal{U}_0(\chi) - m_\pi^2 f_\pi (\sigma - f_\pi)$

explicit chiral symmetry breaking

Chiral invariant part :

$$\mathcal{U}_0(\chi) = \sum_n a_n (\chi - \chi_0)^n$$

expanded in powers of

$$\chi = \frac{1}{2}(\sigma^2 + \pi^2) \quad \chi_0 = f_\pi^2/2 \text{ (vacuum)}$$

$$n_{max} = 4$$

$$a_1, a_2$$

determined by vacuum constants (f_π, m_π, m_σ)

$$a_3, a_4$$

adjustable parameters

- **Scalar** (“sigma”) **field** :
mean field (chiral **order parameter**) plus **fluctuating** pieces.

$$\sigma \text{ mass: } \mathbf{NOT} \text{ to be identified with “}\sigma(500)\text{” : } m_\sigma \simeq 0.9 \text{ GeV}$$

- **Nucleon mass** : $M_N = g\sqrt{2\chi}$... in **vacuum**: $M_N = g f_\pi$ (Goldberger - Treiman)

FRG Flow equations in practice & Fixing the input (contd.)

UV scale :

action $\Gamma_{k=\Lambda}$

$$\Lambda \simeq \Lambda_\chi = 4\pi f_\pi$$

UV

Γ_k

IR

**“full”
effective action**

$$\Gamma_{k=0}$$

- Simplifying assumptions and approximations :
 - derivative expansion
 - no “k-running” of Yukawa coupling

- **k-dependent effective action :**

$$\Gamma_k = \int d^4x \left[\bar{\Psi} i\gamma_\mu \partial^\mu \Psi + \frac{1}{2} \partial_\mu \sigma \partial^\mu \sigma + \frac{1}{2} \partial_\mu \pi \partial^\mu \pi - \bar{\Psi} [g(\sigma + i\gamma_5 \boldsymbol{\tau} \cdot \boldsymbol{\pi}) + \gamma_0 (g_v v + g_w w \tau_3)] \Psi - \mathcal{U}_k(\boldsymbol{\pi}, \sigma; v, w) \right]$$

k-dependent potential

- **Vector fields** v (isoscalar) and w (isovector) encode **short-distance NN dynamics**:
Self-consistently determined background **mean fields** (non-fluctuating)

(**not** to be identified with physical ω and ρ mesons)

- **Effective chemical potentials** of neutrons and protons : $\mu_{n,p}^{\text{eff}} = \mu_{n,p} - g_v v \pm g_w w$

Relevant quantities: $G_v = \frac{g_v^2}{m_V^2}$, $G_w = \frac{g_w^2}{m_V^2}$ \longleftrightarrow **contact terms** in **ChEFT** $G_w \simeq G_v/4 \sim 1 \text{ fm}^2$

FRG Flow equations in practice (contd.)

- **Flow of k-dependent effective potential**

$$k \frac{\partial \mathcal{U}_k}{\partial k}(T, \mu_p, \mu_n; \chi, v, w) = \frac{k^5}{12\pi^2} \left[\frac{1 + 2 f_B(E_\sigma)}{E_\sigma} + \frac{3[1 + 2 f_B(E_\pi)]}{E_\pi} - 4 \sum_{i=p,n} \frac{1 - f_F(E_N - \mu_i^{\text{eff}})}{E_N} \right]$$

$$f_{F,B}(E) = \left[e^{E/T} \pm 1 \right]^{-1} \quad \chi = \frac{1}{2}(\sigma^2 + \pi^2) \quad E_\pi^2 = k^2 + \mathcal{U}'_k(\chi), \quad E_\sigma^2 = k^2 + \mathcal{U}'_k(\chi) + 2\chi \mathcal{U}''_k(\chi),$$

$$E_N^2 = k^2 + 2g^2\chi, \quad \mathcal{U}'_k(\chi) = \frac{\partial \mathcal{U}_k(\chi)}{\partial \chi}, \quad \mu_{n,p}^{\text{eff}} = \mu_{n,p} - g_v v \pm g_w w$$

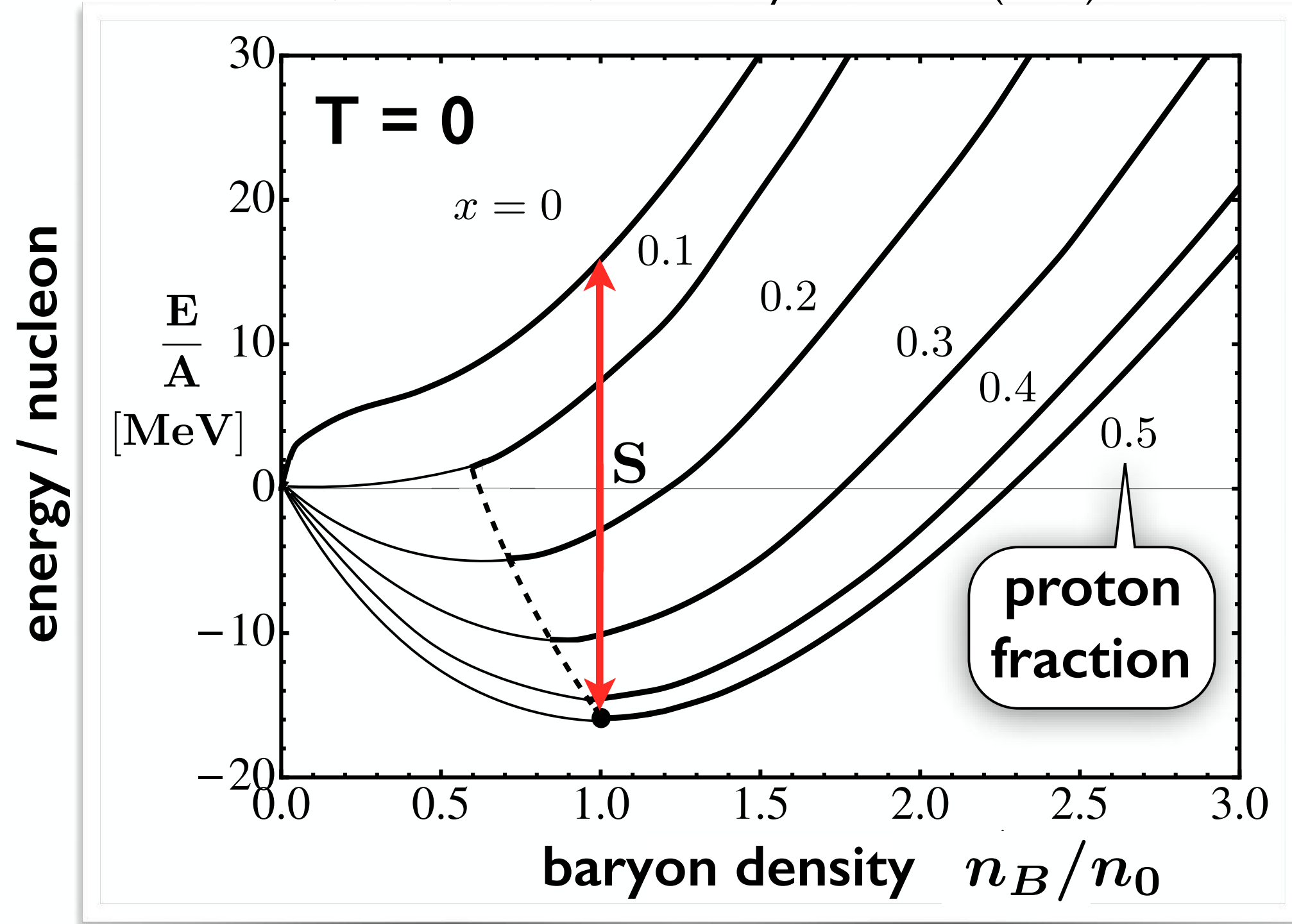
... plus vector field equations, then full system of coupled differential equations solved on a grid.

- **Thermodynamics** : Grand canonical potential $\Omega = -\frac{T}{V} \ln \mathcal{Z} = \Omega_F + \mathcal{U}_{k=0}$

<p>pressure $P = -\Omega$</p> <p>baryon densities $n_i = -\frac{\partial \Omega}{\partial \mu_i}$</p>	<p>entropy density $s = -\frac{\partial \Omega}{\partial T}$</p> <p>energy density $\mathcal{E} = -P + \sum_{i=p,n} \mu_i n_i + Ts$</p>
---	---

From symmetric to asymmetric nuclear matter in the Chiral FRG approach

M. Drews, T. Hell, B. Klein, W.W.: Phys. Rev. D 88 (2013) 096011



- **Symmetry energy $S = 32$ MeV**

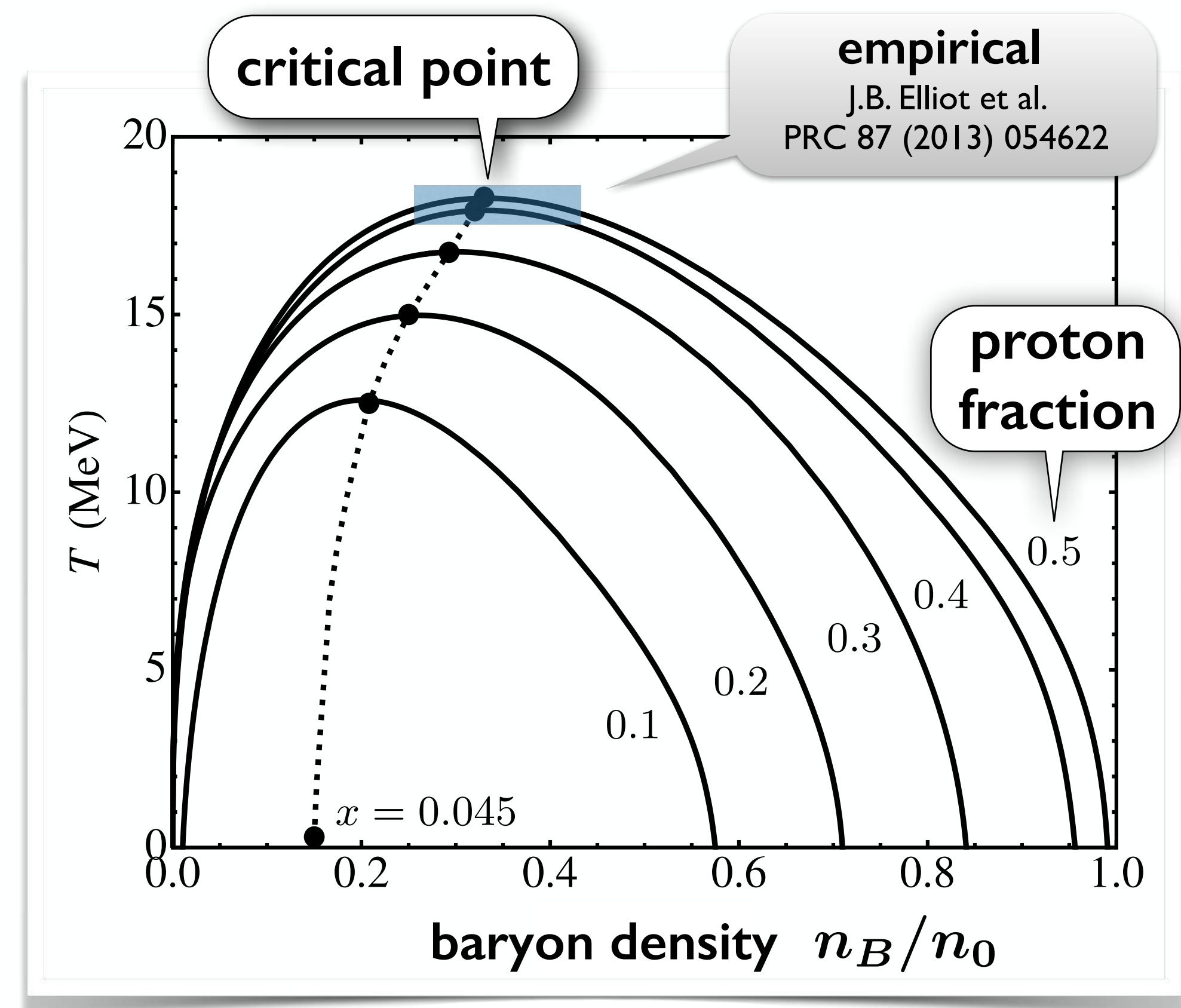
(“empirical” : $S = 32 \pm 2$ MeV)

M. Baldo, G.F. Burgio : Prog. Part. Nucl. Phys. 91 (2016) 203

- **FRG results (non-perturbative) consistent with (perturbative) Chiral EFT calculations**

M. Drews, W.W.: Phys. Rev. C91 (2015) 035802

- **Liquid-gas phase transition :**
Evolution of coexistence regions from **symmetric to asymmetric** nuclear matter



FLUCTUATIONS and PHASES in BARYONIC MATTER

- a closer look -

L. Brandes, N.. Kaiser, W.W.: Eur. Phys.J. A57 (2021) 243

- **Vacuum Fluctuations** (nucleonic zero-point energy / one-loop fermionic effective potential)

... treated as logarithmic correction to mean-field approximation : V. Skokov et al. : Phys. Rev. D82 (2010) 034029

Vacuum part of fermionic grand potential :

$$\delta\Omega_{\text{vac}} = -4 \int \frac{d^3p}{(2\pi)^3} E_N = -\frac{2}{\pi^2} \int dp p^2 \sqrt{p^2 + M_N^2(\sigma)} \xrightarrow[\text{regularisation}]{\text{dimensional}} -\frac{M_N^4}{8\pi^2} \ln \frac{M_N^2}{\Lambda^2}$$

($\Lambda = g f_\pi$)

extended mean-field appr.
(EMF)

$$\Omega_{\text{EMF}} = \underbrace{\Omega_{\text{MF}}}_{\text{mean-field}} - \frac{(g\sigma)^4}{4\pi^2} \ln \frac{\sigma}{f_\pi}$$

vacuum fluctuations

- Note :

Functional Renormalisation Group automatically includes vacuum fluctuations

CHIRAL PHASE TRANSITION in DENSE BARYONIC MATTER ?

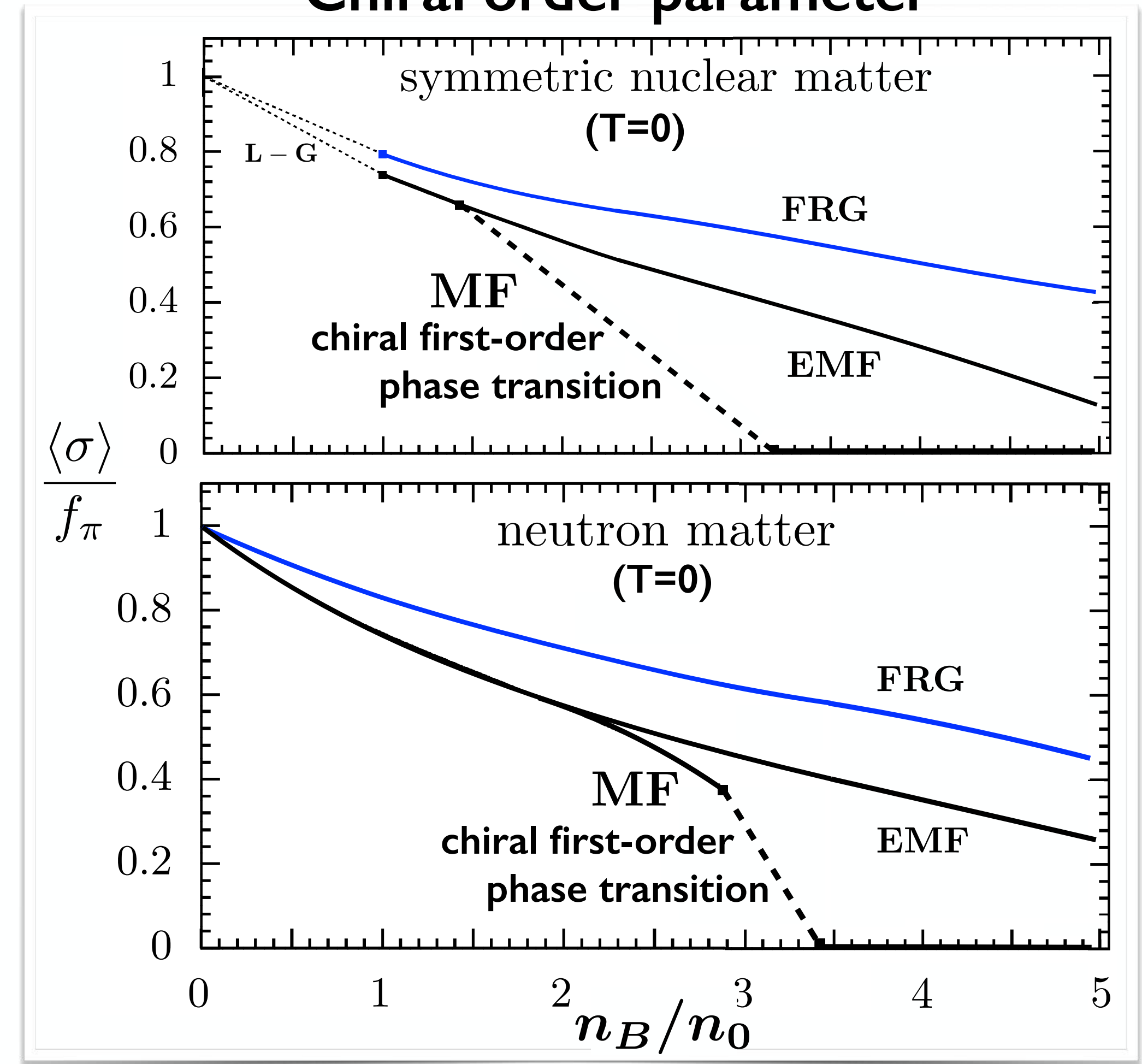
★ Studies in chiral nucleon-meson field theory

M. Drews, W.W.: Prog. Part. Nucl. Phys. 93 (2017) 69 — L. Brandes, N. Kaiser, W.W.: Eur. Phys. J. A57 (2021) 243

- **Mean-field** approximation (MF) :
chiral first-order phase transition
at baryon densities $n_B \sim 2 - 3 n_0$
- **Vacuum fluctuations** (EMF) :
shift **chiral transition** to **high density**
→ **smooth crossover**
- **Functional Renormalisation Group** (FRG) :
non-perturbative loop corrections
involving **pions** & **nucleon-hole** excitations
→ further reinforcement of stabilising effects

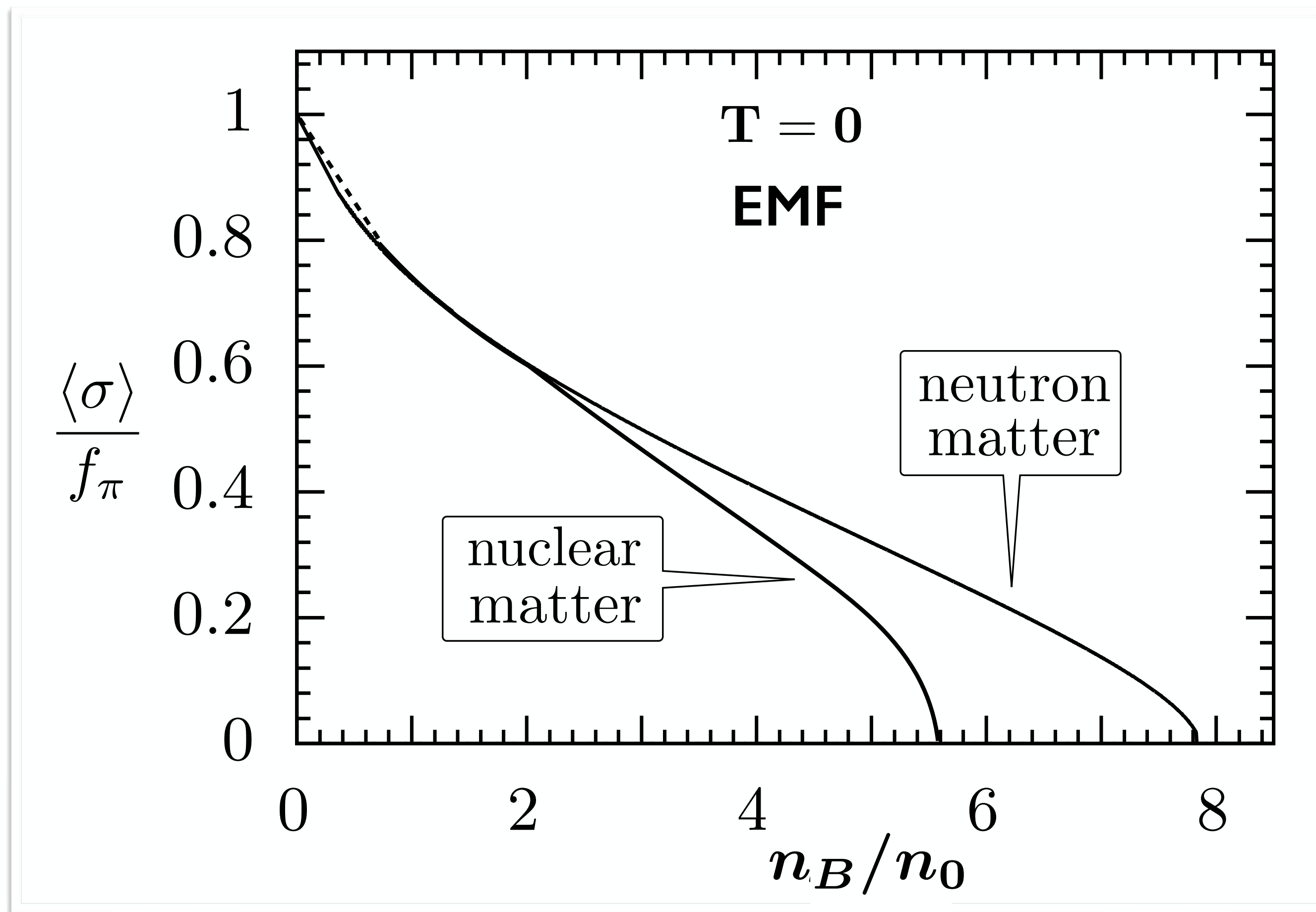
Chiral crossover transition at $n_B > 6 n_0$
far beyond core densities in neutron stars

Chiral order parameter



CHIRAL LIMIT ($m_\pi \rightarrow 0$)

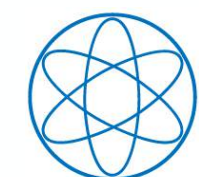
2nd order chiral phase transition in nuclear and neutron matter



L. Brandes, N.. Kaiser, W.W.: Eur. Phys. J. A57 (2021) 243

- Chiral Nucleon-Meson Field Theory
- EMF calculations :
Extended Mean-Field including logarithmic vacuum fluctuations
- Critical densities (chiral limit)
$$n_B^{cr} > 5 n_0$$
- Alternative approach:
Parity-doublet model
 $\{N(1/2^+) - N^*(1/2^-)\}$
Critical densities $n_B^{cr} > 10 n_0$

J. Eser, J.-P. Blaizot : Phys. Rev. C109 (2024) 045201
arXiv:2408.01302



7.

Neutron Star Matter

as a

Relativistic Fermi Liquid

Basics of (Relativistic) Fermi-Liquid Theory

G. Baym, S.A. Chin : Nucl. Phys. A262 (1976) 527

T. Matsui : Nucl. Phys. A370 (1981) 365

- **Variation of the energy** ($T = 0$)

$$\delta E = V \delta \mathcal{E} = \sum_p \varepsilon_p \delta n_p + \frac{1}{2V} \sum_{pp'} \mathcal{F}_{pp'} \delta n_p \delta n_{p'} + \dots \quad n_p = \Theta(\mu - \varepsilon_p)$$

quasiparticle energy

$$\varepsilon_p = \frac{\delta E}{\delta n_p}$$

quasiparticle interaction

$$\mathcal{F}_{pp'} = V \frac{\delta^2 E}{\delta n_p \delta n_{p'}} = f_{pp'} + g_{pp'} \boldsymbol{\sigma} \cdot \boldsymbol{\sigma}'$$

- **Landau effective mass**

$$m^* = \sqrt{p_F^2 + M^2(\rho)}$$

- **Density of states at the Fermi surface**

$$N(0) = \frac{m^* p_F}{\pi^2}$$

- **Landau parameters** Quasiparticle interaction expanded in Legendre series

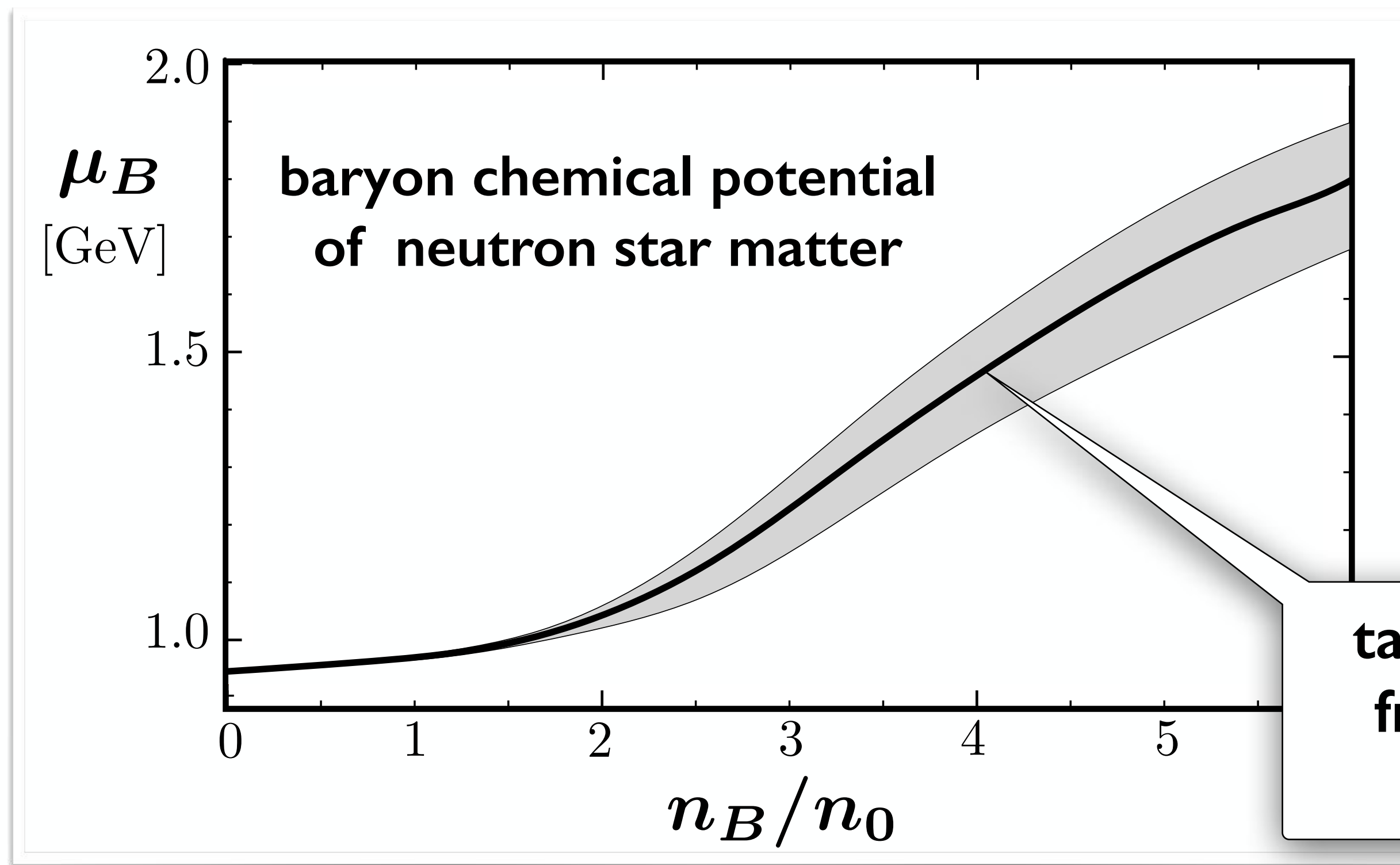
$$f_{pp'} = \sum_{\ell=0}^{\infty} f_{\ell} P_{\ell}(\cos \theta_{pp'}) \quad F_{\ell} = N(0) f_{\ell}$$

DENSE BARYONIC MATTER in NEUTRON STARS as a RELATIVISTIC FERMI LIQUID

B. Friman, W.W. : Rhys. Rev. C100 (2019) 065807

L. Brandes, W.W. : Symmetry 16 (2024) 111

- **Neutron Star Matter : Fermi liquid** / dominantly neutrons + ca. 5 % protons
- **Baryonic Quasiparticles :**
baryons “dressed” by their strong interactions and imbedded in mesonic (multi-pion) field



- **Landau effective mass**

$$m_L^*(n_B) = \sqrt{p_F^2 + M_N^2(n_B)}$$

- **Baryon chemical potential**

$$\mu_B = m_L^*(n_B) + \mathcal{U}(n_B)$$

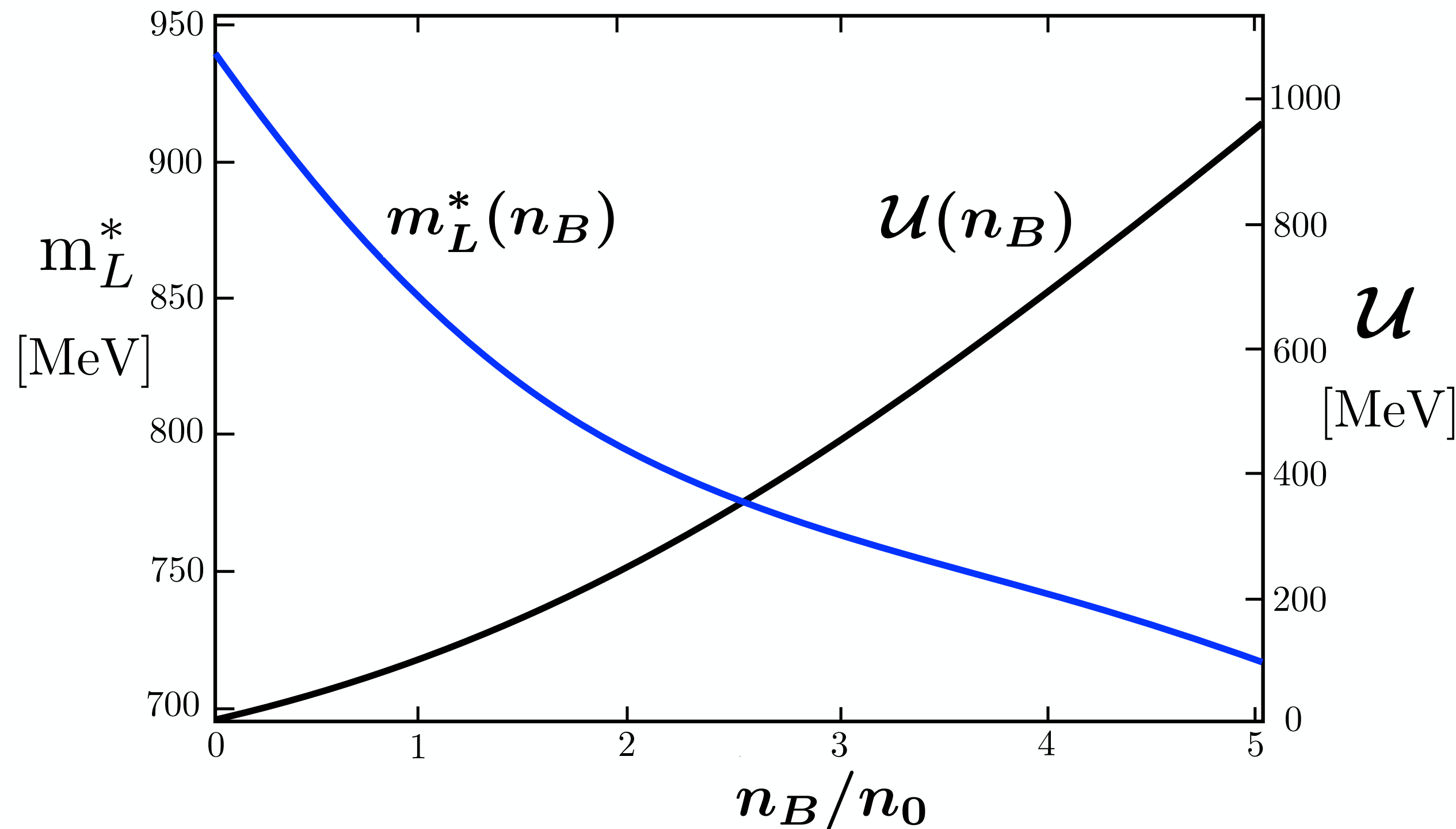
take median of $\mu_B(n_B)$
from Bayesian-inferred
neutron star EoS

quasiparticle
potential

QUASIPARTICLE POTENTIAL and FERMI-LIQUID PARAMETERS

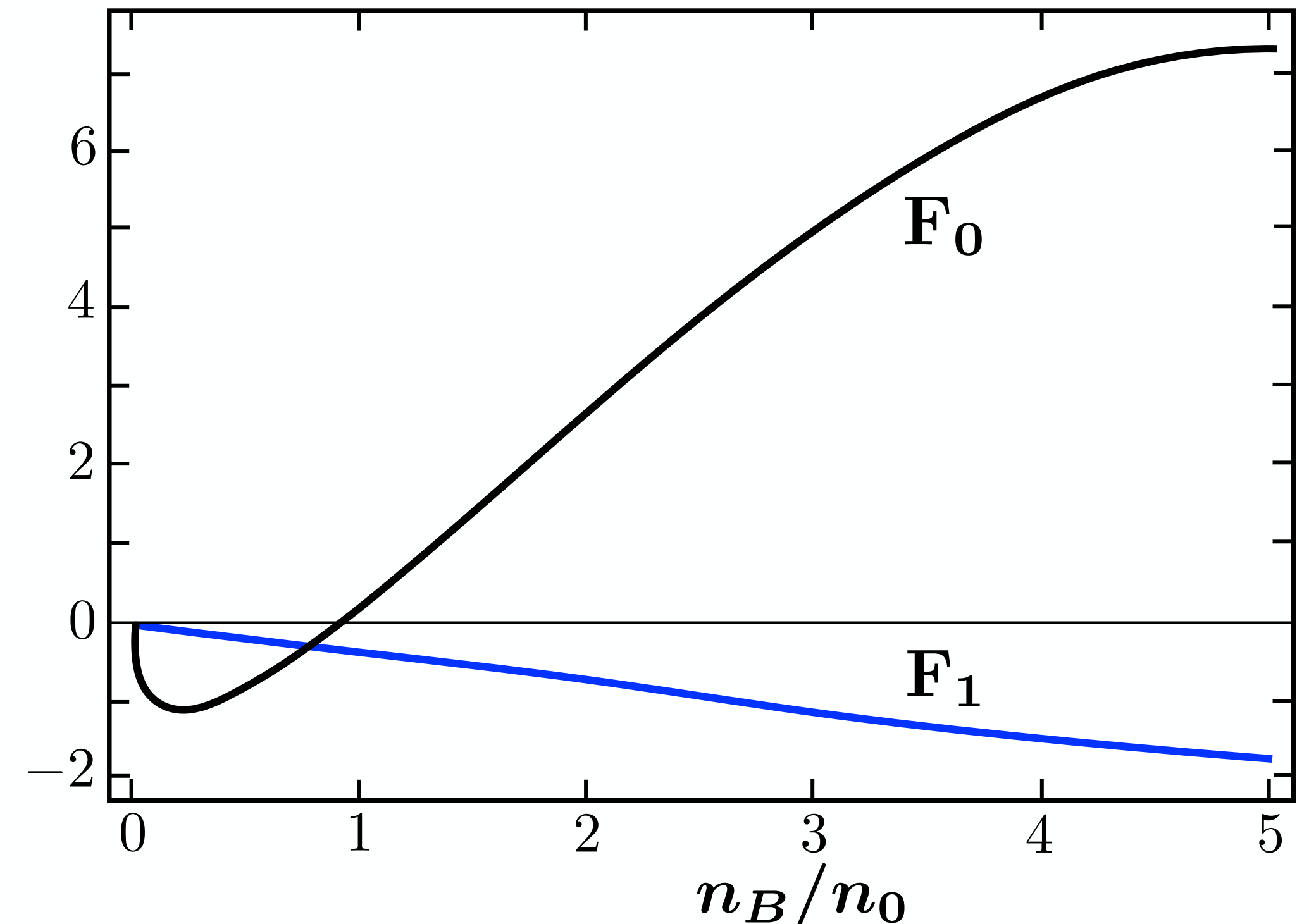
- $m_L^*(n_B)$ from **chiral nucleon-meson field theory & Functional Renormalisation Group**
- **Quasiparticle effective potential**

$$\mathcal{U}(n_B) = \sum_n u_n \left(\frac{n_B}{n_0} \right)^n$$



- **Landau Fermi-Liquid parameters**

$$F_0 = \frac{m_L^* p_F}{\pi^2} \frac{\partial \mu_B}{\partial n_B} - 1 \quad F_1 = -\frac{3\mathcal{U}}{\mu_B}$$

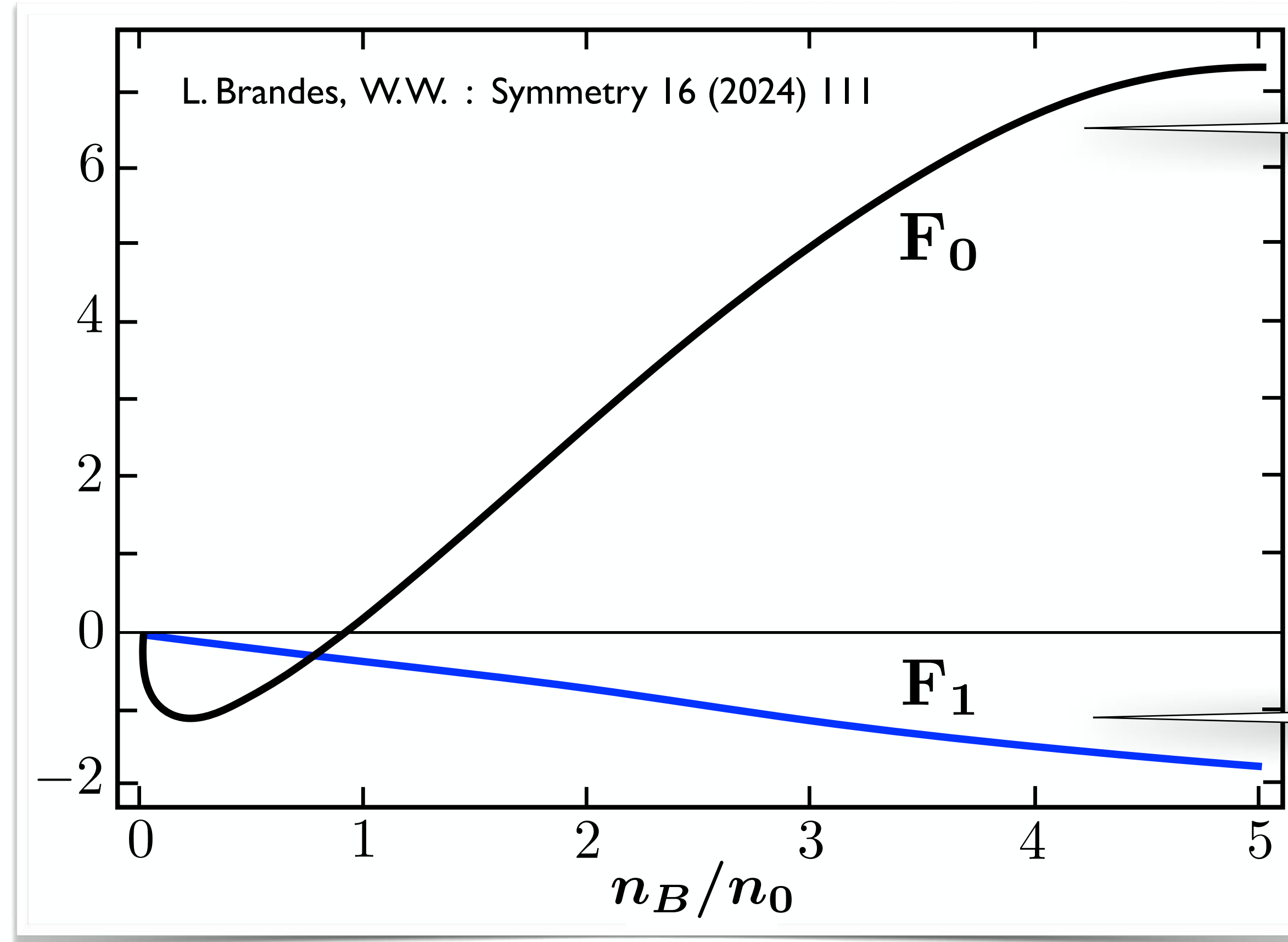


➔ **Strongly repulsive correlations including many-body forces with $n \geq 2$**

LANDAU FERMI-LIQUID PARAMETERS

- Deduced from empirically inferred neutron star matter EoS in combination with Chiral Nucleon-Meson Field Theory & Functional Renormalisation Group

neutron star matter :
a strongly correlated Fermi liquid
...
but not “extreme” !



strongly repulsive many-body correlations

decreasing effective Fermion mass

- Low densities $n_B \lesssim n_0$: good agreement with (perturbative) ChEFT results

J.W. Holt, N.Kaiser, W.W. :
Phys. Rev. C87 (2013) 014338



LANDAU FERMI-LIQUID PARAMETERS (contd.)

- Comparison with atomic liquid helium-3 in its normal phase at low temperature (3 K)

G. Baym, Ch. Pethick : Landau Fermi-Liquid Theory (1991)

- Interaction between He-3 atoms:
attractive van der Waals potential plus strongly **repulsive short-range core**

- Landau Fermi-Liquid parameters of liquid helium-3 at pressures $P = (0 - 30)$ bar:

$$F_0(^3\text{He}) \sim 10 - 70 \qquad F_1(^3\text{He}) \sim 5 - 13$$

D. S. Greywall, Phys. Rev. B33 (1986) 7520

... much larger by magnitude than Landau parameters of neutron star matter !

- Neutron star matter at central densities is a **strongly correlated Fermi system**
... but not as extreme as one might have thought !



SUMMARY

★ **Neutron star matter :**

- ▶ Equation-of-state constrained by steadily expanding observational data base (Multimessenger observations : **stiff EoS** required)
- ▶ $M_{max} \gtrsim 2 M_{\odot}$, $R \simeq 11 - 13$ km
- ▶ **Strong first-order phase transition unlikely**
- ▶ **Not ruled out: baryonic matter or smooth hadrons-to-quarks crossover**

★ **Theoretical concepts :**

ChEFT (perturbative), FRG (non-perturbative), Fermi-Liquid Theory

- ▶ **Conventional** (hadronic) **EoS** consistent with empirical “stiffness” constraints
- ▶ **No chiral phase transition** in neutron-rich matter up to at least $n_B > 5 n_0$

★ **Notes added :**

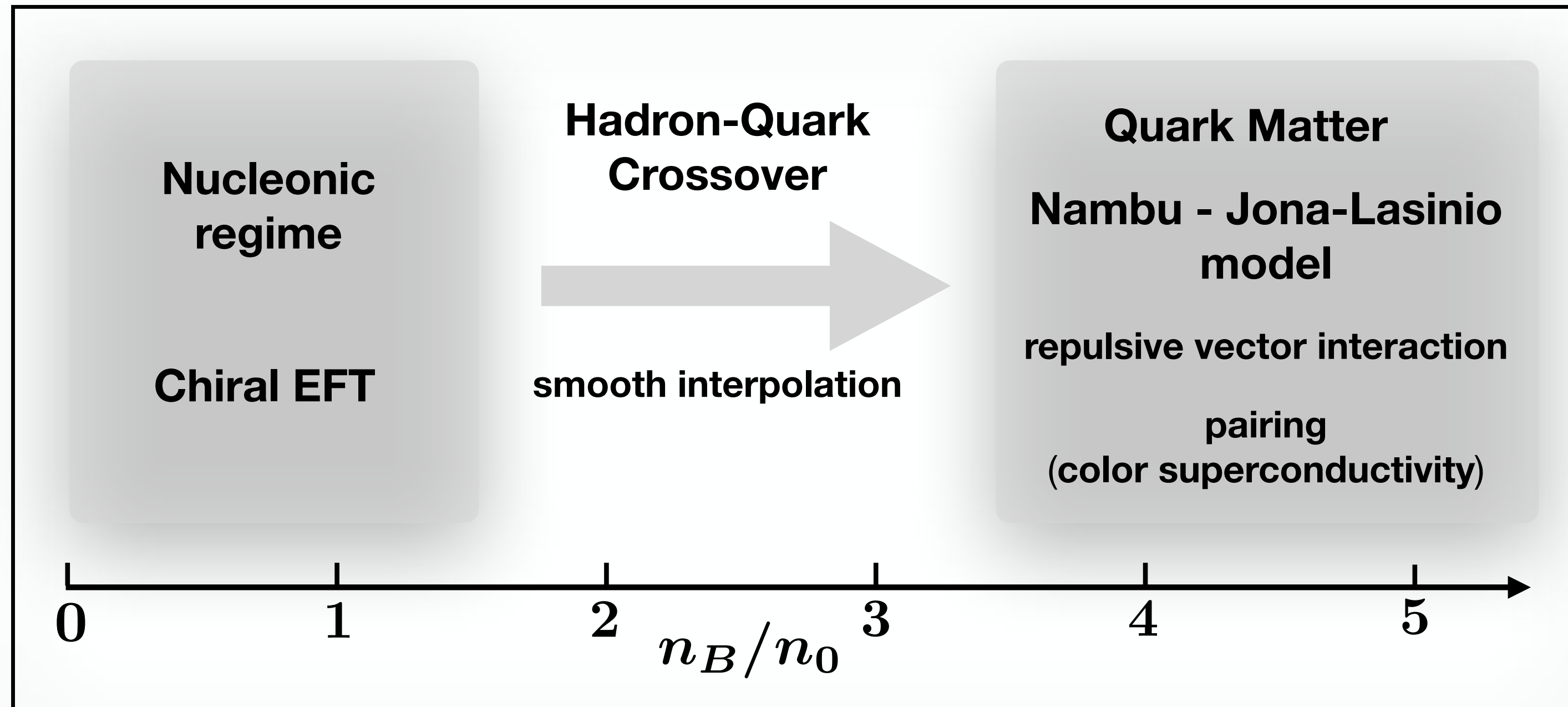
- ▶ **Hadron-Quark Continuity** (successful example: QHC21 equation-of-state)
- ▶ **Superfluidity** (from neutron matter to 2-flavor quark matter)



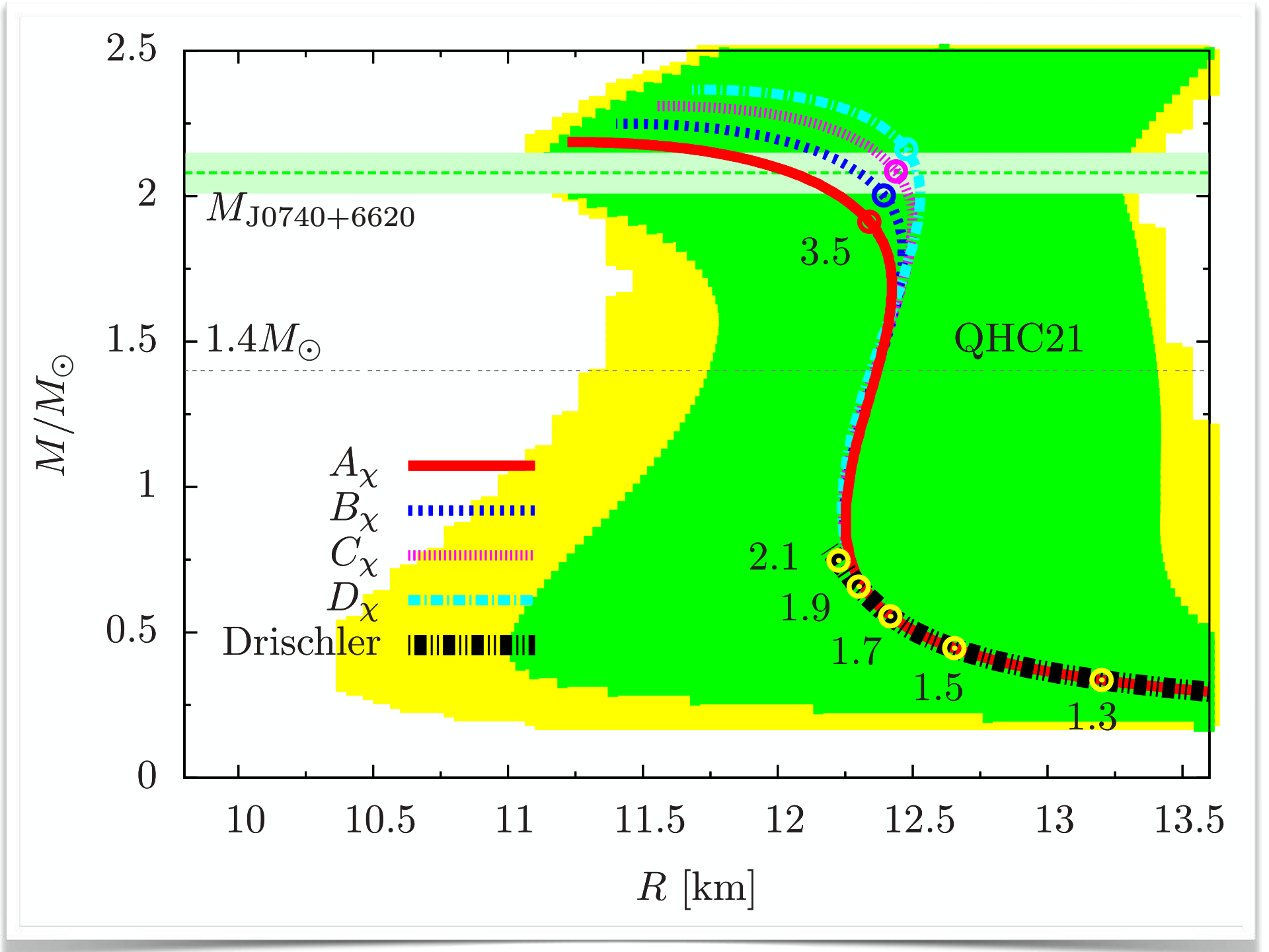
COLD MATTER at EXTREME DENSITIES

Hadron - Quark Continuity

- QHC21 Equation-of-State



T. Kojo, G. Baym, T. Hatsuda : *Astroph. J.* 934 (2022) 46



- **NJL model features** : Chiral symmetry restoration Scalar-pseudoscalar coupling G
 Vector coupling $g_V/G \simeq 1.0 - 1.3$ Pairing interaction $H/G \simeq 1.5 - 1.6$
- Intermediate crossover region may involve “quarkyonic” matter

L. McLerran, S. Reddy
Phys. Rev. Lett. 122 (2019) 122701

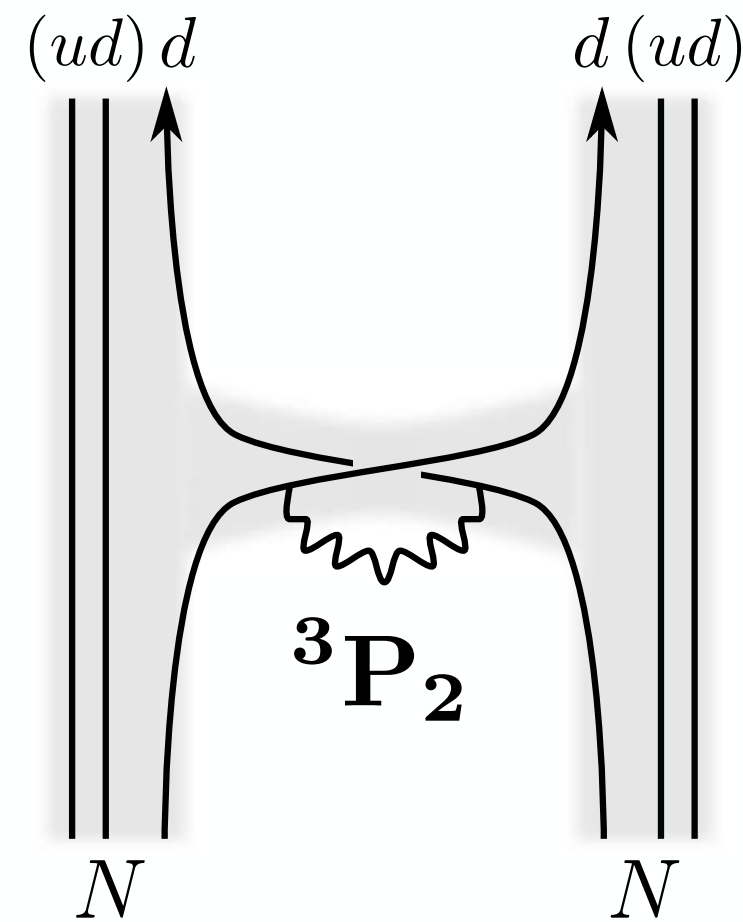
COLD MATTER at EXTREME DENSITIES

Hadron - Quark Continuity (contd.)

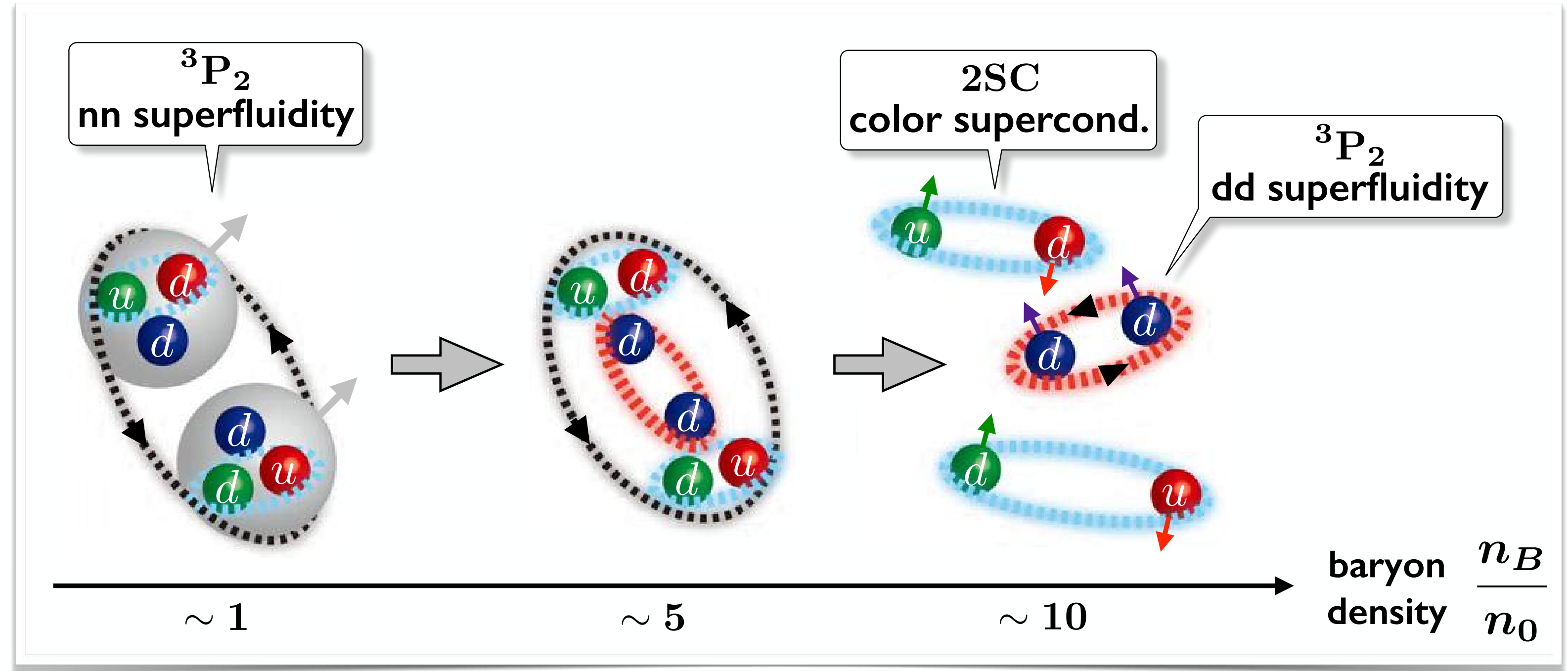
- **Continuity** test case : **superfluidity** from **neutron matter** to $N_f = 2$ **quark matter**

Y. Fujimoto, K. Fukushima, W.W. : Phys. Rev. D 101 (2020) 094009

- Attractive **spin-orbit force** in 3P_2 **nn** and **dd** channels



induces superfluidity in both hadronic and quark phases



- **Continuous matching** of symmetry breaking patterns from **neutron matter** to **2SC + $\langle dd \rangle$ quark matter**

$$[\mathbf{SU}(3)_C] \times \mathbf{SU}(2)_L \times \mathbf{SU}(2)_R \times \mathbf{U}(1)_B \rightarrow [\mathbf{SU}(2)_C] \times \mathbf{SU}(2)_L \times \mathbf{SU}(2)_R \times \mathbf{U}(1)_{C+B}$$

global color chiral symmetry baryon no.

broken by $\langle dd \rangle$ condensate

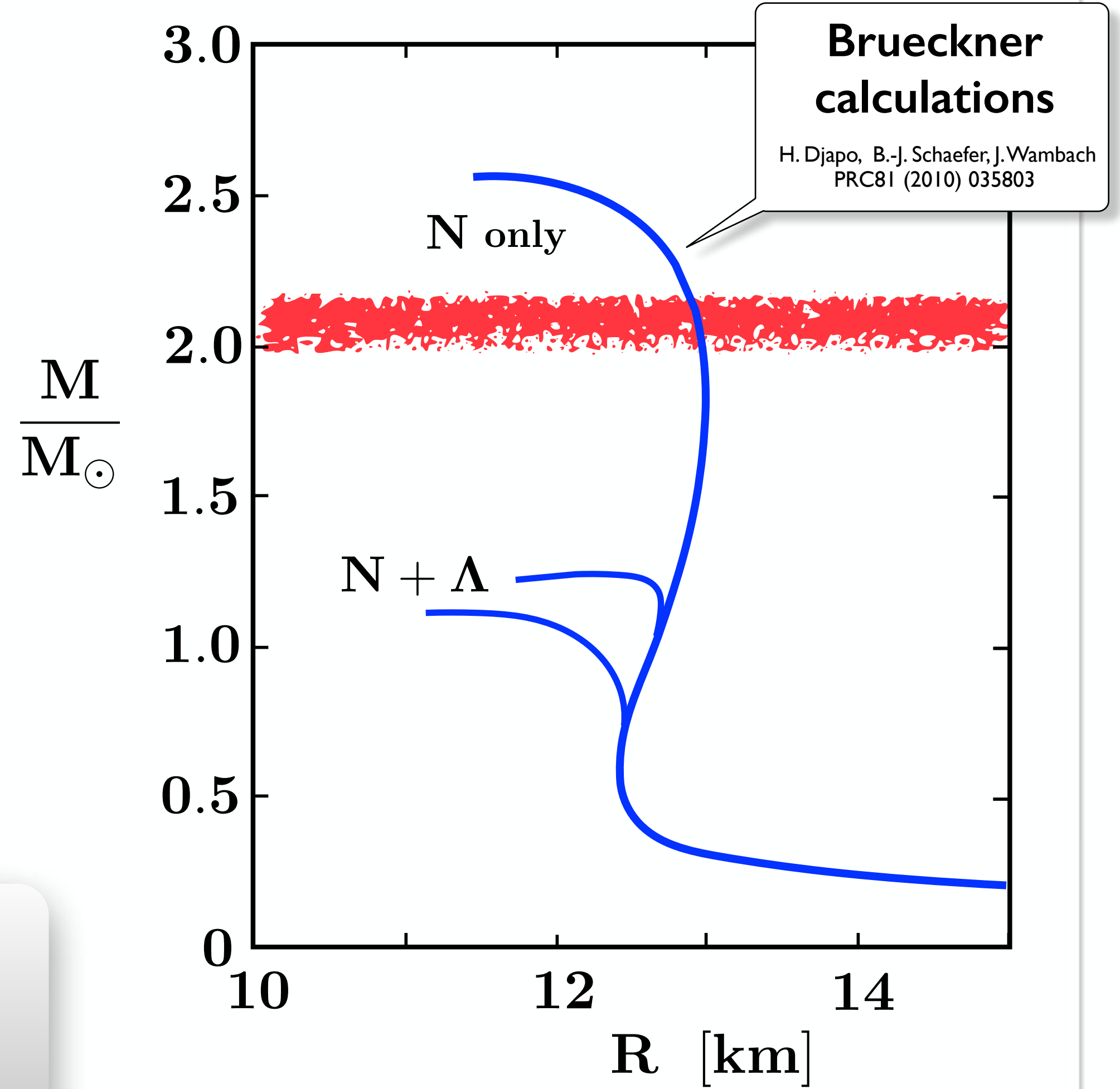
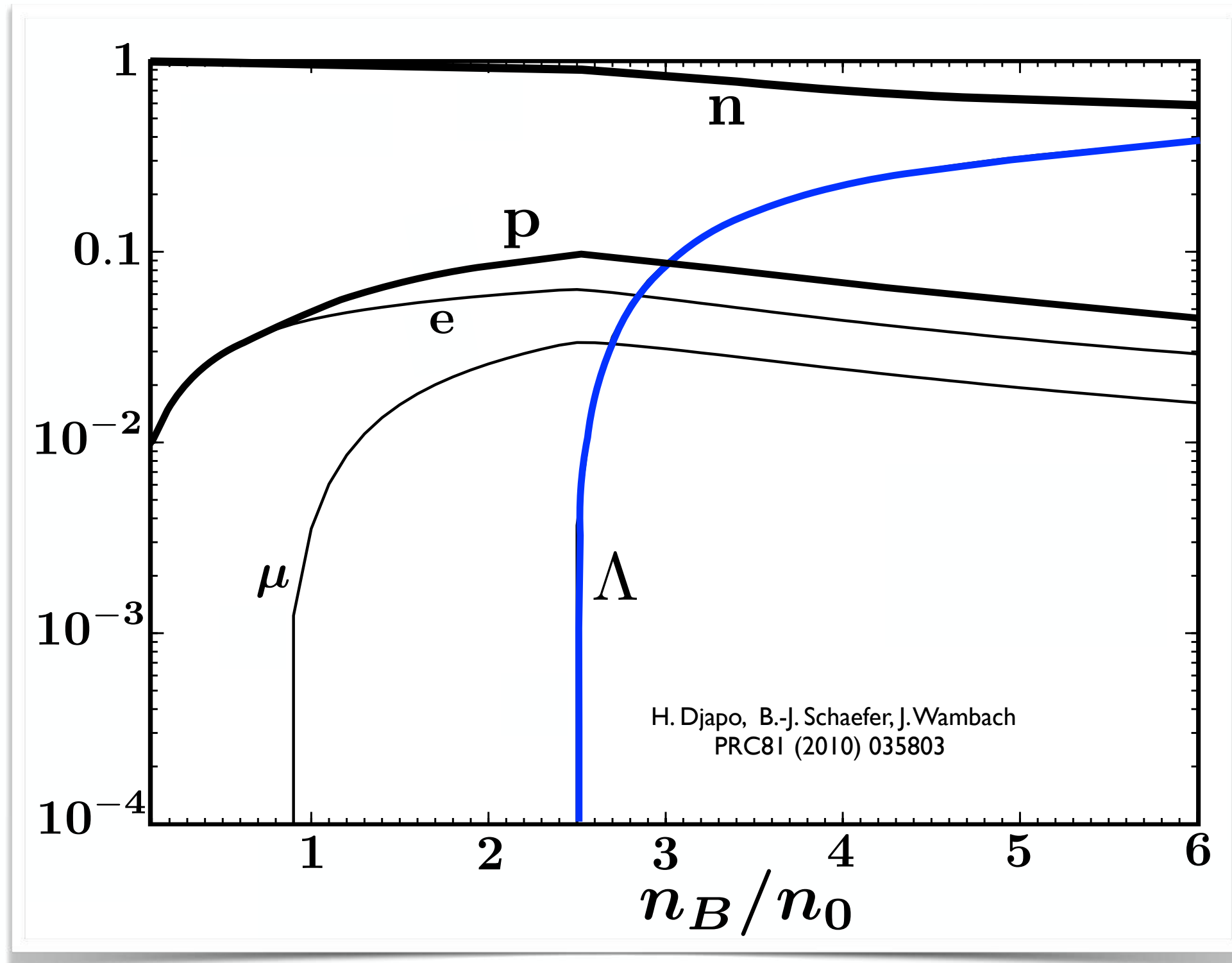
8.

Hyperon-Nuclear Interactions and Strangeness in Dense Matter

- **Chiral SU(3) Effective Field Theory of Hyperon-Nucleon Interactions**
- **Hyperon - NN Three-Body Forces**
- **“Hyperon Puzzle” in Neutron Stars ?**



NEUTRON STAR MATTER including **HYPERONS**



- Inclusion of hyperons :

EoS too soft to support 2-solar-mass n-stars, unless:
strong repulsion in **YN** and/or **YNN** interactions

$$\begin{pmatrix} \frac{\Sigma^0}{\sqrt{2}} + \frac{\Lambda}{\sqrt{6}} & \Sigma^+ & p \\ \Sigma^- & -\frac{\Sigma^0}{\sqrt{2}} + \frac{\Lambda}{\sqrt{6}} & n \\ -\Xi^- & \Xi^0 & -\frac{2\Lambda}{\sqrt{6}} \end{pmatrix}$$

BARYON-BARYON INTERACTIONS

from
CHIRAL SU(3)_L × SU(3)_R EFFECTIVE FIELD THEORY

$$\begin{pmatrix} \frac{\pi^0}{\sqrt{2}} + \frac{\eta}{\sqrt{6}} & \pi^+ & K^+ \\ \pi^- & -\frac{\pi^0}{\sqrt{2}} + \frac{\eta}{\sqrt{6}} & K^0 \\ K^- & \bar{K}^0 & -\frac{2\eta}{\sqrt{6}} \end{pmatrix}$$

	BB interactions
LO	
NLO	
N ² LO	
N ³ LO	

- Systematically organized hierarchy in powers of Q/Λ
(Q : momentum, energy, pseudoscalar meson masses)

- Hyperon-Nucleon interaction :
still very limited scattering data base

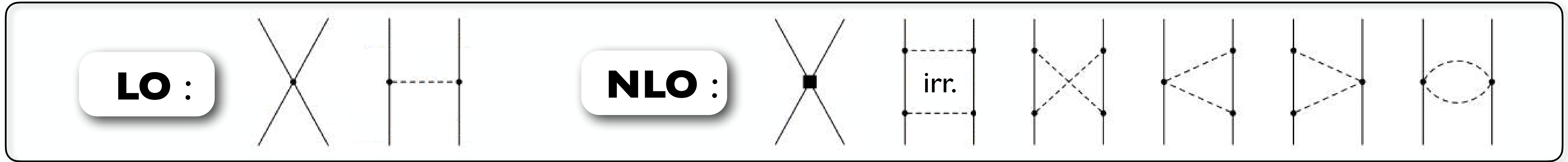


- Restriction to
NLO YN interactions
plus three-body forces

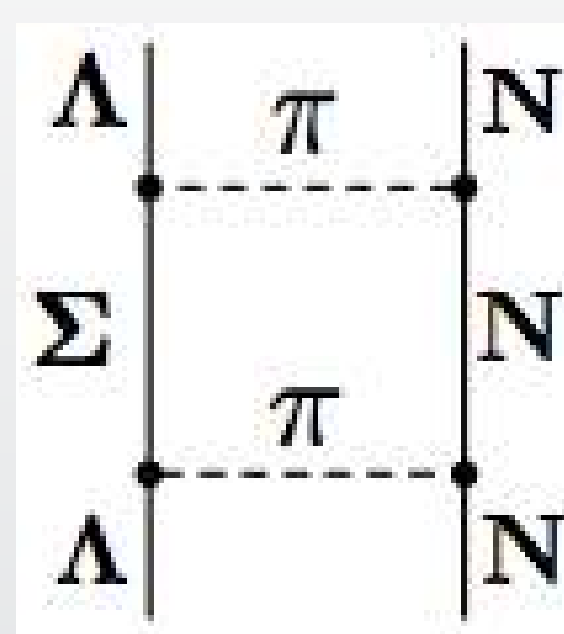
3 – body forces	
N ² LO	
N ³ LO	
4 – body forces	
N ³ LO	

Hyperon - Nucleon Interaction

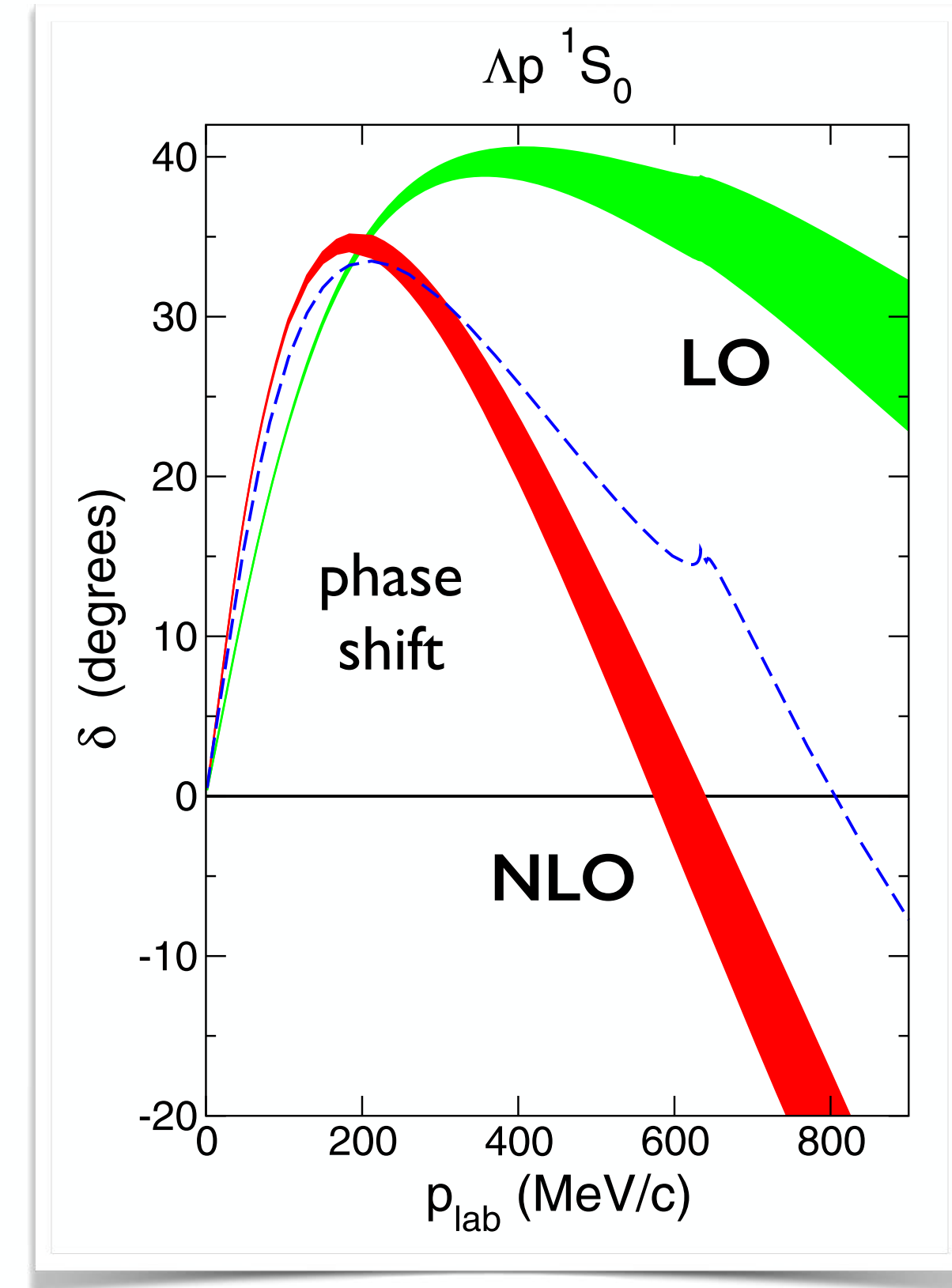
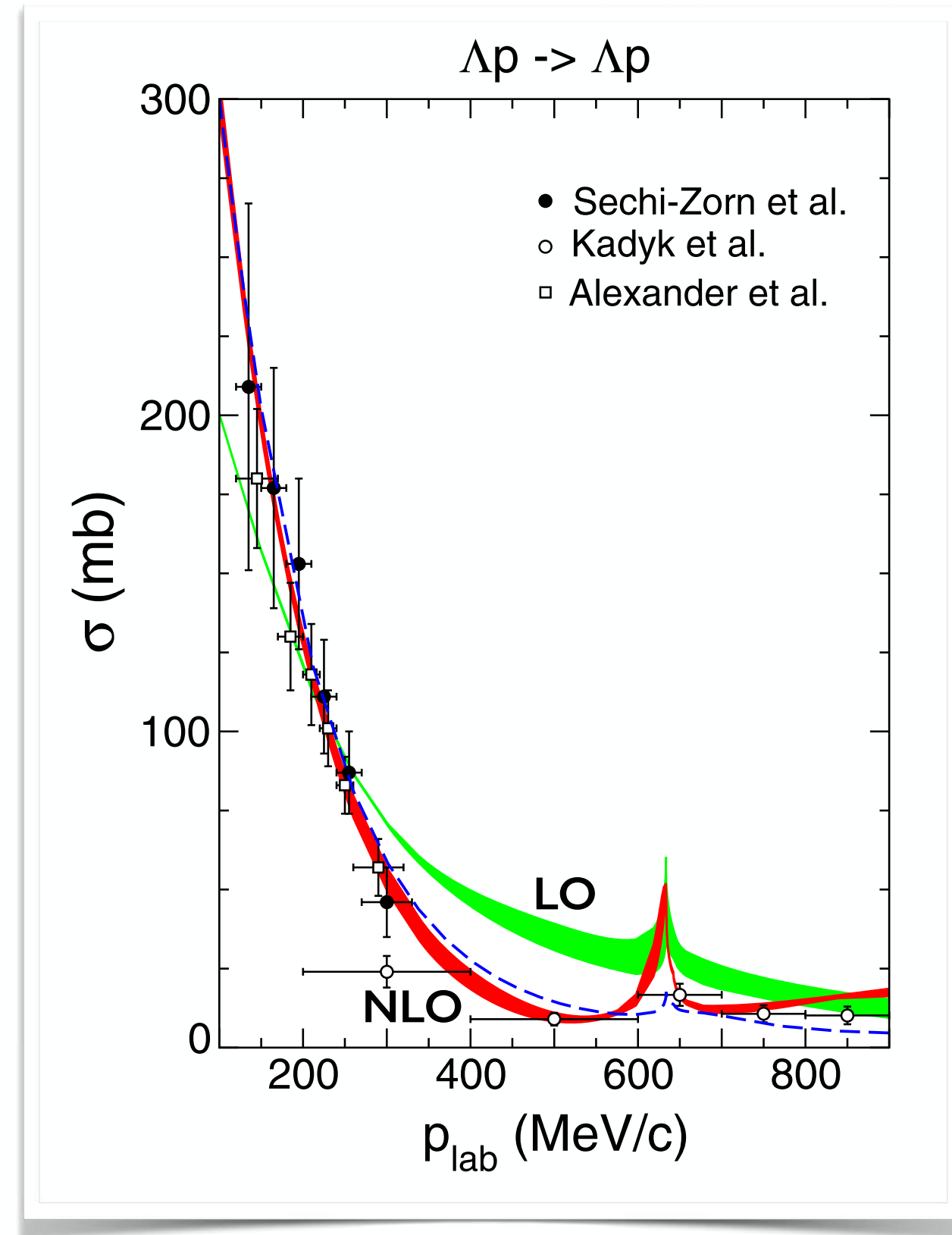
from **CHIRAL SU(3) Effective Field Theory**



ΛN scattering



Important role of $\Lambda N \leftrightarrow \Sigma N$ coupled channels



- moderate attraction at low momenta
 → relevant for hypernuclei
- increasing repulsion at higher momenta
 → relevant for dense baryonic matter

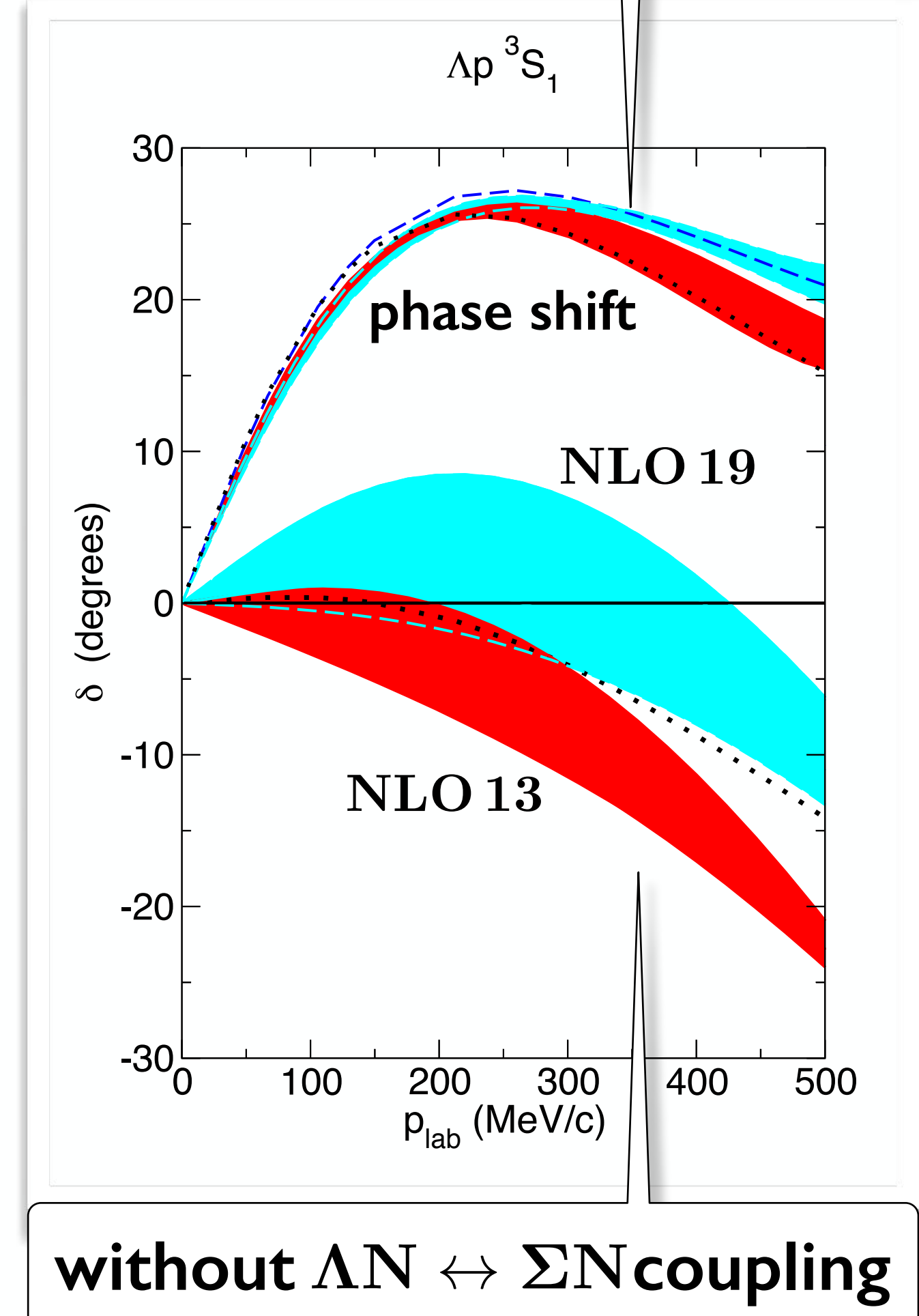
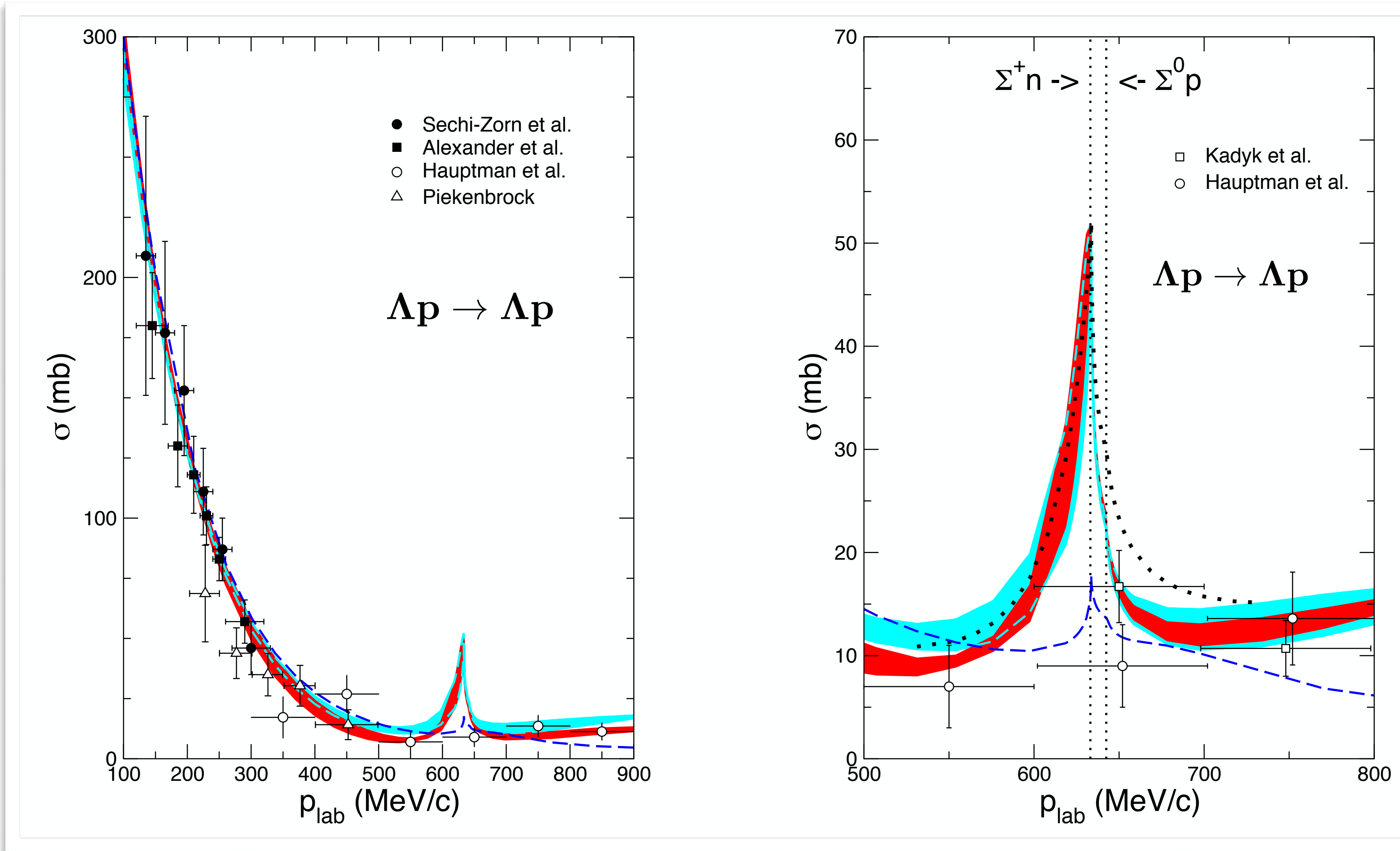
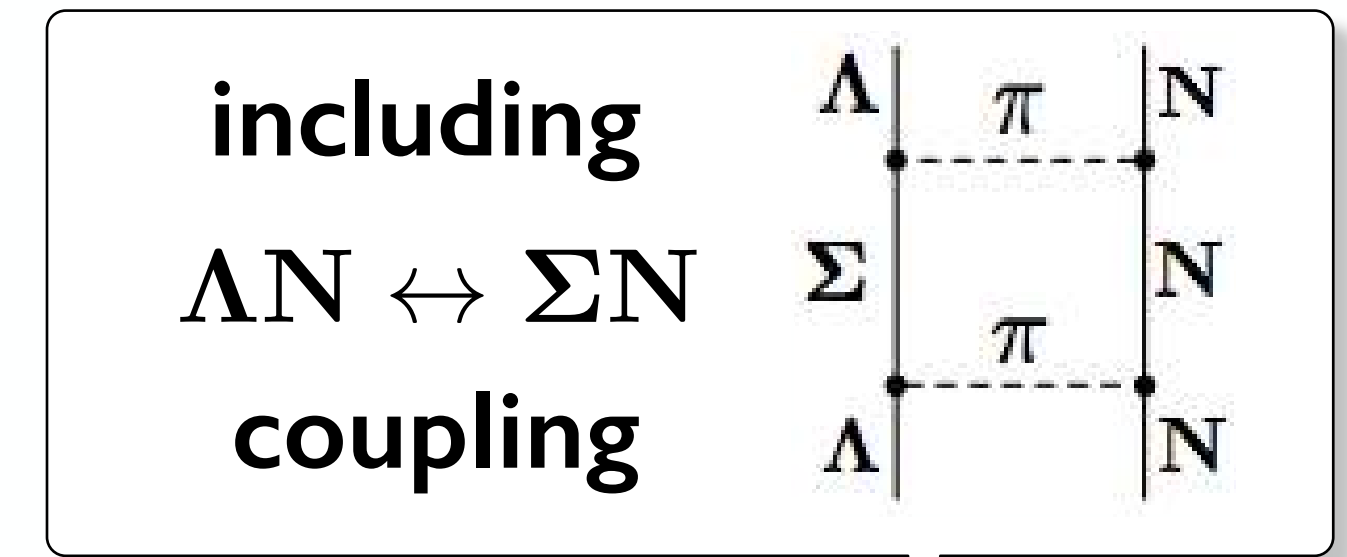
J. Haidenbauer, S. Petschauer, N. Kaiser, U.-G. Meißner, A. Nogga, W.W.
 Nucl. Phys. A 915 (2013) 24



Λ Hyperon - Nucleon Interaction update

J. Haidenbauer, U.-G. Meißner, A. Nogga Eur. Phys. J. A56 (2020) 91

- Reduced no. of independent parameters (contact terms) at NLO by symmetries connecting NN and YN S-waves
 - blue : NLO 19
 - red : NLO 13



without $\Lambda N \leftrightarrow \Sigma N$ coupling

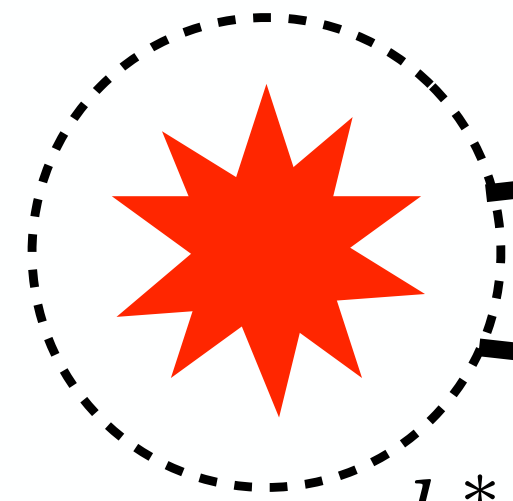
Λp CORRELATION FUNCTION

- Femtoscopia two-particle correlation studies from p p collisions with ALICE @ LHC

L. Fabbietti, V. Mantovani Sarti, O. Vazquez Doce : Ann. Rev. Nucl. Part. Sci. 71 (2021) 377

Source function

$$S(k^*, r)$$



$$k^* = \frac{1}{2} |\mathbf{p}_1 - \mathbf{p}_2|$$

Two-particle wave function

$$\Psi(k^*, r)$$

\mathbf{p}_1

Λp

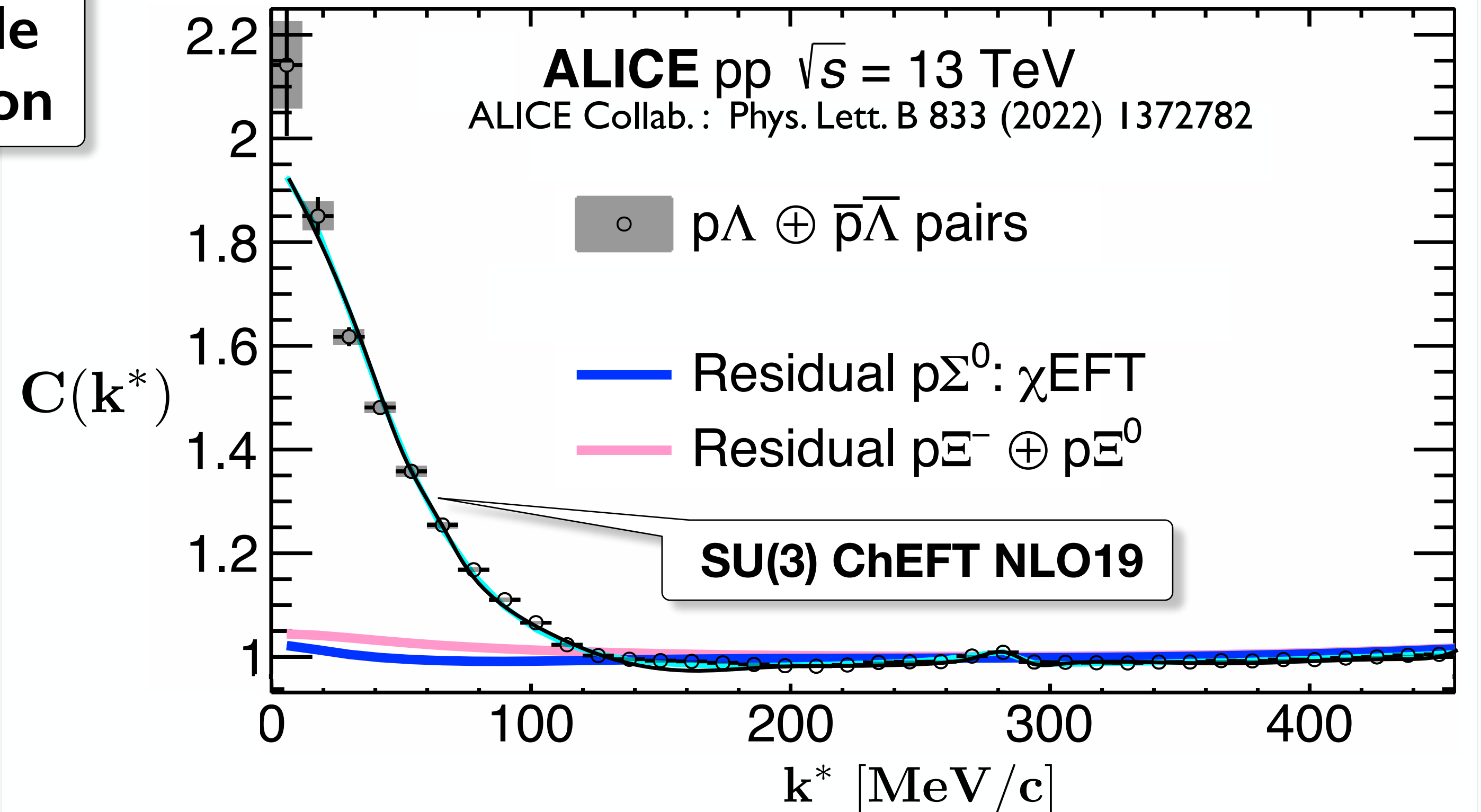
\mathbf{p}_2

- Correlation function

$$C(k^*) = \frac{\langle \mathcal{P}_1(k^*) \mathcal{P}_2(k^*) \rangle}{\langle \mathcal{P}_1(k^*) \rangle \langle \mathcal{P}_2(k^*) \rangle}$$

$$= \int d^3 r S(k^* r) |\Psi(k^* r)|^2$$

- Accurate test of low-momentum Λp interaction



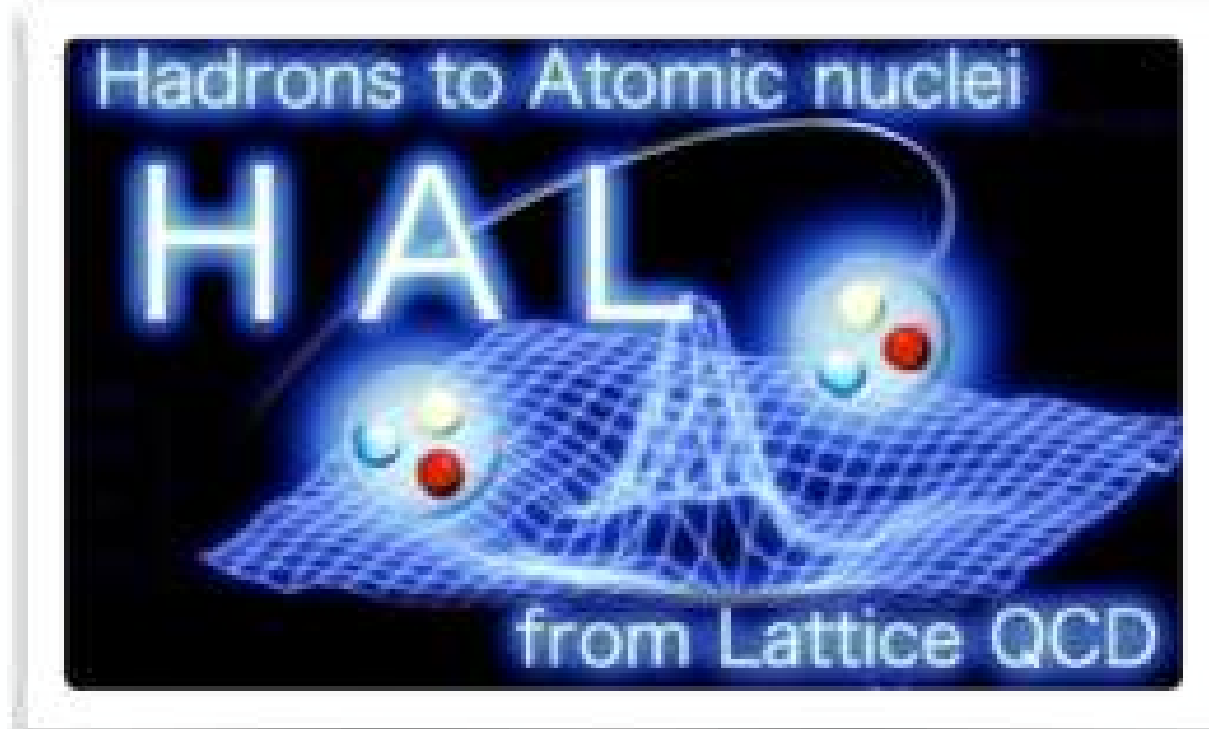
D.L. Mihaylov, J. Haidenbauer, V. Mantovani Sarti,
Phys. Lett. B850 (2024) 138550

Hyperon - Nucleon Interactions from Lattice QCD

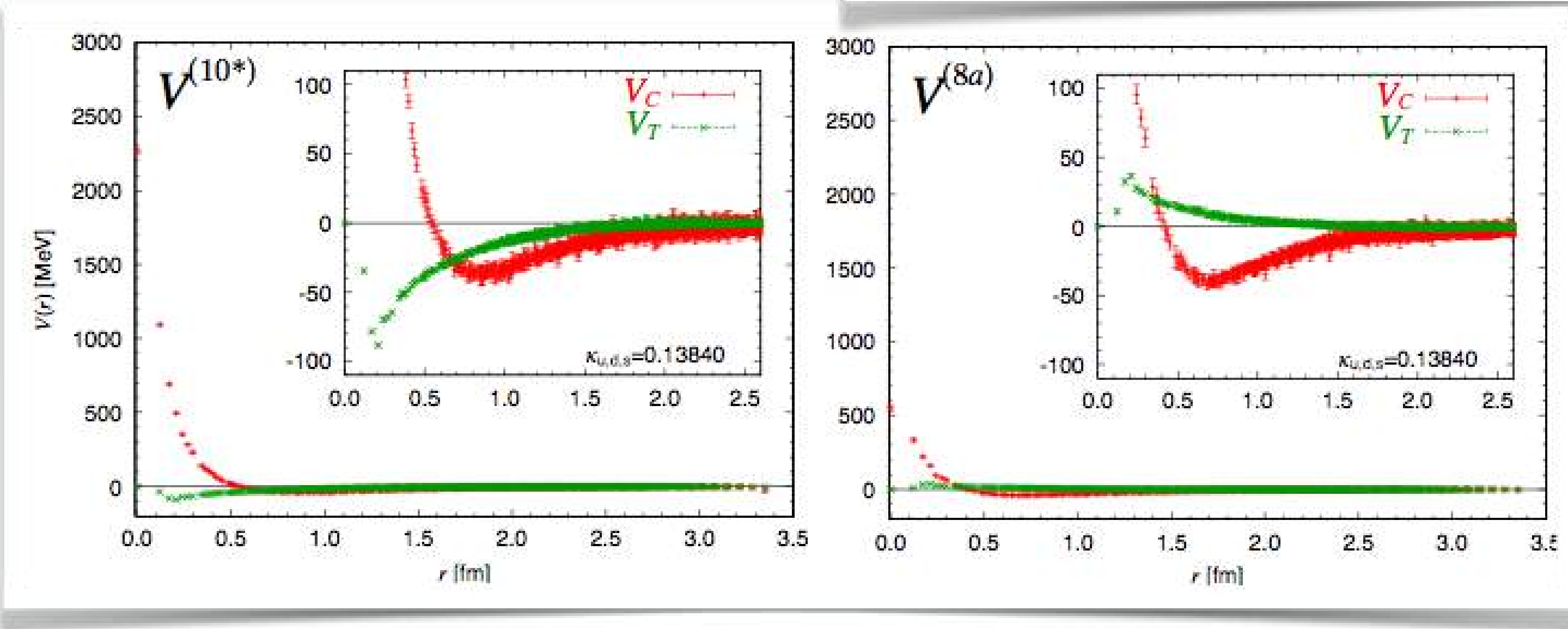
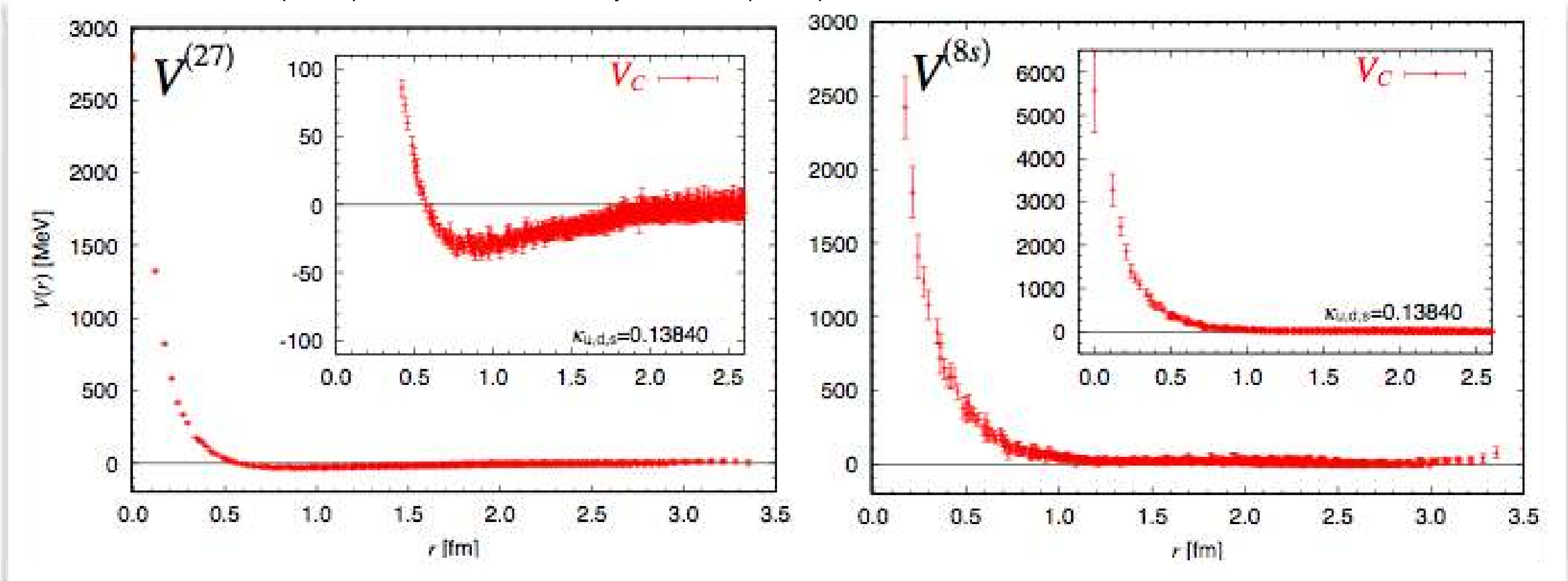
T. Inoue et al.

PTP 124 (2010) 591

Nucl. Phys. A881 (2012) 28



$m_\pi = m_K = 0.47 \text{ GeV}$
towards physical quark masses



SU(3) decomposition

$$\Lambda N(^1S_0) = \frac{9}{10} [27] + \frac{1}{10} [8_s]$$

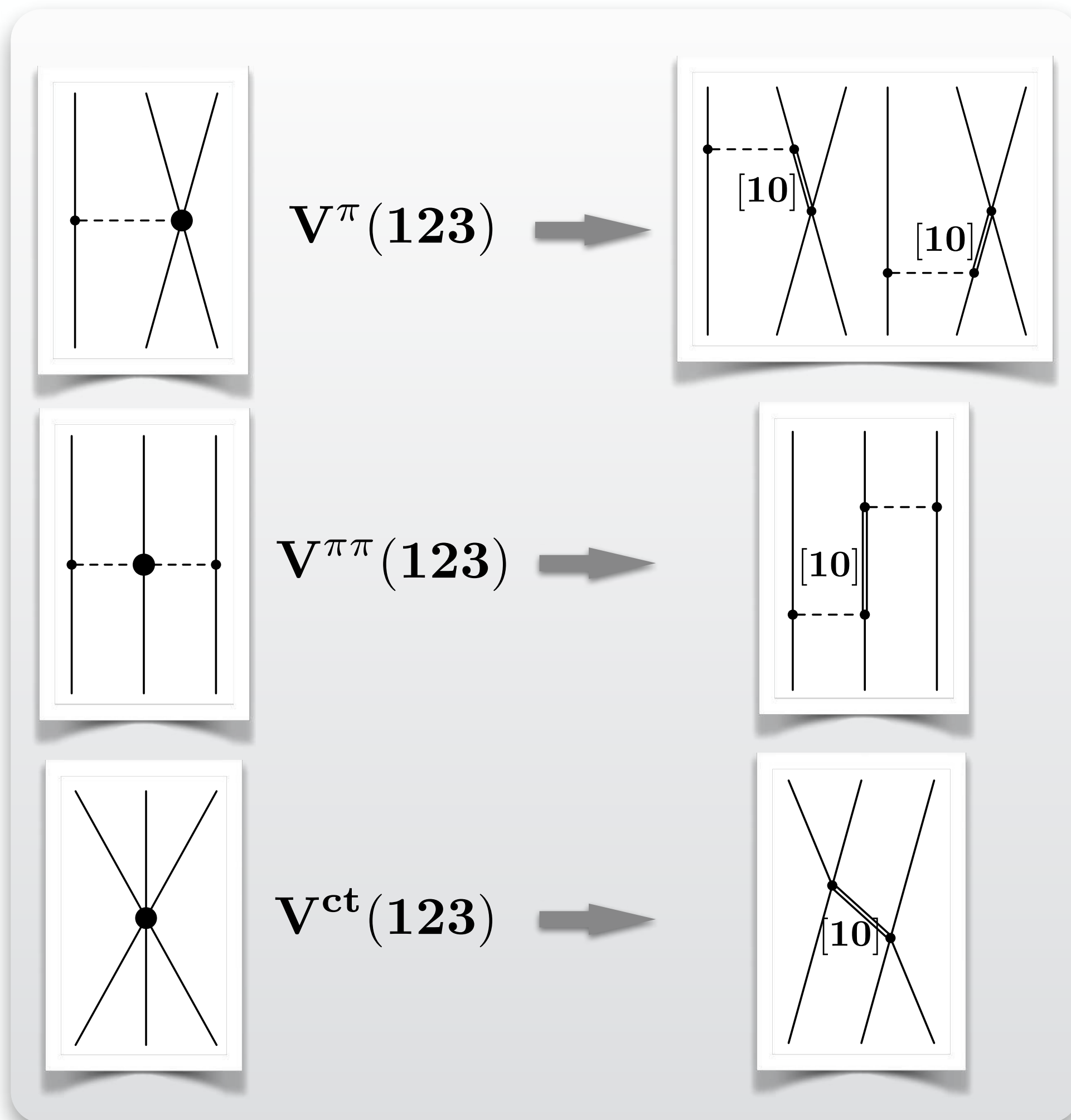
$$\Lambda N(^3S_1) = \frac{1}{2} [10^*] + \frac{1}{2} [8_a]$$

Short-range repulsive core
in all channels

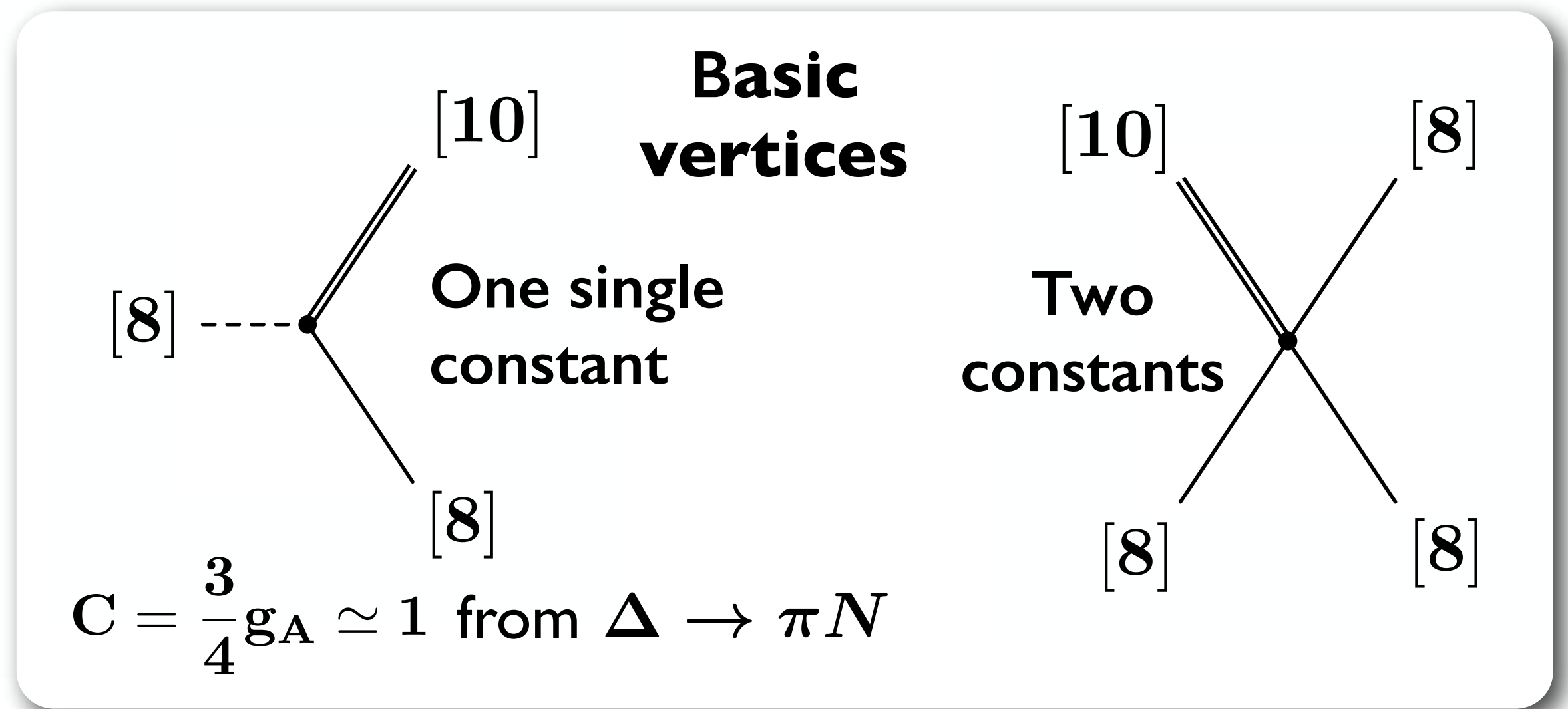
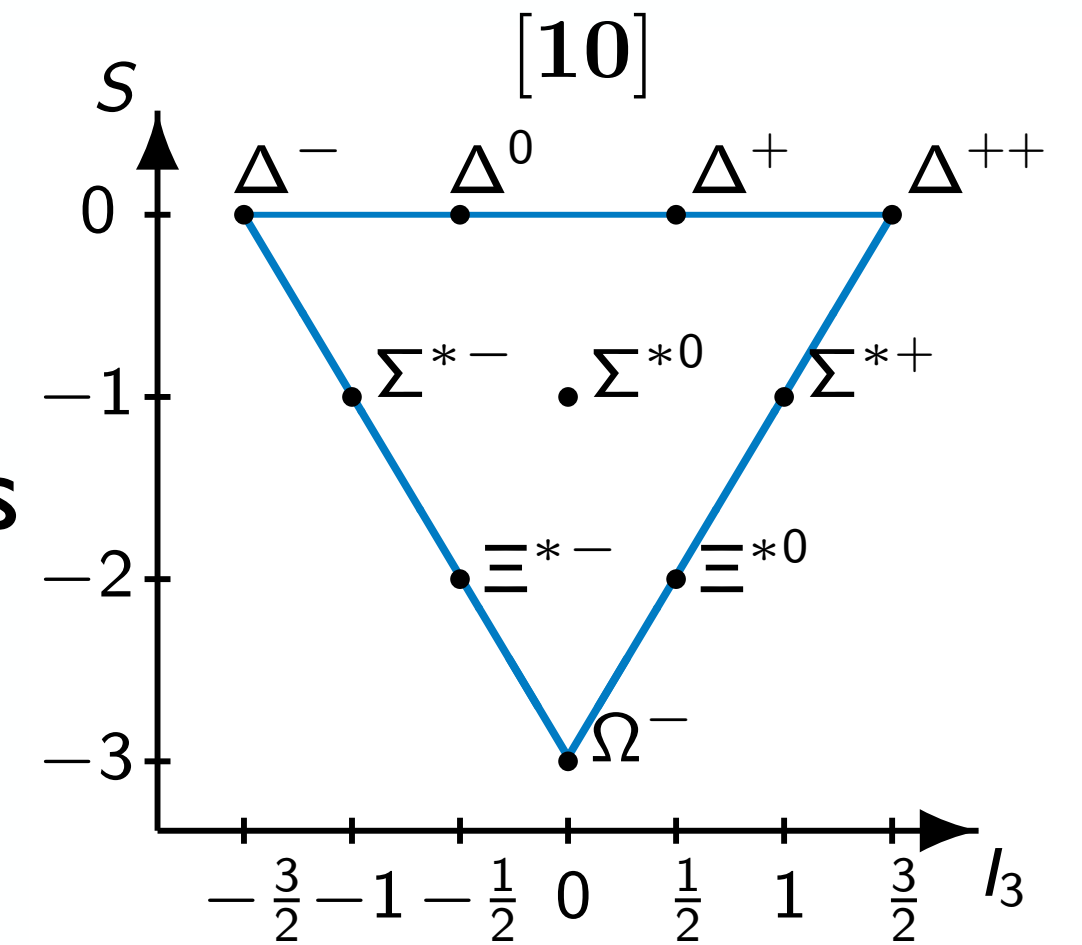
HYPERON-NUCLEON-NUCLEON THREE-BODY FORCES

from Chiral $SU(3)_L \times SU(3)_R$ Effective Field Theory

S. Petschauer, N. Kaiser, J. Haidenbauer, U.-G. Meißner, W.W.: Phys. Rev. C93 (2016) 014001



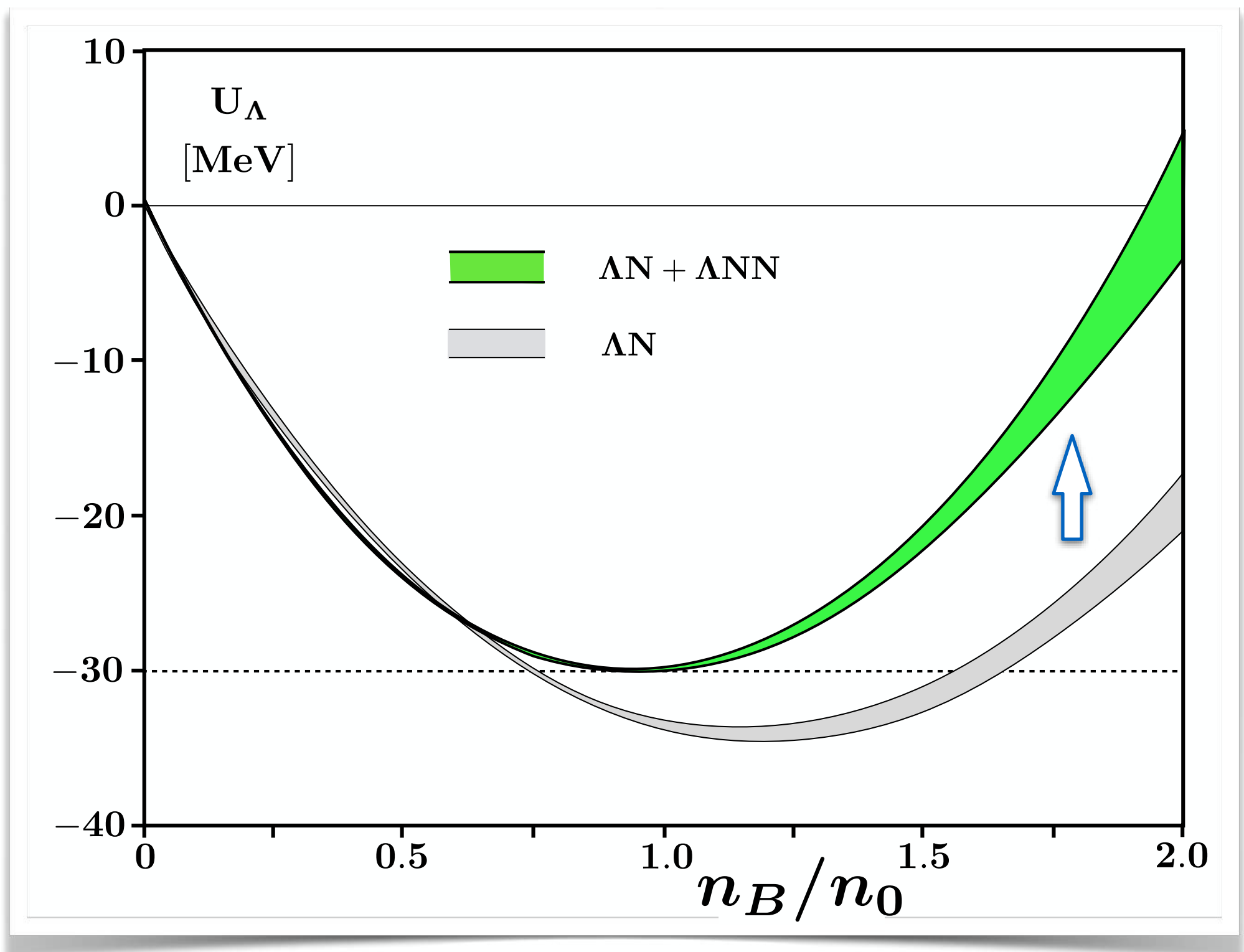
- **Decuplet Dominance** in YNN three-body forces
- Estimates of YNN interactions assuming dominant (Σ^* , Δ) intermediate states



Density dependence of Λ single particle potential

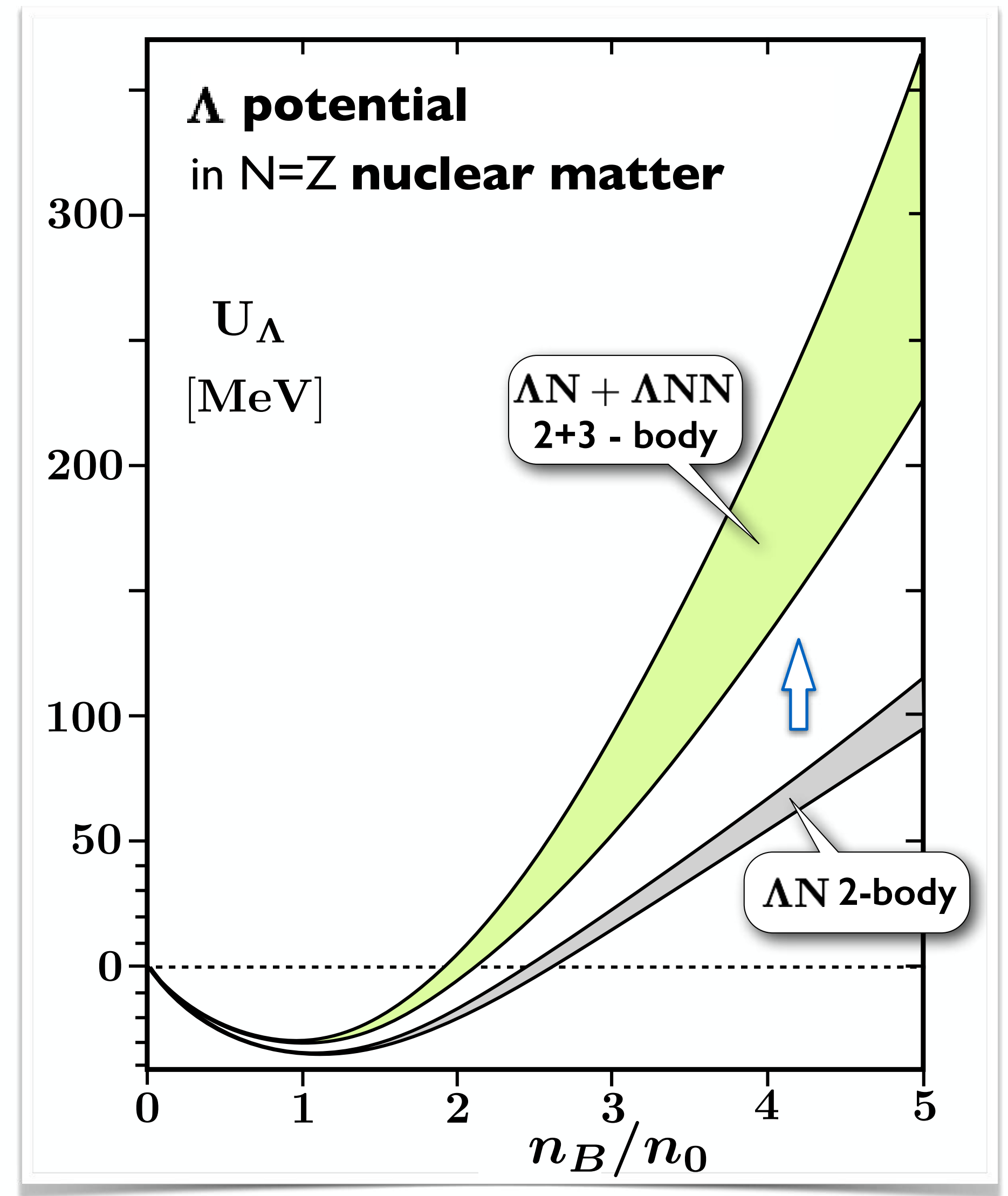
- Coupled-channels G-matrix including $\Lambda NN \leftrightarrow \Sigma NN$
- **Three-body interactions treated as density-dependent effective 2-body forces**

D. Gerstung, N. Kaiser, W.W.: Eur. Phys. J. A56 (2020) 175



Chiral NN (N3LO) + YN (NLO) + NNN+YNN interactions

Strong additional repulsion from YNN three-body forces



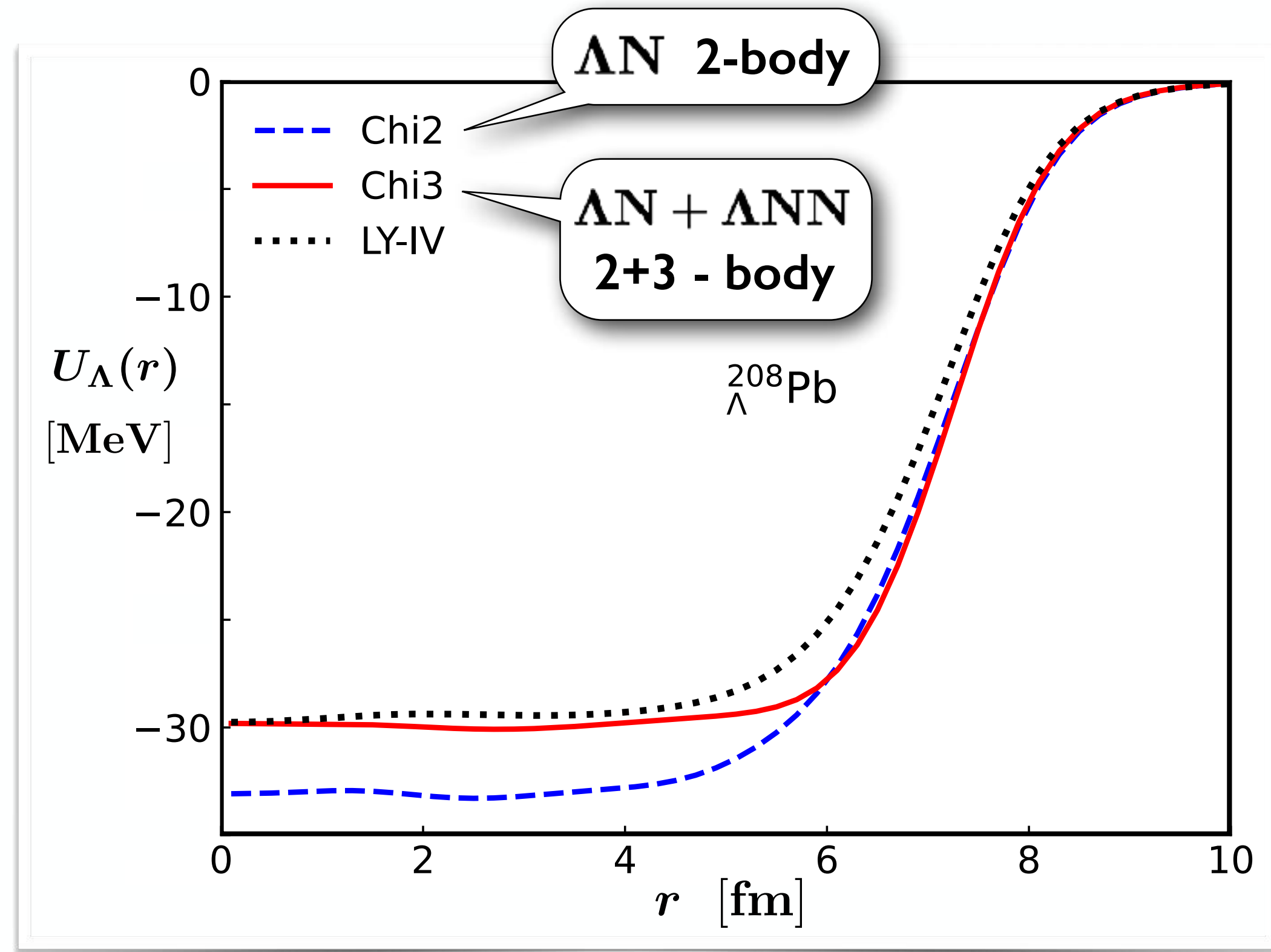
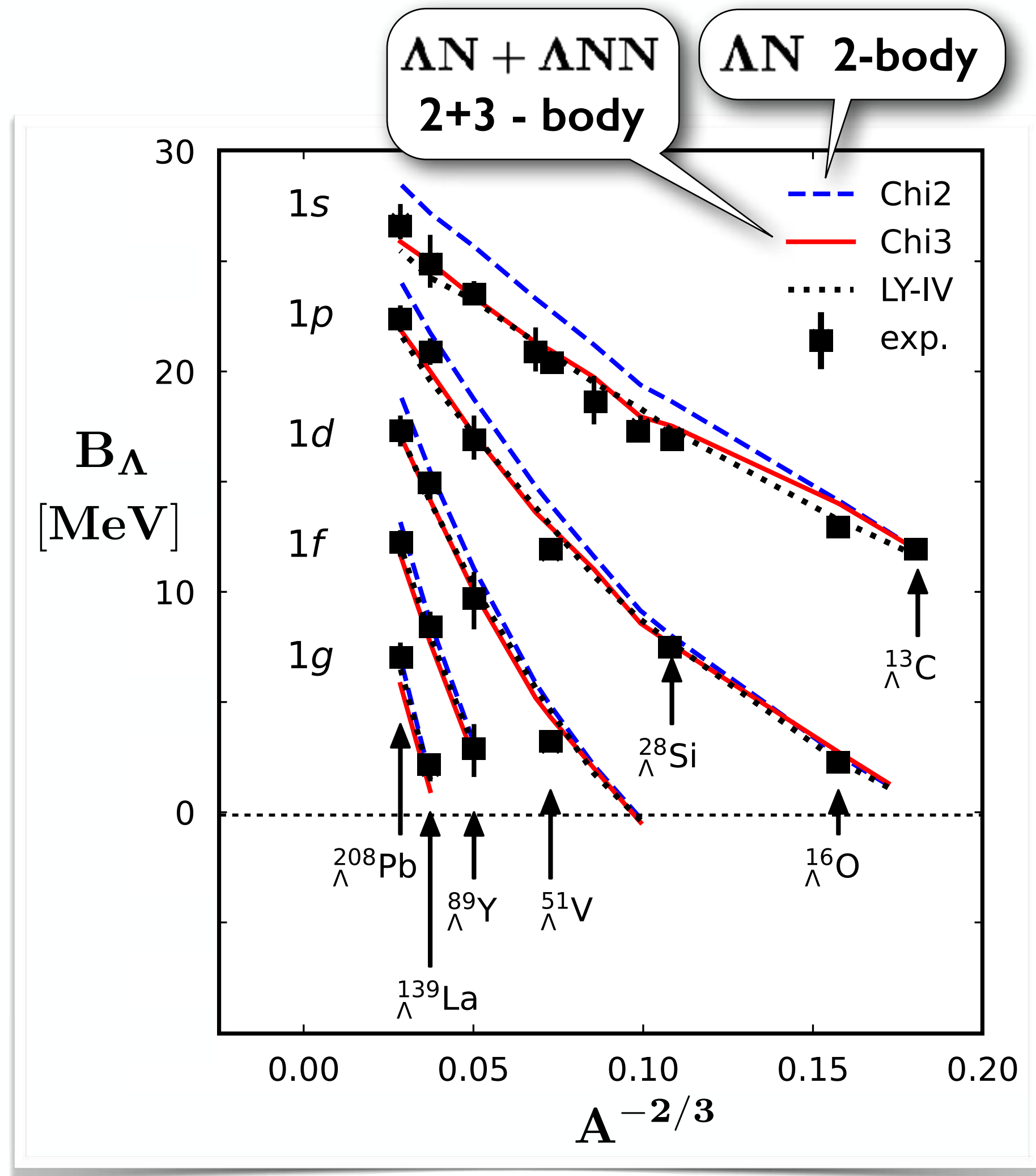
- **Constrained by hypernuclear physics : $U_{\Lambda}(\rho = \rho_0) \simeq -30 \text{ MeV}$**

A. Gal, E. Hungerford, D. Millener
Rev. Mod. Phys. 88 (2016) 035004

Λ HYPERNUCLEI

- Translation of **Chiral NN (N3LO) + YN (NLO) + NNN + YNN** interactions into Skyrme type energy density functional

A. Jinno, K. Murase, Y. Nara, A. Ohnishi : Phys. Rev. C108 (2023) 065803



- Overbinding of Λ with only two-body forces

HYPERNUCLEAR PHENOMENOLOGY

- Recent update on Λ - nuclear binding energies including Λ NN three-body forces
- Two- and three-body hyperon-nucleus potentials using realistic (empirically constrained) density distributions

$$U_{\Lambda}(n_B) = U_0^{(2)}(p_F) \frac{n_B(r)}{n_0} + U_0^{(3)} \left(\frac{n_B(r)}{n_0} \right)^2$$

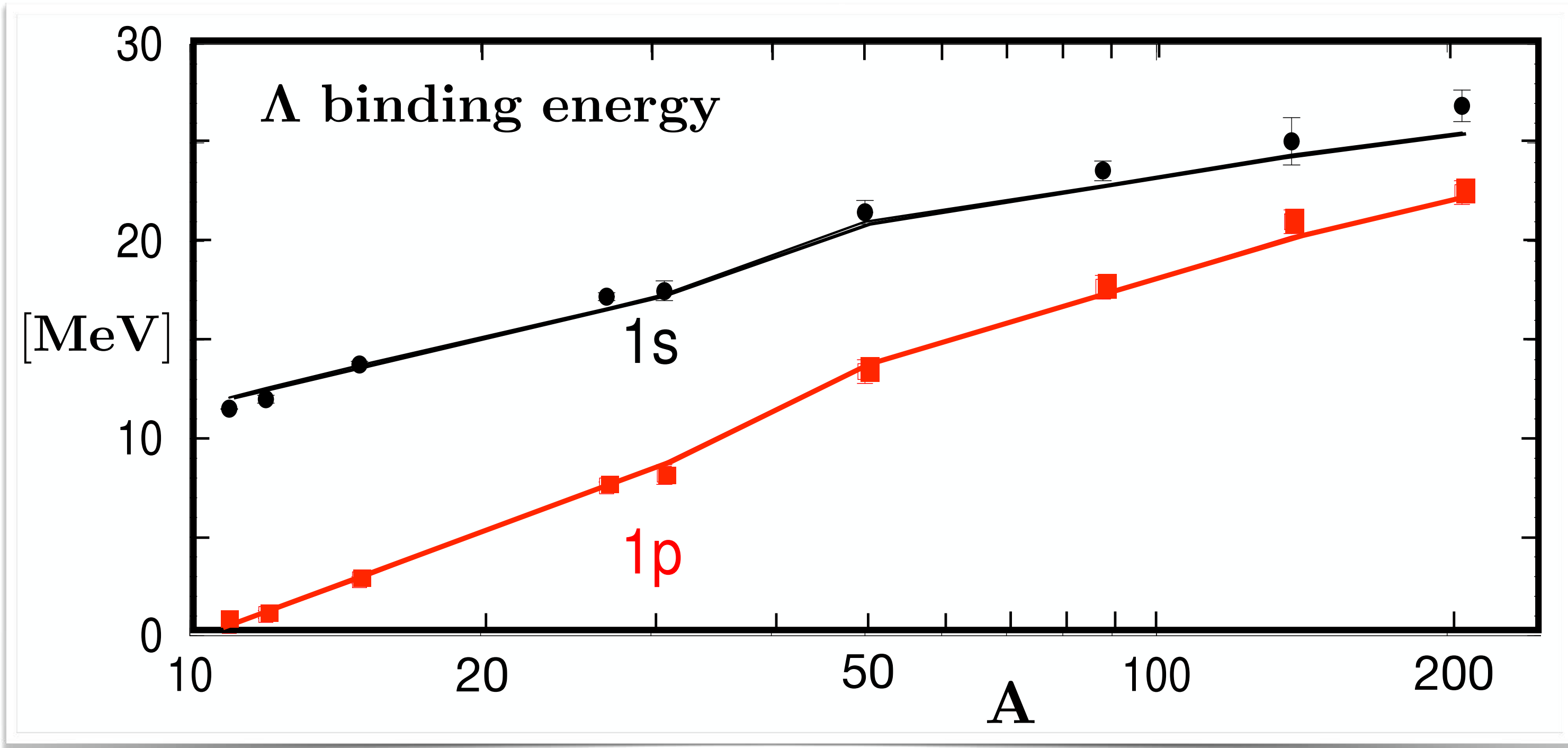
- Pauli correlations important
- Best fit :**

$$U_{\Lambda}(n_0) = -(27.3 \pm 0.6) \text{ MeV}$$

$$U_0^{(2)} = -(38.6 \pm 0.8) \text{ MeV}$$

$$U_0^{(3)} = (11.3 \pm 1.4) \text{ MeV}$$

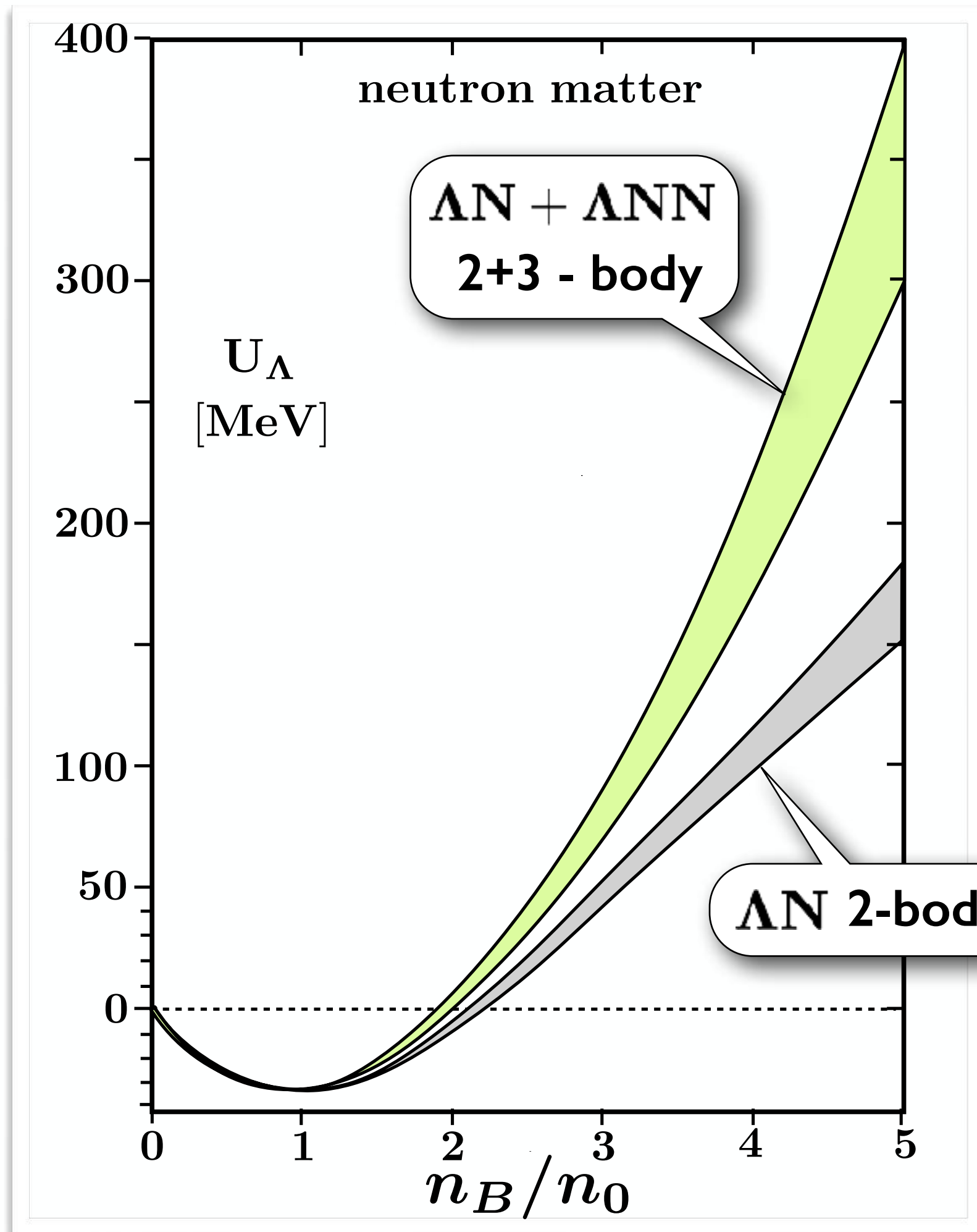
E. Friedman, A. Gal : Phys. Lett. B 837 (2023) 137669 ; Nucl. Phys. A1039 (2023) 122725



- Such **repulsive Λ NN three-body forces** can possibly solve the hyperon puzzle in n-stars

Λ HYPERONS in NEUTRON STARS ?

- Onset condition for appearance of Λ hyperons in neutron stars : Equality of chemical potentials



- Hyperon chemical potential**

in neutron star matter

from
**Chiral SU(3)
EFT interactions**

D. Gerstung, N. Kaiser, W.W.
Eur. Phys. J. A56 (2020) 175

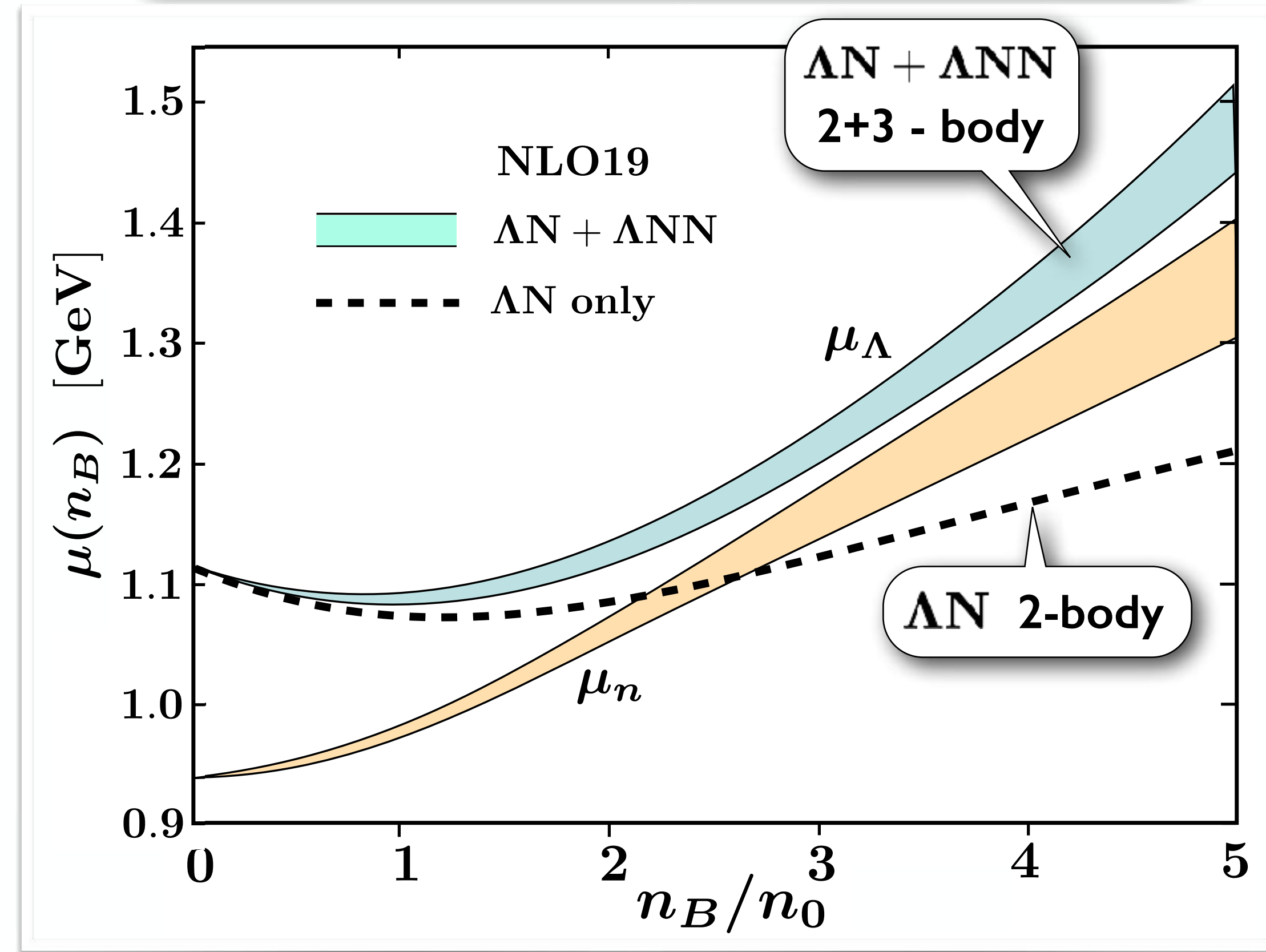
- Neutron chemical potential**

in neutron star matter

from
**Chiral EFT
+ FRG EoS**

M. Drews, W.W.
Prog. Part. Nucl. Phys. 93 (2017) 69

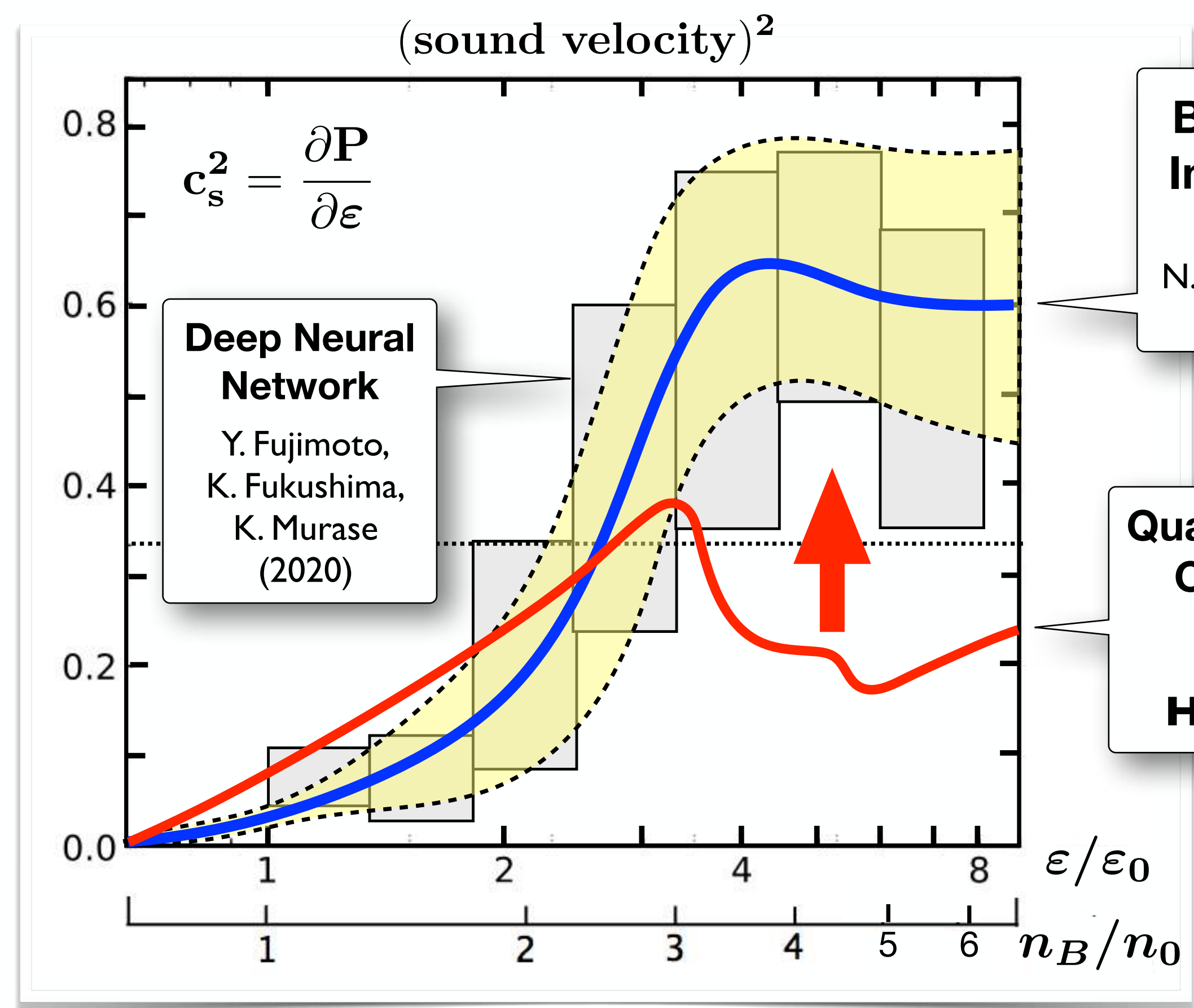
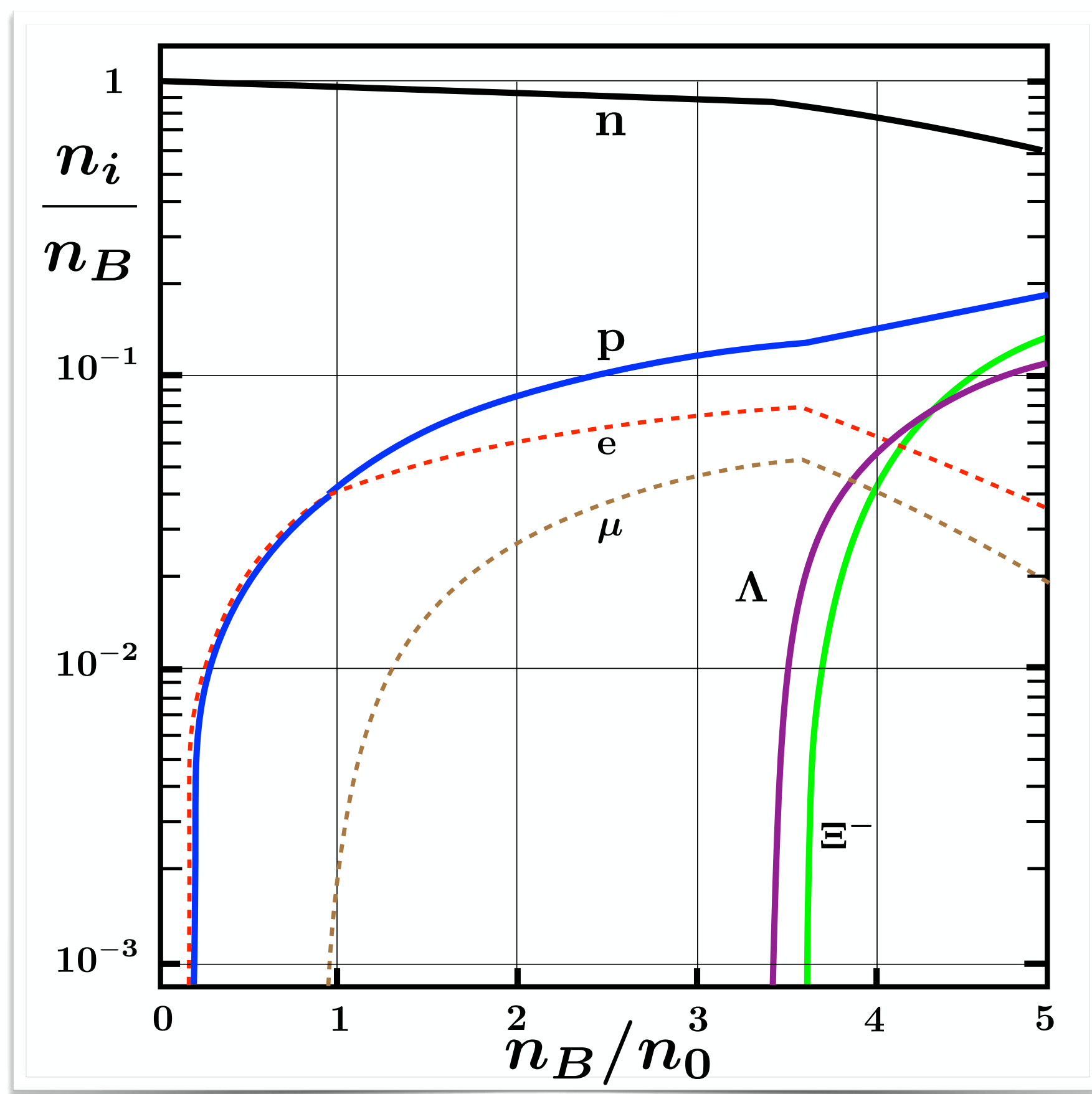
$$\mu_\Lambda = \mu_n \quad \mu_i = \frac{\partial \epsilon}{\partial n_i}$$



NEUTRON STAR MATTER including **HYPERONS**

NO "Hyperon Puzzle" ?

- **Quark - Meson Coupling model** $M_B^* = M_B^{(0)} - g_B \bar{\sigma} + \frac{d_B}{2} (g_B \bar{\sigma})^2$ T.F. Motta, P.A.M. Guichon, A.W. Thomas Nucl. Phys. A1009 (2021) 122157
- **Effective in-medium baryon masses including non-linear dependence on σ field, with scalar polarizability d_B representing e.g. effects of three-body forces**



Strangeness **CONCLUSIONS** and **OUTLOOK**

- ★ Key to **strangeness** in **neutron stars** :
 - ➔ **balance** between **hyperon-nuclear 2-** and **3-body forces**
 - ➔ **overbinding** in **hypernuclei** by two-body interactions compensated by **repulsive** hyperon-nuclear three-body forces
- ★ **Equation-of-state** of **neutron star matter** :
 - ➔ even **stiffer** than previously expected ($M_{\max} \simeq 2.3 M_{\odot}$)
 - ➔ increasingly repulsive hyperon-nuclear many-body forces can prevent appearance of hyperons in neutron star cores
- ★ Further insights and constraints expected :
 - ➔ expanded high-statistics **YN two-body data base**
 - ➔ improved **high-resolution hypernuclear spectroscopy**
 - ➔ growing quantity and quality of **astrophysical data**
focus on EoS and **speed of sound** in **neutron stars**

